

Criteria for cathodic protection of steel in concrete in the context of Arabian Gulf environment

Mohammad Golam Ali

Civil Engineering

October 1991

Abstract

This study attempts to formulate and quantify various relevant considerations which influence the effective cathodic protection of corroding reinforcing steel in concrete structures in the Gulf environment. The parameters included in the research program are: chloride content, temperature, reactive aggregates, depth of reinforcement in a two mat system and secondary effects. It was found that the instant off, shift and decay potentials as well as the current density needed for adequate protection of steel are dependent on the chloride gradient as well as the chloride content in concrete. A 60°-C exposure required only about 20 percent higher level of protection in terms of current density/instant off potential/decay potential for an initial polarization period of two months. Enhanced activation in the initial period reduces the corrosion activity subsequently due to the beneficial electromigration of ions requiring a reduced protection on a long term basis. The decay potential criterion was found to be least sensitive to chloride content, chloride gradient and temperature effect, although it does not explicitly indicate the level of protection current which is automatically adjusted to accommodate the various factors influencing corrosion activity.

In a two mat reinforcement system, the top mat was significantly overprotected when the bottom mat was just adequately protected from the anode source located above the top mat. The top mat suffers overprotection to an extent which would cause an unacceptable 30 percent reduction in the steel-concrete bond in a period of about 8 years. However, the bond reduction for a practical cathodic protection current density of 1-3 ma/ft² was found to be negligible. In high alkali-cement concrete containing reactive aggregates, cathodic protection current significantly advances the cracking time and softens the mortar at the steel-concrete interface reducing compressive strength and hardness.

INFORMATION TO USERS

This manuscript has been reproduced from the microfilm master. UMI films the text directly from the original or copy submitted. Thus, some thesis and dissertation copies are in typewriter face, while others may be from any type of computer printer.

The quality of this reproduction is dependent upon the quality of the copy submitted. Broken or indistinct print, colored or poor quality illustrations and photographs, print bleedthrough, substandard margins, and improper alignment can adversely affect reproduction.

In the unlikely event that the author did not send UMI a complete manuscript and there are missing pages, these will be noted. Also, if unauthorized copyright material had to be removed, a note will indicate the deletion.

Oversize materials (e.g., maps, drawings, charts) are reproduced by sectioning the original, beginning at the upper left-hand corner and continuing from left to right in equal sections with small overlaps. Each original is also photographed in one exposure and is included in reduced form at the back of the book.

Photographs included in the original manuscript have been reproduced xerographically in this copy. Higher quality 6" x 9" black and white photographic prints are available for any photographs or illustrations appearing in this copy for an additional charge. Contact UMI directly to order.

U·M·I

University Microfilms International
A Bell & Howell Information Company
300 North Zeeb Road, Ann Arbor, MI 48106-1346 USA
313/761-4700 800/521-0600

Order Number 9402446

**Criteria for cathodic protection of steel in concrete in the
context of Arabian Gulf environment**

Ali, Mohammad Golam, Ph.D.

King Fahd University of Petroleum and Minerals (Saudi Arabia), 1991

U·M·I
300 N. Zeeb Rd.
Ann Arbor, MI 48106

**CRITERIA FOR CATHODIC PROTECTION OF STEEL
IN CONCRETE IN THE CONTEXT OF
ARABIAN GULF ENVIRONMENT**

BY

MOHAMMAD GOLAM ALI

**A Thesis Presented to the
FACULTY OF THE COLLEGE OF GRADUATE STUDIES
KING FAHD UNIVERSITY OF PETROLEUM & MINERALS
DHAHRAN, SAUDI ARABIA**

**In Partial Fulfillment of the
Requirements for the Degree of**

**DOCTOR OF PHILOSOPHY
In
CIVIL ENGINEERING**

OCTOBER, 1991

KING FAHD UNIVERSITY OF PETROLEUM & MINERALS

DHAHRAN, SAUDI ARABIA

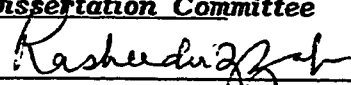
This Dissertation, written by

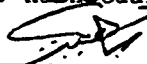
Mohammad Golam Ali


under the direction of his Dissertation Advisor, and approved by his Dissertation Committee, has been presented to and accepted by the Dean of the College of Graduate Studies, in partial fulfillment of the requirements for the degree of

DOCTOR OF PHILOSOPHY IN CIVIL ENGINEERING

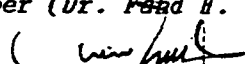
Dissertation Committee

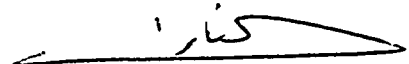

Chairman (Dr. Rasheeduzzafar)



Co-Chairman (Dr. Saadoun S. Al-Saadoun)



Member (Dr. Ahmad S. Al-Gahtani)

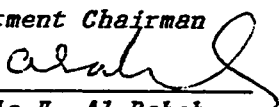

Member (Dr. Fakh H. Dakhil)


Member (Dr. Ghazi J. Al-Sulaimani)


Member (Dr. AlFarabi Sharif)


Member (Dr. Abdallah Shehri)


Dr. Ghazi J. Al-Sulaimani
Department Chairman


Dr. Ala H. Al-Rabeh
Dean College of Graduate Studies

Date : August, 1991



DEDICATED TO

My Parents

ACKNOWLEDGEMENT

Acknowledgement is due to the King Fahd University of Petroleum and Minerals for the support of this research.

I wish to express my sincere appreciation for the guidance and patient support of my Dissertation Supervisor Dr. Rasheeduzzafar for his invaluable counsel in various technical aspects of this work. I also wish to thank my Dissertation co-supervisor Dr. Saadoun S. Al-Saadoun and the other members of my Dissertation Committee Dr. Ahmad S. Al-Gahtani, Dr. Fahad H. Dakhil, Dr. Gazi J. Al-Sulaimani, Dr. Alfarabi Sharif and Dr. Abdullah Shehri for their suggestions during this investigation. I would like to thank Dr. M. Atiquzzaman for his help in designing the current supply unit for this research.

I wish to thank my wife Nazneen Rekha for her patience, good humor, support and assistance during the long course of this work. Thanks are also due to my son Tahseen and daughter Tanzeena for their love and smile which inspired me in doing this research work.

TABLE OF CONTENTS

	Page
List of Tables	xi
List of Figures	xiv
Abstract	xxi
 <i>Chapter 1</i>	 1
Introduction	
 1.1 Magnitude of Corrosion Damage to Reinforced Concrete Structures	 1
1.2 Mechanism of Corrosion of Reinforcement in Concrete	2
1.2.1 Electrochemical Corrosion of Steel in Concrete	2
1.2.2 Corrosion Protection of Steel By Concrete	3
1.2.3 Loss of Corrosion Protection	7
1.2.4 Mechanism of Chloride Corrosion of Steel in Concrete	8
1.2.5 Forms of Reinforcement Corrosion in Concrete	10
1.2.6 Corrosion Products	12
1.3 Corrosion Control in Reinforced Concrete Construction	13
1.4 Status and Potential of Cathodic Protection for Reinforced Concrete Construction	14
1.4.1 Principles of Cathodic Protection	14
1.4.2 Application of Cathodic Protection	23
1.4.3 Advantages of Cathodic Protection	28
1.4.4 Cost	28
1.5 Special Problems of Cathodic Protection in Concrete Structures	29
1.6 Special Problems of Cathodic Protection for Concrete Construction in the Gulf Region	36
1.7 Prevalent Cathodic Protection Criteria and their Application to Reinforced Concrete Structures	37
1.7.1 Criteria Based on Theoretical Considerations	38

	Page
1.7.2 Criteria Based on Laboratory Studies	43
1.7.3 Criteria Based on Field Experience	45
1.8 Unresolved Problems	48
Chapter 2	53
Problem Formulation, Objectives and Research Program	
2.1 Problem Formulation for the Proposed Study	53
2.2 Objectives	58
2.2.1 Developments of Relationships Between Current Density, Polarization Period, Protection Potential and Depolarization Time	58
2.2.2 Effect of Chloride Content of Concrete	58
2.2.3 Effect of Temperature	58
2.2.4 Depth Effect in Two Mat	58
2.2.5 Effect of the Presence of Reactive Aggregate	59
2.2.6 Bond Deterioration Due to Overprotection	59
2.3 Research Program: Theoretical	59
2.4 Research Program: Experimental	61
2.4.1 Developments of Relationships Between Current Density, Polarization Period, Protection Potential and Depolarization Time	61
2.4.2 Effect of Chloride Content of Concrete	63
2.4.3 Effect of Temperature	63
2.4.4 Depth Effect in Two Mat	67
2.4.5 Effect of the Presence of Reactive Aggregate	67
2.4.6 Bond Deterioration Due to Overprotection	67

	Page
Chapter 3	71
Theoretical Study	
3.1 Theoretical Study Related to the Effect of Environmental Parameters on Cathodic Protection Criteria	71
3.1.1 General	71
3.1.2 Concrete Environment in the Arabian Gulf Region	75
3.1.3 The Equilibrium Potential	75
3.1.4 Theoretical Results	76
3.1.5 Discussion	83
3.2 Theoretical Study for Cation Accumulation	84
3.2.1 Origin of Cations in Concrete	84
3.2.2 Movement of the Cations by CP Current	84
 Chapter 4	 88
Methodology of Experimental Research	
4.1 General Description of Instrumentation	88
4.1.1 Potential Wheel-Data Bucket	88
4.1.2 Current Supplying Unit	90
4.1.3 Temperature Chamber	93
4.1.4 Demec Gauge	93
4.1.5 Known Resistors	98
4.1.6 Corrosometer Probes and Ck-3 Corrosometer	98
4.1.7 Half Cells	100
4.1.8 Resistance Meter	100
4.1.9 Fixed D.C. Supply	102
4.1.10 Other Instruments	102
4.2 Monitoring and Evaluation Techniques	104

	Page
4.2.1 Embedded Instrumentation	104
4.2.2 Surface Technique	107
4.2.3 Visual and Physical Examinations	108
4.2.4 Destructive Technique	108
4.3 Procedures and Instrumentation Used to Study the Effect of Chloride Content, Temperature, Depth and Secondary Problems on Cathodic Protection Criteria	108
4.3.1 Developments of Relationships Between Current Density, Polarization Period, Protection Potential and Depolarization Time	108
4.3.2 Chloride Effect on Cathodic Protection Criteria	113
4.3.3 Temperature Effect on Cathodic Protection Criteria and Cathodic Protection Application	121
4.3.4 Depth Effect on Cathodic Protection Criteria	123
4.3.5 Enhancement of Alkali-Silica Reaction Due to Cathodic Protection	129
4.3.6 Degradation of Steel-Concrete Bond Due to Cathodic Protection	132
Chapter 5	140
Experimental Results and Discussion	
5.1 Developments of Relationships Between Current Density, Polarization Period, Protection Potential and Depolarization Time	140
5.1.1 Current Density Needed to Satisfy Prevalent Cathodic Protection Criteria	140
5.1.2 Polarization Period, Current Density and the Cathodic Protection Criteria	142
5.2 Effect of Chloride Content of Concrete on Cathodic Protection Criteria	152
5.2.1 Voltage Drop Across the Resistor in the Control Specimen Which Never Received CP Current	153
5.2.2 Static Potential	156
5.2.3 Instant off Potential	158
5.2.4 Four Hour Decay Potential	165

	Page
5.2.5 Shift Potential	171
5.2.6 Current Density	173
5.2.7 Effectiveness of CP in Arresting Corrosion	181
5.2.8 Summarized Overview	183
5.2.9 Adequacy of Theoretical Model (Established in Art. 3.1) in Predicting the Effect of Chloride in Concrete on Cathodic Protection Potential	187
5.2.10 Effect of Primary Chloride in Concrete on Current-Potential Relationship	188
5.3 Effect of Temperature on Cathodic Protection Criteria and Cathodic Protection Application	189
5.3.1 Temperature Effect on CP Criteria	189
5.3.2 Difficulties in Supplying Impressed Current to Steel in Concrete Specimen Kept at Hot-Dry Environment at Outdoors	203
5.4 Depth Effect on Cathodic Protection Criteria	210
5.5 Enhancement of Alkali-Silica Reaction Due to Cathodic Protection	225
5.5.1 Initiation of Cracks and Total Expansion at the End	227
5.5.2 Compressive Strength	231
5.5.3 Hardness of Mortar	233
5.5.4 Effect on Steel Properties	235
5.5.5 Volume of Gel Formed	235
5.5.6 Scanning Electron Microscopy	238
5.5.7 Summarized Overview	238
5.6 Degradation of Steel-Concrete Bond Due to Cathodic Protection	240
5.6.1 Degradation of Steel-Concrete Bond	240
5.6.2 Movement of Alkali-Cations Due to CP Current	246
5.6.3 Relationship Between the Bond Reduction and Alkali-Cations Concentrations at Steel Surface	250
5.6.4 Movement of Chloride Ions Due to CP Currents	256
5.6.5 Discussion	260

	Page
Chapter 6	
	266
Conclusions and Recommendations	
Chapter 7	
	278
References	

LIST OF TABLES		Page
Table 1.1.	The Reactions Referred to in Chapter 1	4
Table 2.1	The Gulf Parameters Relevant to CP Criteria for Reinforcing Steel in Concrete Structures	56
Table 2.2	Summarized Objectives of the Study	60
Table 2.3	Test Program for Relationship Between Potentials of Steel and Polarization Period	62
Table 2.4	Test Program for Determining the Effect of Chloride Content of Concrete on Static Potentials	64
Table 2.5	Test Program for Determining the Effect of Chloride Content of Concrete and the Chloride Gradient on CP Criteria	65
Table 2.6	Test Program for Determining the Effect of Temperature on Cathodic Protection Criteria	66
Table 2.7	Test Program for Geomorphic Factor: The Presence of Reactive Aggregates and the Increased Alkali-Silica Reactivity Due to Cathodic Protection Current	68
Table 2.8	Determination of the Effect of CP Current Density on the Steel-Concrete Bond	70
Table 3.1	Equilibrium Potential E_o for Different Temperature at a Very Low Iron Ion Concentration (0.056 mg/L. of Solution)	78
Table 4.1	Comparison of the Grading Used in the Research Program and the Grading Used By Others	130
Table 4.2	A Current-Potential Relationship at a Particular Activation Age	137
Table 5.2.1	Effect of Macrocell Chloride Content and Specimen Chloride Content on Voltage Drop Across the 51 Ohm Resistor (Results Are Obtained From Control Specimens at the Age	154

of 14 Days)

Table 5.2.2	Weight Loss of the Coupon Steel and Macrocell Steel for CP Specimen and Control Specimen in Chloride Effect Study. The Result of this Table Shows the Effectiveness of CP in Arresting the Corrosion	182
Table 5.2.3	Protection Level Needed at the Beginning of Activation	184
Table 5.2.4	Maximum Protection Level Recorded During the Observation Period	185
Table 5.3.1	Comparison of the Voltage Drop in the Macrocell and the Static Potential of Steel at Room Temperature Exposure Condition and High Temperature Exposure Condition	190
Table 5.3.2	Comparison of the Protection Level Needed to Protect Steel in Concrete Exposed to Room Temperature of 25 C and Elevated Temperature of 60 C	193
Table 5.4.1	Static Potential of the Main Steel and the Voltage Drop Across the Macrocell in Control Specimen Which Never Received CP Current (32 lbs Chloride Bearing Specimen, 96 lbs Chloride Bearing Macrocell)	213
Table 5.4.2	Static Potential of the Main Steel and the Voltage Drop Across the Macrocell in Control Specimen Which Never Received CP Current (32 lbs Chloride Bearing Specimen, 48 lbs Chloride Bearing Macrocell)	214
Table 5.4.3	Protection Level Needed to Reverse the Current Flow. Depth Effect and Chloride Gradient Effect Are Incorporated Here	216
Table 5.4.4	The Operation Current/Potential Needed for Protection of Bottom Mat at Different Activation Periods (for 32 lbs Chloride Bearing Specimen Having 96 lbs Chloride Bearing Macrocell)	218
Table 5.4.5	The Operation Current/Potential Needed for Protection of Bottom Mat at Different Activation Periods (for 32 lbs Chloride Bearing Specimen Having 48 lbs Chloride Bearing Macrocell)	221

		Page
Table 5.4.6	Current Drawn Up by the Pickup Probes. The Results Show the Efficiency of the Anode System in Supplying Current to the Steel Located At Different Distances From the Anode	224
Table 5.4.7	Weight Loss of the Coupon Steel and Macrocell Steel for CP Specimen in Depth Effect Study. The Results of This Table Shows The Effectiveness of CP in Arresting the Corrosion.	226
Table 5.5.1	Effect of Current Density on Initiation of Crack and Expansion at the End of Observation Period	228
Table 5.5.2	Effect of Current Density on Ductility, Ultimate Strength and Rupture Load of Steel	236
Table 5.5.3	Results Obtained From Simple Staining Technique	237

	LIST OF FIGURES	Page
Fig. 1.1	Theoretical Conditions of Corrosion, Immunity and Passivation of Iron, Assuming Passivation by a Film of Fe_2O_3	6
Fig. 1.2	Schematic Illustration of Local Action Cells (Anode and Cathodes) on a Metal Surface	11
Fig. 1.3	Barrier Repair System	15
Fig. 1.4	Schematic Illustration of Cathodic Protection Principle	17
Fig. 1.5	Cathodic Protection By Superposition of Impressed Current on Local-action Current	18
Fig. 1.6	Polarization Diagram Illustrating Plot of a Current as a Function of Potential for an Anodic and Cathodic Reaction	20
Fig. 1.7	Corrosion Mechanism, Current Flow	21
Fig. 1.8	Polarization Diagram Illustrating How Successive Levels of Cathodic Polarization Reduce the Anodic Current and Thereby Lower Corrosion Rate	22
Fig. 1.9	Schematic Representation of Protection Potential in a E-LogI Plot	24
Fig. 1.10	The Corrosion Mechanism in a Two Mat Reinforcement System (a) Chloride Penetrates Through the Pores of Concrete (b) Chloride Present in Concrete with Its Constituents	32
Fig. 1.11	Schematic Illustration of a Pile Showing How a Lack of Electrical Continuity Between Reinforcing Steel Bars Can Lead to Local Action Corrosion Damage Under Conditions of Cathodic Protection	33
Fig. 1.12	Delamination of Concrete Due to Chloride Attack	33
Fig. 1.13	Tafel Law- Equilibrium Potential and Exchange Currents (a) Reversible Reaction; and (b) Irreversible Reaction	40

		Page
Fig. 2.1	Schematic of the Cathodic Protection Concepts for Reinforcing Steel in Concrete	55
Fig. 3.1	Polarization Curve for an Electrochemical Reaction	73
Fig. 3.2	Interpretation of an Electrolytic Current-Potential Polarization Curve. The Case of Iron in Oxygen-Free 0.1M Solution of NaHCO_3 (PH=8.4)	74
Fig. 3.3	Variation of E_o with Temperature and Fe^{++} Concentration	79
Fig. 3.4	Influence of Chloride on the Behavior of Mild Steel in 0.1 mol/L Solution of NaHCO_3 (PH=8.4), in the Absence of Oxidant (a) No NaCl (b) 0.001 mol/L NaCl (c) 0.01 mol/L NaCl	81
Fig. 4.1	The Potential Wheel Data Logger Used in the Study	89
Fig. 4.2	Electrical Schematic for Impressing Current on Reinforcing Steel in Concrete Specimens	91
Fig. 4.3	The Current Supply Unit Used in the Study	92
Fig. 4.4	The Temperature Chamber Used in the Study	94
Fig. 4.5	Idealized Temperature Expected to Attain Inside the Temperature Chamber	95
Fig. 4.6	Temperature Actually Attained in the Temperature Chamber	96
Fig. 4.7	The Demec Gauge Used in the Test Program for Alkali-Silica Reactivity Study	97
Fig. 4.8	The Corrosometer Probe Used in the Study	99
Fig. 4.9	A Ck-3 Corrosometer Used in the Study	99
Fig. 4.10	The Principle of Half-Cell Potential Measurement	101

		Page
Fig. 4.11	Instrumentation Using Nilson 400 for Resistivity Measurement on Concrete Blocks	103
Fig. 4.12	Artificial Corrosion Macrocell Used in the Test Program	106
Fig. 4.13	Schematic of a Typical Specimen for Study Relating the Current Density with Available CP Criteria	109
Fig. 4.14	Schematic of a Specimen Used in (i) Study on Finding a Relationship Between the Current Density, the Polarization Period and CP Criteria (ii) Study on Enhancement of Alkali-Silica Reaction Due to CP Current	112
Fig. 4.15	A Typical Specimen Used in Study on (i) Chloride Effect (b) High Temperature Effect on CP Criteria	114
Fig. 4.16	Macrocells Positioned in Mold Before Casting of the Specimen	115
Fig. 4.17	Schematic Showing the Direction of Corrosion Current Flow Before Protection and Protection Current Flow After Protection	117
Fig. 4.18	Specimens at Outdoor Exposure. These Specimens were Used in Study on Possible Difficulties of CP Application at High-Temperature Dry Weather Regime	124
Fig. 4.19	A Typical Specimen With Two Mat Reinforcement Arrangement for Depth Effect Study	125
Fig. 4.20	Schematic of the Measurement of Total Circuit Current, Top Mat Current, and Bottom Mat Current in a Two Mat Reinforced Concrete Slab	128
Fig. 4.21	Schematic of a Typical Specimen Used in Bond Study Also Showing Loading Arrangement for the Cantilever Method of Testing for Bond Strength	134
Fig. 4.22	Cantilever Bond Test in Progress with Loading Frame Positioned in the Testing Machine	136

		Page
Fig. 5.1.1	Relationship of the Prevalent Cathodic Protection Criteria and the Current Density	141
Fig. 5.1.2	Variation of Instant Off Potential with Polarization Period for Different Current Densities	143
Fig. 5.1.3	Variation of 4 Hour Decay Potential with Polarization Period For Different Current Densities	146
Fig. 5.1.4	Decay of Potential with Depolarization Time After Different Polarization Periods for 60 ma/sq ft Current density	147
Fig. 5.1.5	Decay of Potential with Depolarization Time After Different Polarization Periods for 20 ma/sq ft Current density	148
Fig. 5.1.6	Decay of Potential with Depolarization Time After Different Polarization Periods for 03 ma/sq ft Current density	149
Fig. 5.1.7	Decay of Potential with Depolarization Time After Different Polarization Periods for 01 ma/sq ft Current density	150
Fig. 5.2.1	Variation of the Static Potential of Steel with Age of the Concrete Specimen	157
Fig. 5.2.2	Instant off Potential Needed to Protect Steel Embedded in Concrete Having 1.5 Chloride Gradient	159
Fig. 5.2.3	Instant off Potential Needed to Protect Steel Embedded in Concrete Having 2.0 Chloride Gradient	160
Fig. 5.2.4	Instant off Potential Needed to Protect Steel Embedded in Concrete Having 4 lbs Chloride Differential	162
Fig. 5.2.5	Instant off Potential Needed to Protect Steel Embedded in Concrete Having 8 lbs Chloride Differential	164
Fig. 5.2.6	Four Hour Decay Potential Needed for Protection of Steel in Concrete Having 1.5 Chloride Gradient	166
Fig. 5.2.7	Four Hour Decay Potential Needed for Protection of Steel in Concrete Having 2.0 Chloride Gradient	167

		Page
Fig. 5.2.8	Four Hour Decay Potential Needed for Protection of Steel in Concrete Having 4 lbs Chloride Differential	169
Fig. 5.2.9	Four Hour Decay Potential Needed for Protection of Steel in Concrete Having 8 lbs Chloride Differential	170
Fig. 5.2.10	Shift Potential Needed for Protection of Steel in Concrete Having Low Chloride Differential(0-4 lbs Cl/yd ³)	172
Fig. 5.2.11	Shift Potential Needed for Protection of Steel in Concrete Having Low Chloride Differential(≥ 0.8 lbs/yd ³)	174
Fig. 5.2.12	Current Density Needed for Protection of Steel in Concrete Having 1.5 Chloride Gradient	175
Fig. 5.2.13	Current Density Needed for Protection of Steel in Concrete Having 2.0 Chloride Gradient	176
Fig. 5.2.14	Current Density Needed for Protection of Steel in Concrete Having 4 lbs Chloride Differential	178
Fig. 5.2.15	Current Density Needed for Protection of Steel in Concrete Having 8 lbs Chloride Differential	180
Fig. 5.3.1	Effect of High Ambient Temperature on Static Potential of Steel	195
Fig. 5.3.2	Effect of Ambient Temperature on Instant Off Potential Needed for Protection	197
Fig. 5.3.3	Effect of Ambient Temperature on 4 Hour Decay Potential Needed for Protection	198
Fig. 5.3.4	Effect of Ambient Temperature on Shift Potential Needed for Protection	199
Fig. 5.3.5	Effect of Ambient Temperature on Current Density Needed for Protection	201

		Page
Fig. 5.3.6	Variation of Current Density With Exposure Period Outdoors	205
Fig. 5.3.7	Current Density During Final Stage of Exposure	206
Fig. 5.3.8	Variation of Concrete Resistivity With Exposure Period at Outdoor	207
Fig. 5.3.9	Variation of Moisture Content With Exposure Period Outdoors	209
Fig. 5.3.10	Variation of Current Density With Resistivity of Concrete	211
Fig. 5.5.1	Cracking Pattern for Different Specimens Used in Alkali-Silica Study	229
Fig. 5.5.2	Effect of Cathodic Protection Current on Compressive Strength of Mortar	232
Fig. 5.5.3	Effect of Cathodic Protection Current on Hardness of Mortar	234
Fig. 5.5.4	Photographs of Scanning Electron Microscopy Analysis. The Mortar Samples were Removed from Steel-Concrete Interface (a) Control Specimen (No Cp Current) (b) CP Specimen	239
Fig. 5.6.1	Typical Load-vs Free End and Loaded End Slips From Bond Strength Test on a Current-Treated Specimen (Impressed Current: 50ma/ft ²), Chloride Content: 2lbs/yd ³)	241
Fig. 5.6.2	Free End Slips Under Bond Test for CP Current-Treated and Control Specimens(Impressed Current: 03ma/ft ²), Chloride Content: 2lbs/yd ³)	243
Fig. 5.6.3	Free End Slips Under Bond Test for CP Current-Treated and Control Specimens(Impressed Current: 50ma/ft ²), Chloride Content: 2lbs/yd ³)	244
Fig. 5.6.4	Reduction in Bond Strength for Different CP Current Densities Impressed on Reinforcing Steel in Chloride	245

		Page
	Contaminated Concrete	
Fig. 5.6.5	Effect of Impressed Current Density on the Concentration of Sodium Ions Near the Reinforcing Steel Surface	247
Fig. 5.6.6	Effect of Impressed Current Density on the Concentration of Potassium Ions Near the Reinforcing Steel Surface	248
Fig. 5.6.7	Na Ion Concentration at Different Locations for Specimens Containing 2 lbs Cl/cu yds of Concrete	251
Fig. 5.6.8	Na Ion Concentration at Different Locations for Specimens Containing 8 lbs Cl/cu yds of Concrete	252
Fig. 5.6.9	K Ion Concentration at Different Locations for Specimens Containing 2 lbs Cl/cu yds of Concrete	253
Fig. 5.6.10	K Ion Concentration at Different Locations for Specimens Containing 8 lbs Cl/cu yds of Concrete	254
Fig. 5.6.11	Reduction in Bond Strength Due to (Na^+ + K^+) Concentrations Near the Reinforcing Steel Surface	255
Fig. 5.6.12	Effect of Impressed Current Density on Chloride Ion Concentration Near the Reinforcing Steel Surface	257
Fig. 5.6.13	Chloride Ion Concentration at Different Locations for Specimens Containing 2 lbs Cl/cu yds of Concrete	258
Fig. 5.6.14	Chloride Ion Concentration at Different Locations for Specimens Containing 8 lbs Cl/cu yds of Concrete	259
Fig. 5.6.15	Corrosion Conditions of Steel Bars Removed From Cathodic Protection Current Treated and Control Specimens (First Bar From Left is From Control Specimen, Other Four Bars Are From Current-Treated Specimens)	261

ABSTRACT

This study attempts to formulate and quantify various relevant considerations which influence the effective cathodic protection of corroding reinforcing steel in concrete structures in the Gulf environment. The parameters included in the research program are: chloride content, temperature, reactive aggregates, depth of reinforcement in a two mat system and secondary effects. It was found that the instant off, shift and decay potentials as well as the current density needed for adequate protection of steel are dependent on the chloride gradient as well as the chloride content in concrete. A 60°C exposure required only about 20 percent higher level of protection in terms of current density/instant off potential/decay potential for an initial polarization period of two months. Enhanced activation in the initial period reduces the corrosion activity subsequently due to the beneficial electromigration of ions requiring a reduced protection on a long term basis. The decay potential criterion was found to be least sensitive to chloride content, chloride gradient and temperature effect, although it does not explicitly indicate the level of protection current which is automatically adjusted to accommodate the various factors influencing corrosion activity.

In a two mat reinforcement system, the top mat was significantly overprotected when the bottom mat was just adequately protected from the anode source located above the top mat. The top mat suffers overprotection to an extent which would cause an unacceptable 30 percent reduction in the steel-concrete bond in a period of about 8 years. However, the bond reduction for a practical cathodic protection current density of 1-3 ma/ ft² was found to be negligible. In high alkali-cement concrete containing reactive aggregates, cathodic protection current significantly advances the cracking time and softens the mortar at the

steel-concrete interface reducing compressive strength and hardness.

ملخص

هذه الدراسة محاولة لصياغة وتقدير الإعتبارات المناسبة المختلفة التي تؤثر في الحماية الكاثودية الفعالة لحديد التسليح الصدأ للمنشآت الخرسانية في بيئة الخليج العربي . إن المتغيرات في هذا البحث تشمل محتوى الكلورايد والحرارة والبحث القابل للتفاعل وعمق حديد التسليح في نظام ذو مستويين مختلفين بالإضافة إلى عوامل أخرى ثانوية . وقد وجد أن الغلق اللحظي وتغيير الجهد تنازلياً وكذلك شدة التيار المطلوبة لحماية الحديد غير معتمدة على ميل ومحتويات الكلورايد في الخرسانة . وقد وضعت توصيات لمستويات الحماية الكافية للحديد على اختلاف تلوث الخرسانة بالكلورايد . وقد وجد أن التعرض الحراري إلى ٦٠ درجة مئوية إذ يحتاج فقط إلى ٢٠٪ زيادة من الحماية بواسطة كثافة التيار أو الجهد اللحظي أو الجهد التفاري لمدة شهرين من الإستقطاب الأولي . إن تعزيز النشاط في الفترة الأولية يخفض نشاط الصدأ فيما بعد . وقد وجدنا أن طريقة الجهد التنازلي تعتبر الأقل تأثيراً في محتوى الكلورايد . ميل الكلورايد وتأثير الحرارة لم توضح مباشرة مستوى حماية التيار الذي عياره أتوماتيكياً لإستيعاب العوامل المختلفة المؤثرة في نشاط الصدأ . وعند استعمال حديد ثنائي في بلاطة خرسانية فإن أعلى البلاطة يمتلك حماية كافية بينما أسفل البلاطة يعتبر محمياً من المصدر الأنودي الموجود في أعلى البلاطة . ونتيجة للحماية الفوقية في المستوى الأعلى فإنه يتسبب في انخفاض الرابطة بين حديد التسليح والخرسانة بمقدار ٣٠٪ في مدة ٨ سنوات . على كل حال انخفاض الرابطة لكثافة التيار الذي يتراوح بين ١-٢ ميلي أمبير لكل قدم مربع في الحماية الكاثودية العملية وجد أنه صغير جداً يمكن إهماله . ولقد وجد من البحث أن الحماية الكاثودية في حالة استعمال خرسانة بها اسمنت ذو قلوية عالية وحصلت نشاط بسبب زيادة التشققات ولذلك يضعف الخرسانة عند سطح التماس بين الحديد والخرسانة ويؤدي أيضاً إلى تقليل مقاومة الخرسانة وقساوتها .

CHAPTER 1

INTRODUCTION

1.1 MAGNITUDE OF CORROSION DAMAGE TO REINFORCED CONCRETE STRUCTURES

Corrosion of reinforcement has been established as the predominant factor causing widespread premature deterioration of concrete construction in the Arabian Gulf States(1-3). Even beyond the corrosive Gulf environment, the last decade has witnessed a growing world-wide concern for problems of corrosion damage in reinforced concrete structures. Corrosion deterioration in bridge decks, parking garages, coastal structures, and in concrete construction with chloride based accelerating agents, currently constitutes probably the single most significant concrete deterioration problem in the world.

In the United States alone, corrosion damage to bridge decks and support structures has been estimated to be over a billion dollars annually. The national Bureau of Standards has reported that in 1975 the national cost of corrosion in the USA was estimated at 70 billion dollars(4,5). Approximately 40 percent of that total was attributed to the corrosion of steel reinforcements in concrete. The National cost of corrosion and corrosion protection in the U.K. has been estimated to 3.5 percent of the GNP of UK(5). For US, this figure is 4.2. In March 1981, the United States General Accounting office estimated the number of deficient bridges to be over 100,000 , with an estimated cost of 33.2 billion dollars to replace or rehabilitate these bridges(6). Approximately 50,000 of the deficient bridges and 11 to 17 billion dollars of the cost are related to the deterioration of

concrete bridge decks. The cost of damage for the Gulf region has not been fully estimated but would probably run into hundreds of millions of dollars.

The deterioration due to corrosion of reinforcing steel gives rise to a familiar sequence of events resulting from more than two fold volume increase associated with the transformation of original metallic iron to iron oxide or rust. The formation of voluminous corrosive products on the steel surface, generates tensile stresses within the surrounding concrete which far exceed its tensile strength, causing cracking and the eventual spalling of the concrete cover to the reinforcement. With corrosion progressing unhampered, and at an enhanced rate, steel and concrete sections are reduced, and eventually bond will be lost between rebars and concrete(7). These effects weaken a structure, and its anticipated maintenance free useful service life of 50-60 years may be reduced to less than 15 years. Even more serious is the hazard caused by falling concrete from buildings and bridges and the unacceptable general appearance of the deterioration.

Once corrosion of reinforcement is initiated and the concrete spalling begins, the repairs and the corrective measures are expensive and tedious, and even then the success of the conventional remedial work in eliminating corrosion is somewhat uncertain.

1.2 MECHANISM OF CORROSION OF REINFORCEMENT IN CONCRETE

1.2.1 Electrochemical Corrosion of Steel in Concrete

Corrosion is the deterioration of the material due to interaction with its

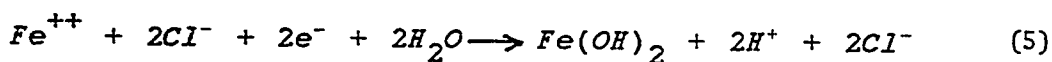
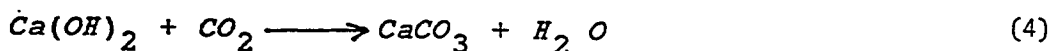
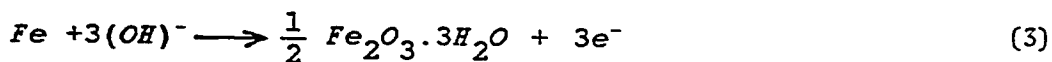
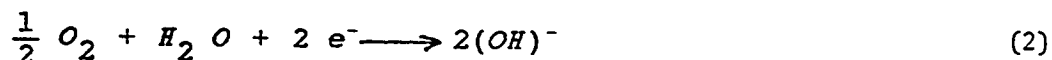
environment. Generally speaking, metal corrodes because the corrosion products are thermodynamically more stable than the metals themselves. The corrosion of reinforcement in concrete is an electrochemical process involving a galvanic cell wherein chemical energy is converted to electrical energy. In the Gulf region electrochemical reactions result from chloride-laden pore moisture in contact with the reinforcement(8). For such reactions to occur on embedded steel in concrete, there must exist on or around the rebar in the steel concrete system areas of **differential electro-chemical potential** which are electrically connected in concrete by an **electrolyte**. This electrolyte exists in the form of salt laden pore fluid in the Gulf concrete. When these conditions are met, corrosion occurs through the dissolution of metal ions to the moisture, leaving electrons behind (Reaction 1). By definition, this is an anodic reaction and the areas that corrode are called **anodic**. The remaining electrons move through the conductor metal from the anodic areas to non-corroding locations where they react with either water or oxygen to form hydroxyl ions (Reaction 2). By definition, this is a cathodic reaction and the locations at which this occurs are called **cathodes**. The electrons neutralize cations in the electrolyte, thus completing the electrical circuit.

Differences in metal potential may be obtainable either due to differences in metal itself (metal defects or differential impurities), or much more readily due to differences in the physical and or chemical environment of highly heterogeneous concrete. The later may result due to differences in alkalinity, chloride concentrations, oxygen availability, segregation, compaction, bleeding, permeability and the exposure conditions.

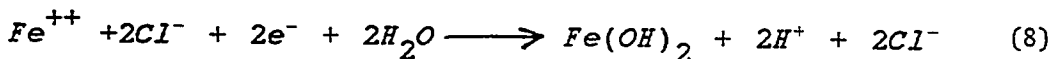
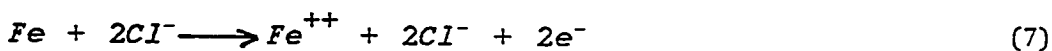
1.2.2 Corrosion Protection of Steel by Concrete

The usual chloride free environment of uncarbonated concrete is highly

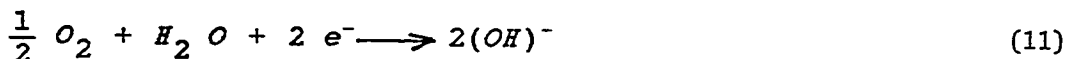
Table 1.1 The Reactions Referred to in Chapter 1



* In Absence of Oxygen



* In Presence of Oxygen



protective against corrosion of embedded steel for three reasons. Firstly, the aqueous environment within concrete matrix is characterized by significant presence of highly alkaline uncombined water in the well-distributed pores or voids of concrete; this environment passivates steel against corrosion. Secondly, concrete cover over reinforcement forms a defensive shield/barrier against the ingress of chlorides(from external source) and oxygen required for cathodic depolarization. Thirdly, concrete offers high resistivity to the flow of corrosion current.

A major application of thermodynamics to corrosion phenomena is the potential-PH plot known as Pourbiax diagram (9) using thermodynamic stability criteria and solubility data. Potential-PH diagram for a metal shows the equilibrium regions where the specific metal is in a state of immunity, passivity or corrosion. Fig. 1.1 shows the potential-PH plot for iron which is essentially the same for carbon steel. The plot shows that the redox potential for the hydrogen electrode lies above the region of immunity for iron in both acid and alkaline solutions implying that iron will dissolve with the evolution of hydrogen in solutions of all PH values. However, passivity for iron/steel is indicated in an alkaline environment characterized by a PH range of 9.5 to 12.5. From the standpoint of electrochemical behavior of steel in concrete, the most significant feature is the highly alkaline nature of the hydrated cement and its aqueous phase. Calcium hydroxide constitutes, on an average 20 percent of the hydrated products and passes into solution till the pore water is saturated and acquires a high degree of alkalinity corresponding to a PH of 12.5. Excess $\text{Ca}(\text{OH})_2$ is precipitated in crystalline form and constitutes a source of reserve basicity which buffers the concrete system against a reduction of alkalinity. With hydration, the pore liquid becomes increasingly concentrated with respect to the readily dissolvable sodium

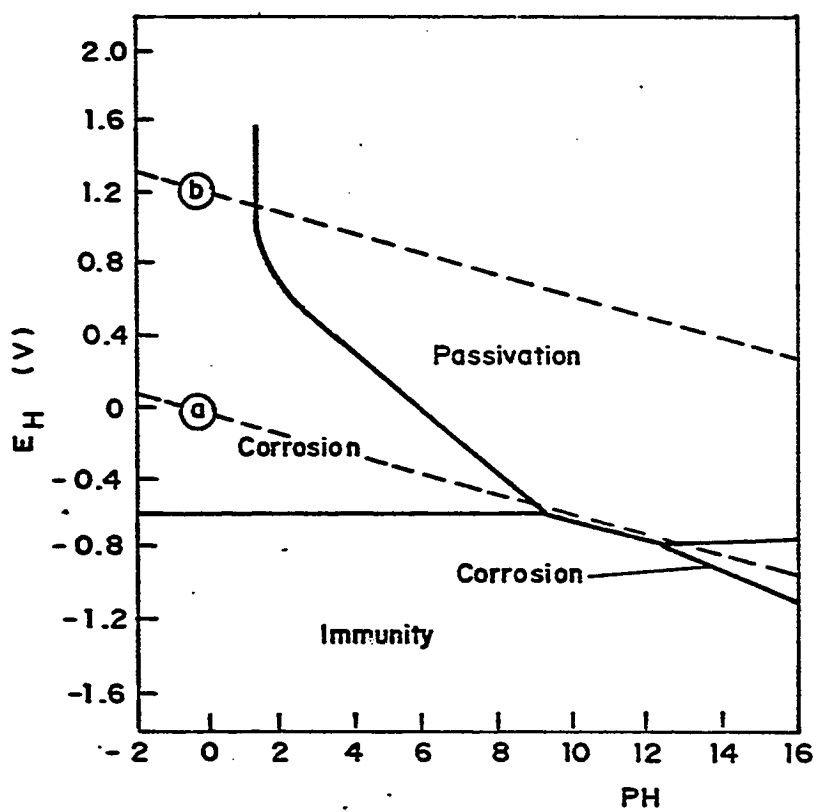


Fig. 1.1 Theoretical Conditions of Corrosion, Immunity and Passivation of Iron, Assuming Passivation by a Film of Fe_2O_3

and potassium hydroxides further raising the PH to values in excess of 13 within a few weeks of hydration(10). Due to sufficient hydroxyl activity in the highly alkaline pore solution of concrete, the passivity of steel in concrete system is specifically attributed to the formation of a protective submicroscopically thin oxide film in accordance with Reaction 3(11), signifying virtually complete inhibition of the anodic reaction associated with dissolution of metal (Reaction 1). Since the rate of corrosion is governed by the slowest partial anodic or cathodic reaction, passivation at anodic sites implies the stoppage of corrosion for all practical purposes. The exact composition of the corrosion passivating film is uncertain, but it is generally regarded to be comprising predominantly of Fe_2O_3 or Fe_3O_4 (12). However, it is agreed that its formation, stability, integrity and protective quality are characterized by high alkalinity(OH^- ions) and oxygen availability. A reduction in alkalinity lowers the protective quality of the film. Experience indicates a PH level of at least 11.5 in order to provide good electrochemical protection(16). If PH drops to 9.5/9 the protective oxide film is decomposed and its corrosion inhibition effect is eliminated(13).

1.2.3 Loss of Corrosion Protection

For initiation of rebar corrosion, the protective oxide film on steel surface must decompose; it may be disrupted by two specific circumstances which are of considerable significance to rebar corrosion mechanism in concrete. First, when the atmospheric carbondioxide makes an ingress into the concrete matrix and its penetrating front advances deep enough to intercept the steel reinforcement. The ready combination of carbondioxide with the calcium hydroxide of cement paste (Reaction 4) tends to neutralize alkalinity below PH 9 as this reaction signifies consumption of hydroxyl ions. Second, the presence of chlorides in concrete is

specially effective in eliminating passivity, because chloride ion has been described as a "specific and unique destroyer" of the passivating film(14).

In a cover concrete of adequate thickness and quality, which has been properly compacted and is free of honeycombs and other surface defects, the depth of carbonation is approximately proportional to the square root of the time of exposure. Normal outdoor air contains 0.03 percent carbondioxide and many investigations have shown that this depth does not exceed 5-8 mm after 10 years of exposure to the normal outdoor environment(15). Carbonation, therefore, has a significantly lesser corrosion promoting role compared to chlorides.

1.2.4 Mechanism of Chloride Corrosion of Steel in Concrete

The unusual high incidence of corrosion against the highly chloride -polluted environment puts the chloride ion as the most important cause for steel corrosion in the Gulf region. Chloride concentrations as high as 110 lbs/cu.yds have been observed in the Gulf concretes(16) whereas concentrations in excess of the usual chloride limit values of 0.15 percent(ACI specification) and 0.40 percent (B.S specification) are a common occurrence. Chlorides enter the concrete in this region either through constituent materials or through curing water and the environment.

In an attempt to elucidate the role of chlorides in the corrosion process, Hausmann(17) has proposed the "chloride threshold" concept. The chloride threshold theory states that there is a critical concentration of chloride ion above which corrosion of rebar will occur and below which the passive condition is maintained. Hausman's electrochemical studies show that chloride tolerance

increased as the PH of the solution was increased. Hausmann suggests that these results indicate that there is a competition between the hydroxyl and chloride ions; the corrosive action of the chloride ions is continuously opposed by the passive film-producing action of the hydroxyl ions. At low levels of chlorides the hydroxyl ions passivate the metal in accordance with Reaction 3. With increasing chloride concentration, a point is reached where the corrosion process, represented by Reaction 5, balances the passivating action of hydroxyl ions. Further increases in the chloride concentration cause the passive film to break down and corrosion occurs. According to Hausmann, the ratio of the combined Cl to OH concentration should not exceed a threshold of 0.60. Part of the total chloride may combine with the compositional phases of cement ,specially with C_3A phase, to form insoluble compounds such as calcium chloroaluminates. In practical terms, the minimum concentration of water soluble uncombined chloride ions (expressed as percentage by weight of cement) which will induce corrosion of embedded reinforcement, has been reported to be 0.40 percent, based on laboratory electrochemical study(18) , whereas the corrosion threshold for full size concretes has been found to be 0.15 percent chloride (19).

The precise mechanism by which chlorides actually disrupt the passivating film is not resolved as yet. One explanation is that chloride ions are able to diffuse through the passivating film and bond with the iron atoms in accordance with Reaction 6. Another is that when present in quantities beyond the critical value, they effectively sabotage the passive film producing action of hydroxyl ions, rendering steel surface exposed to corrosive action.

The chloride corrosion reactions at anodes and cathodes in the absence and presence of oxygen are shown in Reactions 7 through 12. It may be noted:

(i) the chloride corrosion causes a rapid reduction in the alkalinity at anodic sites to a PH level of about 5, due to the iron chloride complexing followed by the hydrolysis and the release of hydrogen (Reaction 9) and, (ii) chloride is regenerated which would perpetuate the corrosion even without further chloride addition.

Reaction 9 at the cathode in the absence of oxygen is characterized by an emission of hydrogen gas which is plated at the cathodic sites causing its polarization. This stoppage of the cathodic partial reaction would normally stifle corrosion at the anode. An adequate supply of dissolved oxygen is necessary for cathodic depolarization and is, therefore, a pre-requisite parameter to sustain the corrosion at the anodic sites.

1.2.5 Forms of Reinforcement Corrosion in Concrete

Chloride corrosion in concrete may take place by both of the two common mechanisms: **micro-cell** as well as **macro-cell**. The first type is the general form of uniform corrosion, which occurs with a general loss of passivity due either to carbonation or to the presence of excessive amounts of chlorides. Chlorides are more or less continuously distributed in the concrete surrounding the surface of the rebar. During microcell corrosion, very small anodes and cathodes are established on the metal surface (Fig. 1.2). The position of cell components is in a state of constant flux. With time uniform general corrosion occurs over the entire metal surface. The electrochemical potential is similar to that of corroding steel in other environments, typically -450 mv to -600 mv saturated calomel electrode (SCE), and the potential gradients are not very steep. The **macrocell** corrosion mechanism is characterized by a form of localized pitting corrosion that often occurs in concrete structures. During localized corrosion, the anodic and

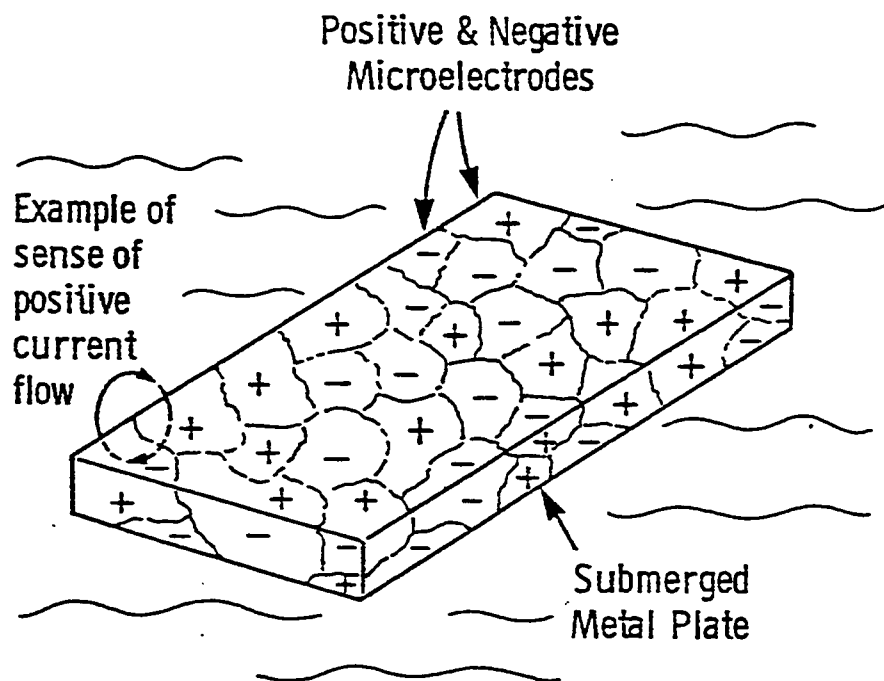


Fig. 1.2 Schematic Illustration of Local Action Cells (Anode and Cathodes) on a Metal Surface

cathodic reactions take place simultaneously on separate areas of the metal surface. Macro corrosion is essentially initiated by differential PH and or differential chloride cells. Corrosion occurs at well defined small anodic sites of high chloride concentration and low PH by a pitting mechanism. In this situation a large area of passive steel acts as the cathode. The result is rapid, spotty corrosion followed by concrete cracking at total iron losses as low as 0.5 to 2 percent of the rebar volume(20). Further, only a small percentage(10 percent or less) of the total bar surface may be visibly corroded when initial cracking occurs. The average potential is between that of passive steel and that of the local anodes, typically -200 to -500 mv(SCE).

1.2.6 Corrosion Products

Corrosion products formed at anodic sites depend on an interactive effect of oxygen supply, alkalinity and type of corrosion cell developed at anodic sites. These are seldom of a single compositional variety. More than one hydroxide of iron may exist concomitantly at the corrosion areas. The chloride corrosion products coexisting at corrosion sites, where measured PH was as low as 4.6, are reported to be white ferrous hydroxide and yellowish-green to greenish blue products(21), which may have been ferrous chloride (FeCl_2) and hydrated ferrous chloride ($\text{FeCl}_2 \cdot \text{H}_2\text{O}$) respectively. In conjunction with low PH values, significant amounts of black granular corrosion products (Fe_3O_4) are also observed implying that at least small amounts of oxygen had been available at corrosion sites(Reaction 13).

1.3 CORROSION CONTROL IN REINFORCED CONCRETE CONSTRUCTION

Several potential corrosion control measures have been proposed(22) and are in current use on concrete structures affected by the rebar corrosion problem.

These include measures which:

- (i) exclude chloride ingress and oxygen diffusion through the use of dense impermeable quality concrete, concrete membranes, coatings, penetrants, sealing materials, high density overlays and increased cover to reinforcement
- (ii) retard corrosion by the use of chemical corrosion inhibitors such as sodium benzoate, sodium nitrite or calcium/chromate complexes and also by chloride removal through electro-chemical techniques
- (iii) specify the use of corrosion resistant reinforcement comprising epoxy coated, stainless clad and galvanized rebars.

In the last decade cathodic protection has emerged not only as a strong corrosion control and prevention technique but also as a most viable rehabilitation method for rebar corrosion damaged concrete structures. It has been successfully used on full-scale installations of more than 150 major constructions such as bridge decks, marine structures, parking garages, prestressed and concrete coated pipes in the United States, Canada and Europe alone. Cathodic protection is now being strongly proposed for several high profile reinforced concrete construction applications in the Gulf region. The Manama Sitra causeway bridges linking the island of Sitra and the mainland at Manama in Bahrain, Power transmission tower foundations in Eastern Saudi Arabia and severely corrosion damaged underground power cable manholes in Jubail are some of the proposed applications in this region.

Currently the only comprehensive rehabilitation repair technique available for corrosion damaged concrete is the barrier repair system shown in Fig. 1.3(23). It, however, suffers from several deficiencies including those of cumbersome application and concomitant differential embedment of reinforcement in chloride free and chloride contaminated concretes.

Cathodic protection as a corrosion control technology was first logistically demonstrated by Stratfull in 1972(24) at the Sly park bridge deck on a small installation. Since then the U.S. Federal Highway Administration (FHWA) and the Ontario Ministry of Transportation, Canada have actively tried and developed the technology for application to salt-damaged reinforced concrete bridge decks. Its viability as a preventive and rehabilitation option for chloride induced corrosion of reinforced concrete structures can be adjudged from the following FHWA position statement(25):

“ The only rehabilitation technique that has proven to stop corrosion in salt contaminated bridge decks regardless of the chloride content of the concrete is cathodic protection”.

This evaluation explicitly verifies the efficacy of the cathodic protection and further implies that the conventional techniques such as modified concrete overlays and coatings have not proven to be significantly successful chloride corrosion protection methods.

1.4 STATUS AND POTENTIAL OF CATHODIC PROTECTION FOR REINFORCED CONCRETE CONSTRUCTION

1.4.1 Principles of Cathodic Protection

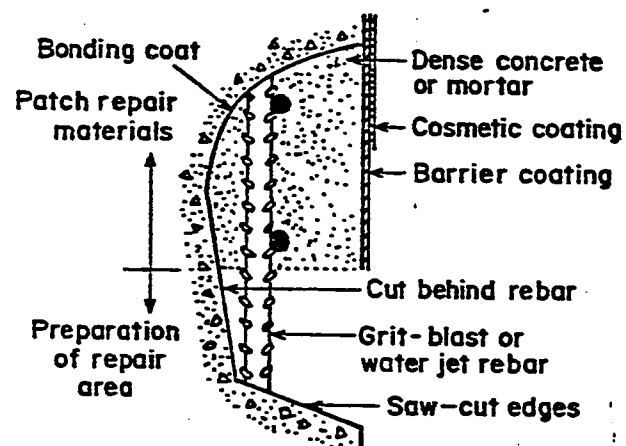


Fig. 1.3 Barrier Repair System

The logistics of the cathodic protection principle is shown in Fig. 1.4. A metal(reinforcement) located in an ionically conducting environment(pore fluid of concrete) can be protected from corrosion by connecting it to a current source of negative polarity,i.e. a current source which will supply electrons to the metal (reinforcement) and will cause a current to flow in the opposite direction through the ionically conducting environment (concrete) and onto the metal (reinforcement). The current is passed into the electrically conducting environment(concrete) via a second electrode(auxiliary anode) and passes through the solution by ionic conduction. Therefore only parts of the metals(reinforcement) which are in contact with the electrolyte (concrete), thereby completing the electrical circuit, can be protected by this technique.

Simply stated, on the strength of the fact that anodic and cathodic reactions (Reactions 1 and 2) are reversible, a negative charge externally imposed on the steel reinforcement by connecting it to the negative terminal of the power source, will attract and retain the Fe^{++} ions from migrating into solution ($2\text{e}^- + \text{Fe}^{++} \longrightarrow \text{Fe}^0$). The rebar in chloride contaminated concrete will have on its surface a large number of anodes and cathodes as a result of the multiple micro and macro cells present(Fig. 1.2). Once the cathodic protection current is applied, however, the entire structure becomes the cathode, or **electron donor**, and the positive terminal of the power source becomes the anode, or **electron acceptor**. In terms of superposition of impressed current on local action current, the concept is illustrated in Fig. 1.5. A typical of the numerous local action corrosion cells operative on rebar surface gets the impressed current from the auxiliary anode. Current leaves the auxiliary anode and enters both the cathodic and the anodic areas of the corrosion cells, returning to the source of D.C. current,B.

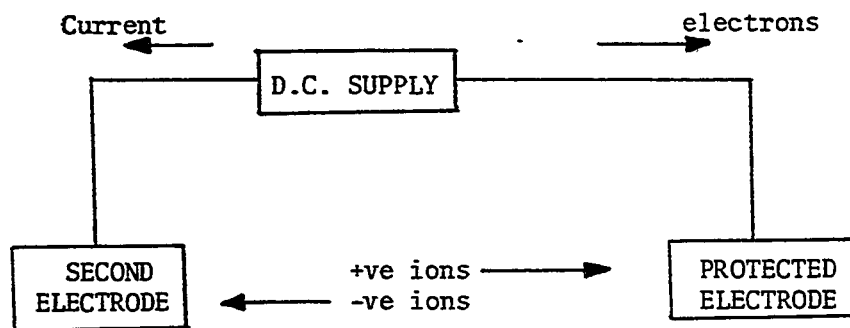


Fig. 1.4 Schematic Illustration of Cathodic Protection Principle

HOW CP WORKS

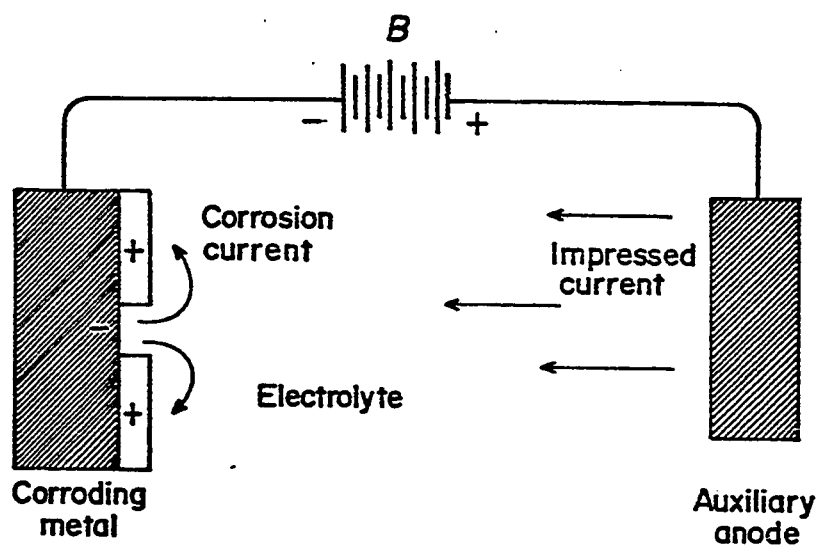


Fig. 1.5 Cathodic Protection By Superposition of Impressed Current on Local-action Current

When the cathodic areas are polarized by the external current to the open circuit potential of the anodes, all the rebar surface becomes equipotential and local action current no longer flows. The rebar surface, therefore, cannot corrode so long as the external current is maintained.

The kinetics of the corresponding electrochemical reactions at the anode and cathode as a function of potential are best illustrated diagrammatically. Fig. 1.6 shows a typical polarization diagram for a corrosion cell of the type operative on the rebar and shown in Fig. 1.5. While corrosion cell potential constitutes the driving force for corrosion, kinetic factors are largely determined by polarization; and it is this latter phenomenon which is most influential with regard to corrosion rate. Thus, it has been determined that potential of an electrode is a function of the net current flowing through it. When a current flows, the potential of the anode becomes more noble(positive) ; and potential of the cathode is more active(negative). This is illustrated by the diagram in Fig. 1.6, where a pair of curves, one expressing the potential current characteristics of the anodic reaction and the other of the cathodic reaction, are shown. For a corrosion exposure involving a low resistance electrolyte, the anodic and cathodic reactions are in balance at ϕ_{corr} , which represents the potential of the rebar corroding at a rate corresponding to the current density I_{corr} .

Now it is recognized that corrosion occurs at anodic sites, where current flows from metal into the electrolyte (Fig. 1.7). If cathodic current is provided by an external source to the metal, then the anodic current is reduced or eliminated altogether. This is conceptually illustrated in Fig 1.8, where four successive degrees of cathodic polarization ranging from free corrosion(no external current -condition 1) to complete protection(no net anodic current -condition 4) are

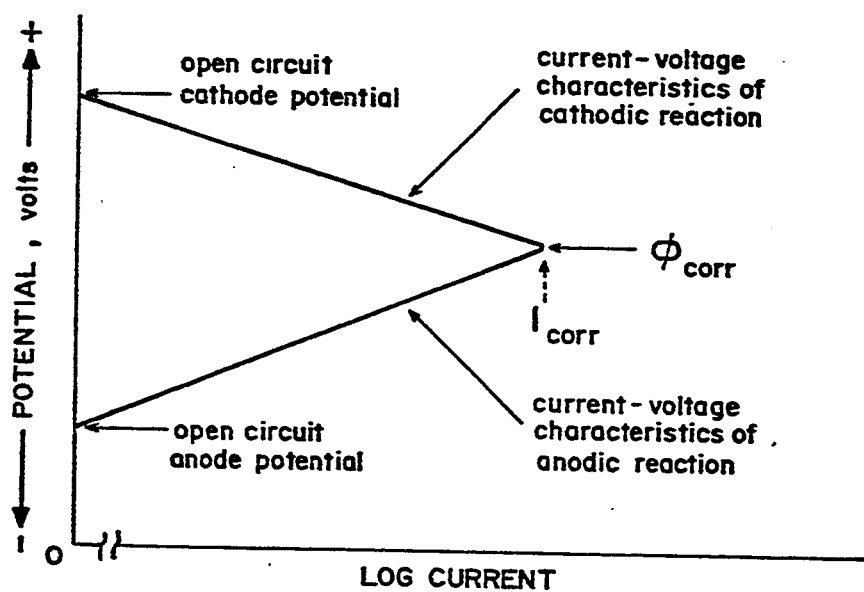


Fig. 1.6 Polarization Diagram Illustrating Plot of Current as a Function of Potential for an Anodic and Cathodic Reaction

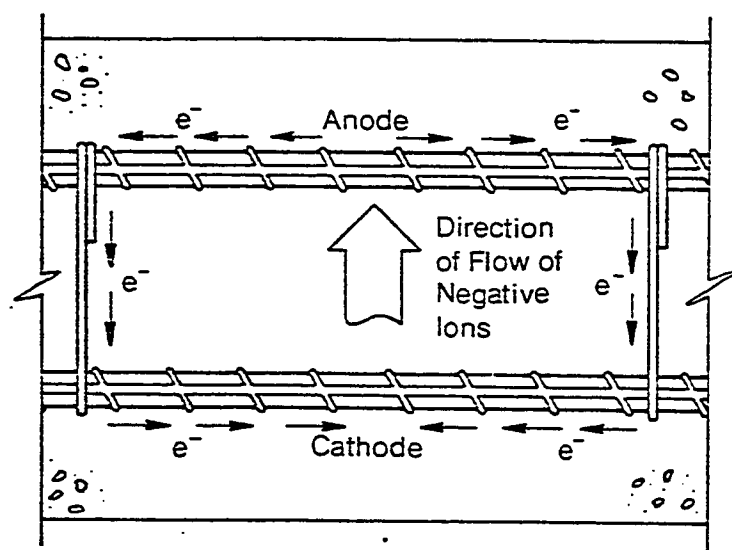


Fig. 1.7 Corrosion Mechanism, Current Flow

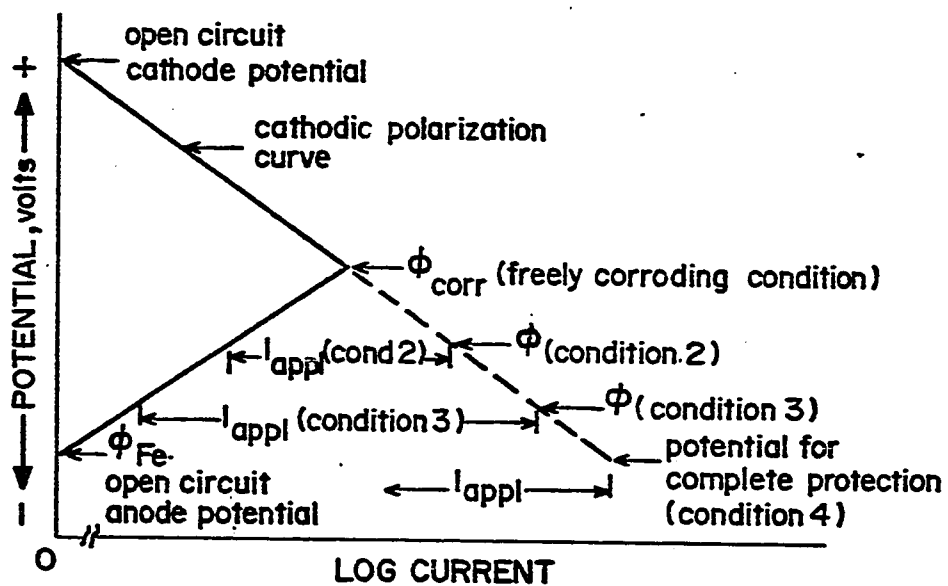


Fig. 1.8 Polarization Diagram Illustrating How Successive Levels of Cathodic Polarization Reduce the Anodic Current and Thereby Lower Corrosion Rate

illustrated. Complete protection is achieved when the metal is polarized to the open circuit potential of the anode(ϕ_{Fe} in Fig 1.8). No additional benefit is derived from polarization to a more negative potential. In fact, several deleterious secondary effects are associated with overprotection. First, it is uneconomical due to the wasteful additional cathodic current; second, it weakens the bond between steel and concrete(26); and third, hydrogen damage of the metal may result specially in high strength steels as used in prestressed concrete construction(27).

Two significant conclusions which are relevant for the proposed research are illustrated by Fig. 1.9;

- (i) As many systems have in actual practice an approximately logarithmic relationship between potential and current density, the effective reduction in corrosion rate often becomes smaller for each incremental negative shift in potential.
- (ii) The corresponding increase in the cathodic current becomes greater for each more negative step potential.

The significance of these conclusions is that partial protection, reducing corrosion to a level that is acceptable, can substantially reduce the consumption of current in an impressed current system. Criteria for protection can therefore be a specific potential, or a specific negative shift of potential from the free corrosion value.

1.4.2 Application of Cathodic Protection

1.4.2.1 General Application

Cathodic protection by sacrificial anode gained acceptance for corrosion control of buoys, ship hulls and various tanks and underground structures in the late 1800's. During the early 1900's the use of impressed current for protection of

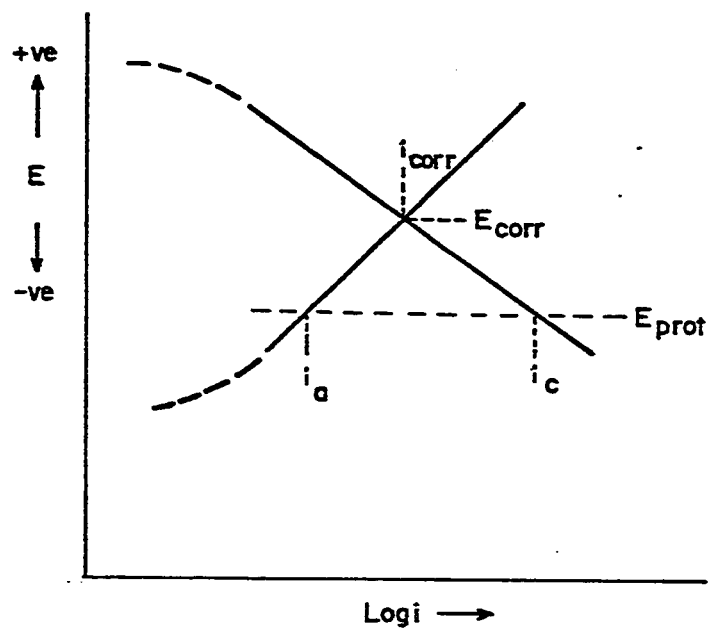


Fig. 1.9 Schematic Representation of Protection Potential in a E-Log i Plot

underground structures came into use, and the application of cathodic protection grew rapidly with the development, in the mid-1930's, of a new source of direct current, known as copper oxide rectifier. Although ships, marine structures, concrete coated piling and nuclear reactor containment vessels are some of the applications, the use of cathodic protection in these areas has not reached major proportions. It is the underground pipelines, underground storage tanks and steel structures in sea water where cathodic protection has been extensively applied. In United States alone there are over one million miles of underground pipelines(28), with much of that quantity cathodically protected with either sacrificial anodes or impressed current. U.S. Government regulations now require cathodic protection on all interstate pipelines(29). Prior to the advent of unleaded fuels and fiber glass storage tanks, many gas stations used a form of cathodic protection for their underground storage tanks.

1.4.2.2 Application to Reinforced Concrete Structures

Although cathodic protection is a well-established means of preventing corrosion for pipelines buried in soil and steel structures located in sea water, the application of this technique to reinforced concrete structures is still in a developmental stage. Concrete is a distinctly different material from soils and saline water in terms of its internal and external environments, conductivity to the flow of electrical currents, inherent heterogeneity of matrix and responses at the steel/encasing-material interface. Even when the principle of protection remains unaltered, this position requires significantly different technology and criteria for corrosion control of reinforcement in concrete structures. This is discussed in greater detail in section 1.5 of this dissertation.

The first serious attempt to apply the impressed current CP system to

control chloride corrosion damage of rebar in reinforced concrete construction was made in early 1970's. Stratfull(30) and others (31,32,33) reported success on its use on bridge deck surfaces. Since reinforced concrete parking garages often suffer the same type of deterioration as bridge decks, in 1977 two cathodic protection installations were made in parking garages, one in Cincinnati, Ohio, and the other in Minneapolis, Minnesota.

Early problems arising from application to concrete structures were found to be with materials, techniques and logistics rather than with the concept. Two features of reinforced concrete structures made the CP installation particularly difficult. First, the high electrical resistivity of concrete which hampers the spreading of the currents from the locations of the anodes to obtain a uniform distribution over the entire reinforcement network. The second feature of importance pertains to a possible lack of electrical continuity among reinforcing steel members.

In view of the significance of a uniform distribution of the impressed current for success in corrosion control, the progress in the application of cathodic protection system to reinforced concrete structures has remained linked to the development of a successful anode system which in addition to spreading the current efficiently, is also easily constructible, durable and capable of operating in the particular conditions appertaining in concrete structures. Therefore, anodes for reinforced concrete systems have been specially developed over the past 10 years to overcome the specific associated problems.

Early CP installations used simple high silicon cast iron anodes in an asphalt overlay made conductive by the addition of coke. Variation in the system

were tried, but as the system cannot be used for vertical and soffit surfaces, and also adds upto 80 mm to the slab thickness, thi limited applicability and the dead weight load penalty were strong negative factors. To avoid the weight and thickness penalties of conductive overlays, anode systems were installed in slots cut into the concrete. Anodes of platinum clad niobium wire and graphite fibers failed due to acid attack of the concrete adjacent to the anodes. It was , however, the advent of conductive coating anode systems in around 1980 that first provided a practical anode system for vertical and soffit surfaces of reinforced concrete. Conductive coating anode systems, using platinum clad niobium or titanium as a primary anode, have seen wide applications. In 1983 a conductive polymer wire, sometimes preassembled into a mesh array, was introduced as an anode for reinforced concrete. This anode has been extensively used in highway bridge and car park decks as well as with a gunite overlay for vertical and soffit surfaces. In 1985, titanium expanded mesh anodes coated with various precious metal oxides by different manufacturers, were introduced concurrently in UK and USA for applications to reinforced concrete.

The power source is generally a direct current rectifier with various control elements. Power requirements for CP system is typically in the range of 40-50 watts or a maximum of 0.02 watt per square feet of concrete surface. For reasons of economy and ease of control, the rectifier units are generally constructed with multiple outputs, each providing an individually adjustable direct current. Control may provide constant current or constant voltage, or constant voltage with a current limit. Automatic systems to maintain constant steel reinforcement/concrete reference potentials have also become available lately.

1.4.3 Advantages of Cathodic Protection

Cathodic protection is becoming more acceptable for concrete construction, and its initial limited application to bridge decks has now been extended to other structures and buildings such as parking facilities, wharves and chemical plants. It offers the following significant advantages:

- * It is the only appropriate method for the rehabilitation of reinforced concrete structures where deterioration has been caused by chloride induced corrosion of the reinforcement. All other rehabilitation techniques in presence of chlorides in concrete are only cosmetic and do not control corrosion on a long term basis. Therefore, it offers an attractive option to replacement, massive concrete removal or a continuous program of patch repairs throughout a structure's life.
- * Provided corrosion of reinforcement has not impaired structural integrity, only minimal concrete repairs are required before a cathodic protection system is installed.
- * The effectiveness of cathodic protection in arresting corrosion can be measured by simple, non-destructive techniques.
- * The cost of applying cathodic protection is only a small fraction of the replacement cost of the threatened structure, and cathodic protection is clearly the least expensive means of providing long-term, maintenance free service life for steel reinforcement in corrosive chloride contaminated environment.

1.4.4 Cost

The cost of cathodic protection is highly variable. In a recent review the capitalized costs (inclusive of first cost, maintenance and power costs) for wire anode (non-overlay) and conductive overlay types of cathodic protection systems have been reported to be US\$ 164.80/ sq.m and US\$ 147.90/sq.m of concrete surface respectively. This may be compared with the capitalized cost for maintaining a typical existing, black-steel-reinforced slab and subsequent replacement with slabs having epoxy coated reinforcing bars which comes to be US\$ 137.78/sq.m. However, the patching or membranes can only be viewed as temporary repair

methods when the concrete down to and below the bar is contaminated with concrete.

Chou (34) gave a comparative cost for a particular bridge deck. For the bridge deck studied, the CP cost was US\$ 41,344 compared with US\$138,396 for total deck replacement. Using an annual worth method, cathodic protection was found to be cheaper by US\$ 3228 to US\$ 5793. Chou suggests that as overlays are now a popular method of deck rehabilitation, it does not cost much more to insert a CP system under the overlay at the same time. The installed cost of most system is less than US\$ 6 per sq. ft.

1.5 SPECIFIC PROBLEMS OF CATHODIC PROTECTION IN CONCRETE STRUCTURES

Reinforced concrete is a composite, highly heterogeneous material made of concrete and embedded steel reinforcement and is markedly different from sea water, ground water and soil which have hitherto formed the conventional electrolyte for numerous successful cathodic protection installations. Plain concrete itself is a diphasic material comprising aggregate particles of various sizes dispersed unevenly in a matrix of cement paste. The most distinctive feature of the concrete make-up is the intrinsic heterogeneity of its matrix. The two phases of concrete structure are neither homogeneously distributed with respect to each other, nor are they themselves homogeneous. The interfacial region between the particles of coarse aggregate and the hardened cement paste forms a third phase which has been identified as a "transition zone" (35). The hardened cement paste is a porous solid comprising of voids, pores and microcracks ranging from 3 mm

(air voids) to 10 nm - 5 μ m (capillary voids) to 5 to 25 \AA (gel pores). These voids and pores are filled with a highly alkaline aqueous phase of PH in the range of 12.5 to 13.5. Apart from the inherent heterogeneities, localized differences are invariably introduced on a macro scale by conditions prevailing during construction. These may produce areas of differential compaction, permeability, resistivity and diffusion. Further, the reinforced concrete structure is commonly exposed to the full impact of the environment and its variations. In terms of its sensitivity to its service environment, concrete has been likened to a living organism. Contrary to its plain rock-like deceptive simplicity, concrete is a highly responsive pseudo-solid system which is affected by any external action such as variation of pressure, temperature or humidity.

The main differences between a conventional cathodic protection installation and reinforced concrete may be summarized as follows:

- * the pore fluid which constitutes the effective electrolyte is highly alkaline and is discontinuously distributed along the rebar through a rigid concrete matrix of low diffusivity to water and oxygen.

- * In conventional cathodic protection applications, the electrolyte being sea water, ground water or soil is usually near neutral (PH 6-8) and is semi-infinite, making it possible for the auxiliary anode to be located remote from the structure. In reinforced concrete structures the highly alkaline electrolyte has finite boundaries, and is neither immersed nor buried. This makes it imperative that the auxiliary anode be applied and distributed over the surface of the structure itself, close to the steel cathode (reinforcement) to be protected.

- * Concrete has a highly variable electrical resistivity in the range of 157 ohm-cm to 157,500 ohm-cm (36). Another estimate is on the order of 10^4 ohm-cm for wet concrete and as high as 10^{11} ohm-cm for dry concrete(37). A third study(38) puts the range at $6.5-11.4 \times 10^5$ ohm-cm. Compared with an estimated resistivity of less than 2000 ohm-cm for soils and 30 ohm-cm for sea water, this makes dry concrete an effective insulator (also compare with 17×10^{-7} ohm-cm for copper and 97×10^{-7} ohm-cm for iron). However, Lewis and Copenhagen(39) have reported that in coastal atmosphere where sea salt and moisture can penetrate the concrete, resistivities as low as 100 ohm-cm have been observed. Concretes buried in moist soil are reported to have resistivities in the range of 3000 to 8000 ohm-cm(40). These data emphasize the high degree of variability of

concrete resistivity, high insular nature of dry concrete, very drastic reductions in the resistivity values of moist concrete, and the significance of the conjoint moisture and salt action in the conductance of electrical charges through the concrete matrix.

The high resistivity of dry concrete can strongly thwart the flow and distribution of cathodic current from auxiliary anode to the reinforcement network. Further, the areawise and timewise variations in the resistivity linked to the temperature and humidity fluctuations in concrete and surrounding environment can cause a highly uneven distribution of the protective current and therefore can result in inhomogeneous levels of protection. Thus reinforcement in close proximity of the anodes receives more current and is overprotected, whereas more distant reinforcement receives only a small fraction of the impressed current and remains underprotected. This would particularly pose problems of corrosion control in a structure with a two mat system, specially if the distant mat is also positioned in a highly chloride contaminated concrete (Fig 1.10).

* The nature of cathodic polarization at steel-concrete interface differs significantly from steel in water or soil.

* The established cathodic protection criteria for steel in near neutral electrolytes (seawater, groundwater and soils) cannot be applied to steel in concrete which forms a distinctly different medium of embedment.

In addition to these fundamental differences between the conventional cathodic protection installation and those applied to concrete there are several significant distinctive problems of logistics and secondary effects which are characteristic of only reinforced concrete construction.

The first such feature of importance pertains to a possible lack of electrical continuity among reinforcing steel members. In such a situation, to protect all the elements of the system the locations of the discontinuities will have to be identified, the areas of the structure to be protected will have to be configured into discrete zones and reinforcement has to be connected to the rectifiers at several locations to provide protection coverage to reinforcement in these discrete zones. In practice this could be cost prohibitive and virtually impossible in retrofitting already-cast concrete elements. Further, at the points at which current enters the bar from moist concrete electrolyte, the bar will be somewhat

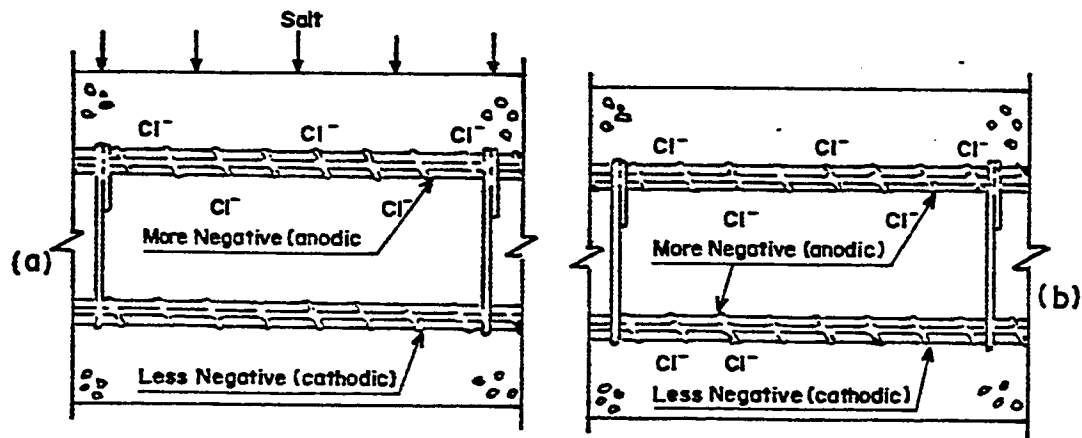


Fig. 1.10 The Corrosion Mechanism in a Two Mat Reinforcement System
 (a) Chloride Penetrates Through the Pores of Concrete
 (b) Chloride Present in Concrete with Its Constituents

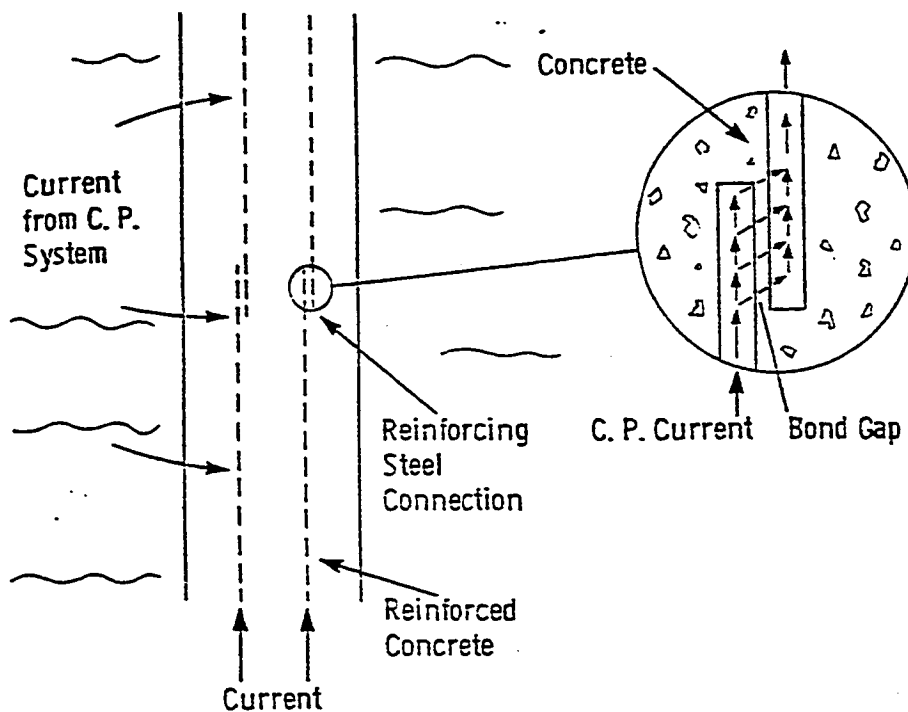


Fig. 1.11 Schematic Illustration of a Pile Showing How a Lack of Electrical Continuity Between Reinforcing Steel Bars Can Lead to Local Corrosion Damage Under Conditions of Cathodic Protection

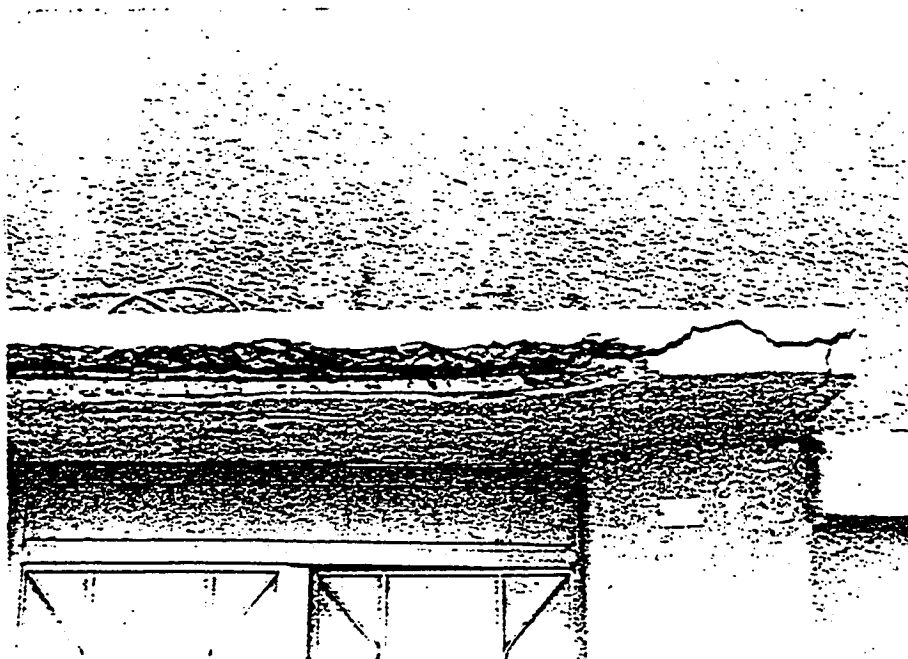


Fig. 1.12 Delamination of Concrete Due to Chloride Attack

protected. At the point at which the current leaves the bar, the steel will experience rapid corrosion at a faster rate than before the CP was applied. This situation is shown schematically in Fig. 1.11.

The **second** problem could arise in regions of a structure where concrete itself is discontinuous primarily due to delamination caused by the expansive corrosion products (Fig. 1.12).

The **third** difficulty pertains to the possibility of a reduction in steel concrete bond due to the action of cathodic polarization. The cathodic action is characterized by a generation of hydroxyl ions at the cathodic steel surface (Reaction 9) and a build up of the sodium (Na^+) and potassium (K^+) ions of the hydrated cement at the regions near the rebar due to the action of the impressed current(41). A high concomitant concentration of hydroxyl ions (OH^-) and sodium (Na^+) and potassium (K^+) cations results in the formation of calcium and potassium hydroxides (electrons being supplied by the rectifier). These hydroxides are known to attack calcium and aluminate silicates thereby "softening" the steel interface concrete causing a **degradation in bond** (42,43). The loss in bond strength was observed to be roughly proportional to the applied current upto 3400 amp-hr/sq. ft(44). This phenomenon is a matter of concern about the long term effects of cathodic protection.

Yet **another possible side effect** of the generation of hydroxyl ions due to cathodic polarization is to raise their concentration in pore fluids to a level where silica of reactive aggregates, if present in concrete, would readily react with high levels of alkalis (sodium and potassium) developed at the steel concrete interface due to the impressed current. The alkali-silica reaction is associated with severe cracking and disintegration of the concrete(45,46). Since this reaction takes

place at the cathodic steel surface, it would also have a deleterious effect on the bond strength of the reinforcement. No planned research has as yet been carried out on this aspect.

A further detrimental possibility in reinforced concrete structures is the evolution of hydrogen gas at the steel surface. If the impressed cathode potential exceeds the hydrogen over-voltage potential (-1.17 V SCE), it would cause the evolution of hydrogen as a result of the electrolysis of water(47). Much of the supplied current is then expended in the electrolysis of water rather than the protection of steel, and the hydrogen gas could possibly enter the stressed steel, specially high grade steel, causing its embrittlement and cracking(27).

One more deleterious side effect is anodic rather than cathodic in nature. The anodic reaction in the presence of chlorides (Reaction 7) would normally result in the reduction of PH at anodic sites and the generation of chloride ions. The negatively charged chloride ions in the vicinity of the anode, would also have a tendency to migrate towards the anodic site. This would generate chlorine gas in a low PH environment. Some reaction is then most likely to take place with the alkaline base of the anode. This reaction is expected to promote the detachment or delamination of the anode from the main body of the structure causing failure of the cathodic protection system.

The concrete factors discussed above can be summarized as :

- * The highly alkaline nature of concrete (PH 12.5-13.5) compared to the near neutral (PH 6-8) nature of sea water, groundwater or soil.
- * Very high and significantly variable values of electrical resistivity.
- * Extreme polarizability of steel-concrete interface.
- * Significant variations in the environment of concrete in different zones of the same structure.
- * Significant changes in the concrete environment of the same

structure with time.

* The reduction in the bond strength of the steel-concrete interface due to concrete softening, hydrogen evolution and possible alkali-silica reactions.

1.6 SPECIAL PROBLEMS OF CATHODIC PROTECTION FOR CONCRETE CONSTRUCTION IN THE GULF REGION

The aggressive climatic conditions prevailing in the Arabian Gulf have a definite influence on the cathodic protection criteria for the reinforcement in concrete structures. The microenvironment within the concrete as well as outside varies significantly in this region. High and variable chloride presence in concrete, high diurnal and seasonal variations of ambient temperature, special CP application such as protection of bottom mat by placing anode at the top, possibility of reactive aggregate usage and the possibility of bond loss associated with the protection of bottom mat by placing anode at the top are some of the distinctive features which are special only to the Gulf concrete.

The Middle East factors which markedly influence current requirements are summarized in the followings:

- (i) Very high and very variable concentrations of chlorides in the Gulf concrete
- (ii) Temperature effects which render the surface concrete very dry and could therefore significantly hamper the protection current flow from the auxiliary anode to the level of the reinforcement
- (iii) The chloride and corrosion configuration in a two mat reinforcement system in the Middle East is significantly different from that obtainable on bridge decks in the United States. In most flexural members the bottom mat of the reinforcement is several times more voluminous than the top mat. In bridge slabs the bottom mat typically comprises 75 % of the total reinforcement compared to 25 % in the top mat. In bridge decks it is usually considered necessary to protect only the upper layer of the reinforcement, as the deicing chloride salts penetrate through the top surface of the slab and accumulate predominantly around and in the vicinity of top rebars. Penetration

of chlorides, water and oxygen to the lower layer may take many years and would always be significantly less in terms of levels of concentration and attack.

The top mat-oriented chloride and corrosion profile commensurates very well with conventional anode application close to the top surface. In this position the anode is in close proximity to the corrosion prone upper layer of reinforcement which may receive about 10 times (48) more protection current than the more distant bottom reinforcement layer located in chloride free concrete.

In the Gulf conditions, where chlorides routinely enter the concrete mix constituents, chloride inclusion and not chloride penetration is the dominant chloride contamination mechanism. The chloride distribution is therefore more uniform across the depth, and the bottom mat is most likely to be as corrosion prone as the top mat. Further, it would constitute a far higher ratio of the reinforcing steel area to the concrete surface area than the top layer reinforcement. Since the **steel to concrete ratio controls the protection current density**, allowing for current drain with concrete depth, a far higher current density may be needed to fully protect the bottom mat in the Gulf conditions than in the usual bridge deck installations in the United States. This high density protection current may severely overprotect the top mat with associated deleterious secondary effects.

* The possibility of reactive aggregate usage is noticeably higher in the Gulf conditions(49,50). This raises concerns about deleterious secondary effects related to concrete disintegration and loss of bond at the steel-concrete interface even in concretes made with low -alkali cements as alkali cations (Na^+ , K^+), tend to migrate and accumulate around the reinforcement due to the impressed current.

1.7 PREVALENT CATHODIC PROTECTION CRITERIA AND THEIR APPLICATION TO REINFORCED CONCRETE STRUCTURES

Literature search indicates at least eight possible criteria for protection of steel against corrosion. However, except for two, all have been proposed in the context of protecting buried steel pipelines and tanks or for steel in sea water.

These eight criteria are:

- (1) Potential to place steel in the "immune" area of the potential-PII diagram.
- (2) Break point in E-LogI curve- constant potential

- (3) Break-point in E-LogI curve- constant current
- (4) Potential shift to -0.50 V copper sulfate electrode (CSE) for uncorroded steel in chloride contaminated concrete to **prevent onset** of corrosion and a potential shift to -0.71 V CSE to **arrest** corrosion in an actively corroding steel in chloride contaminated concrete
- (5) -0.77 V CSE "instant off" potential
- (6) -0.85 V CSE "instant off" potential
- (7) An "instant off" potential at least 300 mV more negative than the original before cathodic protection static potential
- (8) A decay of at least 100 mV measured over a 4 hour period between the "instant off" potential and the fully polarized potential.

The bases of these criteria is traced to three different approaches: firstly, **theoretical**, derived from thermodynamics and kinetic factors determined by polarization (criteria 1,2 and 3); secondly, **laboratory based studies** (criteria 4 and 5); thirdly, **field practices** (criteria 6,7 and 8).

1.7.1 Criteria Based on Theoretical Considerations

1.7.1.1 *Potentials for the Placement of steel in the "Immune" Area of the Potential-PH Diagram*

For steel in water at PH values below 10, the potential-PH diagram indicates "immunity" from corrosion at potentials below -0.62 V standard hydrogen electrode (SHE) or -0.94 V CSE. However, the concrete environment has a PH of 12.5-13.5 and hence for steel in concrete the applicable "immunity" potential is shifted to a value:

$$\begin{aligned}
 E &= -0.09-0.059 \text{ PH} \\
 &= -0.820 \text{ V SHE or } -1.13 \text{ V CSE}
 \end{aligned}$$

The shortcoming of this simplified criterion is that it does not take into account different gulf factors such as the high and variable chloride content in concrete and the concrete surface temperature. Moreover, accumulated field experience strongly negates this theoretical value on the grounds that the corresponding high levels of protective current are economically wasteful and technically undesirable due to the secondary deleterious effects of overprotection. The significantly more negative value compared to that of steel in water (PH= 7), however, indicates that the criterion for protection of steel in concrete is likely to be more stringent than for steel in seawater, groundwater or soil.

1.7.1.2 Criteria Based on E-LogI Techniques

A quantitative evaluation of corrosion kinetics in electrochemical terms is based on a determination of the anodic or cathodic corrosion current I_{corr} at the mixed potential E_{corr} . Under these conditions, for a corrosion exposure involving a low resistance electrolyte or closely located anode and cathode, the anodic and cathodic reactions are in balance, signifying that the same current flows through the anodic and cathodic regions; this makes the metal surface equipotential at E_{corr} . This equilibrium renders I_{corr} determination impossible by simple and direct methods. One indirect method of I_{corr} determination is to make the metal surface acquire a potential other than E_{corr} by applying a potential scan. This would enable current measurements to be carried out for incremental potentials and a plot of potentials(E) against current(I) on a logarithmic scale is obtained. This is called a Tafel plot(Fig. 1.13). The use of E-LogI curve was first made by Stern and Geary (51) in 1957 for developing a cathodic protection criteria for steel.

The metal surface under actual service conditions is far from being equipotential and is characterized by the presence of some areas which are more posi-

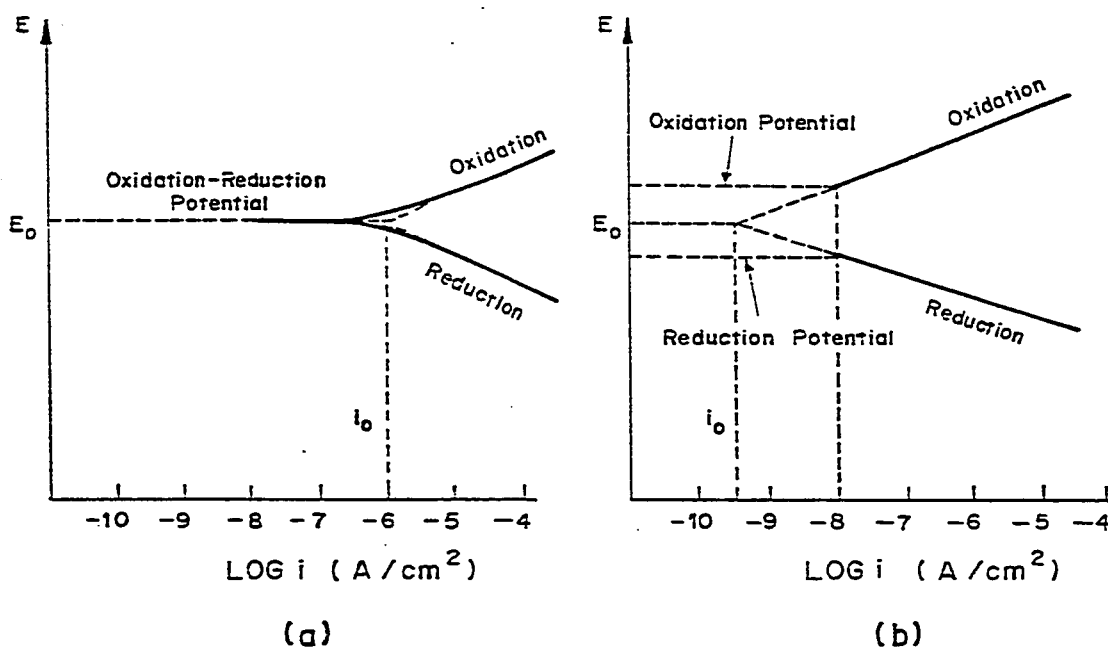


Fig. 1.13 Tafel Law- Equilibrium Potential and Exchange Currents
(a) Reversible Reaction; and (b) Irreversible Reaction

tive and others more negative than the mean potential. The impressed cathodic current will be distributed between the various small cathodic areas depending upon their relative potentials and other characteristics. The combined effect of these small cathodic areas represents the measured combined mean potential which will initially be linear. With incremental impressed current, the plot is depressed in the form of a curve as the individual areas become polarized. The process will continue until each of the areas is polarized, when the curve will again become a straight line. Complete protection will be obtainable when all the areas are polarized so that the current needed for protection will be defined by the point which causes the E-LogI plot to become a straight sloping line. The assumption is that this state represents the current or potential at which the most anodic areas are polarized or eliminated. This signifies that either the anodic area or the total anodic current is now insignificant.

From the E-LogI plot the predicted protection current (I_{CP}) or the protection potential (E_{CP}) can be adopted.

Another related technique is to plot a linear polarization curve on the basis of the polarization resistance equation

$$I_{corr} = \frac{\beta_a \beta_c}{2.3(\beta_a + \beta_c)R_p}$$

where β_a and β_c are the measured slopes of the anodic and cathodic Tafel portions of the E-LogI curves and $R_p (\frac{\delta E}{\delta I})$ is the polarization resistance, being the slope of the linear polarization curve. Knowing I_{corr} , β_a and β_c the relationship between impressed current and the potential shift can be obtained.

Application of E-LogI and linear polarization techniques to formulate

cathodic protection criteria is still in its infancy and at a developmental stage. Although these techniques are justifiably applicable to the steel concrete interface, there are two significant problems in their application to concrete structures. First, there are as yet no well formulated guidelines for running the E-LogI tests and the interpretation of the results requires considerable experimental judgement. Secondly, the technique suffers from the serious drawback of being overly sensitive to changes in the environmental conditions after the E-LogI scan has been completed and the evaluated potential imposed. For example, an increase in chloride concentrations at the steel-concrete interface after the original survey, would most likely change the E-LogI curve, rendering the initially adequate protection inadequate with time.

In spite of these possible drawbacks the E-LogI technique offers significant promise and need to be further researched. It is now a well documented fact in the concrete corrosion literature that different corrosion conditions pertain on different areas of the same structure, and they also widely vary from structure to structure. This makes it illogical to apply an across-the-board protection potential/current for different areas of the same structure or for different structures experiencing widely differing corrosion damage. Schutt(52), therefore, measured a separate E-LogI curve on each section of a structure, using current-off techniques, and applied separate protection potentials for each section, based on its E-LogI data.

Schell and Manning(53) have evaluated E-LogI and linear polarization techniques on eight experimental cathodic protection systems installed on piers of the Burlington Bay Skyway, Canada. Each covered 40 sq. meter of large rectangular reinforced concrete columns having similar reinforcing steel patterns and similar exposure conditions. They report wide variations in the corrosion currents

and protection currents predicted by F-LogI tests. The corrosion and protection currents ranged from 51 to 300 mA and 4.2 to 36.8 mA respectively, and varied quite considerably from cell to cell within each system during the same test, indicating that each cell "sees" only a localized area. Agreement between corrosion current values predicted by the E-LogI plot and those calculated from the linear polarization test data was very good.

Stratfull(54) also evaluated E-LogI technique along with several other currently prevalent cathodic protection criteria on a salvaged section of a bridge deck used as a test slab. He concludes that the E-LogI constant current technique is applicable as a cathodic protection criteria for bridge decks. However, the technique needs the use of sufficient test points to develop an accurate prediction curve. The results showed that compared to other criteria the E-LogI constant current criteria indicated many-fold less current density for protection.

A recent review of protection criteria for buried pipelines(55) is critical of the E-LogI determination criterion in applications to steel in aerated electrolytes. A distinct initiation of the straight Tafel slope (necessary for the interpretation of the data) may be masked by the controlling rate of diffusion of oxygen to the cathodic surface. Most reinforced concrete applications can be considered to constitute an aerated electrolyte.

1.7.2 Criteria Based on Laboratory Studies:

Two extensive studies(56,57) have been undertaken to evolve a cathodic protection criteria based on simulation of the pore moisture electrolyte conditions in concrete by the use of saturated calcium hydroxide solutions. In his electrochemical study carried out on saturated lime solutions containing 0.64 molar (4.4 percent) NaCl to simulate highly chloride contaminated concrete, Hausmann(56)

has made a distinction between uncorroded and corroded steel. Based on this investigation, he suggests that corrosion of uncorroded steel in a highly chloride contaminated concrete can be prevented if steel potential is shifted to a minimum value of -0.50 V (CSE). To arrest the progress of corrosion in a corroded steel, the polarization potential of the steel should be shifted to -0.71 V (CSE).

In a second cathodic protection criteria study carried out by Vrable(57) on simulated and actual concretes, several environments were used at the steel/concrete interface(no corrosion-no chloride; no corrosion-chloride; corrosion-chloride). The results show that complete protection against pitting as well as general corrosion is obtained at a steel polarization potential of -0.77 V(CSE). This investigation also specified an upper polarization limit of -1.1 V(CSE) to avoid overprotection and its possible detrimental secondary effects related with the degradation of bond between steel and concrete due to hydrogen evolution. The upper limit of -1.1 V(CSE) was based on Vrable's finding that the visible hydrogen evolution potential for steel in concrete is at -1.17 V(CSE).

Studies involving the use of simulated concrete pore solutions are clearly far removed from the complexities of real concrete environments and raise some legitimate uncertainties. However, they do bring out some broad trends which are directly relevant to cathodic protection criteria evaluation:

- * Differing chloride-corrosion conditions at the steel-concrete interface may necessitate different criteria for protection
- * Protection can be achieved at potentials much below the theoretical immunity values
- * Protection can be achieved at potentials somewhat more noble than those applicable for steel-in-soil or steel-in-seawater.

1.7.3 Criteria Based on Field Experience

1.7.3.1 *-0.85 V CSE "instant off" potential*

-0.85 V (CSE) criterion signifies that the corrosion of reinforcement would be arrested when its electrode potential is depressed by polarization from its naturally occurring static potential to a potential value of -0.85 V (CSE). Although this criterion was first suggested for underground pipeline(58) it is by far the most commonly used cathodic protection standard for reinforcement embedded in concrete(59,60,61). Further, although empirical in nature and developed primarily from field experience, it has a theoretical basis. It attempts to satisfy the cathodic protection principle that protection of a structure is achieved when all points on the structure are polarized to a potential more negative than the most anodic site on the structure(62,63).

The "instant off" potential compared to "current on" value has the advantage that it eliminates the complexity of making corrective voltage allowance for IR drop in the "current on" position. Further, the "instant Off" value directly addresses to the fact that since the change in potential for protection is achieved by polarization, it is logical to measure the adequacy of protection by the residual polarization immediately on switching-off the cathodic protection current.

Although most extensively used for reinforced concrete structures, the -0.85 V CSE criterion has been frequently criticized on the ground that it provides severe overprotection(53,54,48,64), with current densities in the range where a slow loss of bond between reinforcing steel and concrete has to be seriously considered in the long run.

Chang et al(48) have reported results of cathodic protection tests on four bridge decks. They have reported current densities in the range of 1.3-9.9

mA/sq.ft and 1.8-25.8 mA/sq.ft for polarization levels of -0.78 V (CSE) and -0.85 V (CSE) respectively. These current densities indicate that although the -0.85 V (CSE) polarization does provide protection, it is obviously excessive and a more noble potential would suffice.

Stratfull(54) carried out cathodic protection tests on the salvaged section of a bridge deck using several cathodic protection criteria. He reported 40-fold current densities with the -0.85 V (CSE) criterion compared to 100 mV shift and E-logI criteria.

Schell and Manning(53) installed eight experimental cathodic protection systems on piers of the Burlington Bay Skyway and measured the instant off potential which did not satisfy the -0.85V (CSE) criteria. They state:

"It would appear that this (-0.85 V CSE) may be an overly strict criteria for use on reinforced concrete structures".

1.7.3.2 300 mV "Instant Off" More Negative Polarization Shift Criterion

The 300 mV polarization shift criterion implies that the difference in voltage between the static (before cathodic protection) and the "instant off" potential must be at least 300 mV at all locations of a structure or the instant off potential must be 300 mV more negative than the static potential before the operation of the cathodic protection system. The 300 mV is determined by reading the halfcell potential immediately after turning the cathodic protection currents off.

The 300 mV polarization shift criterion is based upon field experience and is reported to be generally used for bare or uncoated steel pipelines buried in soil(65,66).

The 300 mV shift criterion has been evaluated by Schell and Manning(53)

for piers with corroding reinforcement. On the basis of linear polarization data they consider 300 mV shift criterion to be fairly conservative. However, they also report considerable logistic problems in maintaining this criteria due to significant variations in the static potentials of reinforcement with seasonal changes. This necessitated periodic reestablishment of the static potentials involving considerable practical difficulties. They report that "where static potentials changed significantly from season to season, the shift between instant-off potentials and a static potential measured at a different time of the year often gave a very distorted picture of system operation". Also, this static potential varies widely with chloride content of concrete (67,68). Data on the dependence of shift potential on the chloride content of concrete is still to be developed.

Stratfull(53) has also evaluated 300 mV shift criterion on a bridge deck used for cathodic protection testing. The current densities required to maintain 300 mV shift were found to be about twice the current densities required by the E-LogI and 100 mV decay criteria.

1.7.3.3 100 mV Polarization Decay Criterion

This criterion specifies a minimum of 100 mV potential decay over all representative points of the structure being protected. The potential decay is to be determined as the difference between the "instantaneous off" potential and the potential measured at the corresponding location of the structure after a period during which the cathodic protection system remains turned off. The period between "instant off" potential and the decay potential measurement is typically 4 hours.

Stratfull(54) in an evaluation of cathodic protection criteria found that the current requirement for the 100 mV decay criterion was of the same order as for E-LogI criterion.

In view of the negative aspects of the potential shift criteria based on the wide variations of original static potentials with environmental changes and the invalidity of the single potential criteria for a structure having widely varying static potentials(including passive potentials) reflecting the varying state of corrosivity, the 100 mV criterion has been tentatively supported as most viable by several studies(69,70).

The four hour decay period has been criticized by Kendell and Pit-house(71) on the basis of observations that (i) at a given current density the time required for full depolarization shift to occur becomes progressively longer with increased system operation and, (ii) operation at higher current densities results in a similar trend. They suggest depolarization testing time to be increased to 24 hours in order to correctly assess the status of any cathodic protection system.

1.8 UNRESOLVED PROBLEMS

The current practice in terms of criteria for the cathodic protection of steel in concrete is entirely based on the past experience with the protection of steel in soil or in seawater. In principle, protection current requirements for reinforcing steel in concrete would be controlled by the following factors: (i) extent and configuration of the reinforcing steel in concrete, (ii) factors affecting corrosion rate, which mainly include chloride concentration at steel-concrete interface, concrete quality, extent of concrete cover and environmental aspects. From the standpoint of these governing considerations, the environment of reinforcing steel in chloride-contaminated concrete is sufficiently different from that of soil or sea-

water. Some of the conditions prevailing in the Middle East with respect to concrete construction significantly exacerbate this differential. Such a position necessitates a reevaluation of the conventional cathodic protection criteria.

The review of the prevalent cathodic protection criteria taken together indicate three trends:

- * Firstly, there is no single criterion which is widely accepted by practitioners. The most commonly used criterion of -0.85 V (CSE) "instant off" potential has by now been widely documented for providing overprotection.

- * Secondly, the criteria currently being applied to reinforced concrete structures were primarily formulated for an entirely different environment of buried steel pipelines and are empirical in nature developed on the basis of field experience.

- * Thirdly, each criterion suffers from one or more significant deficiencies. The "immunity", -0.85 V (CSE), -0.77 V (CSE) criteria are widely documented for providing overprotection; the E-LogI criterion, apart from lack of technical development and standardization, has been shown to give considerable variations within the same cathodic protection system; the 300 mV polarization shift criterion suffers from drastic variations in the static base potential; and the 100 mV decay criterion incorporates uncertainties in depolarization as functions of time and current density.

It is reported that the current requirement for satisfying various CP criteria differs widely (54,72,73,74). The best CP criterion will be the one that can be satisfied with least amount of current supply. A criteria evaluation study is needed which may suggest a criterion that corresponds to a minimum current density at the steel surface. Also, the influence of the current density and the polarization period on the depolarization potential, full depolarization time, the instant off potential and the decay potential has to be resolved.

In the Gulf conditions, where chlorides routinely enter the concrete through mix constituents, chloride inclusion and not chloride penetration is the dominant chloride contamination mechanism. The prevalent CP criteria were formulated for controlling corrosion caused by the chloride penetrated to the steel

surface from deicing salt used at the concrete surface. The CP criteria developed for controlling the corrosion induced by chloride penetration may not be suitable for controlling corrosion caused by chlorides originally present in the mix constituents. Presence of significantly higher chloride in concrete and also the presence of chloride gradient within the same concrete are the unique features for Gulf concrete only. Such a situation necessitates the establishment of CP criteria by incorporating the influence of chloride content and chloride gradient.

High diurnal and seasonal variations of temperature is a significant feature of Gulf environment. At a high temperature condition the corrosion rate of steel in concrete and electromigration of ions at the cathodic site may be significantly different than those at cold weather regime. The prevalent CP criteria were formulated mainly for cold weather regime typical of United States and may not be suitable for controlling corrosion of steel in concrete exposed to a very high temperature condition present in the Gulf region. A study has to be carried out which will incorporate the effect of high temperature on CP criteria.

In the Gulf region, the chloride profiles and the corrosion vulnerability of reinforcement in a two mat reinforcement system is significantly different from that obtainable on bridge decks in the United States. In the U.S., it is usually considered necessary to protect only the upper layer of the reinforcement of a bridge deck, as the deicing chloride salts penetrate through the top surface of the slab and accumulate predominantly around and in the vicinity of top rebars. The top mat-oriented chloride and corrosion profile commensurates very well with conventional anode application close to the top surface. In the Gulf conditions, chlorides routinely enter the concrete through mix constituents. This makes the chloride distribution uniform across the depth and the bottom mat is most likely to be as corrosion prone as the top mat. In this situation, protecting the bottom

mat by placing anode at the top of the slab near the top reinforcement will expose the top mat reinforcement to a significantly higher current density than required for adequate protection. A study has to be carried out which can identify the **degree of overprotection** and its consequences **for the top mat** when both of the top and bottom mat reinforcements are protected using anode at the top surface of the concrete section.

As discussed in the previous paragraph, a significantly higher current density will be encountered in the top mat while fully protecting the bottom mat in the Gulf conditions. This high current density at the top mat reinforcement may cause degradation of steel-concrete bond and an enhancement of the disruption on concrete caused by alkali-silica reaction in case reactive aggregates have been used. Only a limited number of studies is available on the effect of impressed current on bond degradation. A systematic study which can relate the **bond degradation** with the **CP currents** is absent in the literature and needed further attention. Possible dependence of bond reduction and cation accumulation also has to be resolved. Possible usage of reactive aggregate in Gulf concrete raises concerns about deleterious secondary effects which may cause disruption of concrete. Only a small and incomplete study(41) has been made so far on the effect of CP current on alkali-silica reaction. A more systematic study is warranted which will relate the increased disruption caused by enhanced **alkali-silica reaction** and the **CP current**.

It is well known that initially the CP criteria for steel underground pipelines were extended for use in protecting steel in reinforced concrete structures. Although a number of experimental research papers have been published recently, study on the effect of the global environment on CP criteria for steel in concrete structures is still a scare. Unfortunately, attempt has not been made in

the past for logistical and theoretical development of such criteria. A theoretically derived criteria can adequately supplement the criteria derived through experimental study and through field experience. In deriving a CP criteria theoretically, effect of the Gulf environmental factors has to be incorporated on the electrochemical equation from which CP concept can be adopted.

The bond reduction happens possibly due to cation accumulation at the steel concrete interface. No theoretical attempt has been made to correlate the cation accumulation at steel concrete interface with the CP current density and activation period.

CHAPTER 2

PROBLEM FORMULATION, OBJECTIVES AND THE RESEARCH PROGRAM

2.1 PROBLEM FORMULATION FOR THE PROPOSED STUDY

The existing CP criteria may be categorized as broadly based on five concepts; "current on" potential, "instant off" potential, decay potential, shift potential and the protection current or potential determined through E-LogI technique. The E-LogI technique is still in its infancy and at a developmental stage. There are as yet no well formulated guidelines for running the E-LogI tests and the interpretation of the results requires considerable experimental judgement. Also, the E-LogI technique suffers from the serious drawback of being overly sensitive to changes in the environmental conditions after the E-LogI scan has been completed and the evaluated potential imposed. The "current on" potential approach is the most widely used in practical CP installation. However, lately CP practitioners are proposing the omission of this approach due to uncertainties associated with the evaluation of potential corresponding to IR drop. The "instant off" potential approach is a preferred modification of this "current on" approach, as this eliminates potential corresponding to IR drop when current flow occurs during the "current on" phase. Because of the aforesaid well established deficiencies associated with the E-LogI technique and the "current on" potential approach, the present research program will focus on the three other concepts of "instant off", decay and shift potentials. In addition to these three concepts for cathodic protection, a fourth concept based on current density at

the steel surface will also be studied in the proposed research program. Fig. 2.1 illustrates the three CP concepts which can be used to protect reinforcing steel in concrete structures. In the research program, salient Gulf factors which have a bearing on the CP criterion will be incorporated to study the manner and extent in which instant off potential, four hour decay potential and shift potential values are influenced and affected for adequate protection. The quantitative data developed on the effect of the various relevant parameters operative in the Gulf situation on the levels of effective protection required for the corroding reinforcing steel will enable the formulation of criteria for cathodic protection in this region.

The Gulf parameters relevant to CP can be broadly categorized into two types: (a) environmental and (b) special construction features. The Gulf environment related to CP is characterized by: one, a unique climate characterized by higher ambient temperature, two, by the presence of significant chlorides in the environment and concrete and three, by secondary effects such as the possible presence of alkali-reactive aggregates. The special construction feature includes the uniform distribution of primary chlorides across the depth of concrete section which makes the bottom mat as vulnerable to corrosion as the top mat in two mat reinforced concrete slabs. These factors affect corrosion damage and corrosion control by CP in a number of ways. A potential CP criterion in this region should be evaluated and tested against the various effects produced by the aforesaid ambient and geomorphic environmental factors and by the special construction feature. Table 2.1 summarizes the special gulf parameters relevant to cathodic protection criteria for reinforcing steel in concrete. To take into account the effect of special Gulf parameters on CP criteria, the following guidelines will be followed in formulating the problem:

- (1) "Current On" Potential
- (2) "Instant Off" Potential
- (3) Shift Potential
- (4) Decay Potential

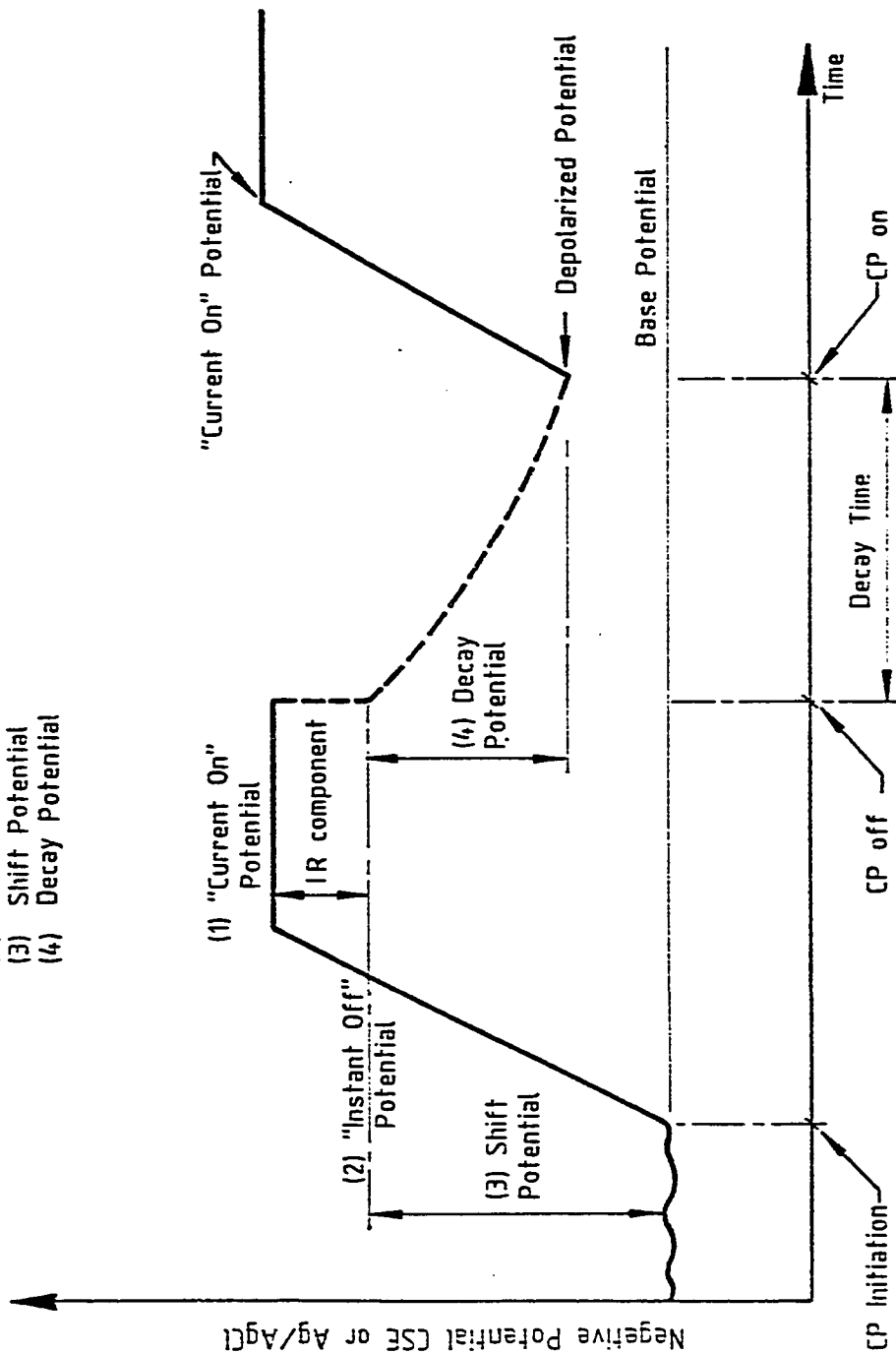
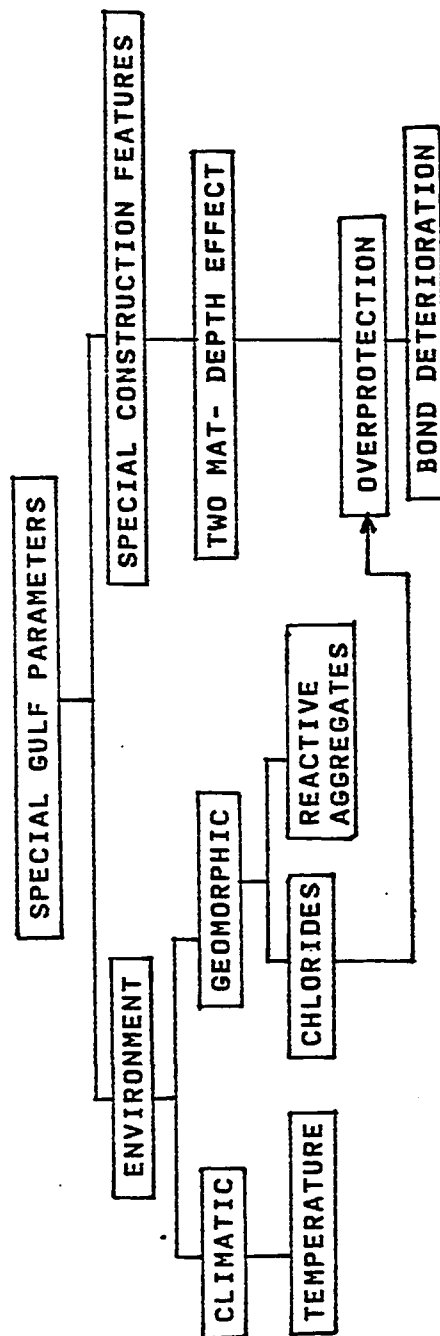


Fig. 2.1 Schematic of the Cathodic Protection Concepts for Reinforcing Steel in Concrete

Table 2.1 The Gulf Parameters Relevant to Cathodic Protection Criteria for Reinforcing Steel in Concrete Structures



- * A reasonable range of chloride contamination in Gulf concrete structures in criteria formulation study.
- * Chloride gradients within the concrete to observe the effect of an unavoidable nonuniform distribution of chlorides on CP criteria.
- * Concrete temperature upto 60°C with a daily variation simulating the typical summer months condition in the criteria establishment study.
- * A typical two mat reinforcement arrangement with lower mat also located in equally chloride contaminated concrete in the two mat-depth effect study.
- * A range of current densities and chloride contents in concrete in the bond reduction study.
- * A range of current densities in the alkali-silica reaction study.

Besides the Gulf parameters discussed above, the prevailing CP criteria need a thorough reevaluation. It is reported elsewhere that the current requirement for satisfying various CP criteria differs widely. Since a high current density at steel surface may cause increased deleterious secondary effects, the optimum CP criterion should be recommended which can be satisfied with the least amount of current density. Also, the possible dependence of the current density and polarization period on the depolarization potential, fully depolarized potential, the instant off potential and the decay potential has to be studied in the quantitative terms.

A theoretical study including the reflection of the Gulf environmental factors on CP criteria can supplement the experimental data. Since the corrosion of reinforcing steel in concrete is an electrochemical process, it should be possible to recommend a corrosion control criteria by including the effect of concrete environment on the electrochemical behavior of reinforcing steel.

2.2 OBJECTIVES

The objective of this study is to formulate various relevant considerations which influence the effective protection of corroding reinforcing steel in concrete structures in the Gulf states and to quantify these effects on cathodic protection. Specifically, the objective is to study the following aspects and to incorporate and interlink the conclusions from these components into recommendations for cathodic protection of reinforcing steel in the Gulf region.

2.2.1 Developments of Relationships Between Current Density, Polarization Period, Protection Potential and Depolarization Time

This study establish the effect of current density and the polarization period on fully depolarized potential, full depolarization time, instant off potential and the decay potential. This study will particularly clarify uncertainty of the depolarization time in the decay potential concepts.

2.2.2 Effect of Chloride Content of Concrete

Chloride study includes development of a data base on static potential as influenced by the absolute chloride content and effect of level of chloride contamination and chloride gradients on the degree of protection required.

2.2.3 Effect of Temperature

This study includes the measurements of shift in static potential, the protection potential and current requirements when the temperature is raised from the room exposure to 60°C simulating typical ambient conditions on concrete surfaces in summer months.

A study of problems related with the supply of the protection current from a commonly available source of 15 DC volt battery in the hot-dry exposure conditions has also been included in this study component.

2.2.4 Depth Effect in Two Mat Reinforcement

Depth study focuses on the degree of overprotection provided to the top mat when the bottom mat is just adequately protected by placing

the anode close to the top mat. The study will be followed by an evaluation of the effect of overprotection on the degradation of steel-concrete bond.

2.2.5 Effect of the Presence of Reactive Aggregates

This component includes a study of the degradation in concrete made with reactive aggregate caused by enhanced alkali-silica reaction due to CP current. Alkali-silica gel formation, advancing of cracking time and softening of concrete characterized by reduction in compressive strength and hardness will be monitored.

2.2.6 Bond Deterioration Due to Overprotection

This study includes the effect of overprotection of top mat which will bring about changes at the steel-concrete interface characterized by the following phenomena:

- (i) degradation of the steel concrete bond as a function of current density, chloride content and cation accumulation.
- (ii) electromigrations of anions and cations from and towards the steel-concrete interface bringing about significant changes in the chloride aggressivity and alkalinity in the vicinity of reinforcing steel.

Table 2.2 Summarizes the objectives of the study.

2.3 RESEARCH PROGRAM: THEORETICAL

A theoretical study was undertaken to find the effect of ambient temperature, humidity and chloride content of concrete on CP criteria. The Nerst equation was used to study the effect of various Gulf environmental parameters such as high ambient temperature, atmospheric humidity and chloride content of concrete on the level of protection required. In another study based on the laws of electric current flow, an attempt was made to develop a relationship between the cation accumulation and the current density.

OBJECTIVES	OVERPROTECTION :Bond Deterioration	<p>* To observe the effect of overprotection of top mat which will bring about changes at the steel-concrete interface characterized by the following phenomena:</p> <p>(i) degradation of the steel concrete bond as a function of current density, chloride content and cation accumulation.</p> <p>(ii) electromigrations of anions and cations from and towards the steel-concrete interface bringing about significant changes in the chloride aggressivity and alkalinity in the vicinity of reinforcing steel.</p>
	GEOMORPHIC FACTOR :Reactive Aggregates	<p>* To observe the degradation in concrete made with reactive aggregate caused by enhanced alkali-silica reaction due to CP current.</p> <p>* Alkali-silica gel formation, advancing of cracking time, and softening of concrete characterized by reduction in compressive strength and hardness will be monitored.</p>
	SPECIAL CONSTRUCTION FEATURES :Depth Effect	<p>* To observe the degree of overprotection provided to the top mat when the bottom mat is just adequately protected by placing the anode close to the top mat. The study will be followed by an evaluation of the effect of overprotection on the degradation of steel-concrete bond.</p>
	CLIMATIC FACTOR Temperature	<p>* To measure the shift in static potential, the protection potential and current requirements when the temperature is raised from the room exposure to 60°C simulating typical ambient conditions on concrete surfaces in summer months.</p> <p>* To observe the problems related with the supply of the protection current from a commonly available source of 15 DC volt battery in the hot-dry exposure conditions.</p>
	GEOMORPHIC FACTOR :Chlorides	<p>*To develop a data base on static potential as influenced by the absolute chloride content</p> <p>* To observe the effect of level of chloride contamination and chloride gradients on the degree of protection required.</p>
	PREVAILING CP CONCEPTS	<p>* To establish the effect of current density and the polarization period on fully depolarized potential, full depolarization time, instant off potential and the decay potential.</p> <p>* To clarify uncertainty of the depolarization time in the decay potential concepts.</p>

Table 2.2 Summarized Objectives of the Study

2.4 RESEARCH PROGRAM: EXPERIMENTAL

The experimental program constitute the major part of the proposed research. A comprehensive experimental research program was carried out in an attempt to achieve the objectives outlined in article 2.2.

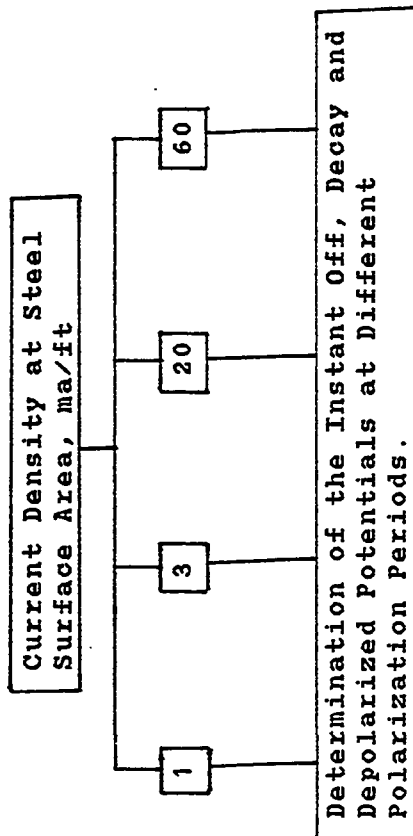
The experimental program is divided broadly in six parts:

2.4.1 Developments of Relationships Between Current Density, Polarization Period, Protection Potential and Depolarization Time

The current densities needed to satisfy prevailing CP concepts were observed. The current density was varied from 0.5 to 15 ma/sq. ft at an interval of 0.5 ma/sq. ft. and at each level of the current density, the instant off, decay and shift potentials were observed.

The effect of current density and polarization period on fully depolarized potential, full depolarization time, instant off potential and the decay potential was also observed in this segment of study. Constant current densities of 1, 3, 20 and 60 ma/sq ft were maintained at the steel surface and the depolarization tests were conducted at different polarization time. The test program for this study is shown in Table 2.3.

Table 2.3 Test Program for Relationship Between Potentials of Steel and Polarization Period



2.4.2 Effect of Chloride Content of Concrete

Chloride contaminations ranging from 0 to 32 lbs/cu yd and chloride gradients ranging from 8 for low chloride bearing concrete to 2 for high chloride bearing concrete were used in the test program to find the effect of chloride contents and chloride gradients on protection potentials and current requirements. The chloride gradient in a concrete was created by using a relatively higher chloride bearing macrocell in concrete and thereafter connecting the macrocell steel and the main steel through an external resistor.

Table 2.4 shows the schematic of the test program for determining the effect of chloride content on static potential of steel. Table 2.5 shows the test program for determining the effect of chloride contents and chloride gradients on CP criteria.

2.4.3 Effect of Temperature

In typical summer months, an ambient temperature of 40°C is common in Gulf countries(75). A temperature of 60°C which included radiation effect, with diurnal variation was simulated in a specially designed temperature chamber. The chloride contents of the specimens were 8 and 32 lbs/cu yds and the chloride gradients were 1.5 and 2.0. The test program for incorporating the temperature effect on CP requirement is shown in Table 2.6.

Specimens were also kept outdoor to study possible difficulties encountered when CP is applied with a commonly available rectifier supply of 15 V DC. The concrete specimens were exposed at outdoors in a period when a hot dry environment prevails in the Eastern region of Saudi Arabia. Electrical resistivity of concrete, moisture content of concrete and the current passing to the steel were recorded at

Table 2.4 Test Program for Determining the Effect of Chloride Content of Concrete on Static Potentials

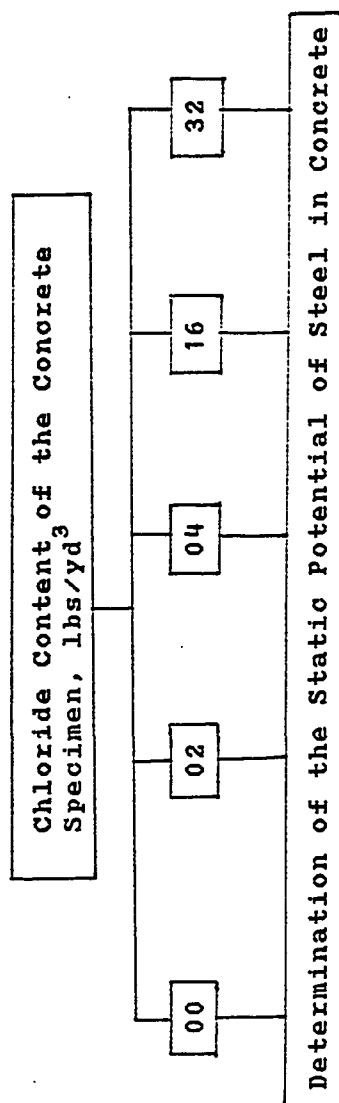
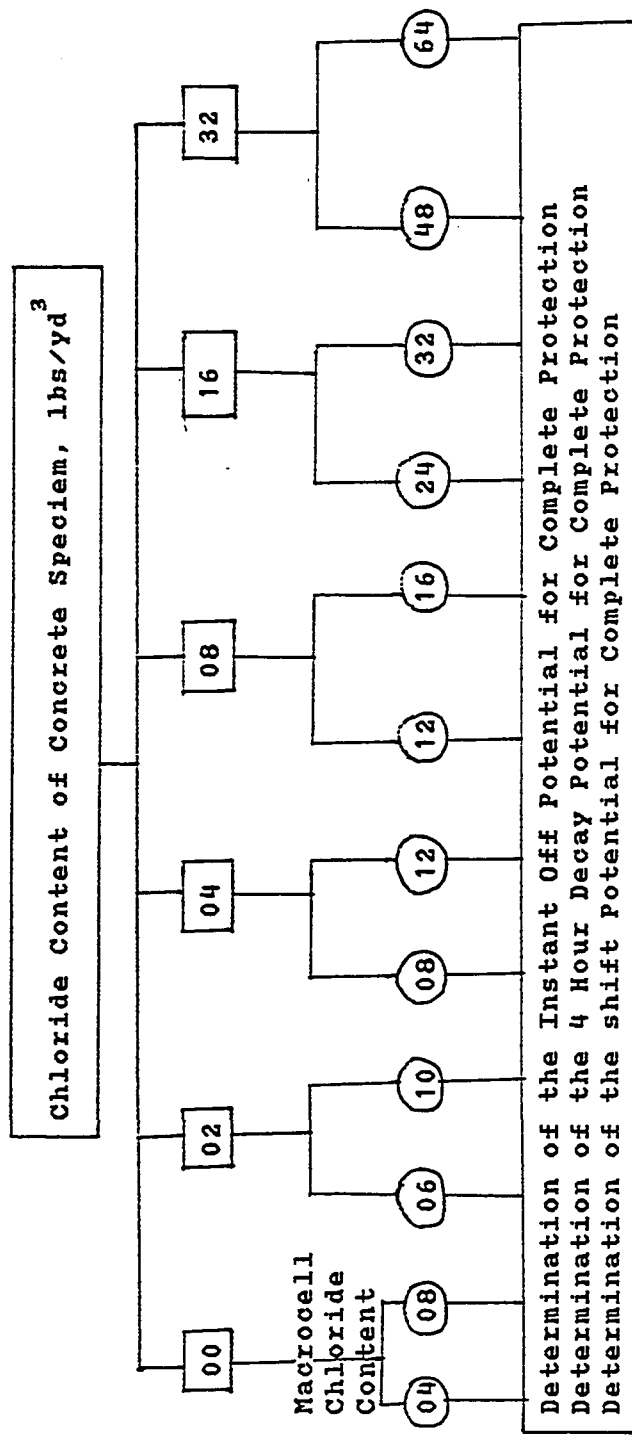


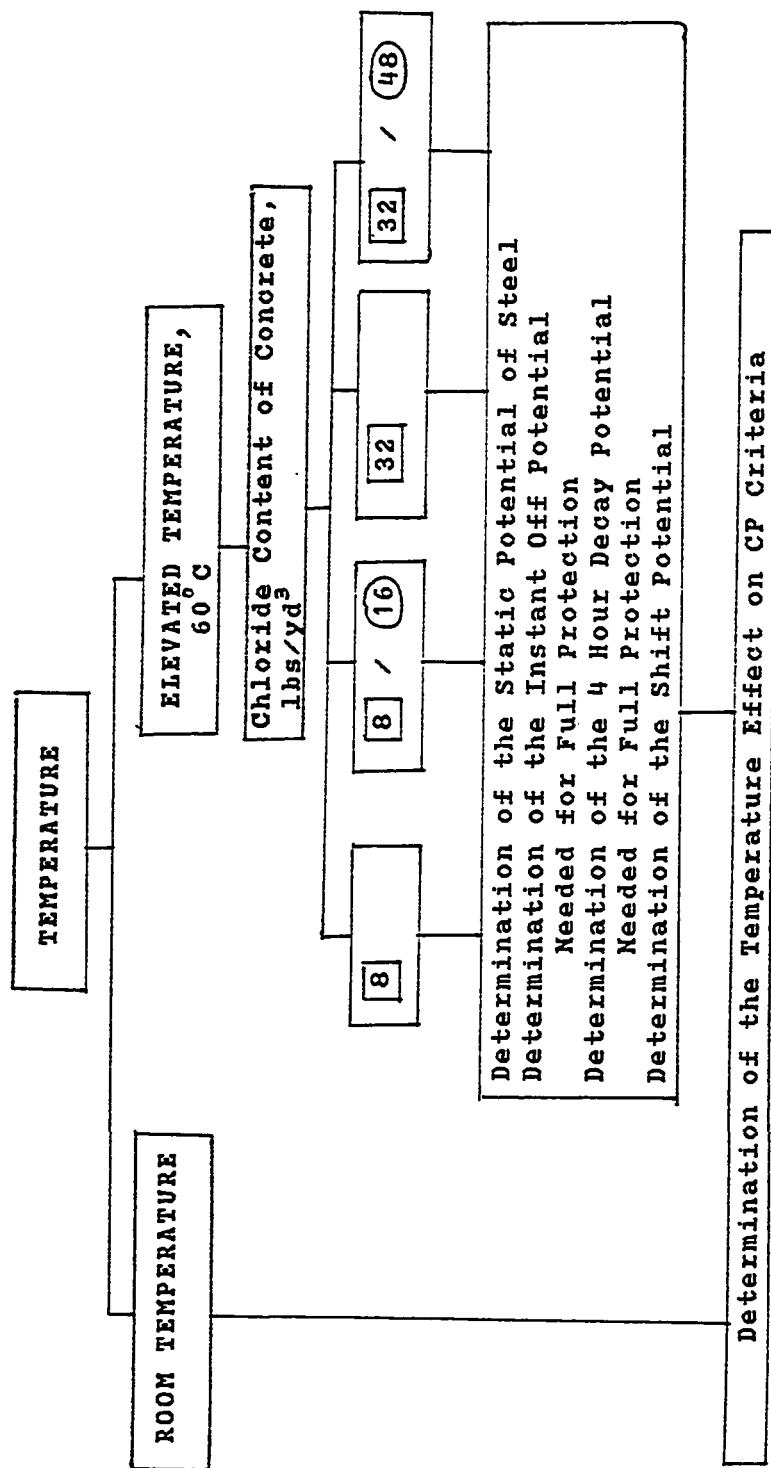
Table 2.5 Test Program for Determining the Effect of Chloride Content of Concrete and the Chloride Gradient on CP Criteria



☐ Chloride Content of the Specimen, lbs/yd³ of Concrete
 ○ Chloride Content of the Macrocell, lbs/yd³ of Concrete

○ Chloride Content of the Macrocell, lbs/yd³ of Concrete

Table 2.6 Test Program for Determining the Effect of Temperature on Cathodic Protection Criteria



☐ Chloride Content of the Specimen

☐ Chloride Content of the Macrocell

different exposure time.

2.4.4 Depth Effect in Two Mat

Both of the top and bottom mats of the two mat reinforcement slab were protected using anode at the top of the slab. The degree of overprotection of the top mat was observed when both the top and bottom mats receive CP currents from the same anode source placed near the top reinforcement. The chloride content of concrete was 32 lbs/cu. yd and the chloride gradients were 1.5 and 3. The ratio of the top and bottom mat reinforcements was 20 percent, a typical value in ordinary reinforced concrete slab in the Gulf region. The distance between the top and bottom mat was 3 inch and the distance between the anode and top mats was 1.5 inch.

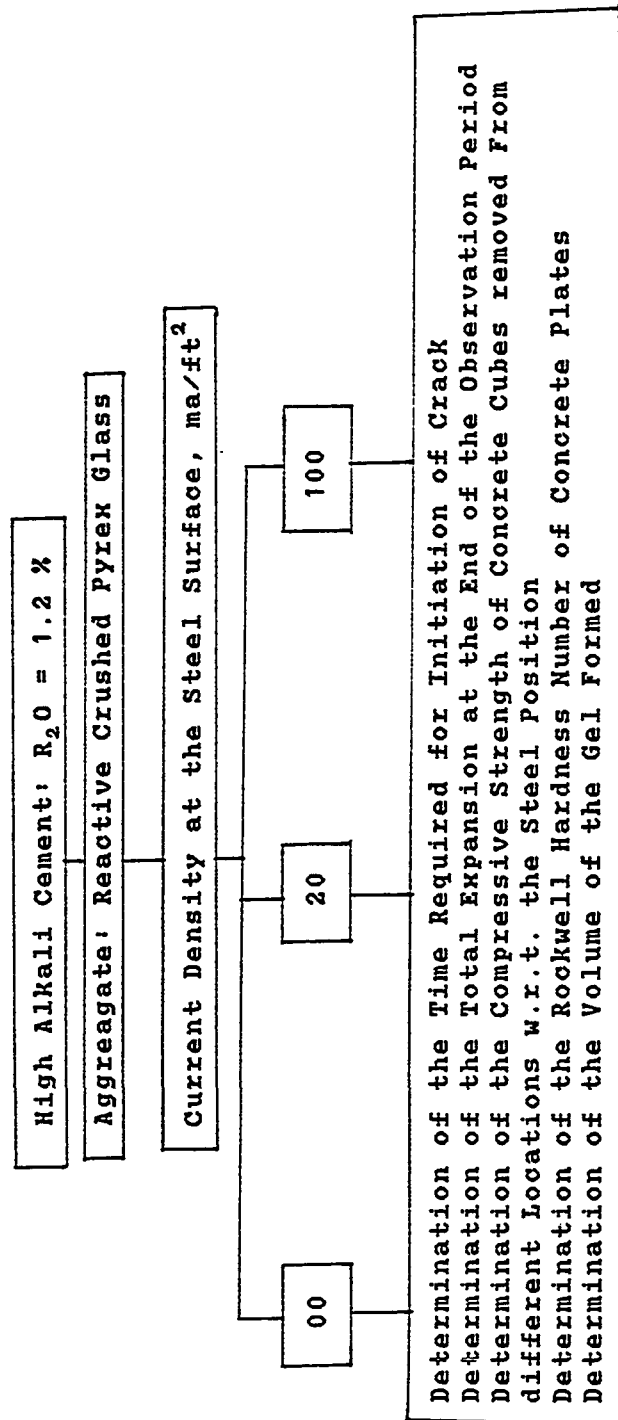
2.4.5 Effect of the Presence of Reactive Aggregate

Mortar prisms made from reactive crushed pyrex glass and 1.2 percent alkali containing cement were subjected to 20 and 100 ma/sq ft currents for a period of 80 days. The observations include time required for initiation of crack, total expansion at the end of observation period, compressive strength and hardness of mortar removed from steel-concrete interface and the volume of alkali-silica gel. The research program would evaluate the enhancement of disintegration of steel encasing concrete as a result of high alkali-silica reaction at the steel-concrete interface caused by high impressed CP current. Test program for alkali-silica reaction study is shown in Table 2.7.

2.4.6 Bond Deterioration Due to Overprotection

Constant current densities of 3, 10, 20 and 50 ma/sq ft were maintained at steel surface for 14 months polarization period. At the end of polarization, pull out

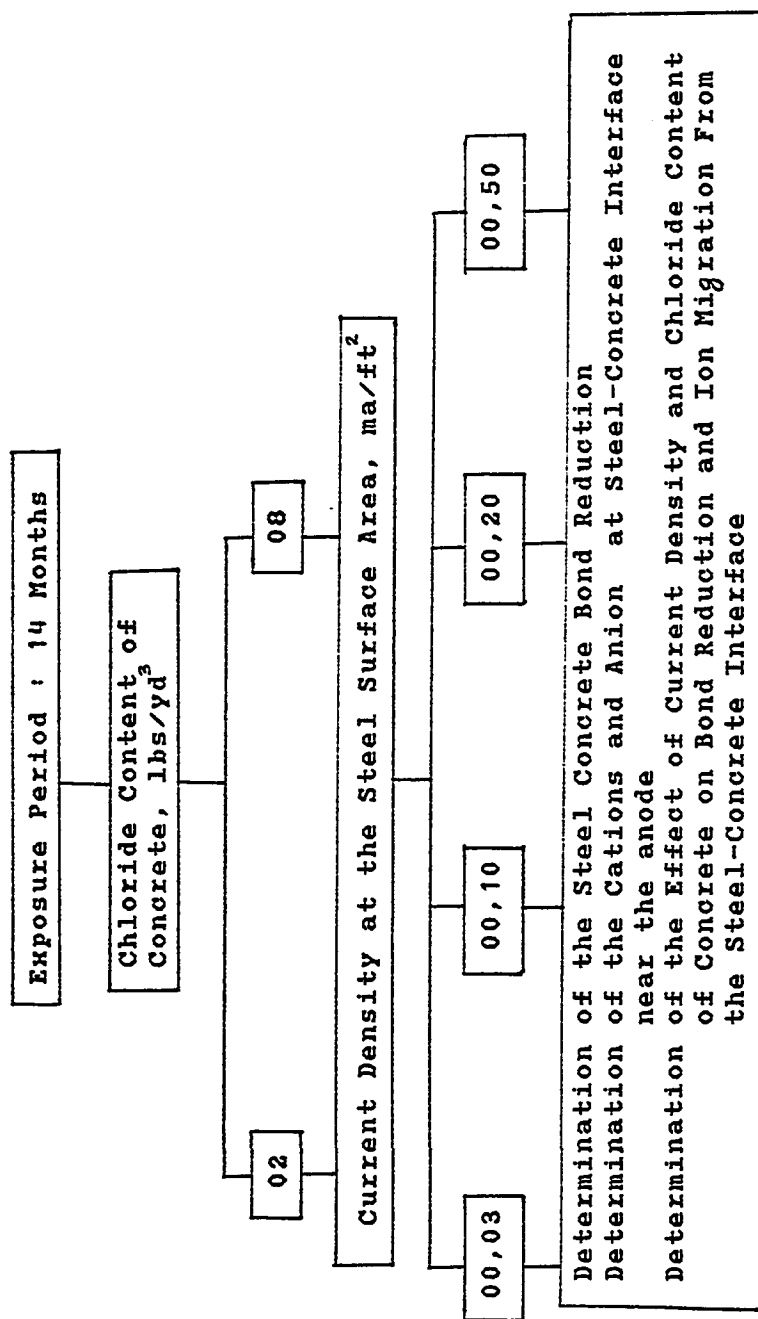
Table 2.7 Test Program for Geomorphio Factor: The Presence of Reactive Aggregates and the Increased Alkali-silica Reactivity Due to Cathodic Protection Current



tests were carried out for bond strength determination and the powder concrete samples were analyzed chemically for determination of the migration characteristics of cations and anions Chloride contaminations of 2 and 8 lbs/cu yd were used in the test specimens. This research program would evaluate the **reduction in the bond** between steel and concrete due to **concrete softening** under the action of high impressed currents, which may possibly be required for lower mat protection in two mat reinforced concrete slab as well as high chloride gradients prevailing in the Gulf region.

Test program for bond study is shown in Table 2.8.

Table 2.8 Determination of the Effect of CP Current Density on the Steel-Concrete Bond



CHAPTER 3

THEORETICAL STUDY

3.1 THEORETICAL STUDY RELATED TO THE EFFECT OF ENVIRONMENTAL PARAMETERS ON CATHODIC PROTECTION CRITERIA

3.1.1 General

This theoretical study is based on the second principle of electrochemical thermodynamics. Since the corrosion of reinforcing steel in concrete is an electrochemical process, mitigation of corrosion is possible by observing the effect of concrete environment on the electrochemical behavior of steel inside concrete. The second principle of electrochemical thermodynamics states that

$$(E-E_o) (i) \geq 0 \quad (1)$$

where, E = reaction potential(electrode potential)

i = reaction current,

E_o = equilibrium potential.

If the reaction potential E is plotted as the ordinate on a graph, with highest potential on the top and the flow of the reaction current i as the abscissa(increasing current to the right), then the influence of this electrode potential on the rate of any electrochemical reaction is represented by a curve ascending from

left to right. This curve is a polarization curve(76). Fig. 3.1 shows such a curve for a single electrochemical reaction. The polarization curve for mild steel in a corrosive environment is shown in Fig. 3.2. Because of the fact that the corrosion reaction (oxidation of metal at the anodic site) is always accompanied by a reduction reaction (evolution of hydrogen at the cathode), the polarization curve for mild steel in a corrosive environment will have two branches as shown in Fig. 3.2. In this Fig., point C represents the equilibrium potential for the corrosion reaction (anodic reaction c) and point A represents equilibrium potential of the cathodic reaction (reaction a) as shown in the Figure. With the change in temperature, humidity, degree of wetness, chloride content, and other environmental factors, the polarization curve also changes. The polarization curve passes through the ordinate (E axis of E-i curve) at E_o , which represents the equilibrium potential(in Fig. 3.2, point C represents the equilibrium potential for anodic reaction). This equilibrium potential changes with temperature, humidity and extent of corrosion. The cathodic protection criteria which are selected after giving proper emphasis on the value of E_o as well as on the polarization curve , are therefore, affected by the environment existing in the Gulf region.

According to Pourbaix(76), when the potential, E, of an electrode is greater (more positive) than the equilibrium potential, E_o , of a reaction, the reaction may only proceed on this electrode in the direction of an oxidation. On the other-hand, when the potential, E, of an electrode is less (more negative) than the equilibrium potential, E_o , the reaction may only proceed on this electrode in the direction of a reduction. In the cathodic protection technique, the electrode potential of steel is depressed to the region of immunity (no corrosion) by supplying continuous electric current from an external source. Cathodic protection

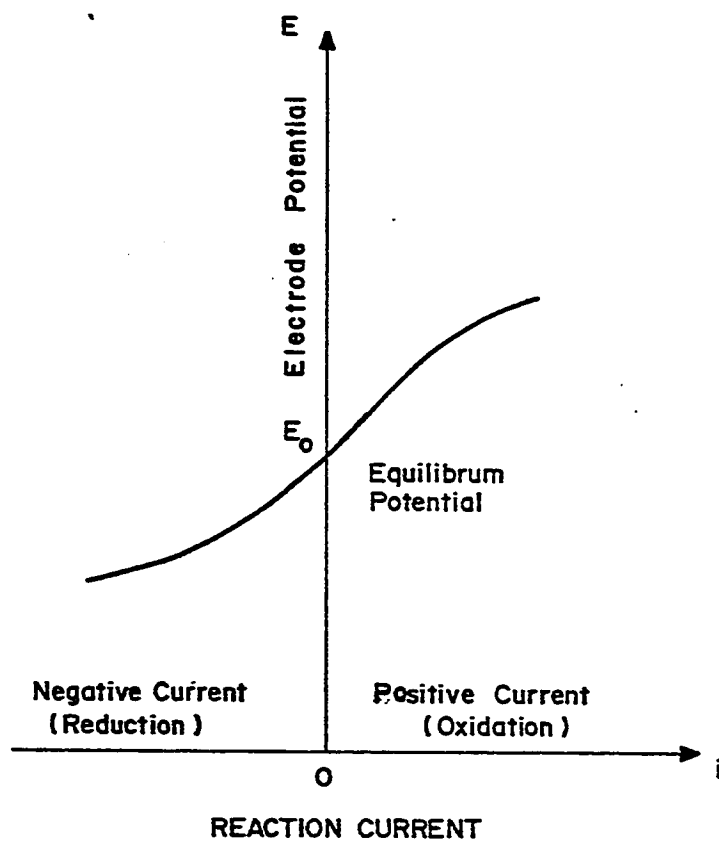


Fig. 3.1 Polarization Curve for an Electrochemical Reaction

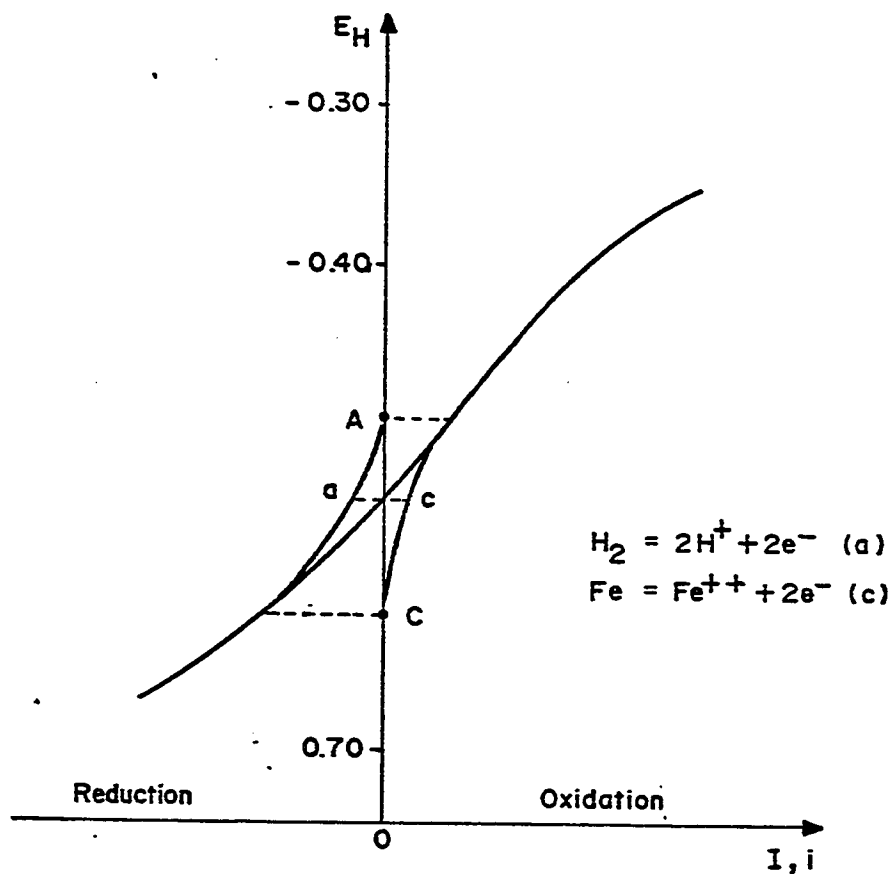


Fig. 3.2 Interpretation of an Electrolytic Current-Potential Polarization Curve. The Case of Iron in Oxygen-free 0.1 M Solution of $NaHCO_3$ (PH=8.4)

will be complete or partial depending on whether or not the protection potential (a value below E_o) is reached. Given that the domain of stability of metallic iron is situated completely below the region of stability of water, it should be noted that the state of cathodic protection by immunity is only maintained by a permanent consumption of energy (electric current) which causes evolution of hydrogen on the surface of the protected steel.

3.1.2 Concrete Environment in the Arabian Gulf Region

In a study(75), it was found that the temperature of concrete in the gulf region varies from 10°C (50°F) in winter to 80°C (176°F) in summer(50°C / 122°F ambient temperature in addition to 30°C / 86°F allowance for direct solar radiation effect). Humidity also varies from a very low value of 5 percent to a very high value of 100 percent. A very high variation in chloride content of concrete has also been noticed in this region(16). A chloride content of as high as 38 kg/cubic meter (110 lb/ yd³) of concrete was found in a concrete sample taken from the Eastern region of Saudi Arabia.

3.1.3 The Equilibrium Potential

The relationship between equilibrium potential and other parameters of an electrochemical reaction is given by:

$$E_o = \sum \frac{v \mu^o}{23060n} + 4.575 \frac{T}{23060n} \sum v \text{Log}\{M\} \quad (2)$$

Where the coefficients v are positive or negative if the reacting elements are on the right side or on the left side of the equilibrium equation.

μ^o = standard chemical potential of the constituent under consideration

n = stoichiometric coefficient of the electrons involved.

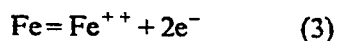
T = absolute temperature

M = activity of the constituent if it is in dissolved state

or,

= fugacity(partial pressure) of the constituent if it is under gaseous state.

For the corrosion of steel, the electrochemical reaction is



For this electrochemical reaction, the expression for E_o will reduce to

$$\begin{aligned} E_o &= \frac{(1)(\mu_{\text{Fe}}^o) + (-1)(\mu_{\text{Fe}^{++}}^o)}{(23,060)(-2)} + \frac{4.575 T}{(23,060)(-2)} (-\text{Log} (\text{Fe}^{++})) \\ &= \frac{(1)(0) + (-1)(-20300)}{(23060)(-2)} + 9.92 * 10^{-5} T \text{Log Fe}^{++} \\ &= -0.441 + 9.92 * 10^{-5} T \text{Log Fe}^{++} \quad (4) \end{aligned}$$

The above equation will provide E_o values in volts, measured with respect to SHE.

3.1.4 Theoretical Results

3.1.4.1 Effect of Temperature

Assuming that iron content of a solution is very low, e.g., 10^{-6} gm-ion Fe/liter or 0.056 mg/liter(this corresponds to a very insignificant corrosion rate), the expression for the equilibrium potential will be reduced to

$$E_o = -0.441 - 5.952 * 10^{-4} T$$

The E_o values for temperature ranges existing in the gulf are calculated and shown in Table 3.1. Fig 3.3 shows the E_o values as affected by the temperature and the concentration of ferrous ion in concrete.

Table 3.1 shows that for a particular ferrous ion content, the change in temperature does not cause an appreciable change in equilibrium potential value. The decrease of E_o value for a change in concrete temperature from 10°C to 80°C is only 0.033 V SHE. However, as shown in Fig. 3.3, this variation of E_o value is noticeable in the case of the variation of the iron ion concentration. As an example, at a constant concrete temperature of 50°C , the E_o values are -0.635 and -0.506 at a concentration of 10^{-6} gm-ion/liter and 10^{-2} gm-ion/liter, respectively.

3.1.4.2 Effect of Humidity

The arabian gulf environment has a relative humidity value ranging from almost 100 percent in a typical summer day to almost zero percent in a typical winter day. At the time of high humidity, concrete voids may be able to attract sufficient water to become saturated, whereas concrete voids may have very little amount of water at a time of low humidity. It is known that the presence of moisture is essential for corrosion reaction to proceed; this implies that high humidity corresponds to the availability of a large amount of Fe^{++} and a low humidity corresponds to a small amount of Fe^{++} . According to Pourbaix, the equilibrium potential of the anodic reaction may change as corrosion proceeds due to its dependence on activity (Fe^{++}) of the reacting species, Fe. This dependence of E_o on the concentration of Fe^{++} is clearly shown in equation 4. Fig.

Table 5.1

E_0 Value for Different Temperatures at a Very Low
Iron Ion Concentration (0.056 mg/liter of Solution)

Temperature, °C	Temperature, °K	E (V), SHE
10	283	-0.609
15	288	-0.612
20	293	-0.615
25	298	-0.618
30	303	-0.621
35	308	-0.624
40	313	-0.627
45	318	-0.630
50	323	-0.633
60	333	-0.639
70	343	-0.645
80	353	-0.651

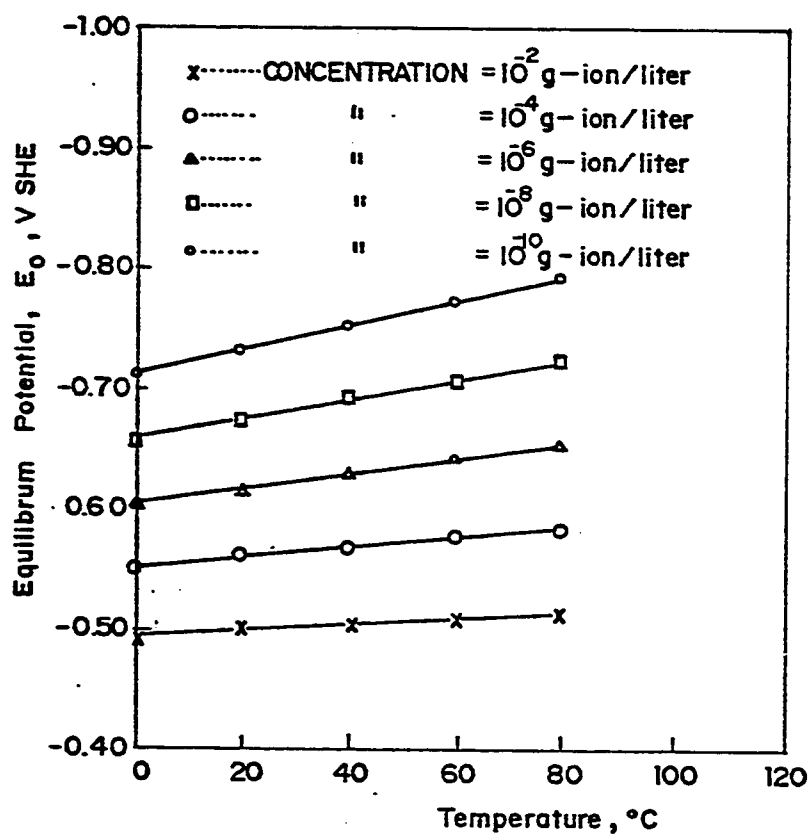
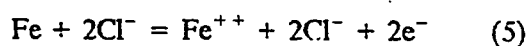


Fig. 3.3 Variation of E_0 With Temperature and Fe^{++} Concentration

3.3 also illustrates the effect of the concentration of Fe^{++} on E_o value. Thus, at a very high humidity regime(high Fe^{++} presence), the E_o value will be higher and at a very low humidity regime, E_o value will be relatively lower. However, it should be noted here that the concentration of ferrous ion will be strictly controlled by the PH of the concrete and the kinetics of $\text{Fe}(\text{OH})_2$ deposition.

3.1.4.3 Influence of Chloride

The corrosion reaction in the presence of chloride ion is



As 2 moles of chloride ions are present on both sides of the above electrochemical reaction, the equation for equilibrium potential E_o for this reaction will be similar to that for reaction 3. Actually, the chloride ions in equation 5 are self generating; once the corrosion reaction starts, the chloride ions produced on the right side of equation 5 will be used on the left side to perpetuate the corrosion reaction. The equilibrium potential value will be unaffected by the amount of chloride ions present in concrete. This theoretical fact has been supported by a related experimental finding as reproduced in Figs. 3.4a, 3.4b and 3.4c (76). These Figures illustrate the current-potential curves in the presence of oxygen free 0.1 M NaHCO_3 solution with varying NaCl concentrations. Examination of these three curves show that:

(1) The addition of chloride does not modify the lower branch of the current potential curve which corresponds to the general corrosion in nonoxidizing or feebly oxidizing media. All these three curves have the same ordinates at C which represent E_o for the anodic reaction (corrosion reaction).

(2) The presence of chloride has the most significant effect on the stability of

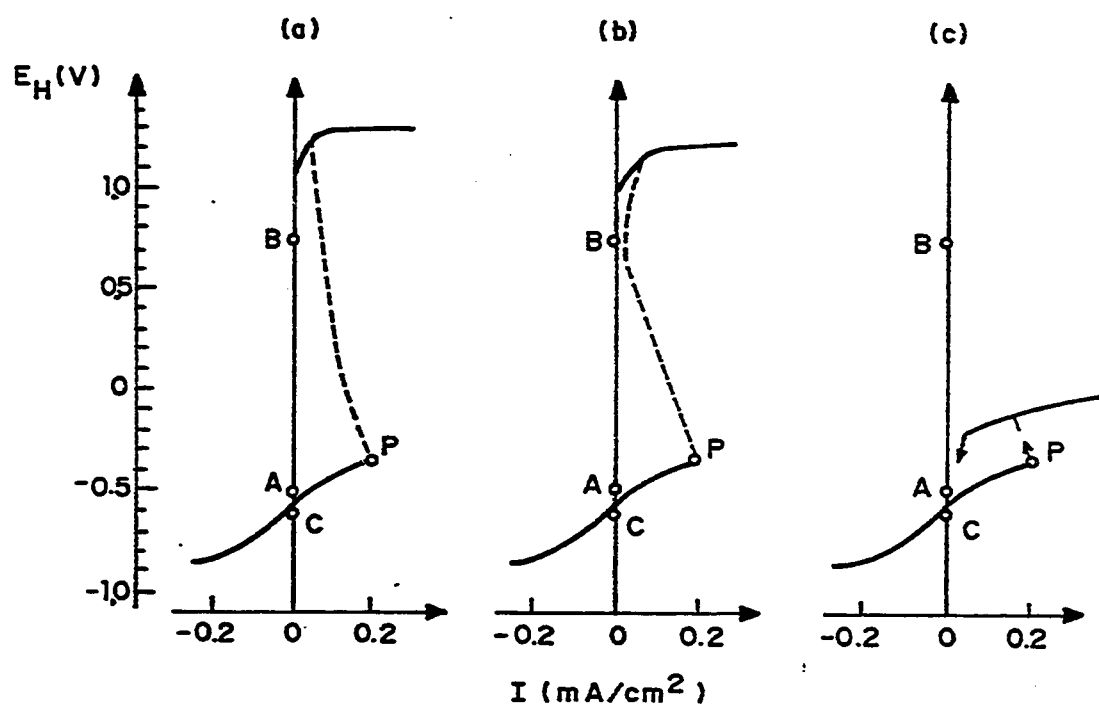


Fig. 3.4 Influence of Chloride on the Behavior of Mild Steel in 0.1 mol/L Solution of NaHCO_3 (PH=8.4), in Absence of Oxidant
 (a) No NaCl (b) 0.001 mol/L NaCl (c) 0.01 mol/L NaCl

the passive film. In Fig. 3.4a, there is a smooth transition to the higher potential. In Fig. 3.4b, there is some instability in approaching the upper portion of the curve. This instability results from the fact that chloride at the higher potential prevents the film from being perfectly protective. At high chloride concentrations (Fig. 3.4c), the potential stabilizes at a relatively lower value and leads to pitting.

The above explanation shows that the equilibrium potential, E_o , is unaffected by chloride ion concentration. However, the modification of the upper portion of the polarization curve due to the increase of chloride ions in concrete poses concern. Fig. 3.4c, which corresponds to presence of high concentration of chloride ions, shows that a small increase of the potential from the equilibrium potential value causes a severe corrosion condition (pitting). Thus, for proper protection against corrosion in case of high chloride concrete, it is safer to lower the potential of the steel by a higher value from the equilibrium potential.

3.1.4.4 Cathodic Protection (CP) Criteria

A number of studies have been made on the CP criteria (29,69,77). Most of the criteria are based on the fact that the potential of the steel is to be lowered to reduce the possibility of corrosion. The equilibrium potential can be used as the bench mark from which the potential is to be lowered. But it is not feasible to lower the steel potential by a large value; because this overprotection of steel may cause a significant reduction in bond between steel and concrete due to accumulation of cations near the steel(26). These unwanted phenomena restrict the lowering of the potential to a value which will protect the steel against corrosion and would not warrant the secondary problems resulting from overprotec-

tion.

3.1.5 Discussion

Since the equilibrium potential depends on the degree of corrosion of the steel in the concrete structure and, also, on the ambient temperature, these factors must have a reflection on the CP potential. The effect of temperature on E_o is insignificant; so it will have very little effect on the CP criteria. The temperature does not significantly require further lowering of the protection potential. An extra lowering by 33 mV may be sufficient for the range of temperature existing in Gulf region.

As shown in Fig. 3.3, since E_o value increases (absolute E_o decreases) with the extent of corrosion, the reinforced concrete in low humidity environment (low corrosion, low Fe^{++}) needs a lower value of CP potential to keep the reinforcement free of corrosion. In case of severe corrosion condition (corresponding to high humidity environment), the CP potential needs to be relatively at a higher value (low absolute E_o value) to stop corrosion at the current rate. However, to stop corrosion completely, the CP potential has to be lowered significantly. Thus, the selected CP potential of steel depends on the level of corrosion adopted as an insignificant value. If a concentration of 10^{-6} gm-ion Fe/liter of solution has been selected as a sufficiently insignificant corrosion value, then a CP potential value lower than -0.60 to -0.65 volt with respect to SHE can be chosen safely.

Chloride content does not affect the equilibrium potential and the protection potential. However, the presence of chloride ion has the most significant effect on the stability of the passive film; a small increase (more positive) of the steel potential from the equilibrium potential value causes a severe corrosion

conditions. High chloride content induces the possibility of pitting in case of improper protection necessitating a slightly lower value for high chloride concretes to be recommended as a further factor of safety against possible corrosion. A potential value more negative than -0.640 V SHE adequately protects the steel against corrosion irrespective of humidity, temperature and chloride content existing in Gulf concrete.

3.2 THEORETICAL STUDY FOR CATION ACCUMULATION

3.2.1 Origin of Cations in Concrete

Cement which is the most important ingredient of concrete contains Na_2O and K_2O , from its raw materials. Generally $\text{Na}_2\text{O} + \text{K}_2\text{O}$ is around 0.5 to 1.3 % by weight of ordinary portland cement(35). A portion of Na_2O and K_2O , is usually combined with the clinker and stays with the clinker minerals. The rest remain in the form of NaOH and KOH in concrete. In aqueous solution, cement alkalis may stay in ionic form as Na^+ , K^+ and OH^- . Ingress of NaCl into the hardened concrete through the pores and also the presence of this salt in mix water and other ingredients of concrete makes the concrete rich in NaCl . The electrolysis of this alkali chloride solution produces chloride at the anode and would free alkali metal at the cathode.



This makes concrete even richer in alkali cations.

3.2.2 Movement of the Cations by CP current

The electronegativity of steel due to CP invariably attracts the positive ions and repulses the negative ions. The concentrations of Na^+ and K^+ will increase near the reinforcement and will decrease some distance away from the reinforcement(43). When CP is applied in reinforced concrete structures, concrete pore fluid will act as an electrolyte to carry the applied CP current to the steel. The conductance of concrete depends upon the velocities as well as the concentrations of its ions. These ions move through the concrete at different velocities. The movable ions in concrete are K^+ , Na^+ , Cl^- , H^+ and OH^- . Absolute velocities of K^+ , Na^+ , Cl^- , H^+ and OH^- at a particular condition were found to be 0.000665, 0.000456, 0.000676, 0.003242 and 0.001802 cm/sec respectively (78). K^+ will share $0.000665 / (0.000665 + 0.000456 + 0.000676 + 0.003242 + 0.001802) = 0.100$ parts of total current applied to the concrete. These values for Na^+ , Cl^- , H^+ and OH^- are 0.067, 0.100, 0.473 and 0.263 respectively. The rate of migration of cations and anions to negative and positive electrodes respectively are in the proportion of their corresponding share to the flow of total current. Thus the migration rate of K^+ is almost equal to that of Cl^- whereas this rate for Na^+ is relatively lower. If 1 Faraday of electricity is passed into the solution, 0.100 equivalent of K^+ and 0.067 equivalent of Na^+ will move to the cathode and 0.100 equivalent of Cl^- will move to the anode.

Since 1 Faraday equals 26.8 A-hours, a current of 26.8 A-hours causes migration of 0.100 and 0.067 equivalent of K^+ and Na^+ respectively towards the cathode(steel). Thus, 1 Ampere of current causes migration of 0.00373 equivalent of K^+ and 0.00250 equivalent of Na^+ per hour. Hence, the concentrations of K^+ and Na^+ near the steel can be written as follows:

Concentration of K^+ , in gm/sq. meter of steel surface area

$$= (1.455 \times 10^{-4}) (\text{current density, in milli amp./sq.meter}) (\text{duration of CP application, in hour}) \text{-----} (7)$$

And,

Concentration of Na^+ , in gm/sq. meter of steel surface area

$$= (0.575 \times 10^{-4}) (\text{current density, in milli amp./sq.meter}) (\text{duration of CP application, in hour}) \text{-----} (8)$$

Both of the above equations demonstrate that the concentrations of Na^+ and K^+ near the steel increase manifold with age and current density. As for example, concentration of K^+ near the steel is 0.943 gm/sq. meter of steel surface area at a current density of 3 ma/sq. meter and at an age of 3 months. This value is 1020 gm/sq. meter of steel area at a current density of 80 ma/sq.meter and at an age of 10 years.

The increased concentrations of these cations near the reinforcement causes a marked weakening of cement matrix thereby reducing the bond between steel and concrete. This fact can be explained broadly in the following manner:

(i) Considering that due to hydrolysis of water, sufficient OH^- will always be present near the reinforcement to combine with Na^+ and K^+ resulting in the formation of NaOH and KOH. These hydroxides are white solids with no cementing properties. As a result, the steel concrete interface will be surrounded by these non-cementitious compounds (35). Moreover, densities of NaOH and KOH are 2.13 gm/ml and 2.004 gm/ml respectively(79) and that of tobermorite gel, which is the most predominant product of hydration, varies from 2.45 gm/ml to 2.53 gm/ml (35). These low density alkali hydroxides would possibly cause local dis-

ruption due to their increased volume.

(ii) Presence of Na_2SO_4 and K_2SO_4 in mix water reduces the strength of cement paste significantly(80). The observed lower strength is due to the change of the structure and due to the change in the intrinsic properties of the hydrates formed under the alkaline condition. Reduction of 28 days strength upto 35% of the control specimen value has been reported with 1.48% K_2O as K_2SO_4 . This reduction was found to be 43 percent by 1.26% Na_2O as Na_2SO_4 . The abundance of Na^+ and K^+ at the steel concrete interface and the ingress of SO_4^- through the pores of concrete makes the environment rich in Na_2SO_4 and K_2SO_4 . Since CP will not be applied before 28 days after casting, the deleterious effects of Na_2SO_4 and K_2SO_4 are limited only to the later strength gain of concrete.

(iii) Enhanced concentrations of the alkali cations will definitely increase the possibility of alkali-silica reactivity. When the soda equivalent R_2O exceeds 0.60 percent by weight of cement in concrete, deterioration due to alkali-silica reactivity becomes a distinct possibility(35).

In actual CP installation in reinforced concrete structure, the current density might be more than 0.279 ma/sq.meter (3 ma/sq.ft.) due to the presence of high chloride gradient within the same concrete. The ingress of NaCl from atmosphere together with the presence of excessive NaCl in mix water and aggregates makes the concrete rich in alkali cations. Thus the concentration of these alkali cations near the rebar in a reinforced concrete structure protected by CP will be at a level dangerous with respect to alkali-silica reactivity and bond reduction.

CHAPTER 4

METHODOLOGY OF RESEARCH

4.1 GENERAL DESCRIPTION OF INSTRUMENTATION

4.1.1 Potential Wheel - Data Bucket

A potential wheel-data logger used to monitor the steel potential values consists of a data bucket, capable of storing a sizable amount of potential data, and a printer. The printer is also capable of drawing contours of the electrode potentials. A hand held terminal connected to the data bucket is used to signal the data bucket for various operations. The potential wheel houses a silver-silver chloride (Ag/AgCl) reference cell. The steel reinforcement and the potential wheel are connected to the data bucket by two separate lead wires. The potential wheel is moved on wet concrete surface to obtain potential readings at various locations. The potential wheel used here has a very high input impedance of 10^{10} ohms so that the observed potential values are unlikely to be affected by the surface dampness and changes in concrete resistivity. Fig. 4.1 shows the potential wheel-data bucket instrument.

This instrument was used in criteria evaluation study (Art. 4.3.1), study of chloride effect on CP criteria (Art. 4.3.2), study of high temperature effect on CP criteria (Art. 4.3.3.1), and depth effect study (Art. 4.3.4).

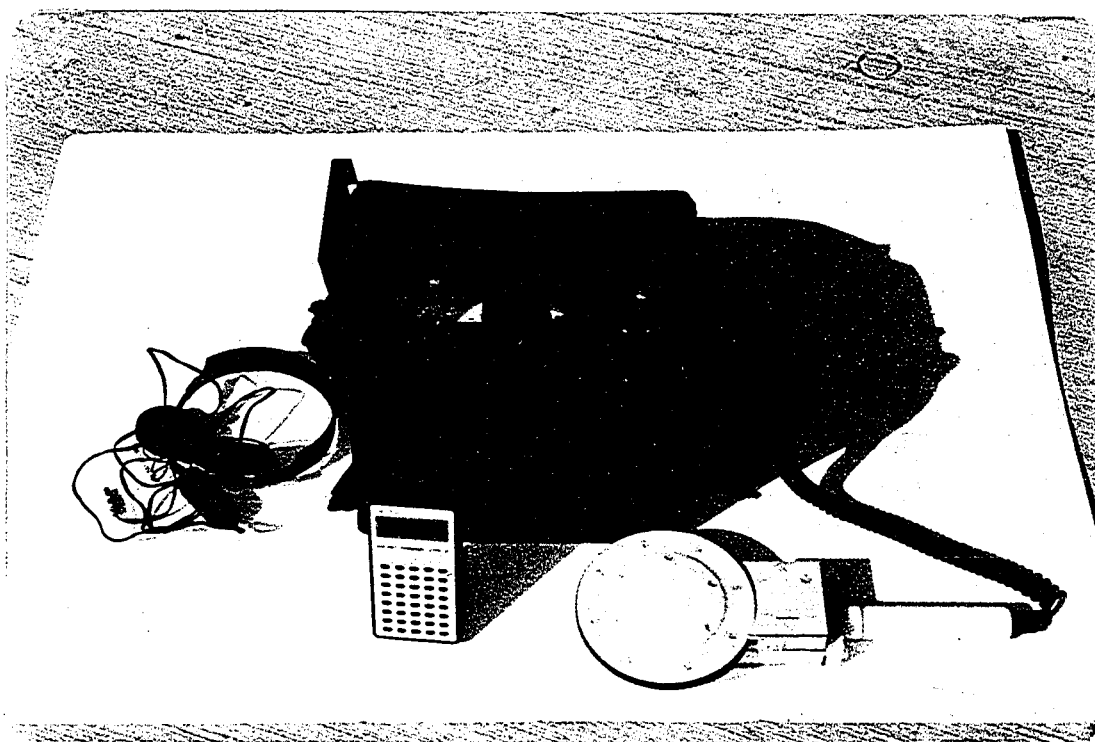


Fig. 4.1 The Potential Wheel Data-Logger Used in
the Study

4.1.2 Current Supplying Unit

The current supplying unit is a rectifier which is a normal DC source with multiple outlets and capability to adjust the current according to the requirement. The circuitry arrangement for the current supplying unit used in the test program is shown in Fig. 4.2. The main components of this instrument are a variac, a rectifier, a capacitor and a number of variable resistors. The variac provides a variable A.C. supply of 0 to 220 volts; the rectifier converts the A.C. supply to D.C. output; the capacitor acts as a low-pass filter to the DC output voltage and the variable resistor adjusts the current supply to a particular specimen. The negative terminal of the D.C. supply is connected to the reinforcing steel, whereas the positive terminal is connected to the anode system. The ammeter, connected in series with the specimen and the variable resistor, measures the current impressed on the steel of each specimen. Current supply to the individual specimen is controlled by the variable resistor connected in series with this specimen. When the required amount of current could not be supplied to the steel in a specimen, even with the maximum adjustment of the potentiometer(variable resistor), the variac was used to change the supply voltage. A current supply unit used in the test program is shown in Fig 4.3.

This instrument was used in criteria evaluation study (Art. 4.3.1), study on chloride effect on CP criteria (Art. 4.3.2), study on enhancement of alkali-silica reaction (Art. 4.3.5), study on temperature effect on CP criteria (Art. 4.3.3.1), study related to depth effect (Art. 4.3.4) and study related to degradation of steel concrete bond (Art. 4.3.6).

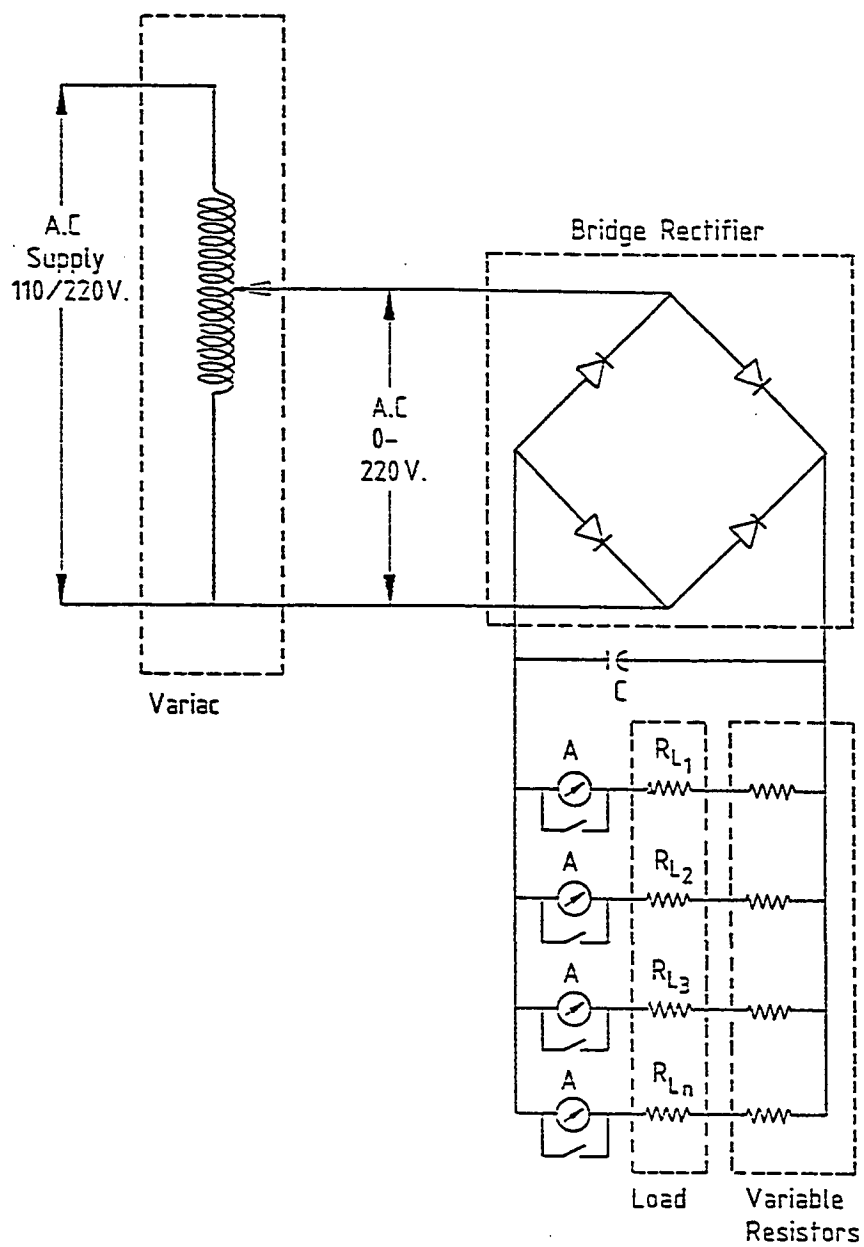


Fig. 4.2 Electrical Schematic for Impressing Current on Reinforcing Steel in Concrete Specimens

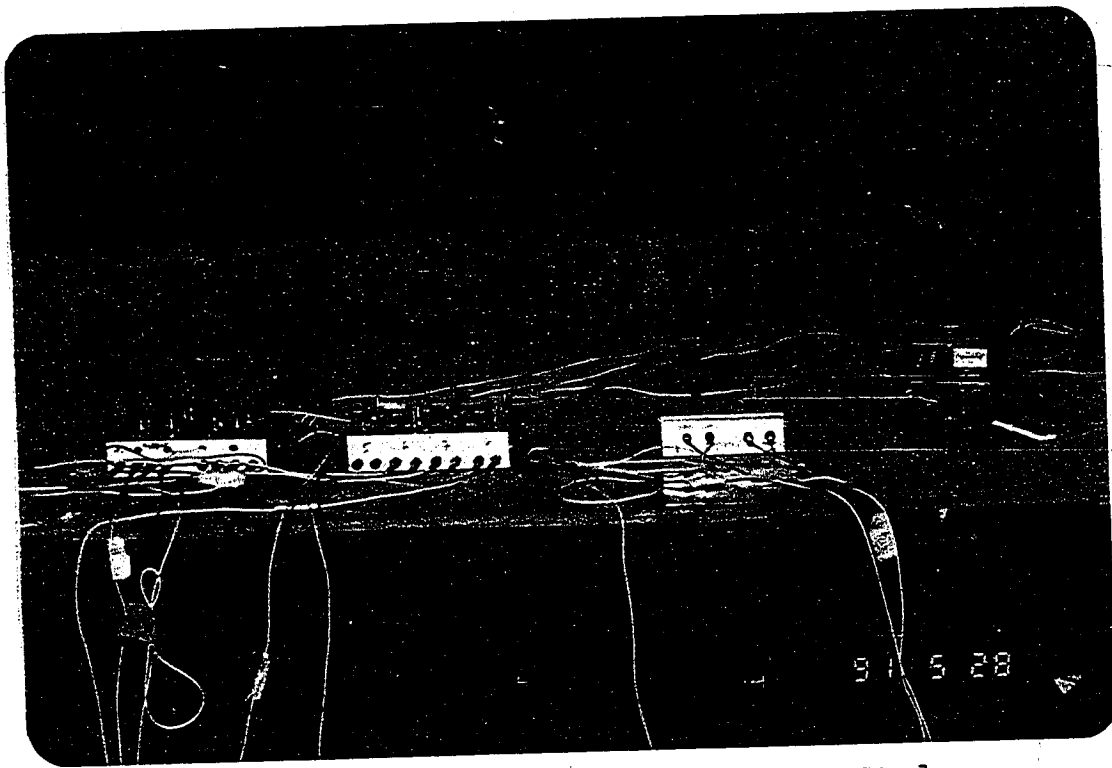


Fig. 4.3 The Current Supply Unit Used in the Study

4.1.3 Temperature Chamber

A temperature chamber, capable of attaining a peak temperature of 60°C , is used in the test program to simulate the concrete surface temperature existing in the Arabian Gulf region. The temperature inside the chamber varied with time according to a predetermined regime which simulates the actual diurnal variation occurring in a typical summer day at Dhahran. Fig 4.4 shows the temperature chamber used in the test program. Fig. 4.5 shows the idealized temperature regime which is expected to attain inside the temperature chamber. The temperature inside the chamber is communicated through a thermostat to the strip chart recorder which records the variation of the chamber temperature. Wires from the specimens were taken out through a small hole included in the chamber. Fig. 4.6 shows the temperature regime actually attained inside the chamber.

The temperature chamber was used in study on temperature effect on CP criteria (Art. 4.3.3.1).

4.1.4 Demec Gauge

A demec gauge with 2 inch gauge length is used to measure the expansions in alkali-silica reactivity specimens and in control specimens having no reactive aggregates. Expansions between two demec disks were measured with this instrument. The demec gauge used in the test program is shown in Fig. 4.7.

This instrument was used in study on enhancement of alkali-silica reaction due to CP current (Art. 4.3.5).

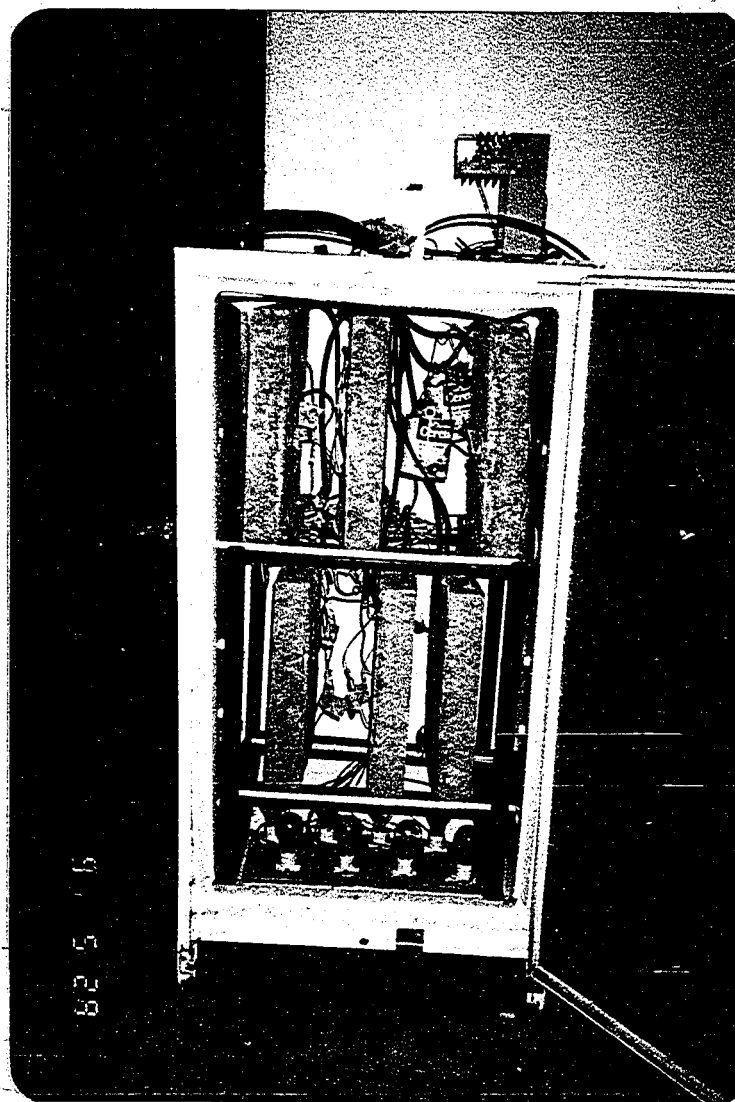


Fig. 4.4 The Temperature Chamber Used in the Study

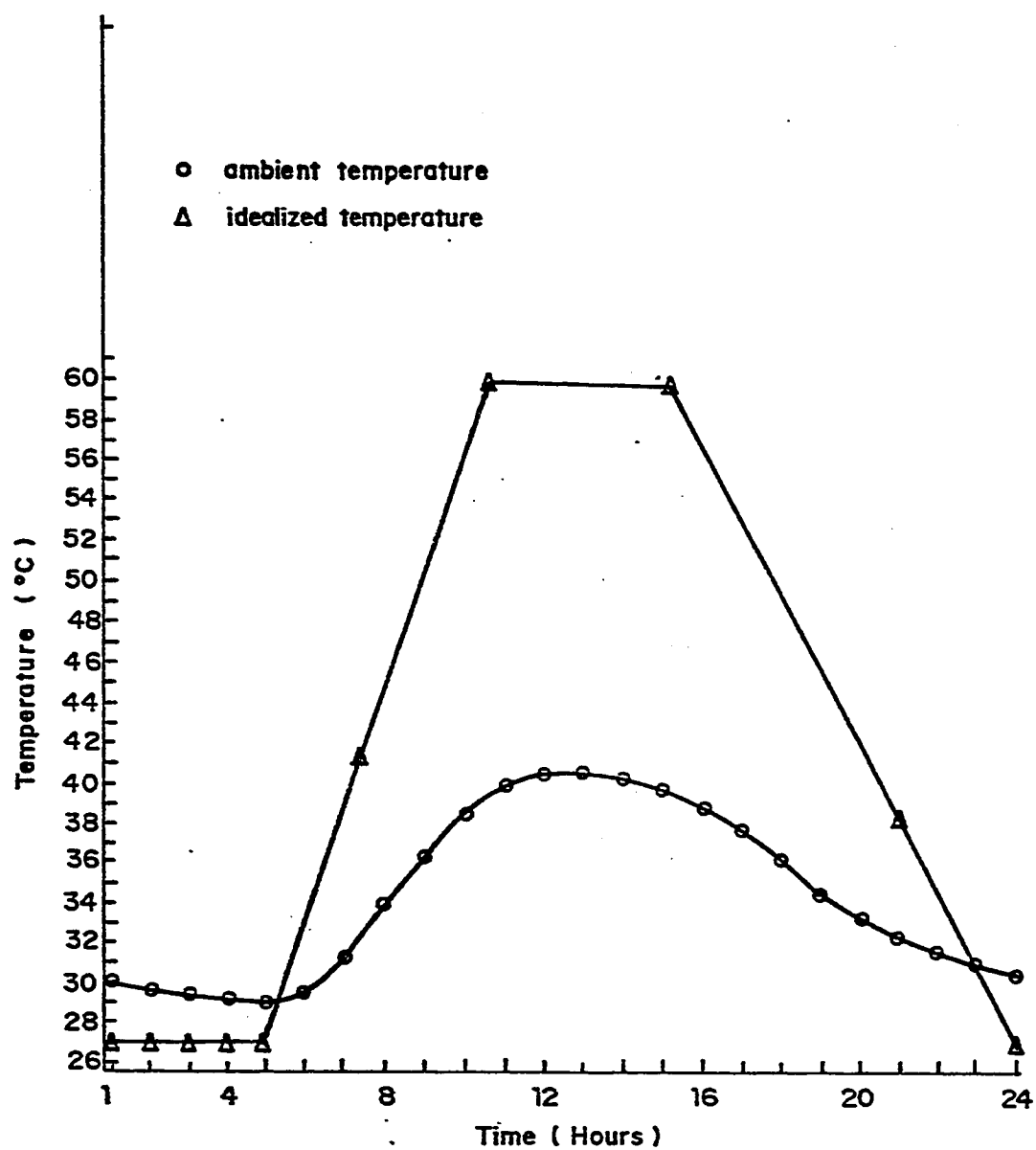


Fig. 4.5 Idealized Temperature Expected to Attain Inside the Temperature Chamber

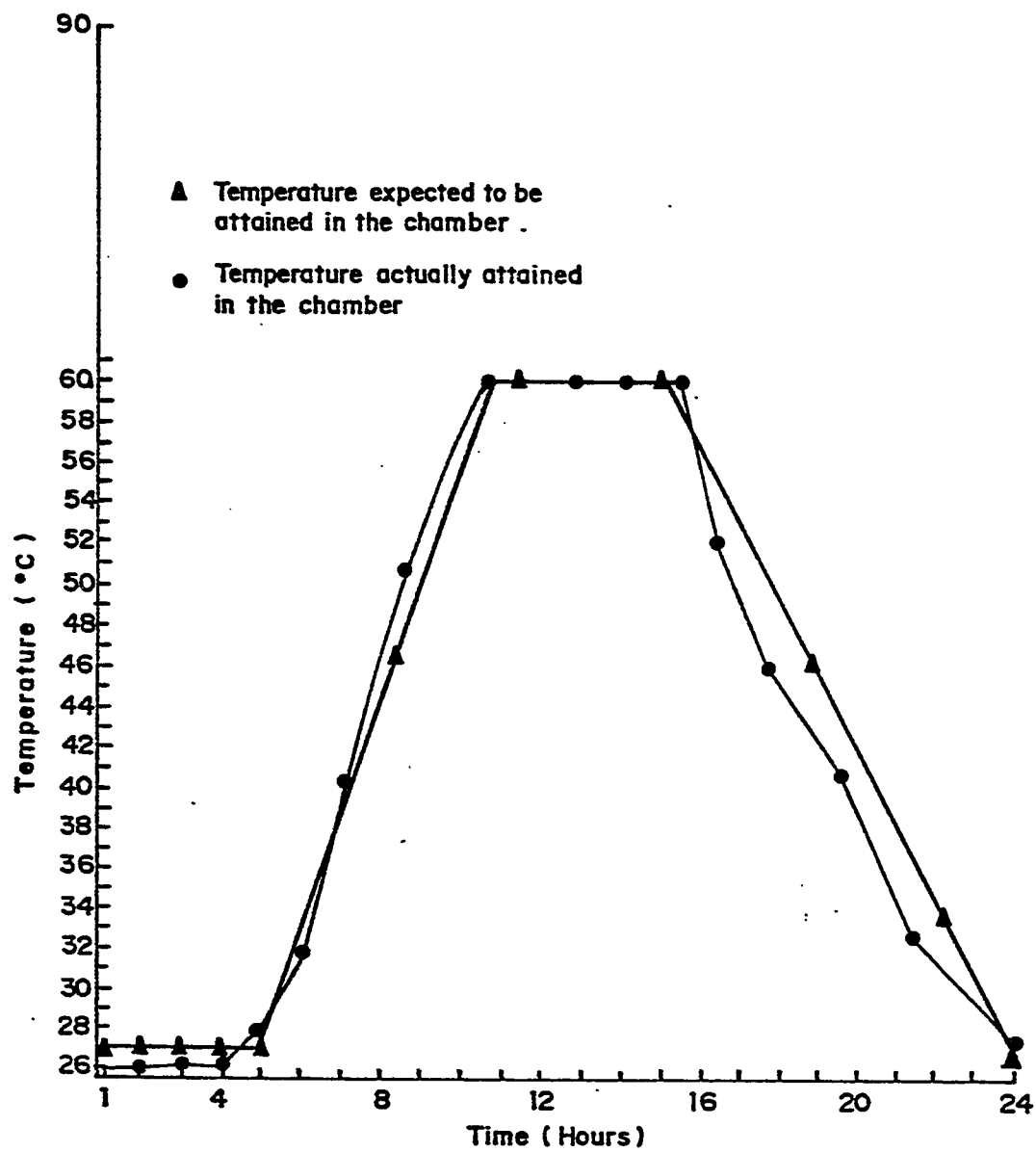


Fig. 4.6 Temperature Actually Attained in the Temperature Chamber

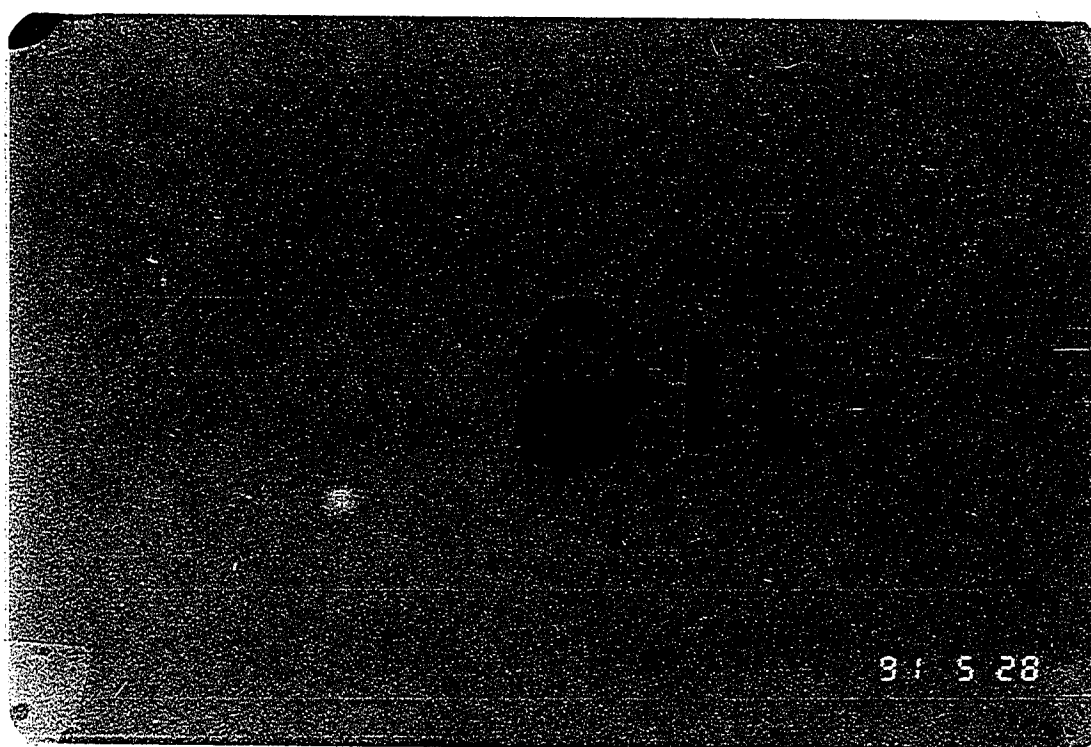


Fig. 4.7 The Demec Gauge Used in the Test Program
for Alkali-silica Reactivity Study

4.1.5 Known Resistors

A number of 51 ohm resistors connect the main steel and the macrocell steel. The voltage drop across the known resistor is the indicator of the corrosion current/protection current flow.

The resistors were used in study on chloride effect on CP criteria (Art. 4.3.2), study on high temperature effect on CP criteria (Art. 4.3.3.1) and study related to depth effect on CP criteria (Art. 4.3.4).

4.1.6 Corrosometer Probes and CK-3 Corrosometer

The corrosion probes indicate corrosion conditions of both of the cathodically protected reinforcement and the unprotected reinforcement. Flat type underground corrosion probes were used in the test program. When the probe is connected with the CK-3 corrosion meter, the corrosion meter reads the metal loss on the digital indicator, in dial divisions (0-1000) which can be converted directly to metal loss by comparison with the probe span. When the probe metal corrodes, the cross-sectional area of the probe metal decreases and consequently the electric resistance of the uncorroded metal sensing element increases. The corrosion meter circuit utilizes this change of resistance to indicate the metal loss on an exposed surface. Any number of probes may be used with a single instrument, with a connection to probe required only at the time a reading is made. Figs. 4.8 and 4.9 show the corrosion probe and the CK-3 instrument respectively.

The corrosion probes were used in study on chloride effect on CP criteria (Art. 4.3.2), study on high temperature effect on CP criteria (Art. 4.3.3.1) and study related to depth effect on CP criteria (Art. 4.3.4).

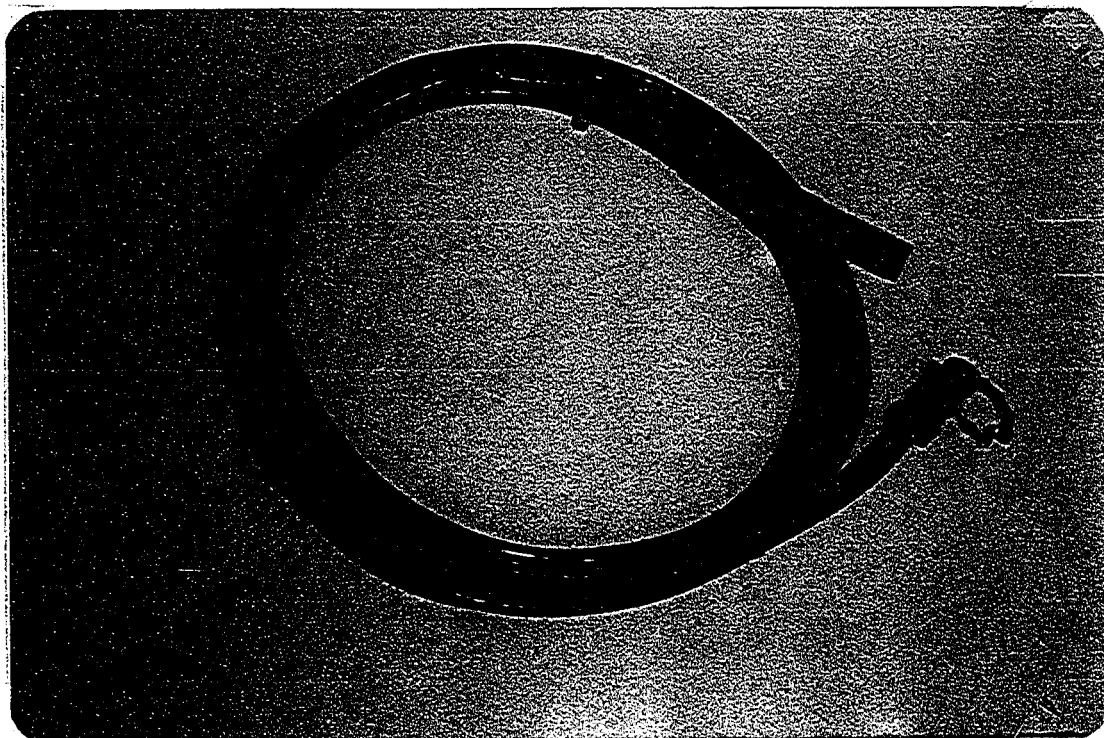


Fig. 4.8 The Corrosometer Probe Used in the Study

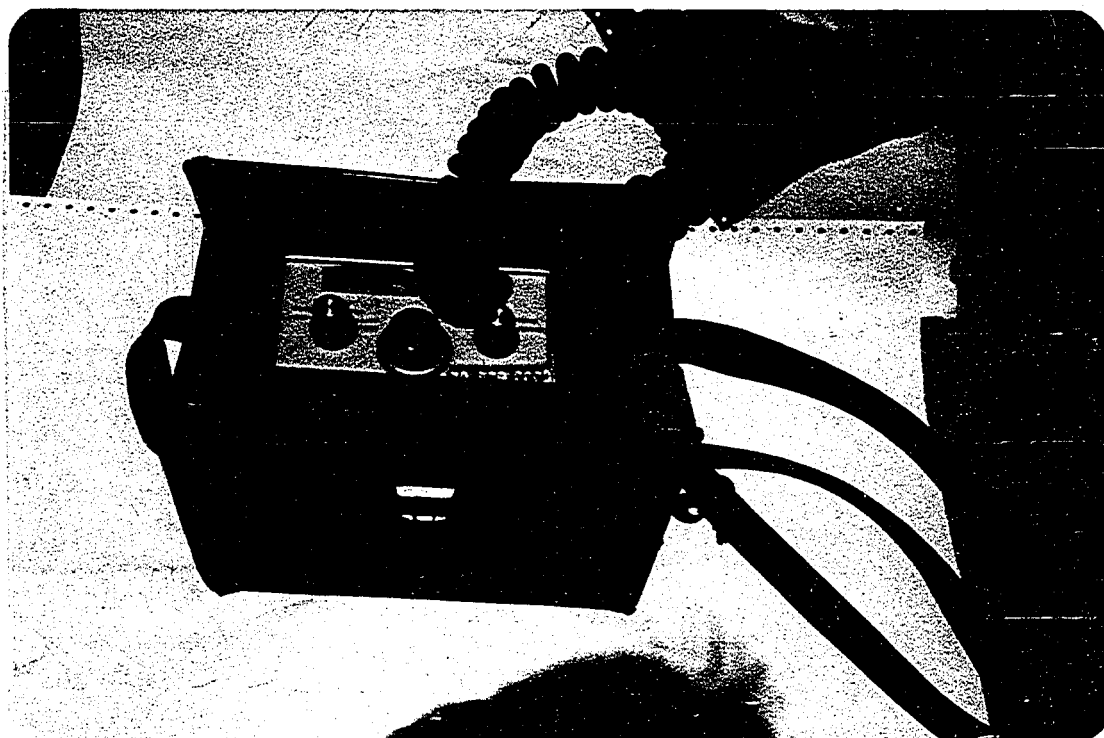


Fig. 4.9 A Ck-3 Corrosometer Used in the Study

4.1.7 Half Cells

Two types of half cells are used in the test program for cross checking the potential data obtained by potential wheel-data bucket.

4.1.7.1 Hand Held Ag-AgCl Half Cells

This type of half cell provides a simpler way of measuring the half cell potential of steel in concrete. The steel reinforcement and the portable half cell are connected to two ends of a high impedance voltmeter by two separate lead wires. The steel electrode potential at a particular location is obtained by moving the half cell to that location. Fig 4.10 shows the principle of half cell operation.

The hand held Ag-AgCl half cell was used in study on chloride effect on CP criteria (Art. 4.3.2).

4.1.7.2 Permanently Embedded Ag-AgCl Half Cells

This half cell is embedded in close proximity of steel reinforcement. The lead wires coming from the steel and the half cell are connected to a high impedance voltmeter. The limitation of this kind of half cell is that it provides steel to concrete potential only at a single location.

The permanently embedded half cell was used in study on chloride effect on CP criteria (Art. 4.3.2) and study related to depth effect on CP criteria (Art. 4.3.4).

4.1.8 Resistance Meter

Nilsson 400 4-pin resistance meter was used in the test program for determination of electrical resistance of concrete. The instrument is a four terminal

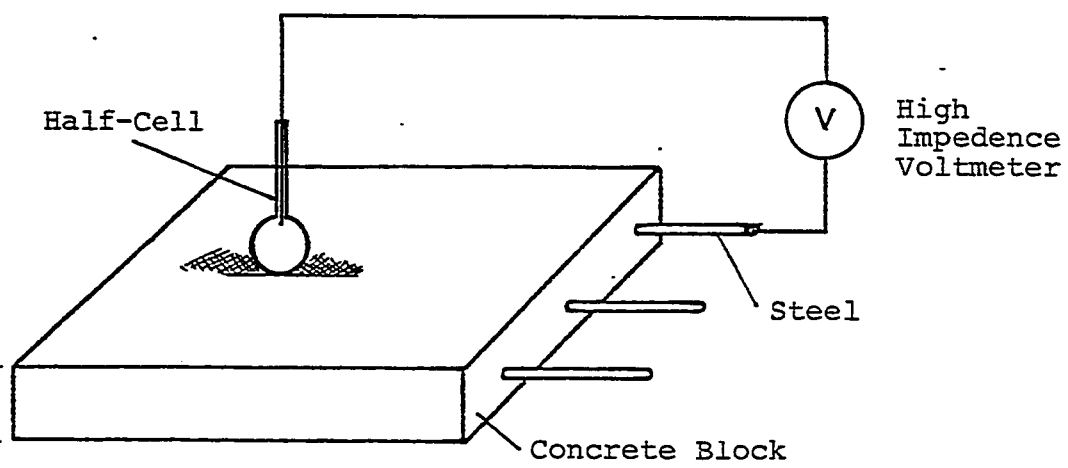


Fig. 4.10 The Principle of Half-Cell Potential Measurement

null balancing ohm meter. It measures resistance directly from 0.01 ohm to 1.1 megaohms. The unit generates a low voltage 97 Hz square wave current between the C1 and C2 binding posts (Fig. 4.11). The detector senses the voltage drop between the P1 and P2 binding posts, compares it to internal standard resistors, and indicates a difference on the null detector. When the null detector is balanced, using the range switch and the dial, the resistance in ohms between P1 and P2 is the dial reading multiplied by the range switch position.

This instrument was used in study on possible difficulties of CP application in concrete exposed to an environment characterized by high temperature and dry weather regime (Art. 4.3.3.2).

4.1.9 Fixed D.C. Supply

15 V DC supply source having 300 mA capacity were used to supply current to steel in the specimens kept at hot-dry environment at outdoors.

This fixed DC supply was used in study on possible difficulties of CP application in concrete exposed to an environment characterized by high temperature and dry weather regime (Art. 4.3.3.2).

4.1.10 Other Instruments

A high precision digital multimeter for measuring the voltage drop across the known resistor which connects the macrocell steel and the specimen steel, two highly accurate multimeters for measuring the current flow to the steel, the universal testing machine for tension and compression test, the masonry driller for removing the powder sample from the concrete specimen, masonry saw for cutting the concrete specimen and a number of other small instruments were used in the test program.

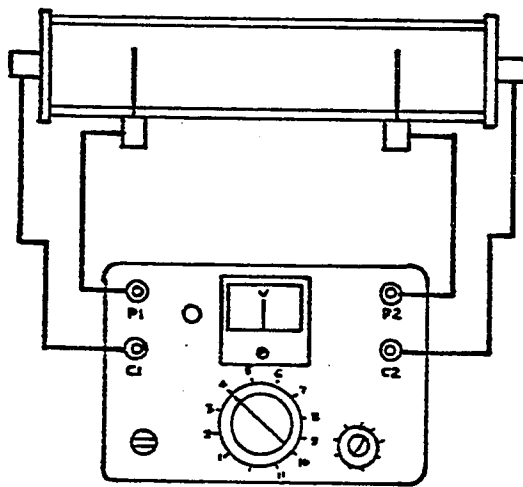


Fig. 4.11 Instrumentation Using Nilson 400 for Resistivity Measurement on Concrete Blocks

4.2 MONITORING AND EVALUATION TECHNIQUES

The techniques to evaluate the cathodic protection systems are broadly categorized into four classes; (1) **embedded instrumentation**, placed in the test slabs at the level of reinforcing steel prior to anode installation. Most of these are monitored remotely at regular intervals throughout the life of the system; (2) **surface techniques**, which monitor the system using portable instrumentations; (3) **visual and physical observation** of the exposed components of each system and (4) **destructive techniques**.

4.2.1 Embedded Instrumentations

Four types of embedded instrumentations are used to measure the subsurface current densities and distribution and/or the measurement of reinforcing steel potentials.

4.2.1.1 *Artificial Corrosion Macrocells*

The macrocells were cast as small concrete cylinders with a short section of rebar (80 mm long) centrally placed on each of the cylinder. The cylindrical macrocell was 3 inch long and 2 inch in diameter. The size of the macrocell steel was the same as that of main steel. The probe (the macrocell) is connected to the reinforcement through a known resistor. By measuring the voltage drop across the resistor, the magnitude and direction of the current flow between the probe and ground (reinforcing steel) can be determined. If the positive voltmeter lead is connected to the ground, a positive voltage reading will indicate that the probe is corroding. A negative sign will indicate that the net current flow is from probe to ground (i.e. the probe is receiving current from the anode system which is

flowing back to the rectifier through the lead connecting the probe to the main steel). Fig. 4.12 shows some of the macrocells used in the test program.

The macrocells were used in study on chloride effect on CP criteria (Art. 4.3.2), study on high temperature effect on CP criteria (Art. 4.3.3.1) and study related to depth effect on CP criteria (Art. 4.3.4).

4.2.1.2 The Current Pick-up Probes

Current pick-up probes comprise a short length rebar attached to a lead wire which is connected through a resistor to the structural steel. The probe rebar is 35 mm long , with size matching the main structural reinforcement. The probe locations are selected in relation to the layout of the primary anode systems, so that the current flow to each probe can be related to the distance of the probe from the primary anode. This makes current pick-up probes useful in examining the current distribution relative to anode position. These probes are also useful in early detection of anode deterioration.

The pick up probes were used in the depth effect study only (Art. 4.3.4).

4.2.1.3 Permanently Embedded Reference Half Cells

Silver-silver chloride half cells are used in the test program. The lead wire of the embedded half cell is connected to one end of the high impedance voltmeter whereas the other end of the voltmeter is connected to ground(reinforcement). Reference cell data may be used in a number of ways to evaluate a cathodic protection system. In order to determine the polarization shift of a reference cell measured from the static potential, power to the system is periodically switched off to allow measurement of static cell potentials. Also by switching off the

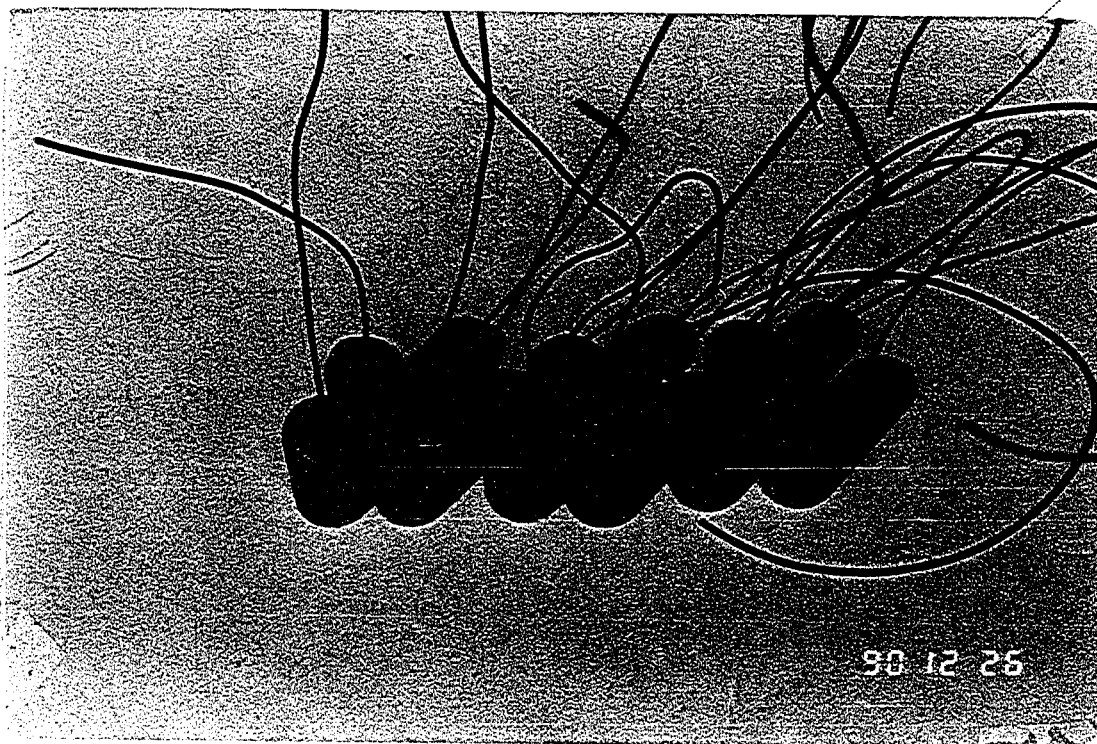


Fig. 4.12 Artificial Corrosion Macrocell Used in the Test Program

power supply, the instant off potential value is measured and compared with the required criteria for protection.

The permanently embedded half cells were used in study on chloride effect on CP criteria (Art. 4.3.2) and study related to depth effect on CP criteria (Art. 4.3.4).

4.2.1.4 Coupon Specimen

Six inch long steel bar having same diameter as that of main steel was used as coupon specimen. They were positioned at the level of the main steel and also were tied with the steel in order to keep them at the same condition. These coupons were removed from the specimen after the observation period and checked for the corrosion condition. Coupons used in the CP specimen should remain corrosion free and the weight loss should be absolutely negligible.

Coupons were used in study on chloride effect on CP criteria (Art.4.3.2), temperature effect on CP criteria (Art. 4.3.3.1) and study on depth effect on CP criteria (Art. 4.3.4).

4.2.2 Surface Technique

Measurement of steel potentials using a portable potential wheel data bucket instrumentation constitutes an extremely effective external technique. Prior to the installation of the cathodic protection system, potentials can be measured at different locations. These potentials are the static potential. During the system operation, half cell survey can be conducted, measuring instant off potentials and the decay potentials. These instant off cell potentials and the decay potentials are the indicative of adequate protection. The difference between

the static potential and the instant off potential is the shift potential.

4.2.3 Visual and Physical Examinations

During the monitoring period, all of the specimens were examined closely for visible signs of deterioration.

4.2.4 Destructive Technique

A number of specimens subjected to cathodic protection current were demolished and the corrosion condition of the protected bars were checked. In the bond study program, powder samples were removed from the specimen after performing the pullout test. In the alkali-silica reactivity program, the specimens were cut down to remove small cubes and small plates for the determination of compressive strength and hardness respectively.

4.3 PROCEDURES AND INSTRUMENTATIONS USED TO STUDY THE EFFECT OF CHLORIDE CONTENT, TEMPERATURE, DEPTH AND SECONDARY PROBLEMS ON CATHODIC PROTECTION CRITERIA

4.3.1 Developments of Relationships Between Current Density, Polarization Period, Protection Potential and Depolarization Time

4.3.1.1 Study on Current Density Needed to Satisfy Different CP Criteria

Test Specimens: Fig. 4.13 shows a typical specimen for study relating the current density with the available CP criteria. All of the specimens were 18 in x 12

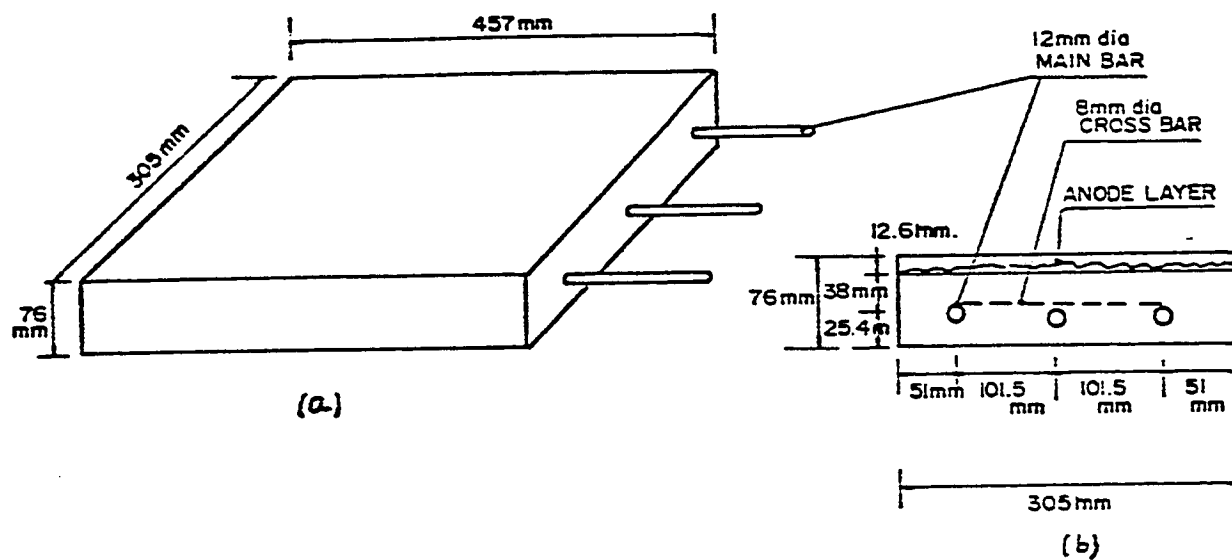


Fig. 4.13 Schematic of a Typical Specimen for Study Relating the Current Density with Available CP Criteria

in x 3 in slab having reinforcement arrangement as shown in Fig. 4.13. The main reinforcement comprises 1/2 in dia, 20 inch long bars with 16 inch embedded inside the concrete. One cross bar, 8 mm dia and 9 inch long, connects the three main steel bars hereby providing electrical continuity between them.

Concrete specimens were cast with a Type V portland cement using a w/c ratio of 0.56, cement content of 550 lbs/ yd³ (327 kg/ m³) and a coarse to fine aggregate ratio of 1.43. Coarse aggregate was crushed limestone with a bulk specific gravity of 2.42 and absorption of 3.8 percent. Beach sand with a specific gravity of 2.70 and absorption of 0.25 percent was used as fine aggregate. Aggregates were washed to remove contamination and dust. Concrete was mixed in a 1/2 ton mixer. ICI H8 tectrode anode used here was properly positioned during casting. A 1/2 inch (12.7 mm) concrete overlay for the anode was used in all of the specimens. No chloride was added with the mix water. The specimens were cured under water for 7 days. Thereafter, curing by covering the specimen with a wet towel was continued till the end of the experimental program.

Approach to the Study: Current supply unit as described in Art. 4.1.2 was used here to supply current to the steel in concrete specimens. The static potential was measured from the control specimen using potential wheel-data logger. The current density in the current treated specimens were changed from 0.25 to 20 ma/sq. ft and at each level of current density, the instant off potential, the decay potential and the shift potential were measured using potential wheel-data logger.

4.3.1.2 *Study on Finding a Relationship Between the Current Density, The Polarization Period and the CP Criteria*

The effect of current density and the polarization period on the depolarized potential, fully depolarized potential and time for its occurrence, the instant off potential and the decay potential were observed in this study.

Test Specimens: The specimens were 4 x 2.5 x 10.5 in (101 x 63 x 267 mm) cement mortar prisms (Fig. 4.14) made with a water cement ratio of 0.6. Two different types of fine aggregates having different specific gravities were used in the preparation of specimens to monitor the effect of aggregate type on the potential readings. A 0.5 in (12.5 mm) diameter, 10.5 in (267 mm) long reinforcing steel bar was embedded throughout the length of the specimen. The distance between the anode and the secondary electrode (the cathode, reinforcing steel) was 3 in (76 mm). The ICI II8 tectrode anode used in the test program was covered with a thin film of mortar. The specimens were demolded after 24 hours and thereafter were cured for 7 days under water.

Approach to the Study: The specimens were subjected to CP current eight days after casting. Some of the specimens were kept as control(never received current). Constant current densities of 01,03,20 and 60 ma/sq ft were maintained throughout the observation period. The first two values are reported in the literature as the current density needed for adequate protection whereas the rest two are observed in case of overprotection. A constant current supply unit as described in Art. 4.1.2 was used here for supplying current to the specimens. The variable resistors and the variac were used to maintain the constant current density in each of the specimen. Potential wheel data bucket was used to measure

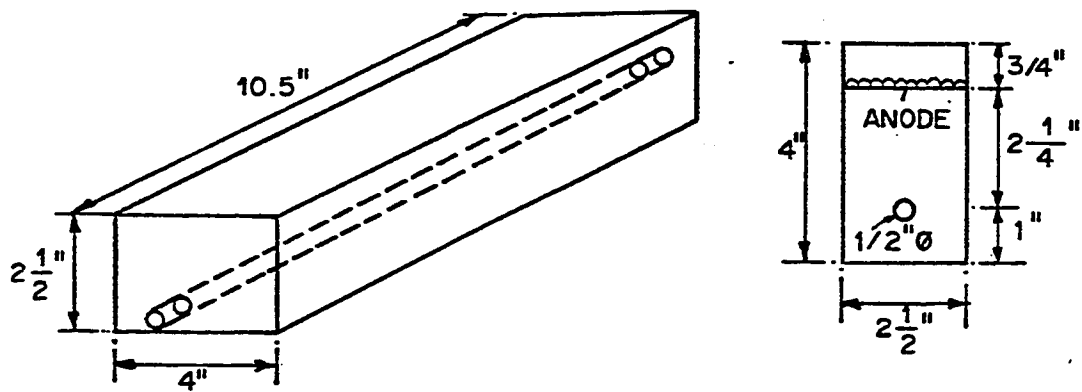


Fig. 4.14 Schematic of Specimen Used in (i) Study on Finding a Relationship Between the Current Density, the Polarization Period and CP Criteria (ii) Study on Enhancement of Alkali-silica Reaction Due to CP Current

the steel potential. The followings were observed in the current treated specimens at different polarization periods:

- * Steel potential immediately after switching off the CP current (i.e. the instant off potential)
- * Steel potential every fifteen minutes from the time the power was switched off. The steel potential measurement was continued upto 4 hours from the time the power was switched off. The four hour decay potential was calculated as the difference between the instant off potential and the potential measured 4 hour after the system was switched off.
- * The depolarized potential was plotted against the depolarization time. From here, the fully depolarized potential and the time for its occurrence were noted.

4.3.2 Chloride Effect on Cathodic Protection Criteria

4.3.2.1 Test Specimens

The Artificial Corrosion Macrocell: The macrocells described in section 4.2.1.1 were cast as small concrete cylinders with a short section of rebar (76 mm long) centrally placed on each of the cylinder. The cylindrical macrocell was 3 in (76 mm) long and 2 in (51 mm) in diameter. The size of the macrocell steel was the same as that of main steel. The concrete mix used in casting the macrocell is exactly similar to that used in casting the main specimen.

Test Specimens: Fig. 4.15 shows a typical specimen for evaluating cathodic protection criteria. In each of the specimen, three macrocells were used. These macrocells were cast prior to the casting of the main specimen and then positioned in the mold one day before casting of the main specimen(Fig. 4.16). The macrocell steel and the main steel were at the same level. All of the specimens were 18 in x 12 in x 3 in slab having reinforcement arrangement as shown in Fig. 4.15. The main reinforcement comprises 1/2 in dia, 20 inch long bars with 16 inch embedded inside the concrete. Three coupon bars were tied with the main steel bars.

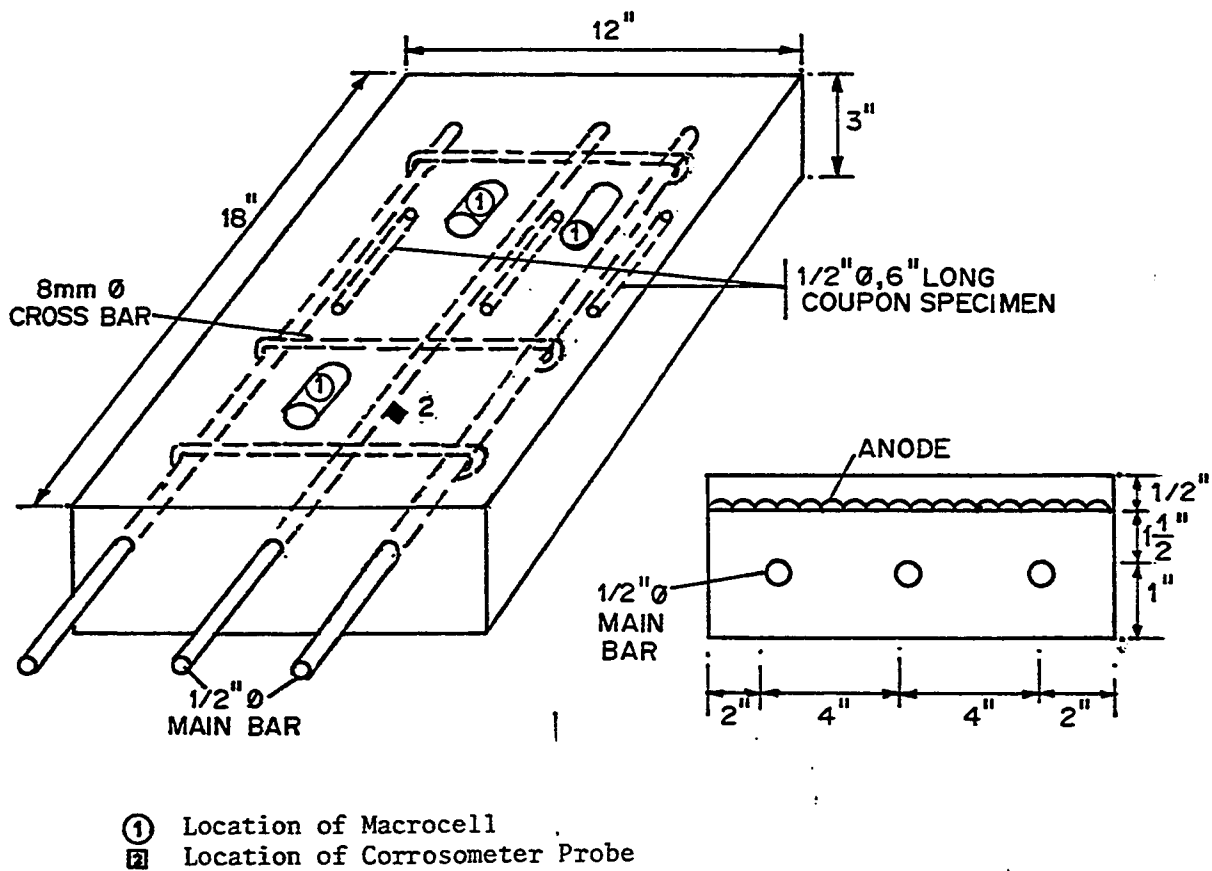


Fig. 4.15 A Typical Specimen Used in Study on (i) Chloride Effect
 (ii) High Temperature Effect on CP Criteria

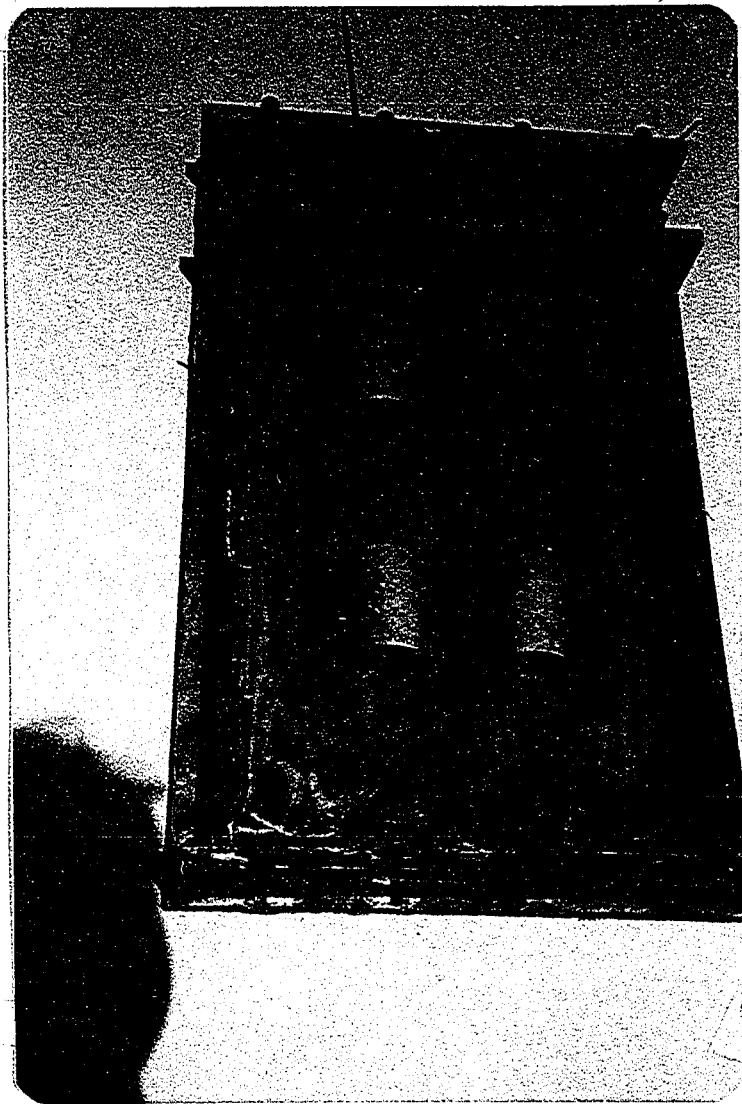


Fig. 4.16 Macrocells Positioned in Mold Before Casting
of the Specimen

One cross bar, 8 mm dia and 9 inch long, connects the three main steel bars hereby providing electrical continuity between them.

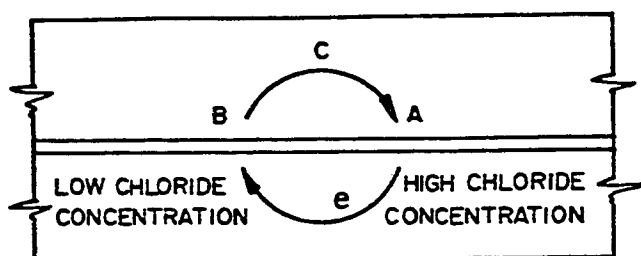
Concrete specimens were cast with a Type V portland cement using a w/c ratio of 0.56, cement content of 550 lbs/ yd³ (327 kg/ m³) and a coarse to fine aggregate ratio of 1.43. Coarse aggregate was crushed limestone with a bulk specific gravity of 2.42 and absorption of 3.8 percent. Beach sand with a specific gravity of 2.70 and absorption of 0.25 percent was used as fine aggregate. Aggregates were washed to remove contamination and dust. Concrete was mixed in a 1/2 ton mixer. ICI H8 Tectrode anode used here was properly positioned during casting. A 1/2 inch (12.7 mm) concrete overlay for the anode was used in all of the specimens. The specimens were demolded one day after casting and were then covered with wet towel for curing. For continued curing, water was sprayed on the specimen regularly several times a day upto 28 days from the date of casting. Curing by immersion in water was not used to avoid chlorides being washed out from the specimen to the surrounding water. The specimens were covered by wet towels throughout the observation period to facilitate CP application.

Chloride Content:

Specimen chloride content, lbs/cu.yds of concrete	0	2	4	8	16	32
---	---	---	---	---	----	----

Macrocell chloride content, lbs/cu.yds of concrete	4,8	6,10	8,12	12,16	24,32	48,64
--	-----	------	------	-------	-------	-------

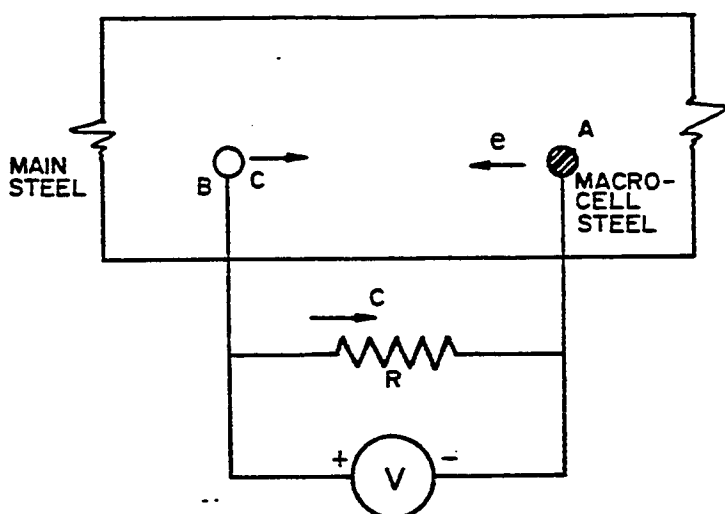
The predetermined amount of chloride content was attained by adding NaCl through the mix water.



Potential of Steel
at A < Potential of
Steel at B

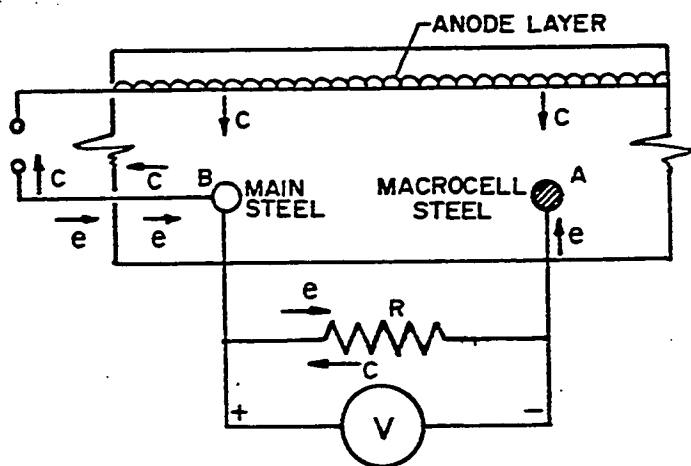
C — Current
e — Electron

(a) A Practical Corrosion Site



Potential of Steel
at A < Potential of
Steel at B

(b) Simulation of An Actual Corrosion Site



* Before CP Application,
Steel at A is Donating
Electron to the Medium

* After CP Application,
Steel at A is Receiving
Electron From the Rect-
fier

Fig. 4.17 Schematic Showing the Direction of Corrosion Current Flow Before Protection and Protection Current Flow After Protection

4.3.2.2 The Approach to the Study

A Practical Corrosion Site: A corrosion site in a reinforced concrete structure is shown in Fig. 4.17a. Anode develops due to high concentration of chloride at a particular location and the corrosion starts at the anodic site. The steel potential at the anodic site is lower (more negative) than that at the cathodic site. The potential difference thus developed causes the corrosion current to flow between the anode and the cathode. The anodic area corrodes and supplies electrons to the cathodic area (Fig. 4.17a)

Simulation of Corrosion Condition : The corrosion situation due to chloride gradient is simulated here. The chloride content of the macrocell was somewhat higher than that in the other parts of the specimen. Because of the high chloride presence in the macrocell, corrosion starts at the macrocell steel first. The steel potential of the macrocell was therefore lower than that of the specimen and it is this potential gradient which drives the corrosion current to flow between the macrocell steel and the specimen steel when they are connected through an external resistor. Two separate lead wires, one coming from the main steel and the other from the macrocell steel, are connected at two sides of a 51 ohm resistor. Fig. 4.17b shows the simulation of the corrosion condition due to chloride gradient. Before application of CP, electrons flow from the macrocell to the main steel and the corrosion current flows from the main steel to the macrocell steel. In this situation, a positive voltage drop across the known resistor is noticed when the positive voltmeter lead was connected to the ground (main steel).

4.3.2.3 Establishment of CP criteria for Adequate Protection

Establishment of the Protection Level: All of the specimens were supplied with

CP currents 14 days after casting. Before application of CP, electrons flow from the macrocell to the main steel and the corrosion current flows from the main steel to the macrocell steel. In this situation, a positive voltage drop across the known resistor is noticed when the positive voltmeter lead was connected to the ground (main steel). The specimens were then activated with impressed DC current and the positive terminal of the supply was connected to the anode whereas the negative terminal was connected to the main steel. The positive voltage drop across the known resistor gradually decreased with the increase of the impressed current and subsequently at a particular level of DC current supply, the voltage drop across the resistor reduced to zero. At this zero voltage drop condition, no local corrosion current flows between the macrocell steel and the specimen steel. In this state, the current passing to the main circuit is the current required for adequate protection. The supply was switched off and the instant off potential, the decay potential and the shift potential were recorded at this stage which corresponded to the protection level necessary for the particular condition of the specimen.

Instant off Potential Measurement: The potentiometer was adjusted until the voltage drop across the known resistor decreased from positive value to zero. The corresponding current supply was maintained for 24 hours. The current supply was then switched off and the steel to electrolyte potential was measured immediately using a potential wheel- data bucket instrument. The potential measured in this manner was recorded as instant off potential. In addition to this measurement the hand held Ag-AgCl half cell and the permanently embedded half cells were used to cross check the potential values recorded by potential wheel-data bucket system. The above operation was continued weekly for a four month activation period.

Four Hour Decay Potential Measurement: The steel to electrolyte potential was measured 4 hours after switching the system off. For this measurement also, the potential wheel data bucket was used primarily and the hand held Ag-AgCl half cell as well as the permanently embedded half cell systems were used to cross check the values obtained by Potential wheel. The difference between the instant off potential and the potential measured 4 hours after switching off the CP current was recorded as the 4 hour decay potential.

Shift Potential Measurement: The potential of steel in the control specimen(never received CP current) was measured by potential wheel. The difference between the instant off potential measured in section 4.3.3.1 and the potential obtained from the corresponding control specimen was recorded as shift potential.

Current Density Measurement: The current passing to the circuit at the onset of protection divided by the steel surface area is reported as the protection current density

4.3.2.4 Checking the Effectiveness of CP Criteria

The effectiveness of different CP criteria, established in section 4.3.2.3, in terms of arresting corrosion was checked using destructive techniques. After the activation period, the specimens were broken for the retrieval of the coupon bars. The coupon bars removed from both the CP specimen and the control specimen were checked for corrosion condition. Also the weight loss percentage was calculated. In some selected specimens, corrosion probes were used. The corrosion probe readings indicate the corrosion rate in both of the control specimen (no CP current) and the CP specimen.

4.3.3 Temperature Effect on Cathodic Protection Criteria and Cathodic Protection Application

4.3.3.1 High Temperature Effect on CP Criteria

Test Specimens: The specimens used in this study are exactly same as those described in section 4.3.2.1 for chloride effect study. Concrete specimens were cast with a Type V portland cement using a w/c ratio of 0.56, cement content of 550 lbs/ yd³ (327 kg/ m³) and a coarse to fine aggregate ratio of 1.43. Coarse aggregate was crushed limestone with a bulk specific gravity of 2.42 and absorption of 3.8 percent. Beach sand with a specific gravity of 2.70 and absorption of 0.25 percent was used as fine aggregate. Aggregates were washed to remove contamination and dust. Concrete was mixed in a 1/2 ton mixer. ICI H8 Tectrode anode used here was properly positioned during casting. A 1/2 inch (12.7 mm) concrete overlay for the anode was used in all of the specimens. The specimens were demolded one day after casting and were then covered with wet towel for curing. The towels were kept wet throughout the 4 months observation period. The specimens were kept inside the temperature chamber 7 days after casting.

Chloride Content

Specimen chloride content, lbs/cu.yd of concrete	8	32
Macrocell chloride content, lbs/cu.yd of concrete	16	48

The predetermined amount of chloride contamination was attained by adding NaCl with the mixing water.

Approach to the Criteria Study: The specimens were supplied with CP currents 14 days after casting. The approach is the same as described in section 4.3.2.2 with the difference that here the specimens were kept inside the temperature chamber. The temperature chamber simulated typical summer climatic condition characterized by high temperature and high humidity.

Establishment of CP Criteria for Adequate Protection: The current reversal technique as described in section 4.3.2.3 was used to achieve the protection level of the reinforcing steel. The protection current density was maintained for 24 hours and then the current supply was switched off. The instant off potential, the four hour decay potential, the shift potential and the current density required for protection of steel were measured using the technique described in section 4.3.2.3 for chloride effect study. The results obtained here were compared with those obtained in section 4.3.2.3 for chloride effect study at room temperature and the effect of temperature on the static potential, four hour decay potential, instant off potential and the shift potential were observed.

4.3.3.2 Study on Possible Difficulties of CP Application at High Temperature and Dry Weather Regime

At high temperature and dry weather regime, the concrete immediately below the anode layer may become very dry. This dry concrete may act as a barrier for the protection current to flow from anode to the steel reinforcement. A small research program was undertaken which studies the possible problems in terms of current supply to the steel when CP is used to protect the reinforcing steel in concrete structures, located in hot-dry environment, using a low rectifier output of 15 V DC.

Test Specimens: The specimens and the concrete mix used in this study are exactly same as those described in section 4.3.2.1 for chloride effect study. In addition to the 18 in x 12 in x 3 in slab specimens, 3 concrete cylinders 3 in x 6 in were also cast. The slab samples and the cylinders were demolded one day after casting and cured under water for 28 days. At the end of curing, the slabs and the cylinders were kept in hot and dry outdoor environment. These cylinders were used to study the effect of outdoor environment on electrical resistivity of concrete.

Approach to the Study: After curing, the specimens were kept outdoors. Fig. 4.18 shows the specimens in the outdoor environment. Current was supplied to each of the sample by a 15 V DC supply. The positive end of the supply was connected to the anode and the negative end was connected to the steel. The current passing to the individual specimen was measured using highly accurate digital multimeter, the electrical resistivity of concrete was measured using Nilsson 400, 4 pin resistance meter and the moisture content was measured from the concrete powder removed from the specimen. The current passing to the steel, the electrical resistivity of concrete and the moisture content of concrete were measured twice a week. The measurement was continued until a very negligible current was passing to the steel.

4.3.4 Depth Effect on Cathodic Protection Criteria

4.3.4.1 Test Specimens

Fig. 4.19 shows a typical specimen for evaluating the depth effect on CP criteria. Two mat reinforcements were used in the specimen; the top mat comprises 25 percent of the total reinforcement. The slab was 18 in x 12 in x 6 in in size and

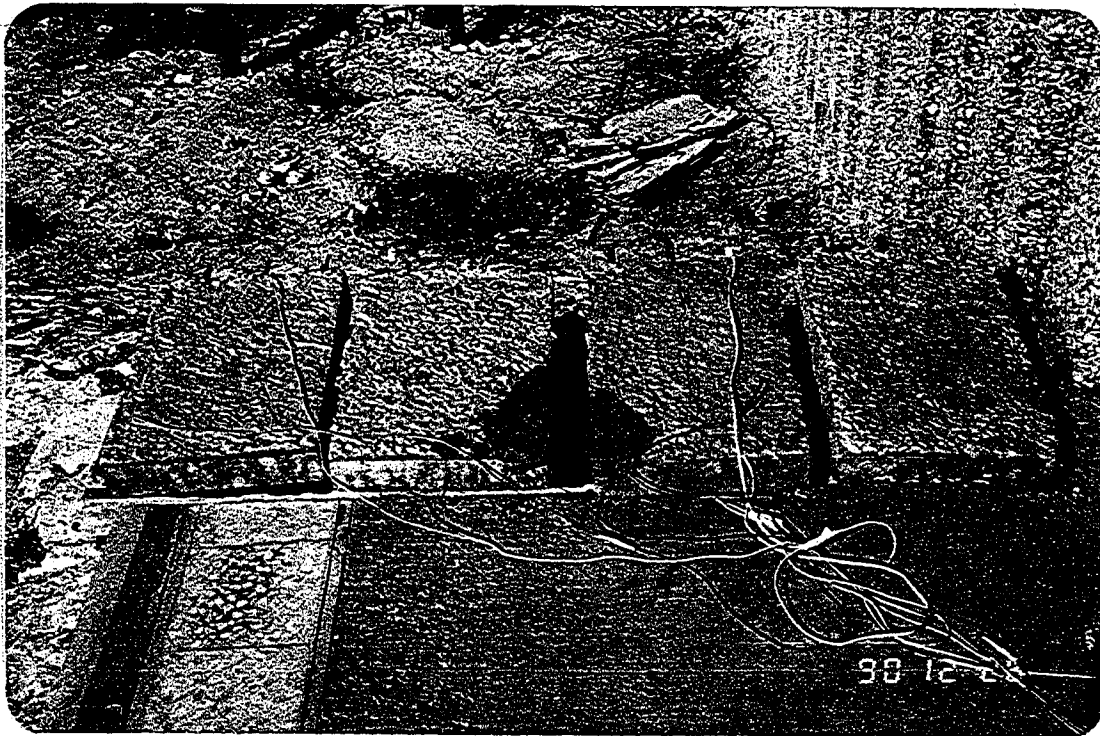


Fig. 4.18 Specimens at Outdoor Exposure. These Specimens were Used in Study on Possible Difficulties of CP Application at High Temperature-Dry Weather Regime

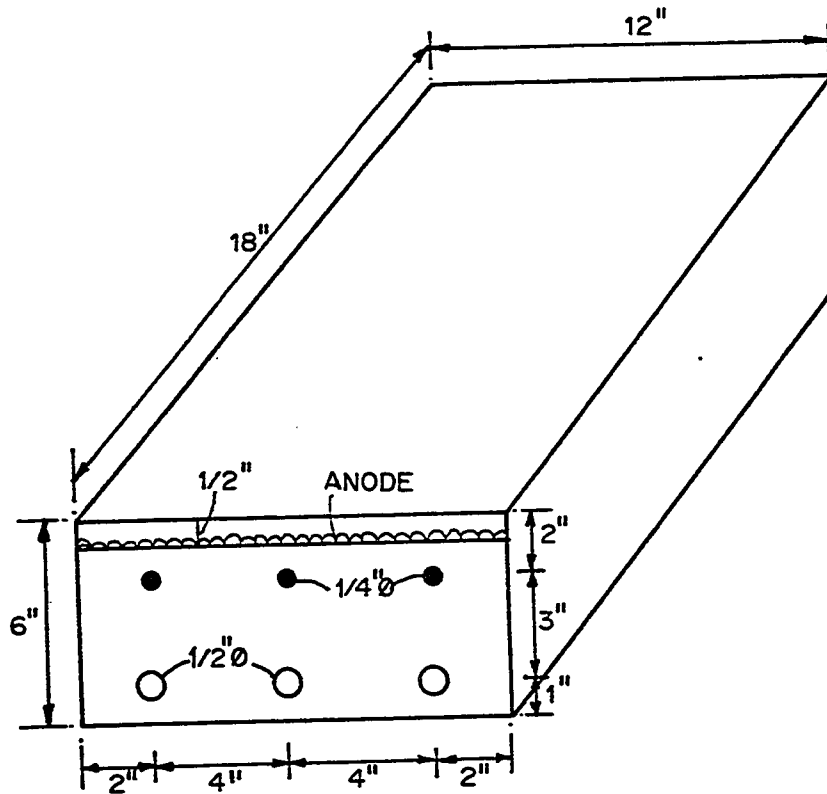


Fig. 4.19 A Typical Specimen with Two Mat Reinforcement Arrangement for Depth Effect Study

the top mat reinforcements comprises 3 bars, 1/4 in (6 mm) dia, 20 in long with 16 in embedded inside the concrete. The bottom mat also comprises 3 bars, 1/2 in (12 mm) dia, 20 in long with 16 in embedded inside the concrete. A set of three coupon bars, 6 in long 1/2 in (12 mm) dia, were tied with the three bottom mat steel bars and another set of three coupon bars, 6 in long 6 mm dia, were tied with the three top mat steel bars. Cylindrical macrocells as described in section 4.2.1.1 were used here for simulating the actual corrosion condition in the specimen. In each of the specimen, six macrocells were used, three of them at the top mat level and three at the bottom mat level. The macrocell steel and the main steel were of the same 6 mm and 12 mm diameters and they were placed at the same level. These macrocells were cast prior to the casting of the main specimen and then positioned in the mold one day before casting of the main specimen. The concrete mix used in casting the macrocell was exactly similar to that used in casting the main specimen. Electrical continuity was attained for all of the three main bars constituting top reinforcement using electrical wires. Bottom mat reinforcements were also made electrically continuous in the same manner.

Concrete specimens were cast with a Type V portland cement using a w/c ratio of 0.56, cement content of 550 lbs/ yd³ (327 kg/ m³) and a coarse to fine aggregate ratio of 1.43. Coarse aggregate was crushed limestone with a bulk specific gravity of 2.42 and absorption of 3.8 percent. Beach sand with a specific gravity of 2.70 and absorption of 0.25 percent was used as fine aggregate. Aggregates were washed to remove contamination and dust. Concrete was mixed in a 1/2 ton mixer. ICI H8 tectrode anode used here was properly positioned during casting. A 1/2 inch (12.7 mm) concrete overlay for the anode was used in all of the specimens. The specimens were demolded one day after casting and were

then covered with wet towel for curing. For continued curing, water was sprayed on the specimen regularly several times a day upto 28 days from the date of casting. Curing by immersion in water was not used to avoid chloride being washed out from the specimen to the surrounding water. The specimens were covered by wet towels throughout the observation period to facilitate CP application.

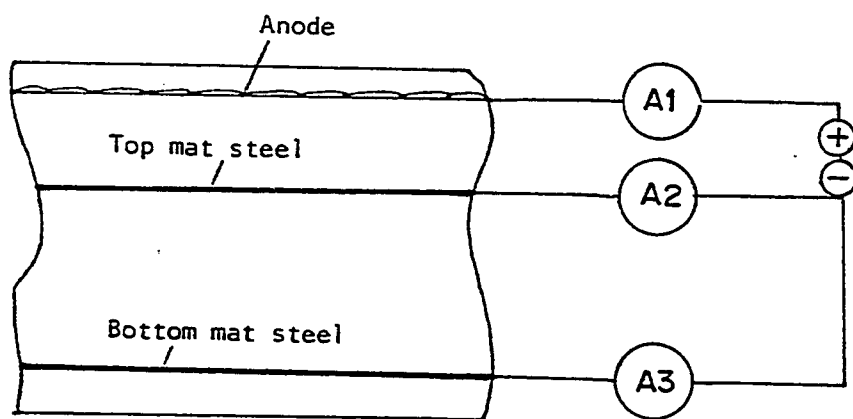
NaCl was added with the mix water in an amount equivalent to 32 lbs/yd³ of concrete. Two sets of specimens were cast. The macrocell chloride contents were 48 and 96 lbs/ yd³ of concrete in the first and second sets respectively.

4.3.4.2 Approach to the Study

The current reversal technique used here for depth effect study was exactly same as described in section 4.3.2.2 for chloride effect study. The specimens were subjected to CP current 14 days after casting.

Establishment of CP Criteria for Proper Protection: The total current passing to the individual circuit was divided to feed both the top and the bottom mats. The total circuit current as well as the top and bottom mat currents were measured using high precision ammeter connected in series as shown in Fig. 4.20.

Top Mat Protection Only: Using the current reversal technique, protection level of the top mat was achieved first. At this condition, the total current passing to an individual specimen as well as the top and bottom mat currents were recorded. The current supply was switched off and the steel potentials for top and bottom mat reinforcements were measured immediately using the potential wheel data logger. The potentials measured in this manner are recorded as instant off potential values. The steel to electrolyte potentials were measured 4 hours after



A_1 measures the total current

A_2 measures the top mat current

A_3 measures the bottom mat current

Fig. 4.20 Schematic of the Measurement of Total Circuit Current, Top Mat Current, and Bottom Mat Current in a Two Mat Reinforced Concrete Slab

switching off the CP current. The difference between the instant off potential and the potential measured 4 hour after switching the system off was recorded as the decay potential. The difference between the static potential (measured from control specimen) and the instant off potential is the shift potential.

Bottom Mat Protection and the Overprotection of Top Mat: Current reversal technique was used again to achieve the protection level of the bottom mat. The total circuit current as well as the top and bottom mat current were measured. The instant off potential, the 4 hour decay potential and the shift potential were measured for both of the top and bottom mat steel. The higher current density received by the top mat in the process of providing adequate protection to the bottom mat was recorded as the overprotection current density and the higher potential value of the top mat steel were noted as overprotection potential values.

4.3.5 Enhancement of Alkali-Silica Reaction Due to Cathodic Protection

The increased degradation of concrete caused by increased alkali-silica reaction due to CP current was observed in this part of the study.

4.3.5.1 Test Specimens

The specimens were 10.5 x 4 x 2.5 in (267 x 102 x 63 mm) in size and a single steel bar of 12 mm diameter was embedded in the mortar specimens (Fig. 4.14). Cement mortar specimens were cast with reactive crushed pyrex glass as aggregate. Type V ordinary portland cement was used with cement to aggregate ratio of 1.0 and water to cement ratio of 0.40. Alkali content of the mix was 1.2 percent(Na_2O) equivalent, by weight of cement. Of this 1.2 percent, 0.4 percent was

Table 4.1 Comparison of the Grading Used in the Research Program
and the Grading Used by Others (81, 82)

Sieve No		Weight, % of Total Aggregate			
Passing	Retained on	ASTM C-227	Mehta et al (82)		In the Proposed Research Program
			Alternate 1	Alternate 2	
# 4	# 8	10	-	-	-
# 8	# 16	25	-	-	10
# 16	# 30	25	-	20	40
# 30	# 50	25	100	40	40
# 50	# 100	15	-	40	10

the base alkali present in cement and NaOH was added with the mix water to provide the equivalent amount of 0.8 percent Na_2O . Table 4.1 shows the grading of the aggregate used in the test program and the grading used by others (81,82). ICI Tectrode anode was placed 3 in (76 mm) away from the steel reinforcement during casting of the specimen. The specimens were demolded one day after casting and cured under water for 7 days. Some of the specimens were kept as control (no CP current applied). Also for comparative purpose, a number of specimens were cast with non-reactive sand as aggregate and using the same mix as adopted for casting the reactive mortar specimens. These specimens were also demolded 24 hours after casting and cured under water for 7 days. These specimens were then kept as control (never received current).

4.3.5.2 The Approach to the Study

The specimens were supplied with CP currents 8 days after casting. CP current densities of 20 and 100 ma/sq. ft were maintained throughout the observation period. The current supply unit is the same as described in Art. 4.1.2. The variable resistors and the variac were used to maintain the constant current density in each of the specimen. The specimens were kept in hot and humid environment which is suitable for accelerated alkali-silica reaction (81, 83).

The following observations were made in the alkali-silica reaction study

Appearance of the First Crack: The appearance of crack on CP specimens as well as on the control specimens were observed. The crack in the control specimens also appeared but at much later date. The CP was continued till 15 days after the first sign of crack appeared in the control specimen.

Total Expansion at Failure: The demec gauge was used to measure the total expansion between two demec disks originally placed 2 inch apart.

Compressive Strength of Mortar: After the observation period, the specimens were cut into pieces. 1/2 inch concrete cubes were cut from three locations: near the steel, near the anode and at a location at midpoint between the steel and anode. A large number of concrete cubes were cut from all of the CP specimens and were tested for compressive strength.

Hardness Number of Mortar: In absence of a proper technique of measuring concrete hardness, Rockwell hardness test (84) was used here to determine the relative hardness of mortar. Small plates of mortar, 2.5 in x 1 in x 0.125 in in size, were cut from the CP specimens as well as from the control specimens. The hardness was measured at three locations of the mortar plate, close to the steel, close to the anode and midpoint of steel and anode.

Properties of Steel: After the observation period, the steel embedded in the mortar was taken out and tested for ultimate strength, ductility and rupture strength. This was done for the CP specimens as well as for the control specimens.

Volume of the Gel Formed: Simple staining technique (85) was used to determine the volume of gel formed under the action of CP current as well as in absence of CP. Powdered samples were taken from near the steel and absorbance of the samples were determined using simple staining technique. This absorbance is the indication of the volume of gel formed.

Scanning Electron Microscopy Analysis: Small amount of solid sample was taken out from near the steel of the CP specimen as well as the control specimen for scanning electron microscopy analysis. The photographs taken by SEM technique show the gel structure formed due to alkali-silica reaction. These results were then compared with the standard alkali-silica gel structure found in cement paste by others(86,87).

4.3.6 Degradation of Steel-Concrete Bond Due to Cathodic Protection

4.3.6.1 Test Specimens and Bond Test Methods

Concrete specimens were cast with a Type V portland cement using a w/c ratio of 0.56, cement content of 550 lbs/ yd³ (327 kg/ m³) and a coarse to fine aggregate ratio of 1.43. Coarse aggregate was crushed limestone with a bulk specific gravity of 2.42 and absorption of 3.8 percent. Beach sand with a specific gravity of 2.70 and

absorption of 0.25 percent was used as fine aggregate. Aggregates were washed to remove contamination and dust. Chloride contents of 2 and 8 lbs/ yd³ (0.364 and 1.455 percent by weight of cement) were added to concrete as sodium chloride (NaCl) through mix water. Concrete was mixed in a 1/2 ton mixer. The specimens were demolded 24 hours after casting, and were cured under water for 28 days. After 14 months of impressed current, the cathodically protected specimens along with control specimens were tested for bond strength. The cantilever bond test method adopted in this study necessitated the use of a special bond specimen. Also, the test specimen was designed to fail in bond only. To avoid shear failure in plain concrete at the point of bond breakdown, open stirrups completely detached from the main reinforcement were positioned in the section. This ensures that the stirrups do not interfere with the impressed current as well as with the bond behavior of the main reinforcement. In addition to shear failure considerations, sufficiently low percentage of longitudinal reinforcement was used to avoid concrete compression failure. Pilot tests were carried out to choose such an embedment length that the bar tensile stresses at the point of bond failure were well below the yield value of the Grade 60 deformed steel used in the specimen. For each specimen 7 in (178 mm) length of the bar at one end was inserted in a brass conduit of slightly larger diameter, which was withdrawn before the concrete had hardened. The conduit length was selected to provide the required 4 in (102 mm) embedment exposed to concrete. Typical test specimen showing the location of the main and shear reinforcements as well as the anode is shown in Fig. 4.21.

The schematic of the cantilever bond test is shown in Fig. 4.21. As opposed to the traditional pullout test, both external shear and bending moment are present in the cantilever test, with concrete and steel experiencing similar tensile strains. Such a

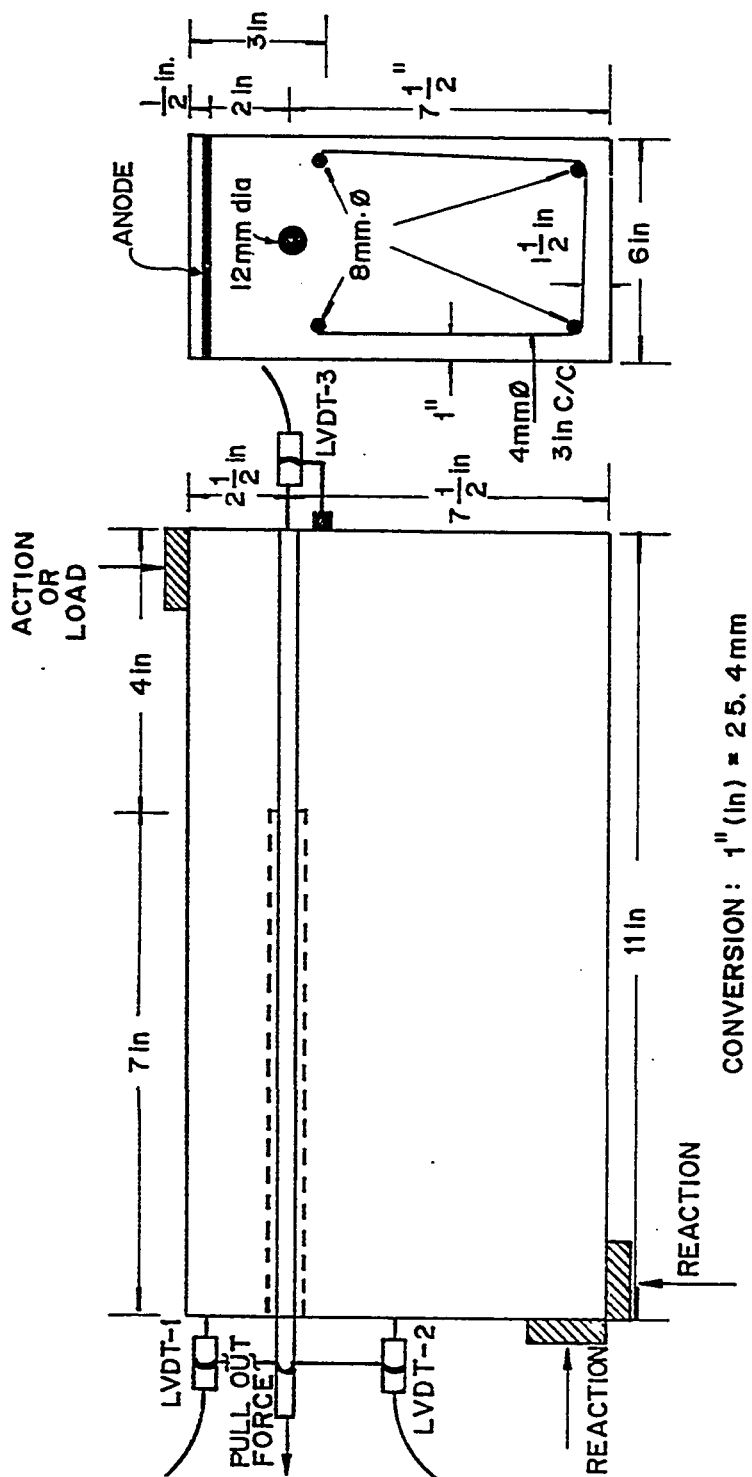


Fig. 4.21 Schematic of a Typical Specimen Used in Bond Study also Showing Loading Arrangement for the Cantilever Method of Testing for Bond Strength

test method, therefore, is more representative of the actual bond stress situation existing along the steel-concrete interface in reinforced concrete flexural members. A special loading frame was designed and fabricated which was positioned in a universal testing machine. Using two LVDTs at the loaded-end and one LVDT at the free-end, the load and the corresponding loaded-end and free-end slips were recorded by an automatic data logging system (Fig. 4.22). For each current density, two test specimens and two control specimens were tested for bond strength and the average values have been used in the interpretation of results. Test and control specimens were made from the same batch of concrete.

4.3.6.2 Approach to the Study

Cathodic protection current was applied to each specimen immediately after removing it from the curing tank. The current supply unit was same as described in Art. 4.1.2. The potentiometers were adjusted twice a week to maintain a predetermined current level. The activation was continued for 14 months. Table 4.2 shows an operational current- steel potential relationship for specimens with 2 and 8 lbs chloride/ yd³ (1.19 and 4.76 kg/ m³) of concrete at a particular activation period. It may be noted that the relationship between the current density and the "instant off" potential, as well as the decay potential is not constant, but changes with the activation period.

Four constant current densities of 3, 10, 20 and 50 ma/ ft² (32.3, 108, 215 and 538 ma/ m²) at the steel surface were used in the test program which also include chloride content of concrete as the second variable. Of the four current densities used in the test program, 03 ma/ ft² corresponds to a level usually used to satisfy

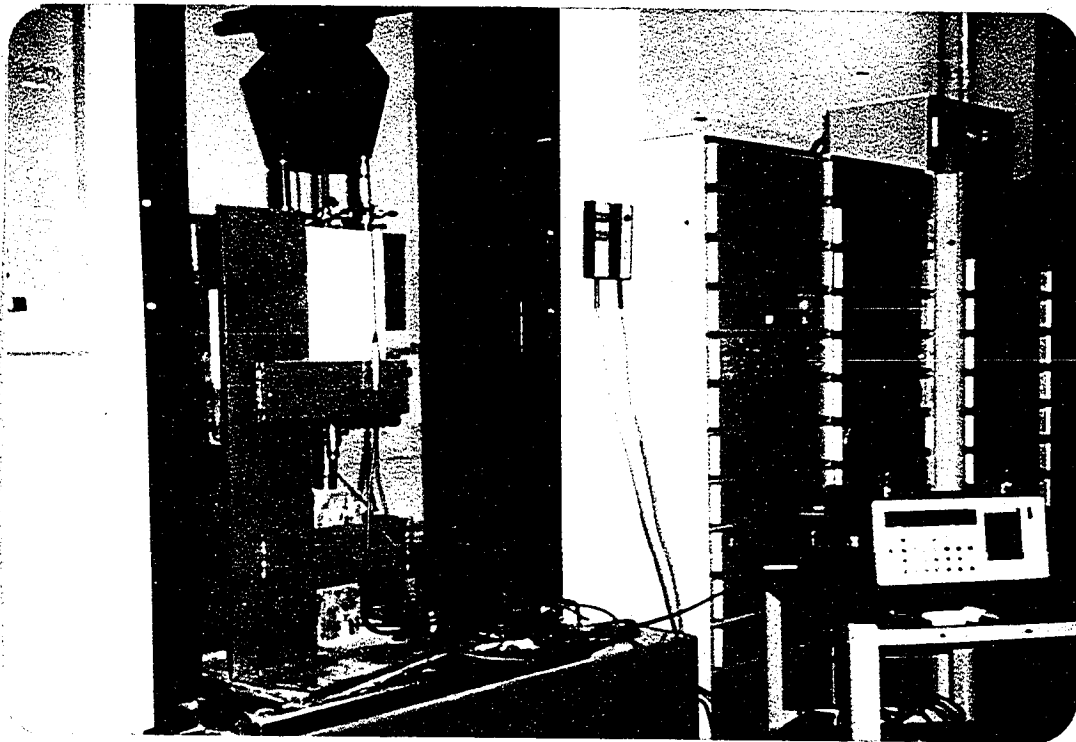


Fig. 4.22 Cantilever Bond Test in Progress with Loading Frame Positioned in the Testing Machine

Table 4.2 A Current-Potential Relationship at a Particular Activation Age

Current Density, ma/sq ft	Chloride Content of the Specimen, lbs/cu yd of Concrete			
	02		08	
	Instant off Potential, mV Ag/AgCl	Four Hour Decay Potential, mV	Instant off Potential, mV Ag/AgCl	Four Hour Decay Potential, mV
03	500	144	590	152
10	706	376	765	270
20	864	390	934	400
50	1634	1050	1995	1130

the existing CP criteria (54,72), whereas the other three values (10, 20 and 50 ma/ft²) may correspond to situations of overprotection of steel in concrete.

It may, however, be noted that in some chloride corrosion situations CP current densities significantly higher than 03 ma/ft² may be needed to provide adequate protection. For example, such a situation may arise in structures with high chloride gradients, or in the case of two-mat slabs containing primary chlorides in the original mix, where depth effect between anode near the top surface and the bottom mat reinforcement necessitates higher CP current densities to protect the bottom reinforcement. It has been observed that in a high chloride gradient situation, when the bottom mat had to be protected through an anode near the top surface in a two mat reinforced slab, a current density as high as 9 ma/ft² (97 ma/m²) was required to adequately protect the reinforcement against corrosion. Thus a current density of 10 ma/ft² may cover such extreme case of cathodic protection. The current densities of 20 and 50 ma/ft² have been used to cover overprotection situations as well as to accelerate possible interface bond deterioration effect for results within a reasonable time frame. Discounting a significant change in the basic mechanism of bond degradation at concrete steel interface under high current densities, a given loss of bond caused by a certain ampere-hour/ft² may be converted to give a reasonable estimate of the time required to cause the same order of bond loss at a practical value of CP current density.

4.3.6.3 Chemical Analysis

After the completion of the bond test on each specimen, the steel bar was removed and inspected for the corrosion condition. Using a masonry driller, concrete powdered samples were obtained for testing from three locations; near the steel, near the

anode and midpoint of the steel and the anode. Chemical analysis for determining potassium (K^+), and sodium (Na^+), in concrete was performed by dissolving the concrete powder with acid; the solution was analyzed using atomic absorption as described by Perkin Elmer(88). Using acid extraction technique chloride concentration was determined by a microprocessor ion analyzer in conjunction with a solid-state chloride ion activity double junction reference electrode. The values obtained were regularly checked by titration using the Gran Plot method (89).

4.3.6.4 Determination of the Steel-Concrete Bond Deterioration Due to CP Current

Bond strength and chemical analysis results obtained from current treated specimens were compared with the corresponding values measured in the control specimens. The magnitude of the bond reduction was correlated to the current density and chloride content of concrete. The effect of current density on the accumulation of the cations near the steel surface and the migration of anions from the vicinity of steel surface were observed. The results obtained here may be used to suggest a current density that can be applied without causing significant steel-concrete bond deterioration in the conditions prevailing in the Gulf region.

CHAPTER 5

EXPERIMENTAL RESULTS AND DISCUSSIONS

5.1 DEVELOPMENTS OF RELATIONSHIPS BETWEEN CURRENT DENSITY, POLARIZATION PERIOD, PROTECTION POTENTIAL AND DEPOLARIZATION TIME

5.1.1 Current Density Needed to Satisfy Prevalent Cathodic Protection Criteria

Current density at the steel surface was varied from 0.25 to 15 ma/ft² with an increment of 0.50 ma/ft² in a 24 hour period. A constant current corresponding to a particular current density was maintained at the steel surface for 20 hours and the "current on" potential was measured using a potential wheel data logger. The supply was then turned off and the "instant off", the 4 hour decay and the shift potentials were measured. After 4 hours from the time the system was turned off, the specimens were activated again and treated for 20 hours with a constant current corresponding to a relatively higher current density. Steel potentials were measured again corresponding to this high current density and the process was continued till a current density of 15 ma/ft² was attained at the steel surface.

Fig. 5.1.1 shows the "current on", the "instant off", the 4 hour "decay" and "shift" potentials recorded at different current densities applied to steel in chloride free concrete. The data of this Figure demonstrate that increased protection potentials are attained on the steel surface at higher current densities. The minimum current density of 1.2 ma/sq ft is needed to satisfy the 100 mV decay criterion whereas the maximum

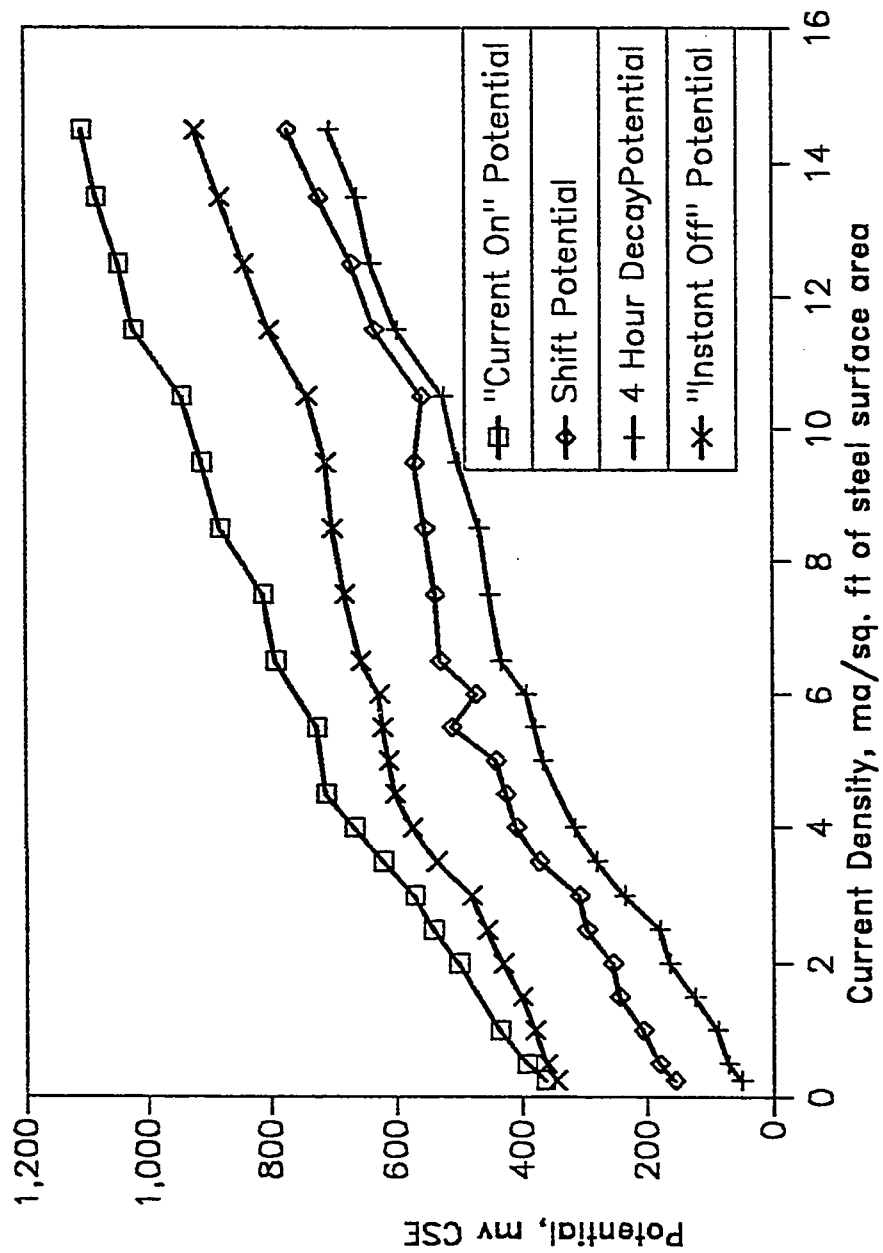


Fig. 5.1.1 Relationship of the Prevalent Cathodic Protection Criteria and the Current Density

current density of 14 ma/sq ft is required to satisfy the -850 mV CSE instant off potential criterion; for the 300 mV shift criterion an intermediate current density value of 3.2 ma/sq ft is needed. The findings here are in line with those reported by stratfull(54). Since the current density required to satisfy the 100 mV decay criterion is significantly lower than the current densities needed to satisfy either the -850 mV CSE instant off potential or the 300 mV shift from the base potential, the 100 mV decay criterion is regarded as the most acceptable amongst the available four CP criteria.

5.1.2 Polarization Period, Current Density and the Cathodic Protection Criteria

Current densities used in the test program are 1, 3, 20 and 60 ma/ ft² based on steel surface area. In reinforced concrete members, the first two values are commonly adopted in the application of normal CP criteria, whereas the later two values correspond to situations of overprotection for the reinforcing steel. Immediately after 7 days curing period, CP current was applied to the reinforcing steel. The potentiometers were adjusted on a weekly basis to maintain constant current flow in each of the specimens. The steel potentials vary only marginally along the length of the bar. To take this variation into consideration, for each specimen an average value of the series of potential readings for a particular scan is reported here. For specimens subjected to 1 and 3 ma/ ft² current densities, potential data for maximum polarization period of 45 days are available, whereas the potential data for the 20 and 60 ma/ ft² current densities were obtained for a prolonged polarization period of 136 days.

5.1.2.1 Instant Off Potential Value

Fig. 5.1.2 shows the relationship between the "instant off" potential value, the polarization period and the current density. The data show that "instant off"

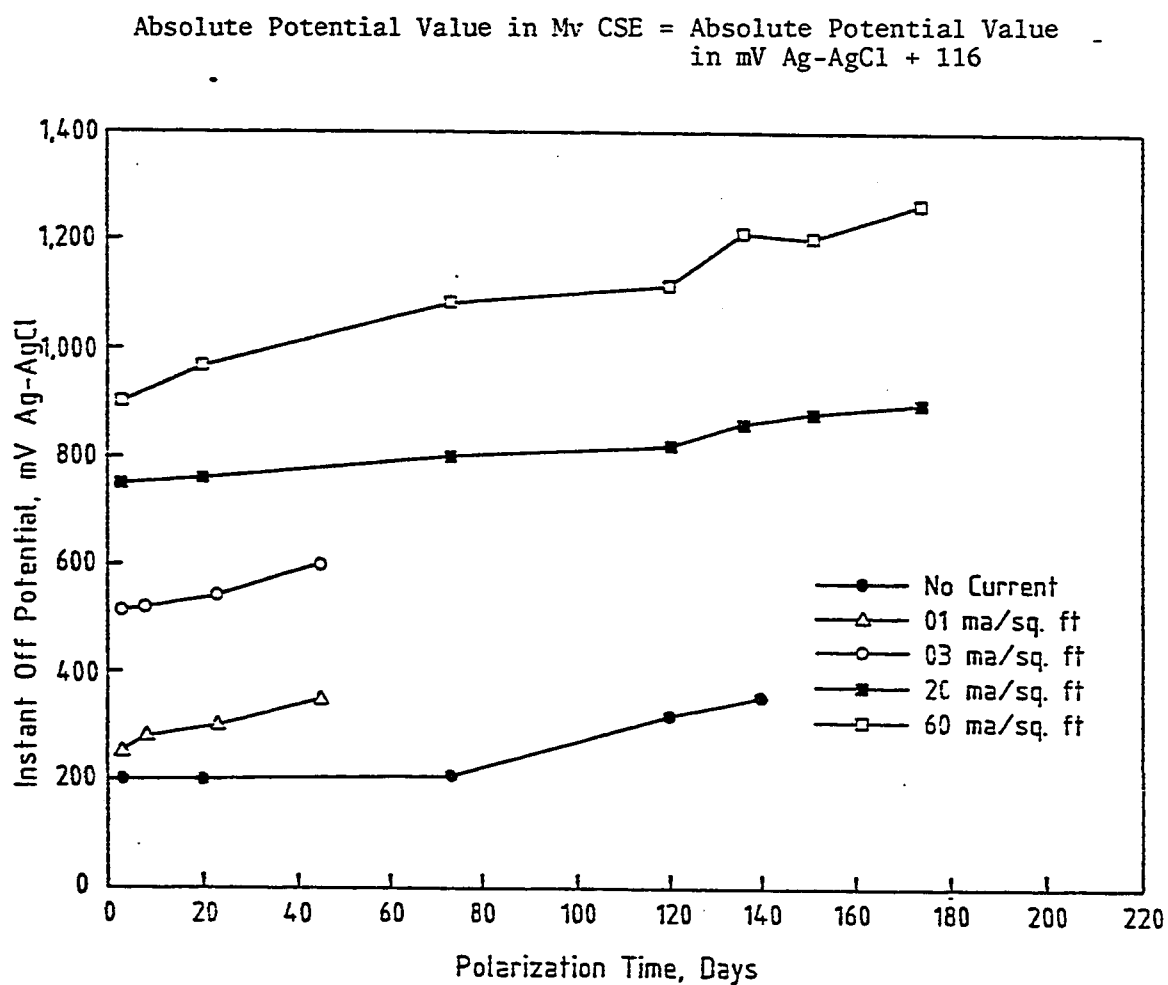


Fig. 5.1.2 Variation of Instant Off Potential with Polarization Period for Different Current Densities

potential varies with polarization period and current density. Variation of "instant off" potential with current density is clearly understandable in view of the fact that a higher current density causes increased polarization and consequently a higher "instant off" potential value would result. For a given current density, an increase in the "instant off" potential with an increase in the polarization period complicates the situation, because in CP practice a protection potential value is adopted irrespective of the polarization time. It is clear from Fig. 5.1.2 that to obtain a predetermined "instant off" potential value, an appropriately reduced current density will have to be used if reinforcing steel is to be polarized for a prolonged period.

At the initial stage of polarization, a current density much higher than 3 ma/ft² is needed for attaining an "instant off" potential value of -850 mV CSE (-734 mV Ag/AgCl); in fact, the data show that a high current density close to 15 ma/ft² may be needed to achieve a -850 mV CSE (-734 mV Ag/AgCl) "instant off" potential value. However, the trend of 3 ma/ft² curve in Fig. 5.1.2 indicates that a current density of 3 ma/ft² is likely to satisfy the "instant off" potential criteria if the steel is polarized for several months. Fig. 5.1.2 also suggests that the "instant off" potential value corresponding to 1 ma/ft² current density is very low(-250 mV Ag/AgCl at 3 days of polarization) and falls significantly short of the proposed -850 mV CSE (-734 mV Ag/AgCl) "instant off" potential criterion. The above discussion indicates that the commonly adopted current densities in the range of 1 to 3 ma/ft² would fail to polarize the reinforcing steel sufficiently to achieve the -850 mV CSE "instant off" potential criterion. In particular, a current density of 1 ma/ft² of the steel surface area may satisfy the -850 mV CSE "instant off" potential criterion only if the steel is polarized for years.

5.1.2.2 Decay Potential Value

Fig. 5.1.3 shows that the 4 hour decay potential value is also dependent on polarization period and current density. As polarization time increases, the 4 hour decay potential also increases. Higher current densities polarize the steel to a greater extent so that the depolarization level is also higher at higher current densities. After 7 days of polarization, a 1 ma/ft^2 CP current density provides insignificant (40 mV) decay potential in 4 hours. However, this low current density satisfies 100 mV decay criterion if reinforcing steel is polarized for at least 42 days. At 7 days polarization period, 3 ma/ft^2 current density provides 175 mV decay potential in 4 hours. These data support the contention that CP current in the range of 1 to 3 ma/ft^2 would satisfy the 100 mV 4 hour decay potential criterion. To obtain a decay potential of 100 mV or more at the very beginning of polarization, a current density of 3 ma/ft^2 , or even somewhat less, would be sufficient as against the fact that a current density of less than 3 ma/ft^2 would certainly not satisfy the -850 mV CSE "instant off" criterion at the beginning of polarization. These findings support Stratfull's (24) observations that the decay potential criterion would need significantly less current density compared to the "instant off" potential criterion. The low current density required to satisfy 100 mV decay criterion makes the decay criterion approach more attractive to the CP practitioners. High current density could exacerbate possible secondary deleterious effects such as reduction in steel concrete bond (26) and enhancement of alkali-silica reactivity (41) if reactive aggregates are present in concrete. Induction of these secondary deleterious effects would be greatly reduced and delayed if 100 mV decay criterion is adopted instead of -850 mV CSE "instant off" criterion.

Figs. 5.1.4 through 5.1.7 show the dependence of depolarized steel potential on the polarization period and the current density. These presentations show an asymptotic variation of the depolarization curves for all the four CP current

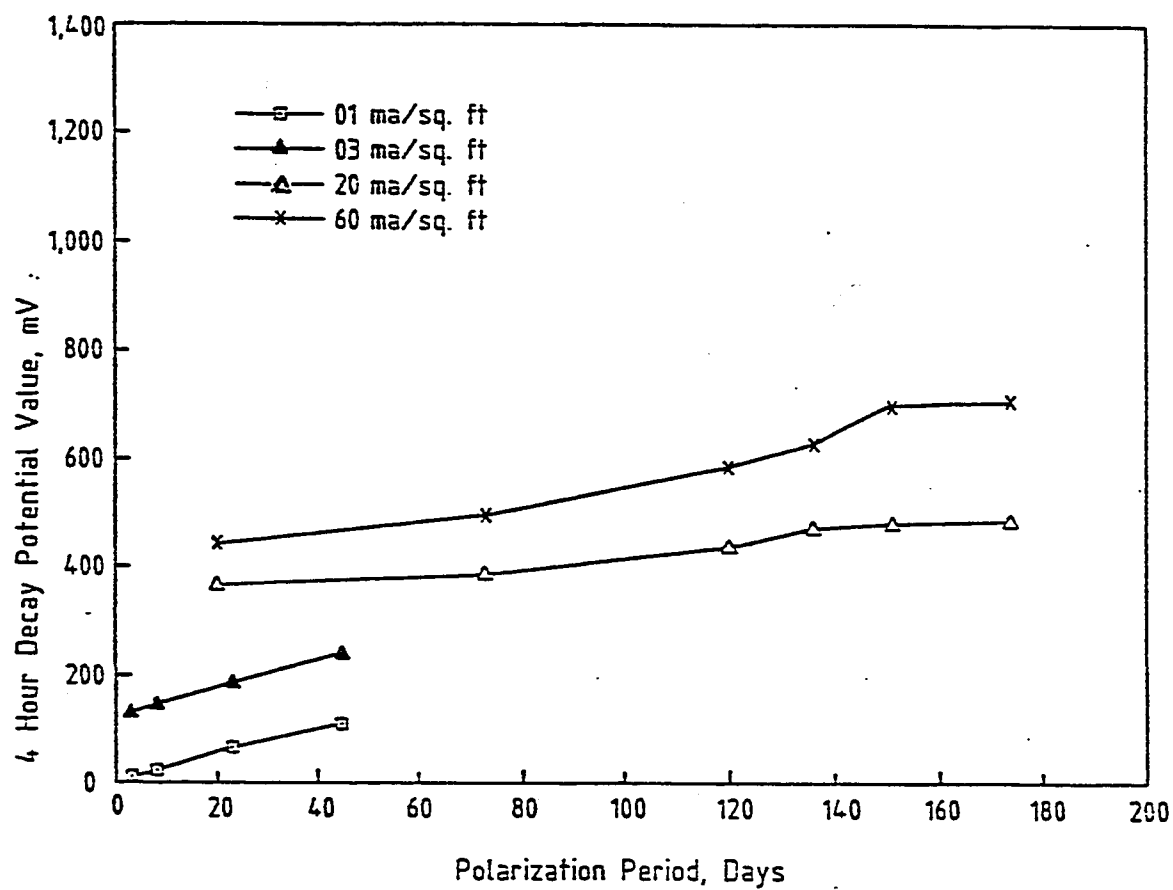


Fig. 5.1.3 Variation of Four Hour Decay Potential with Polarization Period for Different Current Densities

Absolute Potential Value in mV CSE = Absolute Potential Value in
mV Ag-AgCl + 116

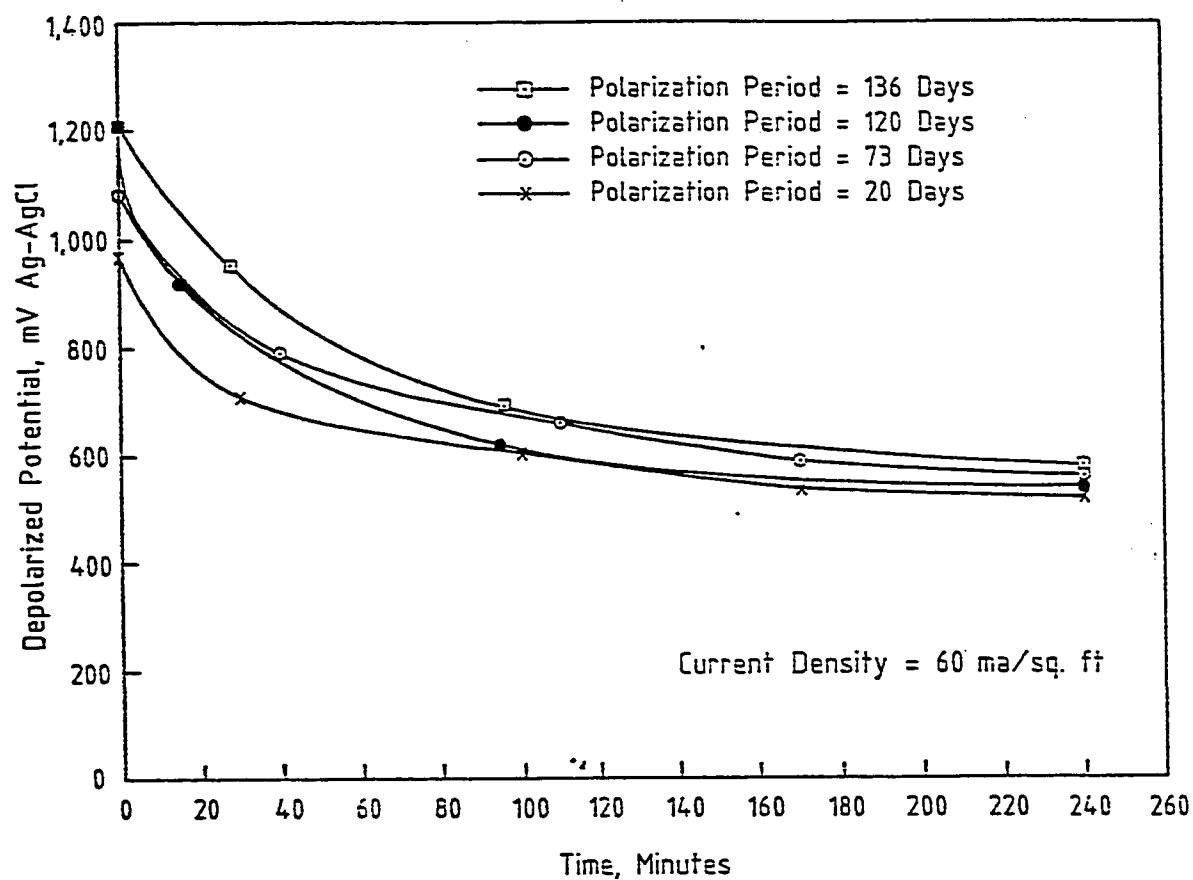


Fig. 5.1.4 Decay of Potential with Depolarization Time After Different Polarization Periods for 60 ma/sq ft Current Density

Absolute Potential Value in mV CSE = Absolute Potential Value in
mV Ag-AgCl + 116

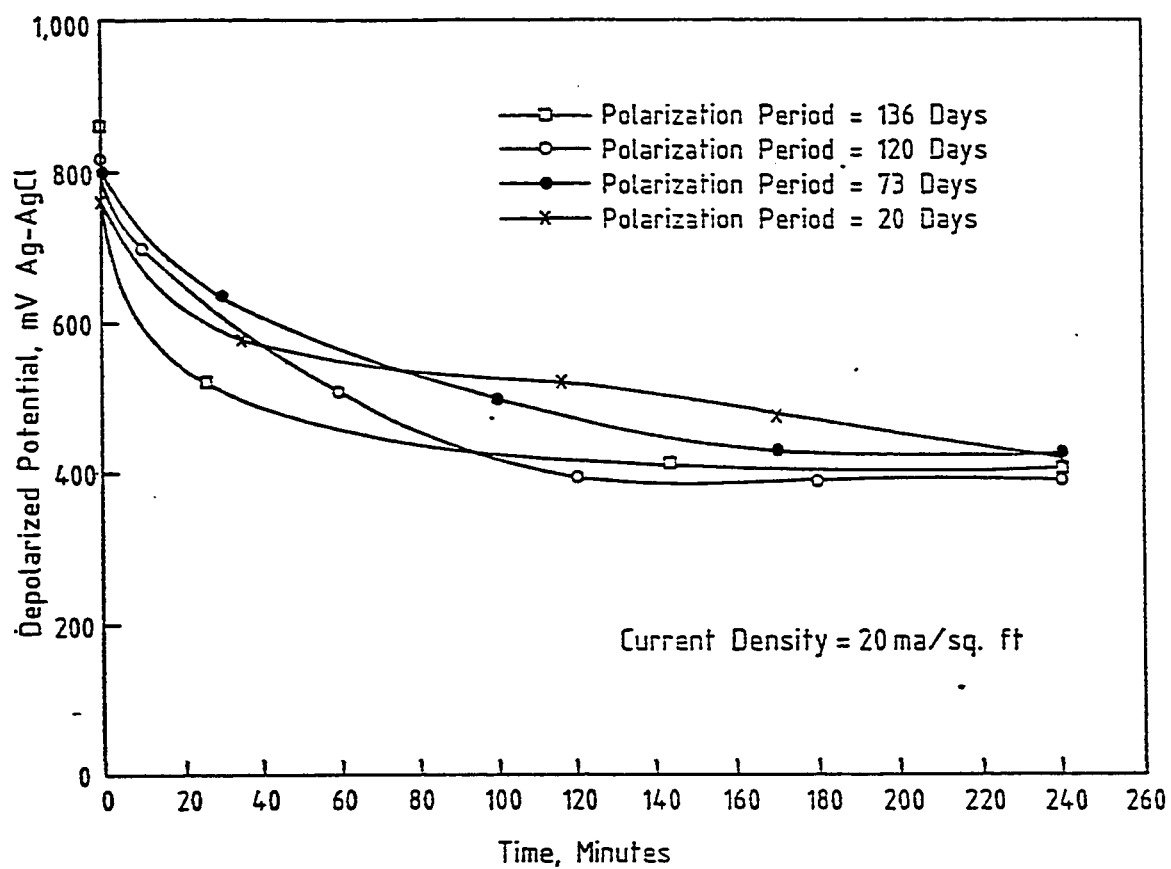


Fig. 5.1.5 Decay of Potentials with Depolarization time After Different Polarization Periods for 20 ma/sq ft Current Density

Absolute Potential mV CSE = Absolute Potential in mV Ag-AgCl
+ 116

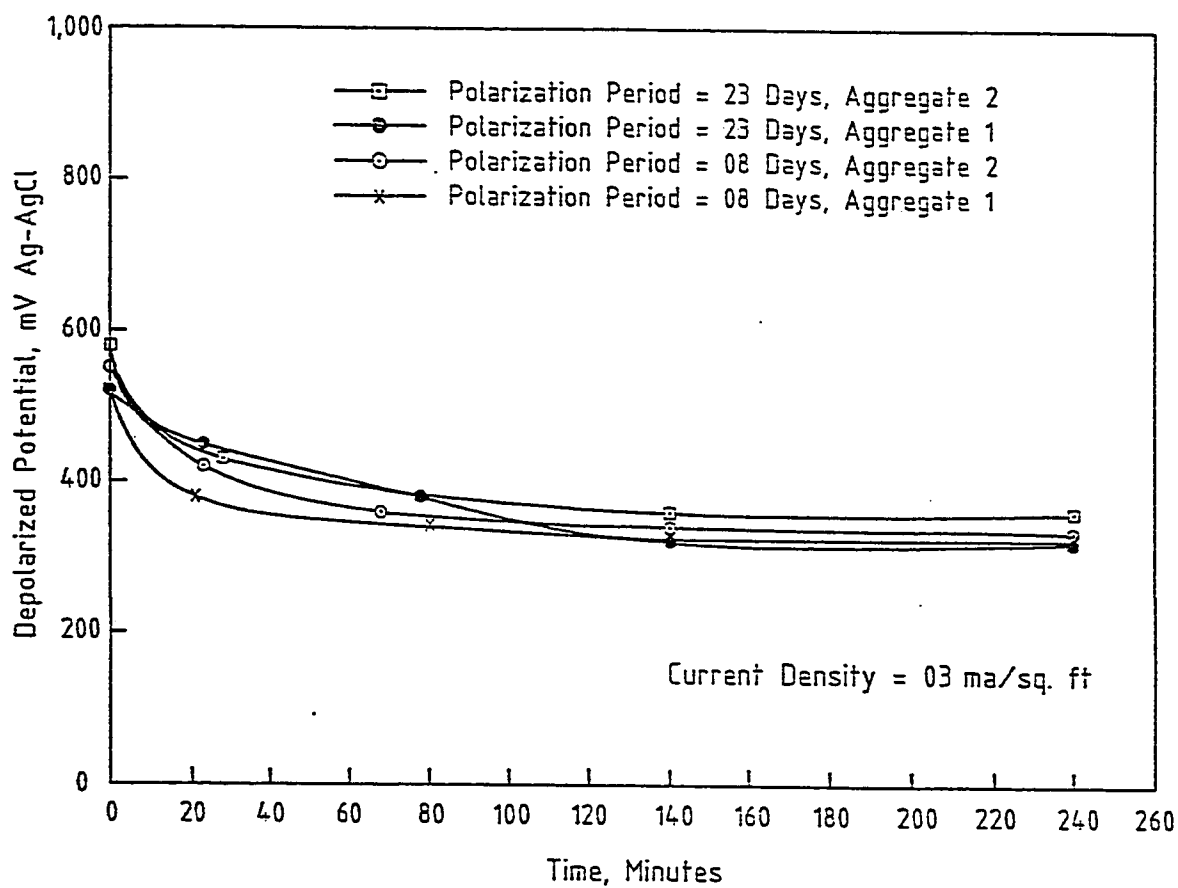


Fig. 5.1.6 Decay Potentials with Depolarization Time After Different Polarization Periods for 3 ma/sq ft Current Density

Absolute Potential in mV CSE = Absolute Potential in mV Ag-AgCl + 116

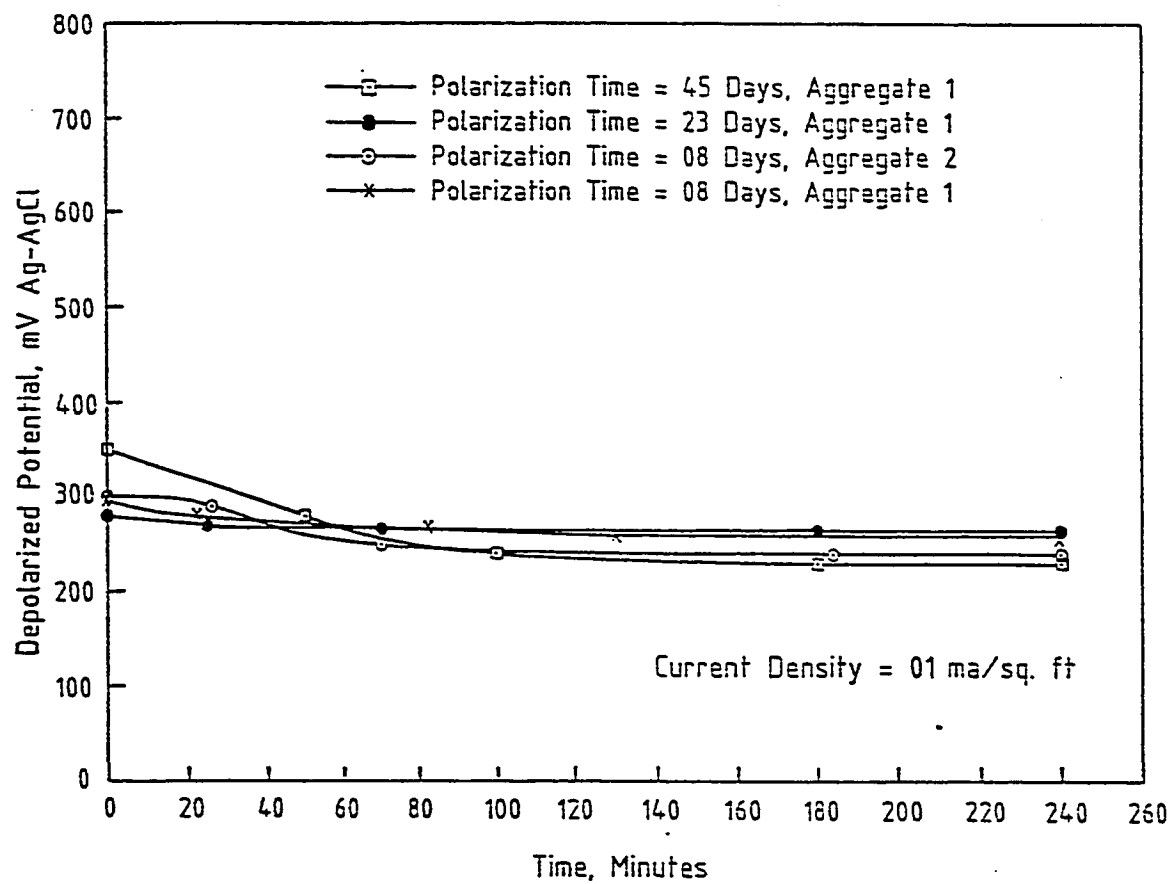


Fig. 5.1.7 Decay of Potential with Depolarization Time After Different Polarization Periods and Two Types of Aggregates for 1 ma/sq ft Current Density

densities. Complete depolarization of steel potential occurs at 70, 140 , 200 and 240 minutes after discontinuing the CP current for current densities of 1, 3, 20 and 60 ma/ ft² respectively. The dependence of a fully depolarized potential on current density is clearly shown in Figs. 5.1.4 through 5.1.7. For a three week polarization period, fully depolarized potentials were observed to be 240, 330 , 420 and 570 mV Ag/AgCl at current densities of 1, 3, 20 and 60 ma/ ft² respectively. However, the data of Figs. 5.1.4 through 5.1.7 show that the depolarized potential is by and large independent of the polarization period.

5.1.2.3 Effect of the Type of Aggregates

Figs. 5.1.6 and 5.1.7 show the influence of aggregate type on depolarization. Fine aggregates used have different specific gravities. Figs. 5.1.6 and 5.1.7 clearly show that the aggregate type has no effect on the "instant off" potential and decay potential values. "Instant off" potentials, decay potentials and the fully depolarized potential values are identical for the two types of aggregates used.

5.1.2.4 Polarization Period and CP criteria

It is clear from the discussion of the results presented in Figs. 5.1.2 through 5.1.7 that more rational CP criteria would be formulated if polarization period is included along with the instant off potential and the decay potential values. Steel polarizes due to the movement of ions from and toward the steel concrete interface. It is the current density which controls this ionic movement. Adequate protection as well as overprotection of steel are directly related to the movement of anions and cations between the negatively charged steel and positively charged secondary anode. The authors feel that it is more logical to develop CP criteria in terms of current density instead of steel potential values as used in CP practice.

5.2 EFFECT OF CHLORIDE CONTENT OF CONCRETE ON CATHODIC PROTECTION CRITERIA

Due to an uneven chloride distribution in a practical reinforced concrete structure, the steel reinforcement becomes anodic at some locations and cathodic at other locations. Anode develops due to high concentration of chloride at a particular location and the corrosion starts at the anodic site. The steel potential at the anodic site is lower (more negative) than that at the cathodic site. The potential difference thus developed causes the corrosion current to flow between the anode and the cathode. The anodic area corrodes and supplies electrons to the cathodic area. A practical corrosion situation due to chloride gradient is simulated in laboratory by inserting macrocell in the specimen; the chloride content of the macrocell was higher than that of the specimen. When the macrocell steel is connected to the specimen steel through a small resistor, both the macrocell steel and the specimen steel act together as a single system of reinforcement in the slab. The specimen achieves an uneven chloride distribution in this way; the chloride differential in the specimen is created by the difference in chloride content of the specimen concrete and the macrocell concrete. The chloride gradient in a specimen is the ratio of the chloride content of the macrocell concrete and the specimen concrete. Because of the high chloride presence in the macrocell, corrosion starts at the macrocell steel first. The macrocell steel becomes anodic and the specimen steel becomes cathodic in this situation. The steel potential of the macrocell is therefore lower than that of the specimen and it is this potential gradient which drives the corrosion current to flow between the macrocell steel

and the specimen steel when they are connected through an external resistor.

The results obtained in the study are analyzed by focusing on three factors: first, the effect of the absolute chloride content of the specimen, second, the effect of the chloride gradient, third, the effect of the chloride difference between the specimen and macrocell concrete. It is possible that the chloride gradient in a specimen is relatively higher whereas the chloride difference in the same specimen is relatively lower. Also a low chloride gradient may correspond to a high chloride difference in the specimen. For example, for 2-lbs chloride bearing specimen having 6 lbs chloride bearing macrocell, the chloride difference is only 4 lbs whereas the chloride gradient is 3.0. On the other hand, for 32 lbs-chloride bearing specimen having 48 lbs chloride bearing macrocell, the chloride difference is 16 lbs whereas the chloride gradient is only 1.5.

5.2.1 Voltage Drop Across the Resistor in the Control Specimen Which Never Received CP Current

Table 5.2.1 shows the effect of chloride content of concrete specimens and the chloride gradient on the voltage drop across the known resistor which connects the macrocell steel and the specimen steel. As the positive end of the voltmeter was connected to the lead wire from the specimen steel and the negative end of the voltmeter was connected to the lead wire from the macrocell steel, a positive voltage drop is indicative of the corrosion current flow between the macrocell steel and the specimen steel. Data of Table 5.2.1 show that the voltage drop across the resistor is dependent on both chloride content of the specimen and the

Table 5.2.1 Effect of Macrocell Chloride Content and Specimen Chloride Content on Voltage Drop Across the 51 ohm Resistor (Results Are Obtained from Contrl Specimen At the Age of 14 Days).

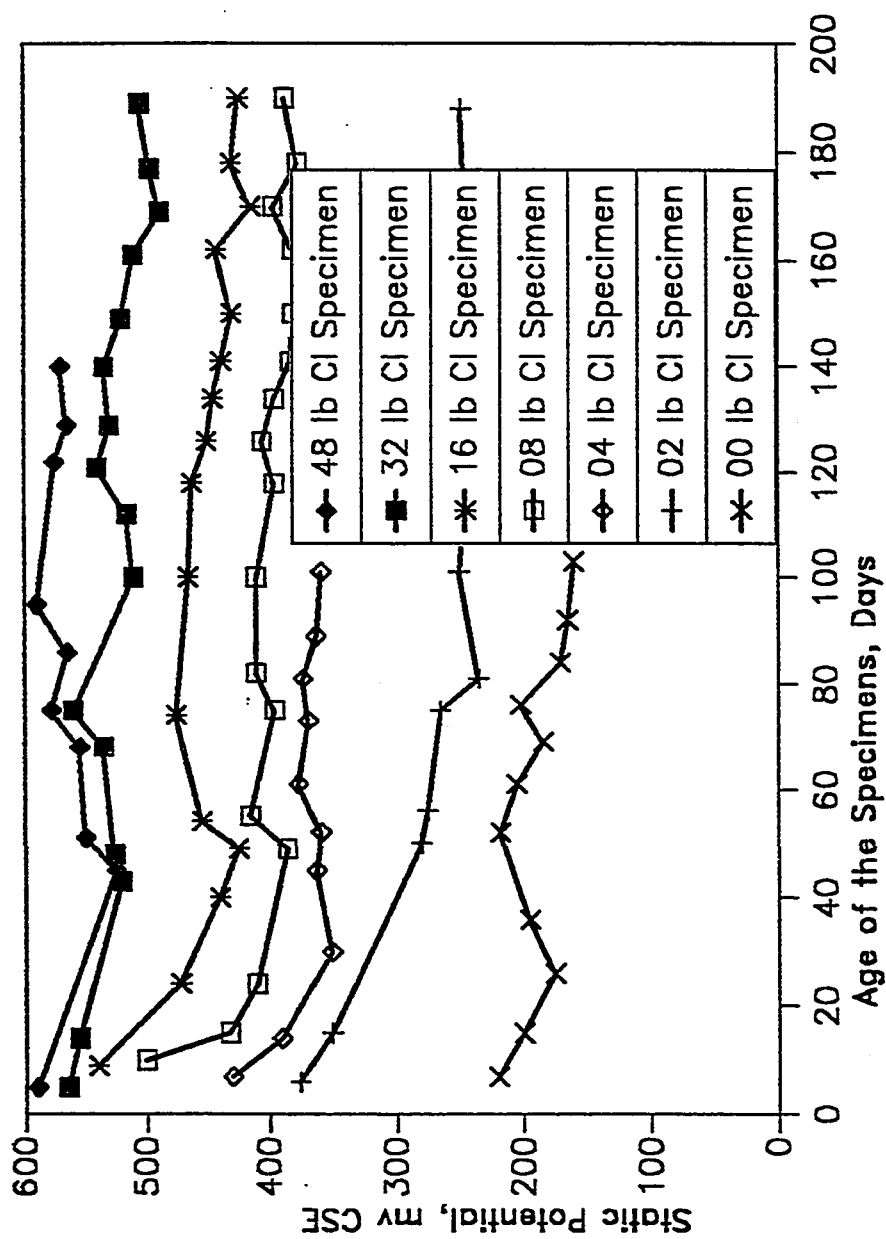
Specimen Chloride Content, lb/yd ³ of Concrete	Macrocell Chloride Content, lb/yd ³ of Concrete	Chloride Gradient Between Macrocell and the Specimen	Chloride Difference Between Macrocell and the Specimen, lb/yd ³	Ratio of Macrocell Steel Area to Specimen Steel Area	Voltage Drop Across the Resistor Which Connects the Macrocell Steel and the Specimen Steel
32	96	3.0	64	0.125	14.9
	64	2.0	32	0.125	8.36
	48	1.5	16	0.125	4.8
16	32	2.0	16	0.125	6.44
	24	1.5	8	0.125	3.12
8	16	2.0	8	0.125	5.84
	12	1.5	4	0.125	2.71
4	12	3.0	8	0.125	2.74
	8	2.0	4	0.125	2.50
2	10	5.0	8	0.125	3.86
	6	3.0	4	0.125	2.52
0	8	-	8	0.125	4.65
	4	-	4	0.125	3.65

chloride gradient. For a chloride gradient of 2.0, the voltage drop across the resistor was found to be 2.5, 5.84, 6.44 and 8.36 mV in the 4, 8, 16 and 32 lbs chloride-bearing concrete specimens respectively. For a particular chloride gradient, a higher voltage drop across the known resistors in high chloride contaminated specimen is attributable to the higher difference in chloride content of the specimen concrete and the macrocell concrete. For example, with a chloride gradient of 2.0, the difference in chloride content of the specimen and macrocell is only 4 lbs in 4 lbs chloride-bearing specimen whereas the value is 32 lbs for 32 lbs chloride-bearing specimen. Here the voltage drop in the latter case (8.36 mV) is significantly higher than the voltage drop (2.5 mV) in the former case. For a specified chloride content of the specimen, the voltage drop depends on the chloride gradient in the specimen. For example, in 32 lbs chloride-bearing concrete, voltage drops were found to be 3.8, 8.36 and 14.9 mV for chloride gradients of 1.5, 2 and 3 respectively. Higher voltage drop at higher gradient is attributable to the greater difference in the potentials of the macrocell steel and the specimen steel. A higher potential difference between the macrocell and the specimen steel drives a higher amount of current flow through the known resistor which connects the macrocell steel and the specimen steel. For 8 lbs chloride difference between the specimen and the macrocell concrete, the voltage drop in 0 lb specimen was found to be higher than that in 2 lbs chloride bearing specimen; this is because the potential difference between the steel embedded in 0 lb chloride bearing concrete specimens and 8 lbs chloride-bearing macrocell concrete is much higher than the potential difference between the steel embedded in 2 lbs chloride bearing specimens and 10 lbs chloride bearing-macrocell concrete. The voltage drop across the known resistor is dependent more on the chloride differential within the same specimen and less on the chloride content of the specimen. As an

example, for an 8 lbs chloride differential in 8 lbs- and 16 lbs- chloride bearing specimens, the voltage drop across the resistor in 16 lbs specimen is only 3.12 whereas the value is 5.84 for 8 lbs chloride bearing specimen. Because of the fact that the macrocell steel and the specimen steel were connected through known 51 ohm resistors in all of the specimens, the voltage drop is an indirect indicator of the flow of corrosion current between the steel in relatively higher chloride contaminated macrocell and relatively lower chloride contaminated specimen.

5.2.2 Static Potentials

The static potentials of steel for different chloride bearing specimens at different ages are shown in Fig 5.2.1. This Figure clearly shows the dependence of static potential on the chloride content of concrete; a higher static steel potential is measured in higher chloride-bearing specimen. All the curves show the highest static potential values initially which subsequently dropped to a slightly lower value and then continued to show a nearly steady trend. This is possibly because a passive potential of steel is obtained when a gamma ferric oxide film ($\gamma\text{-Fe}_2\text{O}_3$) forms around the steel. Due to the presence of excessive water in the specimen during the early ages, a significantly reduced oxygen ingress takes place to the steel interface which may not be sufficient for the formation of the gamma ferric oxide film. Subsequently, formation of this film around the steel surface at a later age due to the availability of sufficient oxygen around it lowers the static potential to a value smaller than the initial highest value. Static potential of the steel measured in the concrete specimens without chlorides always stayed in the range of -200 mV CSE which is numerically higher than -350 mV CSE, the Van Daeveer corrosion potential. For 2 lbs chloride bearing specimen (0.364 percent



Variation of Static Potential of Steel With Age of the Concrete Specimen

Fig. 5.2.1 Variation of the Static Potential of Steel With Age of the Concrete Specimen

by weight of cement), the static potential remained below the threshold corrosion potential(-350 mV CSE) value throughout the observation period. This suggests that the ACI chloride limit of 0.15 percent free chlorides by weight of cement (approximately 1 lb/ yd³ of concrete) as well as the B.S. total chloride limit of 0.4 percent by weight of cement (approximately 2.5 lbs/ yd³ of concrete) for the no corrosion situation can be safely adopted as the threshold chloride limit values in the concrete mix. The static potentials measured in the 4 lbs and higher chloride bearing specimens are found to be numerically lower than the corrosion potential, i.e., < -350 mV CSE. A passive potential, > -350 mV CSE, was never measured in 4 lbs and other higher chloride bearing specimens. This is presumably because when steel is embedded in concrete containing sufficient internal chloride salts, it is brought into contact with an aggressive chloride-rich environment right at the time of casting, before an effective passive film of gamma ferric oxide and a surrounding lime-rich zone of hydration products have had time to form. The direct dependence of static potential on the chloride content of concrete is possibly due to a higher degree of corrosion aggressivity in environments characterized by a higher chloride content of concrete.

5.2.3 Instant Off Potential

Figs. 5.2.2 and 5.2.3 show the instant off potential needed for overcoming the chloride gradients of 1.5 and 2.0. The data of these Figures clearly show the dependence of instant off potential value on the chloride content of the specimen as well as the chloride gradient. For a chloride gradient of 1.5, instant off protection potential values of 470, 525 and 620 mV CSE are required initially in 8, 16 and 32 lbs per cu. yds chloride bearing concrete specimens respectively, whereas

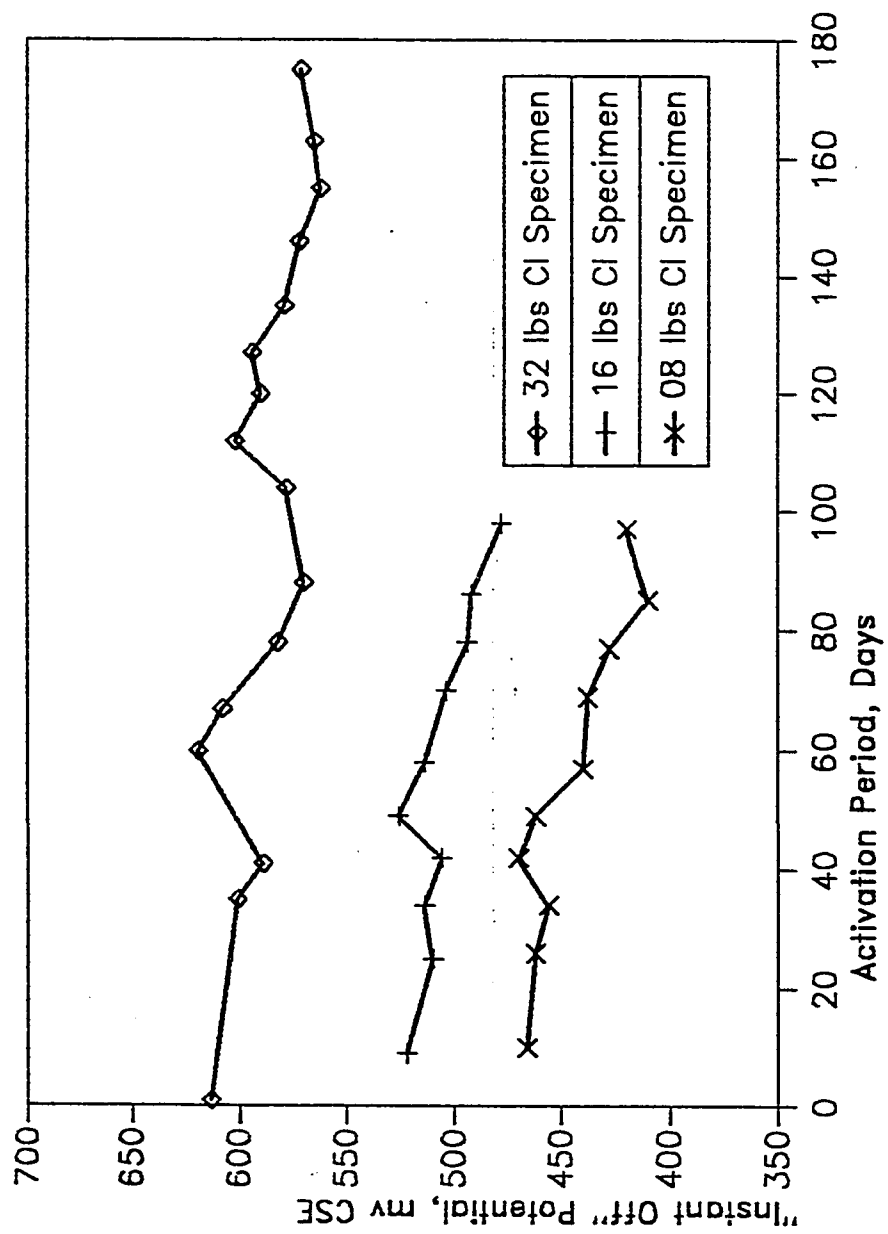


Fig. 5.2.2 Instant off Potential Needed to Protect Steel Embedded in Concrete Having 1.5 Chloride Gradient

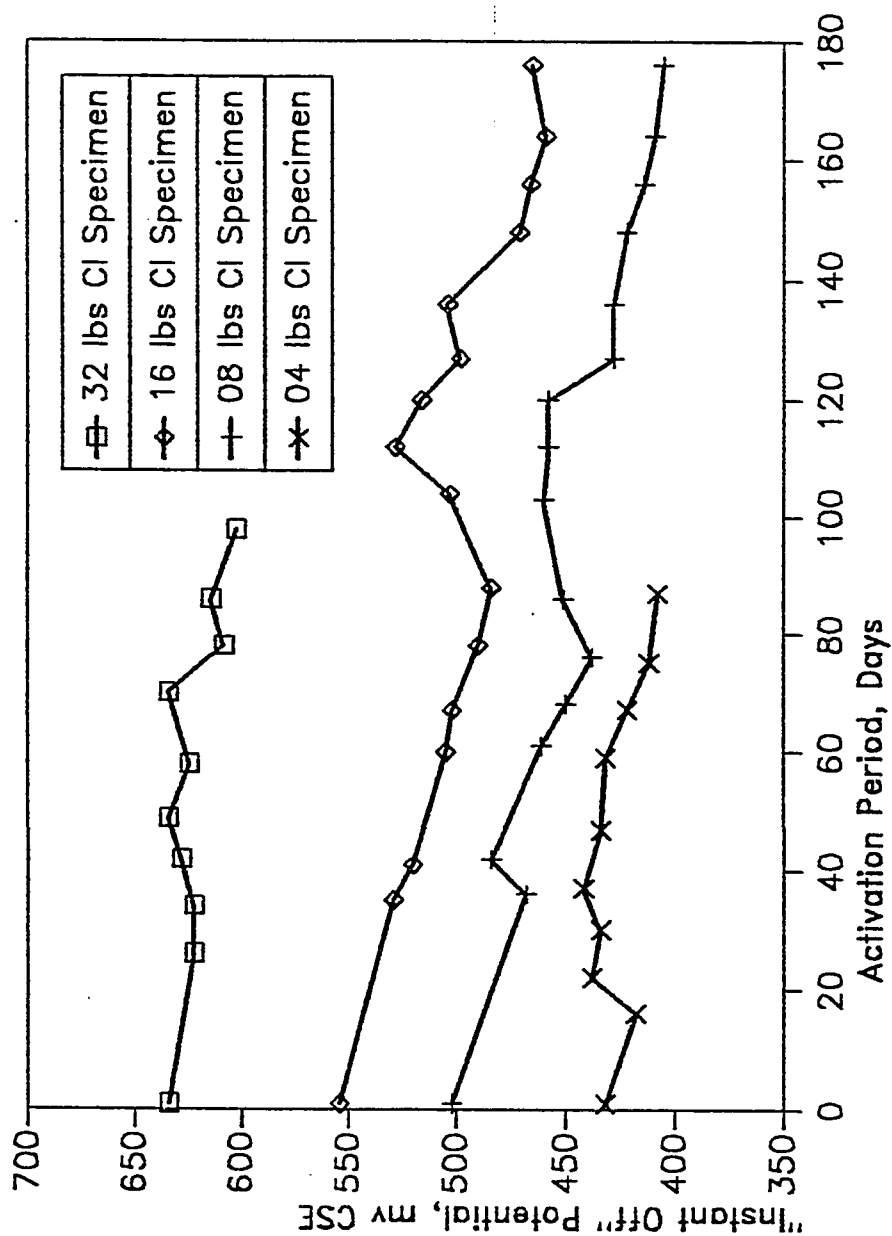


Fig. 5.2.3 Instant off Potential Needed to Protect Steel in Concrete Having 2.0 Chloride Gradient

for a macrocell to specimen chloride content ratio of 2.0, the corresponding protection levels are recorded to 505, 555 and 640 mV CSE. For a particular chloride bearing concrete, higher instant off protection potential is needed when the chloride gradient is higher. This is because of the fact that static potential of steel (Fig. 5.2.1) is found proportional to the chloride content of concrete. For a given chloride content in concrete, a higher difference in static potential between the specimen steel and the macrocell steel is noticed when the chloride gradient is higher. In a situation of higher chloride gradient, when the specimen steel and the macrocell steel are connected through an external resistor and the voltage drop across the resistor is measured by placing the positive end of the voltmeter to the resistors end connecting the specimen steel, and the negative end of the voltmeter to the resistors end connecting the macrocell steel, a higher positive voltage drop has been measured (Table 5.2.1). To cancel this higher voltage drop across the resistor, a higher current density is needed; a higher current density gives a high instant off potential reading. The direct dependence of instant off potential on the chloride content of concrete for a particular chloride gradient is ascribable to the higher static potential obtained for steel embedded in higher chloride-bearing concrete.

Fig. 5.2.4 shows the protection level needed for 4 lbs chloride difference between the specimen and macrocell. For a 4 lbs chloride difference, the instant off protection potential needed for 0 and 2 lbs specimens are more or less same. From the standpoint of higher chloride gradient existing in the 0 lb specimen compared to the 2 lbs chloride bearing specimen, a higher instant off potential is indicated for protecting the higher gradient 0 lb specimen. On the other hand, from the standpoint of higher chloride presence in the 2 lbs chloride bearing specimen compared to the 0 lb specimen, a higher instant off potential is needed to

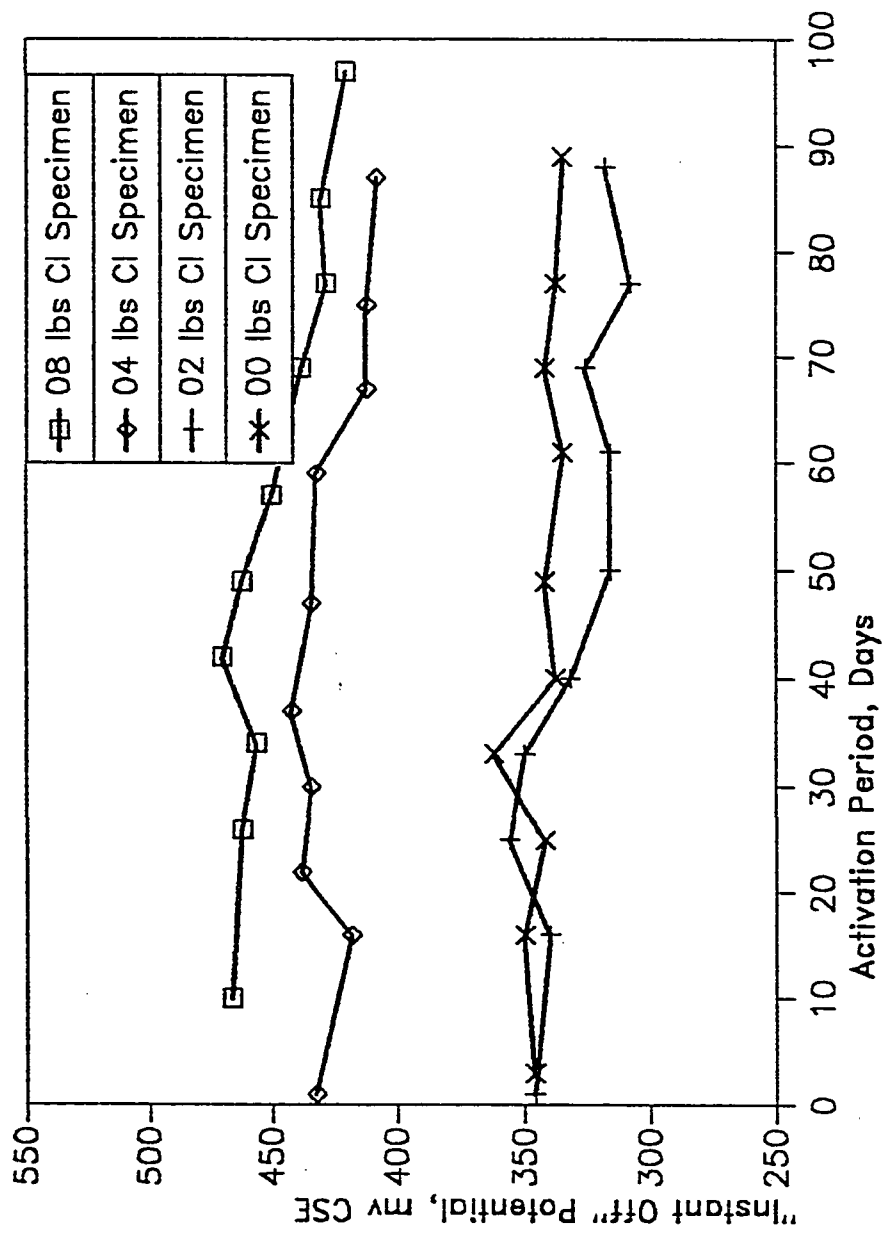


Fig. 5.2.4 Instant off Potential Needed to Protect Steel in Concrete Having 4 lbs Chloride Differential

attain protection in 2 lbs specimen. The same instant off protection potential needed for the 0 and 2 lbs chloride bearing specimens with 4 lbs chloride difference between the specimen and the macrocell suggests that the chloride gradient effect and the chloride level effect somewhat balance each other in this case. Instant off potential needed for the protection of 8 lbs chloride bearing specimen is higher than that needed for 4 lbs chloride bearing specimen. Although the chloride gradient in 4 lbs specimen being 2.0, is higher than that of 8 lbs specimen being 1.5, the higher instant off potential needed for protecting the 8 lbs specimen demonstrates that the effect of chloride level in the specimen is a dominant factor in this case. Moreover, whereas the static potentials measured in the 4 lbs chloride bearing specimen are slightly lower (more negative than -350 mV CSE) than the threshold potential, the static potential values measured in the 8 lbs chloride-bearing specimens are significantly more negative than the -350 mV CSE value. Due to this higher static potential of steel in 8 lbs chloride bearing specimen compare to the 4 lbs specimen and also due to a higher corrosion activity in the 8 lbs chloride-bearing specimen in comparison to 4 lbs specimen, higher instant off protection potential was needed for the 8 lbs chloride-bearing specimen.

Fig. 5.2.5 shows the protection level needed for 8 lbs chloride difference between the specimen and the macrocell. Here again, the instant off potential needed for protecting the 0 lb and 2 lbs specimens are found to be about the same. As explained earlier, possibly the effect of higher chloride gradient in 0 lb specimen in comparison to 2 lbs specimen is balanced by the higher chloride content of the 2 lbs specimen in comparison to 0 lb specimen. The protection potential values for 4 lbs specimen and 8 lbs-specimen are found to be similar with the exception of higher instant off protection potential value for 8 lbs specimen in

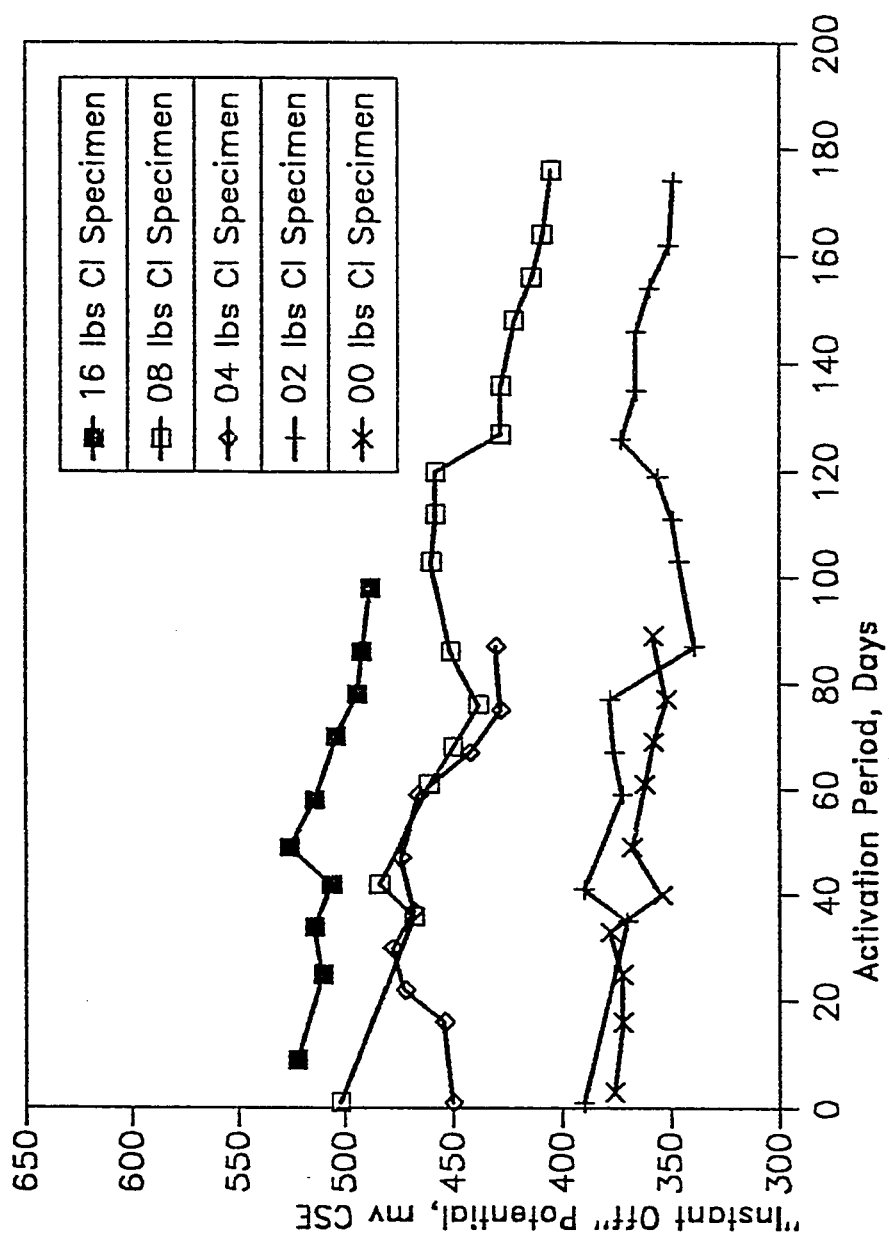


Fig. 5.2.5 Instant Off Potential Needed to Protect Steel in Concrete Specimens Having 8 lbs Chloride Differentials

comparison to 4 lbs specimen at the very beginning of the activation. In this case, the chloride gradients between specimen and the macrocell were 3 and 2 for 4 lbs and 8 lbs specimens respectively. The effect of high chloride gradient is again balanced by the effect of high chloride content of the specimen. The instant off protection values observed in the 16 lbs specimen are higher than those observed for the 2, 4 and 8 lbs specimens although the chloride gradient for the 16 lbs specimen is the lowest; it seems that the higher chloride level of 16 lbs/ yd³ in concrete is the dominant factor in producing the protection potential required. The higher corrosion activity and the higher static potential of the steel embedded in the 16 lbs chloride-bearing concrete, in comparison to the corresponding values in the 2, 4 and 8 lbs-specimens, are the two factors which control the instant off potential values measured in this case.

5.2.4 Four Hour Decay Potential

Fig. 5.2.6 shows the four hour decay potential needed for protecting the specimens having a chloride gradient of 1.5. The decay potential values obtained from the 8 lbs-and 16 lbs-chloride bearing specimens are by and large similar and in the range of 50 mV. The protection level needed for 32 lbs chloride-bearing specimen is about 5-10 mV higher than the level required for 8 and 16 lbs chloride specimens; the values are within 60 mV. This marginal elevation of the protection potential is ascribable to the increased corrosion activity in 32 lbs specimen in comparison to those in 8 and 16 lbs specimens.

Fig. 5.2.7 shows the 4 hour decay potential needed to protect the specimens having a chloride gradient of 2.0. There is significant amount of scatter in

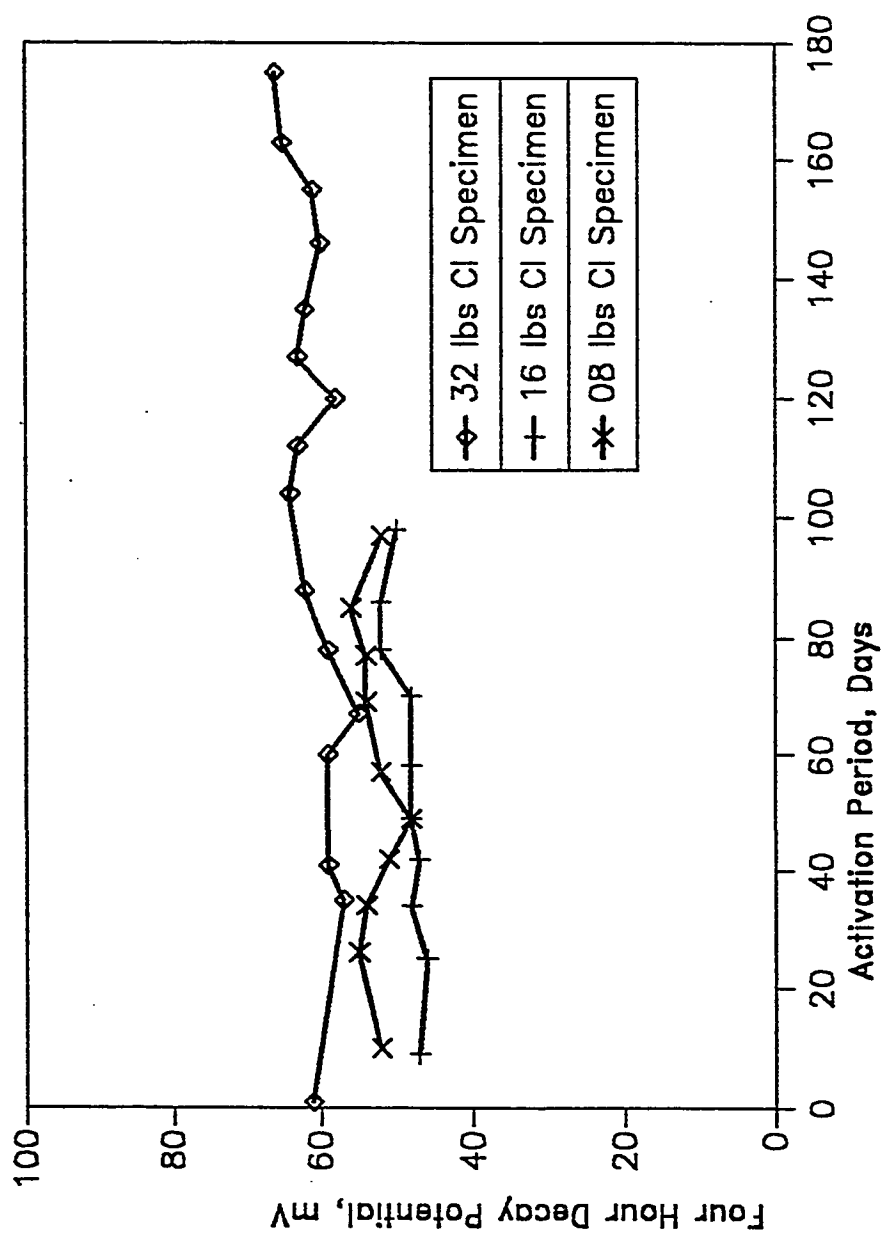


Fig. 5.2.6 Four Hour Decay Potential Needed for Protection of Steel in Concrete Having 1.5 Chloride Gradient

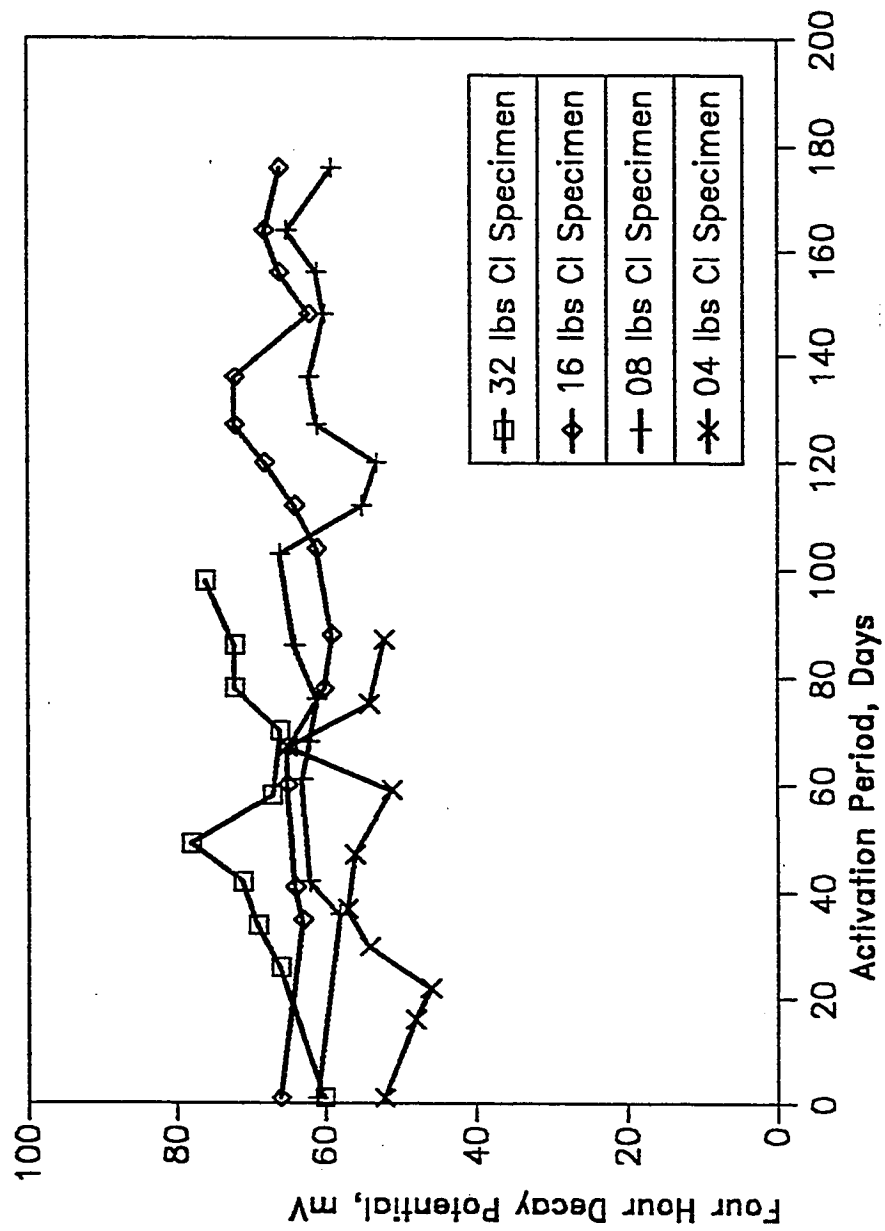


Fig. 5.2.7 Four Hour Decay Potential Needed for Protection of Steel in Concrete Having 2.0 Chloride Gradient

the data of Fig. 5.2.7 which does not show a very well defined relationship between 4 hour decay potential and the chloride content of the specimen. The average protection potential for the 8 and 16 lbs specimens having a chloride gradient of 2.0 is in the range of 55 mV. For the 32 lbs specimen, four hour decay potential as high as 78 mV was recorded.

Figs. 5.2.8 and 5.2.9 show the 4 hour decay potential required for protecting the specimens having 4 and 8 lbs chloride differential. The data of both of these presentations do not show a defined dependence of the 4-hour decay potential on the chloride content of the specimen. Fig. 5.2.9 shows low 4 hour decay potentials only for the 16 lbs chloride specimen. This low decay potential value for the 16 lbs specimen is mainly attributable to the relatively low chloride gradient between the specimen and the macrocell. The chloride gradient for 16 lbs specimen in Fig. 5.2.9 is 1.5 whereas the gradient values are 5, 3 and 2 for the 2, 4 and 8 lbs chloride-bearing specimens respectively. However, the results of Figs. 5.2.8 and 5.2.9 clearly show that for reasonably low levels of chloride contamination in the specimens (0 to 8 lbs per cu. yds of concrete), the decay potential is by and large independent of the difference in chloride content between the specimen and the macrocell; for a 4 lbs chloride difference the decay potentials are in the range of 50 mV whereas for 8 lbs difference, the values are in the range of 65 mV.

The above results clearly demonstrate that the 100 mV decay criterion commonly adopted is overly conservative. For upto 8 lbs chloride contaminated concrete having upto 4 lbs difference in chloride level of the specimen and the macrocell, a protection potential of 60 mV decay in 4 hour may be adequate for effective protection. The four hour decay potential of 70 mV may be adequate for

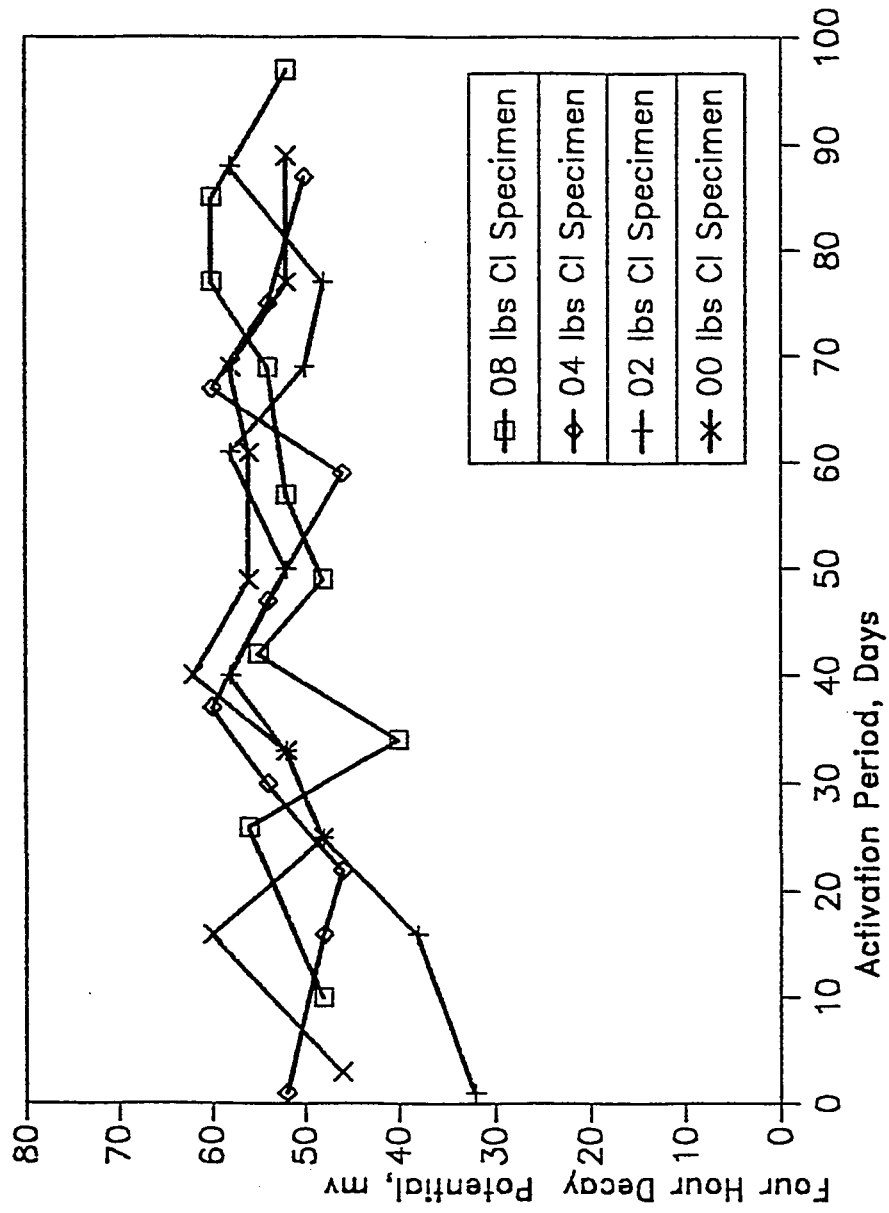


Fig. 5.2.8 Four Hour Decay Potential for Protection of Steel in Concrete Having 4 lbs Chloride Differential

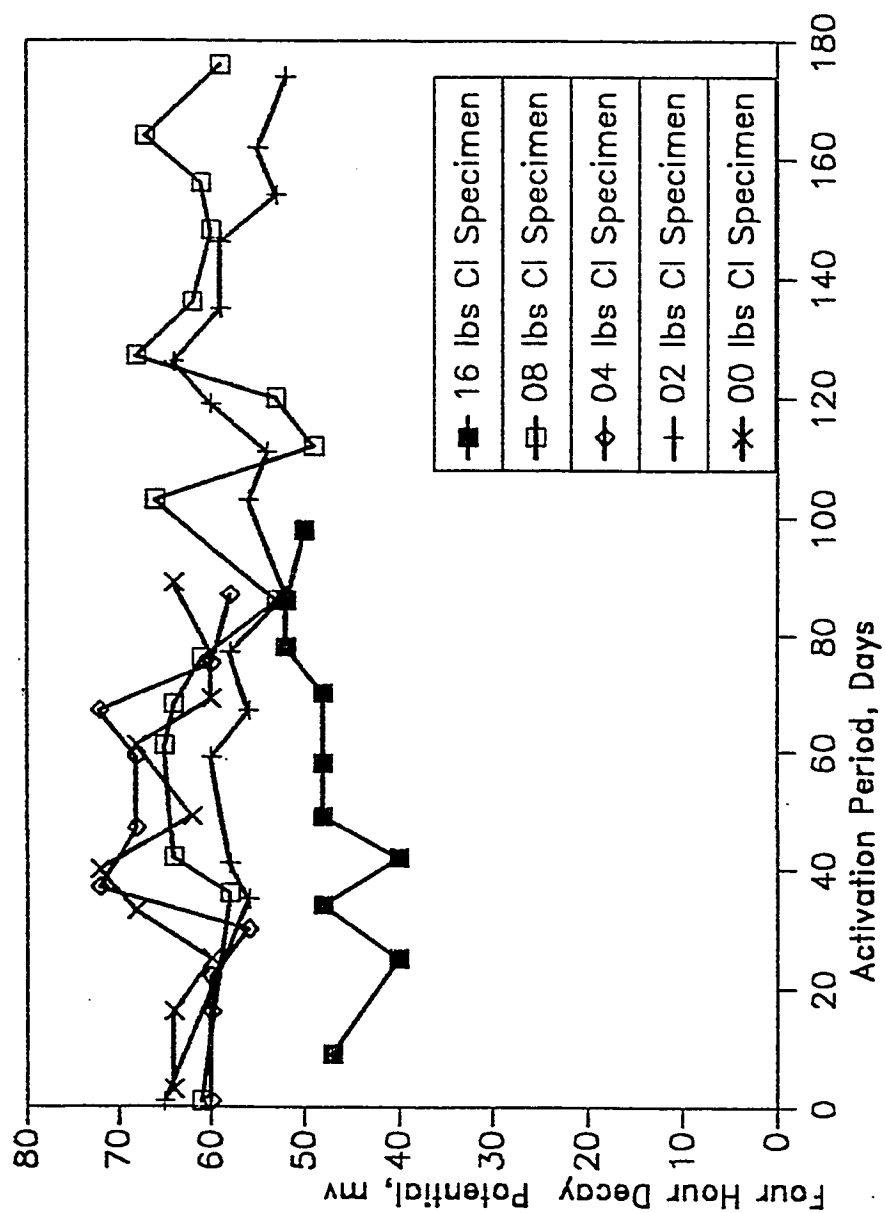


Fig. 5.2.9 Four Hour Decay Potential Needed for Protection of Steel in Concrete Having 8 lbs Chloride Differential

effective protection for upto 16 lbs chloride-bearing concrete having a chloride differential of 8 lbs. For 16 to 32 lbs chloride-bearing concrete having a chloride gradient of 2.0, a four hour decay potential of 80 mV may be sufficient.

5.2.5 Shift Potential

Considering the shift potential values required for protection, the data show that the shift potential is mainly related to the chloride gradient in the specimen. For this reason, the shift potential data are plotted separately for the two groups of specimens; in one group are the low chloride bearing specimens (0 to 4 lbs) having chloride gradients > 2 and in the other group are the high chloride bearing specimens(8 to 32 lbs) having chloride gradients ≤ 2 .

Fig. 5.2.10 shows the shift potential required for low chloride bearing specimens. There is some scatter in the shift potential data with activation period. The 0 lbs chloride bearing specimen showed the highest shift potential with values of 192 mV and 172 mV where the macrocell chloride contents were 8 and 4 lbs respectively. The 2 lbs chloride bearing specimens having 10 lbs chloride bearing macrocell (a chloride gradient of 5) also showed a high shift potential value of 150 mV. For the 2 lbs chloride bearing specimen having 6 lbs chloride bearing macrocell, the shift potential is found to be 70 mV only. The data for 4 lbs chloride bearing specimen with 8 and 12 lbs chloride macrocells showed that higher shift potential is required in specimen coupled with 12 lbs chloride macrocell (a chloride gradient of 3). These data demonstrate that the shift potential is also dependent on the chloride gradient within the specimen; a high chloride gradient needs a higher shift potential for adequate protection against corrosion.

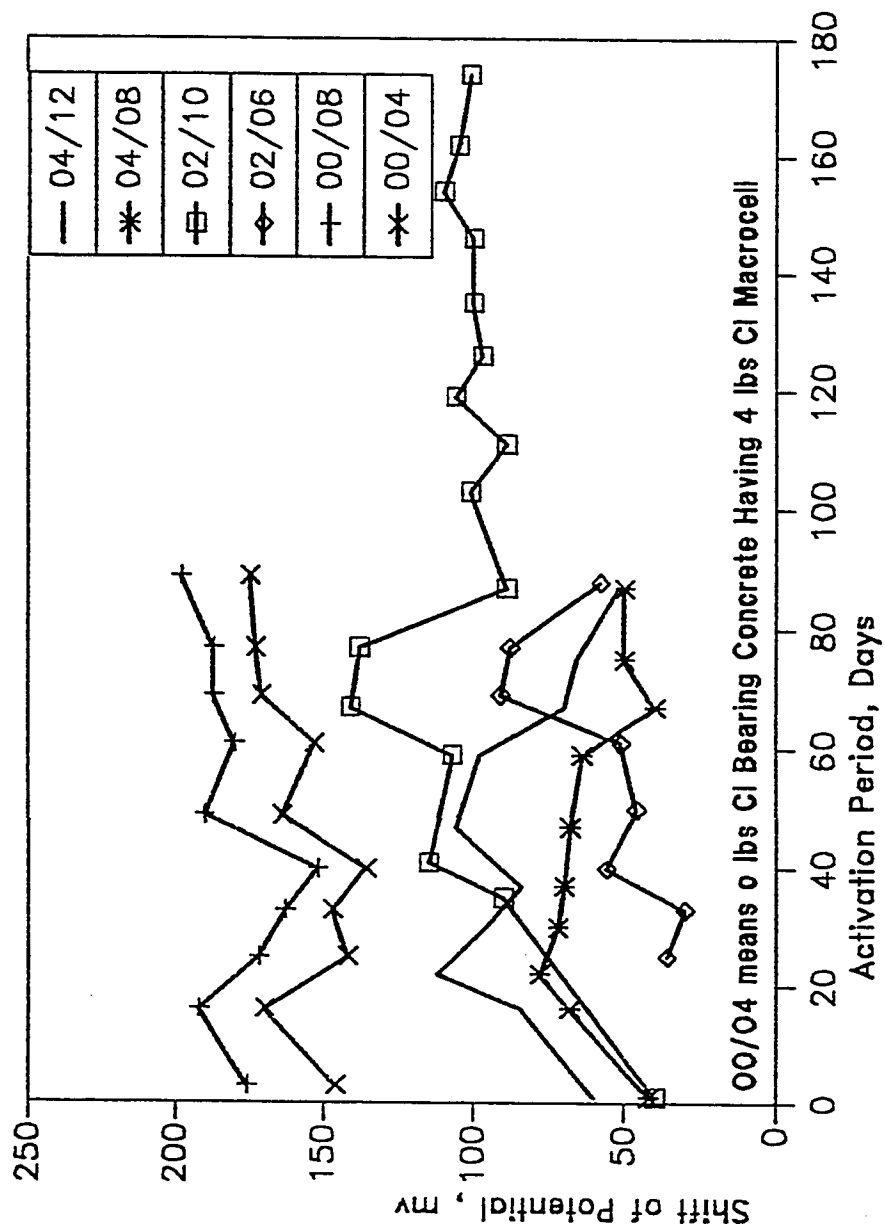


Fig. 5.2.10 Shift Potential Needed for Protection of Steel in Concrete Having Low Chloride Content (0-4 lbs Cl⁻/cu. yd)

Fig. 5.2.11 shows the shift potentials needed for higher chloride bearing specimens. This presentation shows that the shift potential varies from 50 to 100 mV with no apparent relationship between the shift potential value and the chloride content of the specimens. The variation of shift potential with time is attributable to the variation of static potential with time; as the shift potential is the difference between the static potential and the instant off potential. A low shift potential value of 50 to 100 mV for high chloride content specimens is ascribable to the low chloride gradient (≤ 2) used in the high chloride specimens (≥ 8 lbs $\text{Cl}^- / \text{yd}^3$). Moreover, since the static potential of the steel in high chloride bearing specimen is relatively higher, a relatively lower shift in the steel potential is needed for high chloride contaminated concrete to reach the protection level.

5.2.6 Current Density

Figs. 5.2.12 and 5.2.13 show the current density required for protection of steel in concrete specimens having chloride gradients of 1.5 and 2.0 respectively. The data of these Figures clearly show that the current density required at the steel surface is predominantly dependent on the chloride content of the specimen. Fig. 5.2.12 shows that the current density required for 32 lbs chloride bearing specimen is much higher than the densities required for protecting 8 lbs- and 16 lbs-chloride bearing specimens. The applied current has to overcome a differential in potential created by 16 lbs chloride difference in the case of 32 lbs chloride specimen whereas in 8 and 16 lbs chloride bearing specimens, the applied current had to overcome the potentials created by only 4 and 8 lbs chloride differences respectively. Higher is the chloride difference between the specimen and the macro-cell, more is the protection current required for overcoming the voltage drop

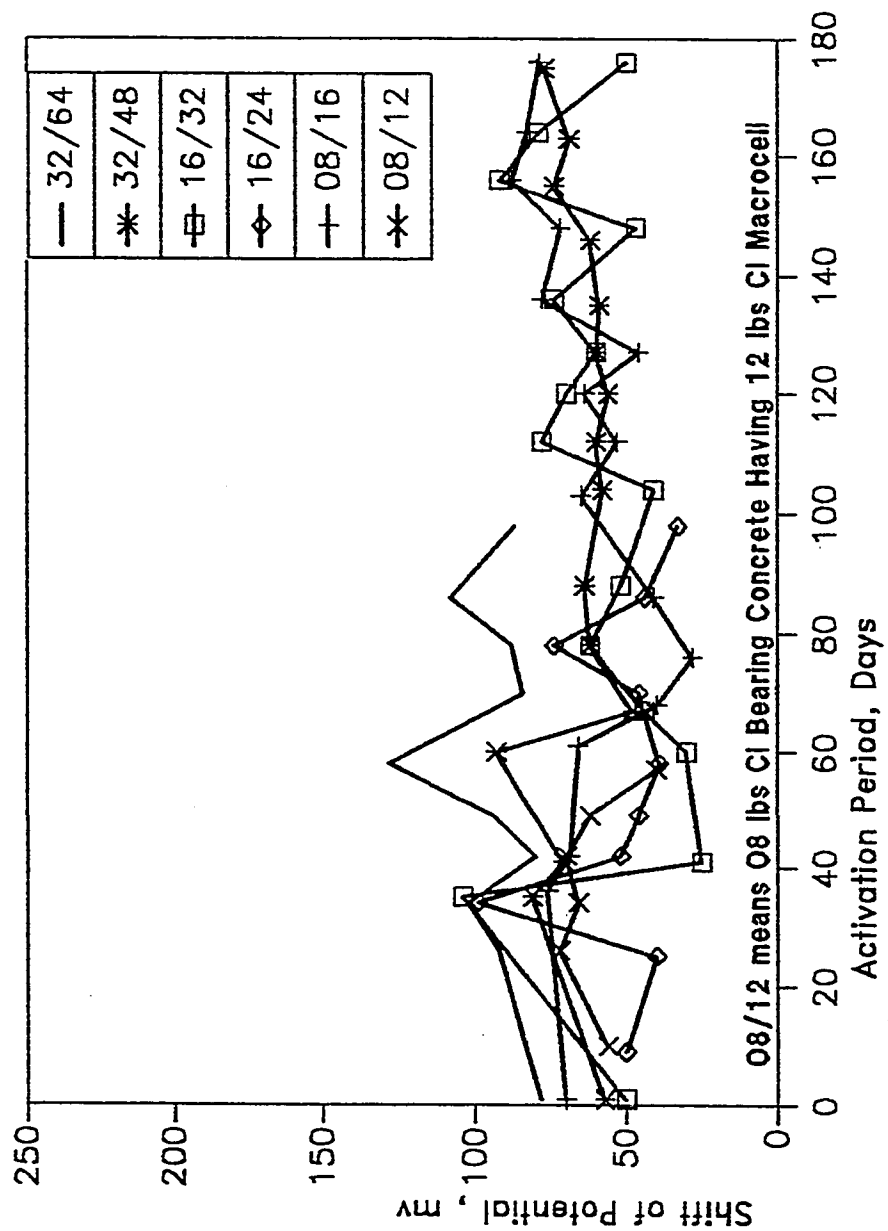


Fig. 5.2.11 Shift Potential Needed for Protection of Steel in Concrete Having High Chloride Content (Greater than 8 lbs/cu yd)

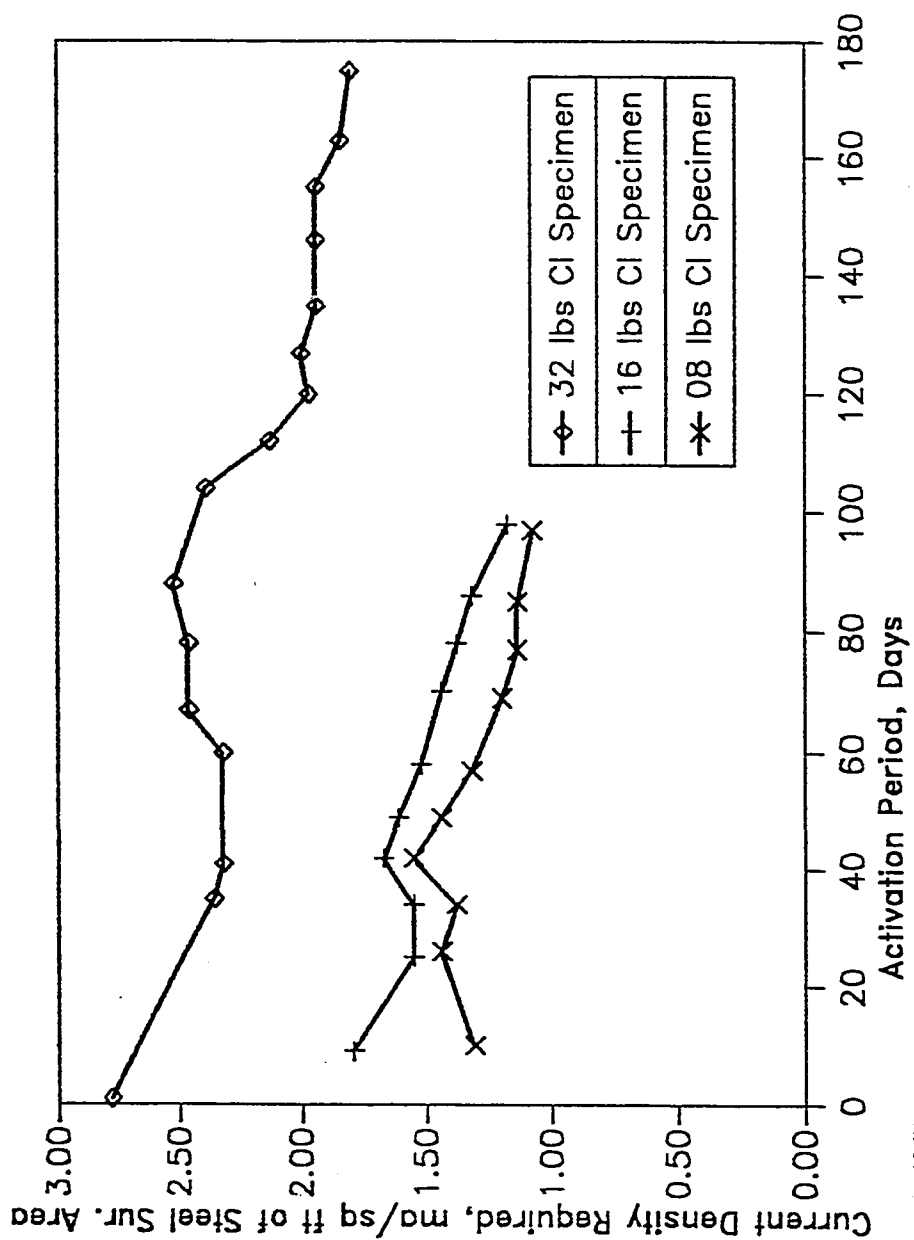


Fig. 5.2.12 Current Density Needed for Protection of Steel in Concrete Having 1.5 Chloride Gradient

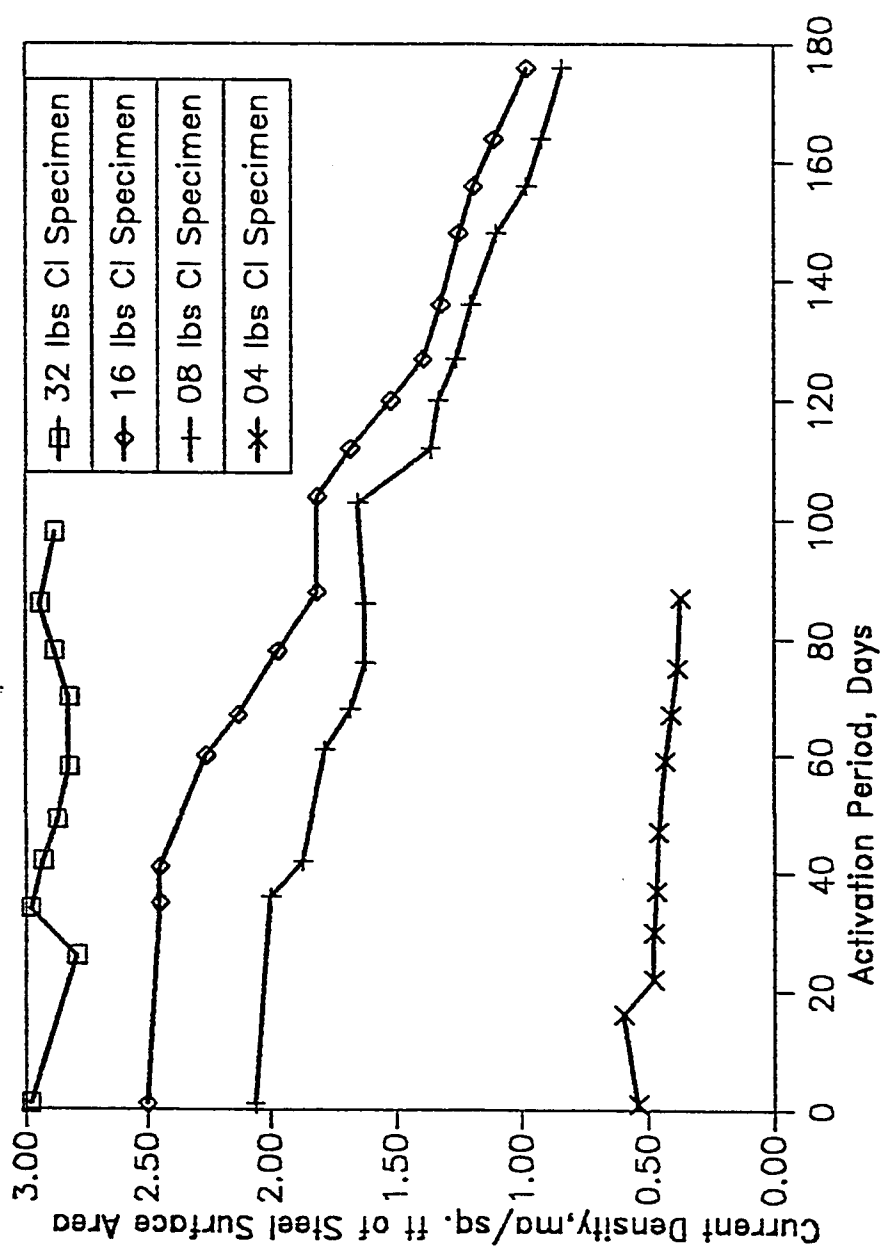


Fig. 5.2.13 Current Density Needed for Protection of Steel in Concrete Having 2.0 Chloride Gradient

across the resistor which connects the steel of the macrocell and the steel of the specimen. The current densities needed are the highest at the beginning of the activation period and are somewhat mitigated with the activation period. The protection current densities needed at the steel surface of the specimens having a chloride gradient of 2.0 are shown in Fig. 5.2.13. This Figure also shows that at the beginning of activation period, highest current density of 2.98 ma/sq ft is required for the 32 lbs specimen coupled with 64 lbs chloride bearing macrocell. The 4 lbs chloride bearing specimen coupled with 8 lbs chloride bearing macrocell needed only a 0.50 ma/sq ft current density for adequate protection. For the same chloride gradient of 2.0, the 8 lbs- and 16 lbs- chloride bearing specimens are observed to require protection current density levels in between those needed for protecting the 4 lbs and 32 lbs chloride bearing specimens. However, a big difference in the protection current density requirement is observed for the 8 lbs and the 4 lbs chloride specimens.

Fig. 5.2.14 shows the protection current density needed to protect the steel in specimen having 4 lbs chloride difference between the macrocell and the specimen concrete. The 2 lbs- and 4 lbs- chloride bearing specimens showed almost similar current density requirements which are of in the order of 0.50 ma/sq ft at steel surface. The interesting point worth noticing is that the 0 lb chloride bearing specimen needed higher impressed current than the 2 and 4 lbs chloride bearing specimens. This is attributable to the fact that the difference in static potential of the macrocell steel and the specimen steel in 0 lb chloride bearing specimen is much higher than the corresponding static potential differences obtained in 2 lbs- and 4 lbs- chloride bearing specimens. A higher current density was needed to overcome this higher potential difference between the specimen steel and the macrocell steel in 0 lb chloride specimen. A higher current density was required

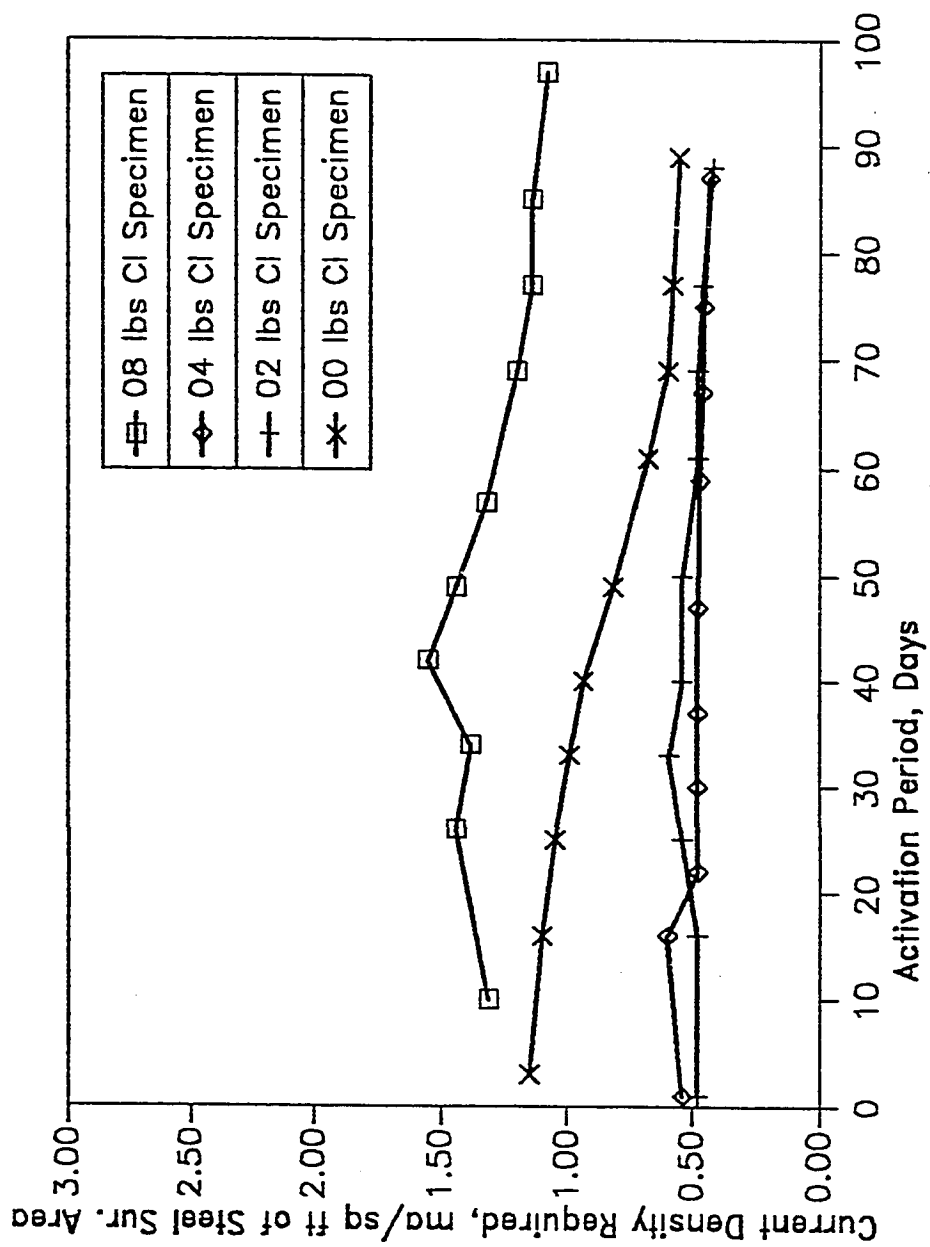


Fig. 5.2.14 Current Density Needed for Protection of Steel in Concrete Having 4 lbs Chloride Differential

for protecting 8 lbs-chloride bearing specimens having 4 lbs chloride differential within the specimen compared to the densities needed for protecting 0, 2 and 4 lbs specimens having the same 4 lbs chloride differential within the same specimen. The chloride content of 2 lbs is lower than the allowable chloride limit (B.S. Specification) for corrosion initiation and the 4 lbs chloride content is slightly above the threshold chloride value. The levels of corrosion activity in the 2 and 4 lbs chloride bearing concrete specimens are significantly lower than in the 8 lbs chloride bearing specimen. The high current density required in 8 lbs specimen is obviously attributed to the higher corrosion activity within the specimen.

Fig. 5.2.15 shows the protection current density needed for steel in specimens having 8 lbs chloride differential. The highest protection current is needed for the 8 lbs chloride bearing specimen and a marginally lower current density is required for the protection of steel in the 16 lbs chloride bearing specimen. Both of the 8 lbs-and 16 lbs-chloride bearing specimens contain chlorides in excess of the allowable limit. Although the higher chlorides in the 16 lbs specimen would result in a higher level of corrosion activity compared to the 8 lbs chloride bearing specimen, the 8 lbs chloride specimen has a higher chloride gradient of 2.0 compared to a lower chloride gradient of 1.5 for the 16 lbs specimen. The higher protection current density for the 8 lbs chloride specimen shows that it is the chloride gradient which dominates the current density requirement. The same trend is noticed in the 0, 2 and 4 lbs specimens having 8 lbs chloride differential within the specimen.

The current density vs. activation period data presented in Figs. 5.2.12 through 5.2.15 clearly show that the current density needed for protection decreases somewhat with the activation period with very few exceptions observed

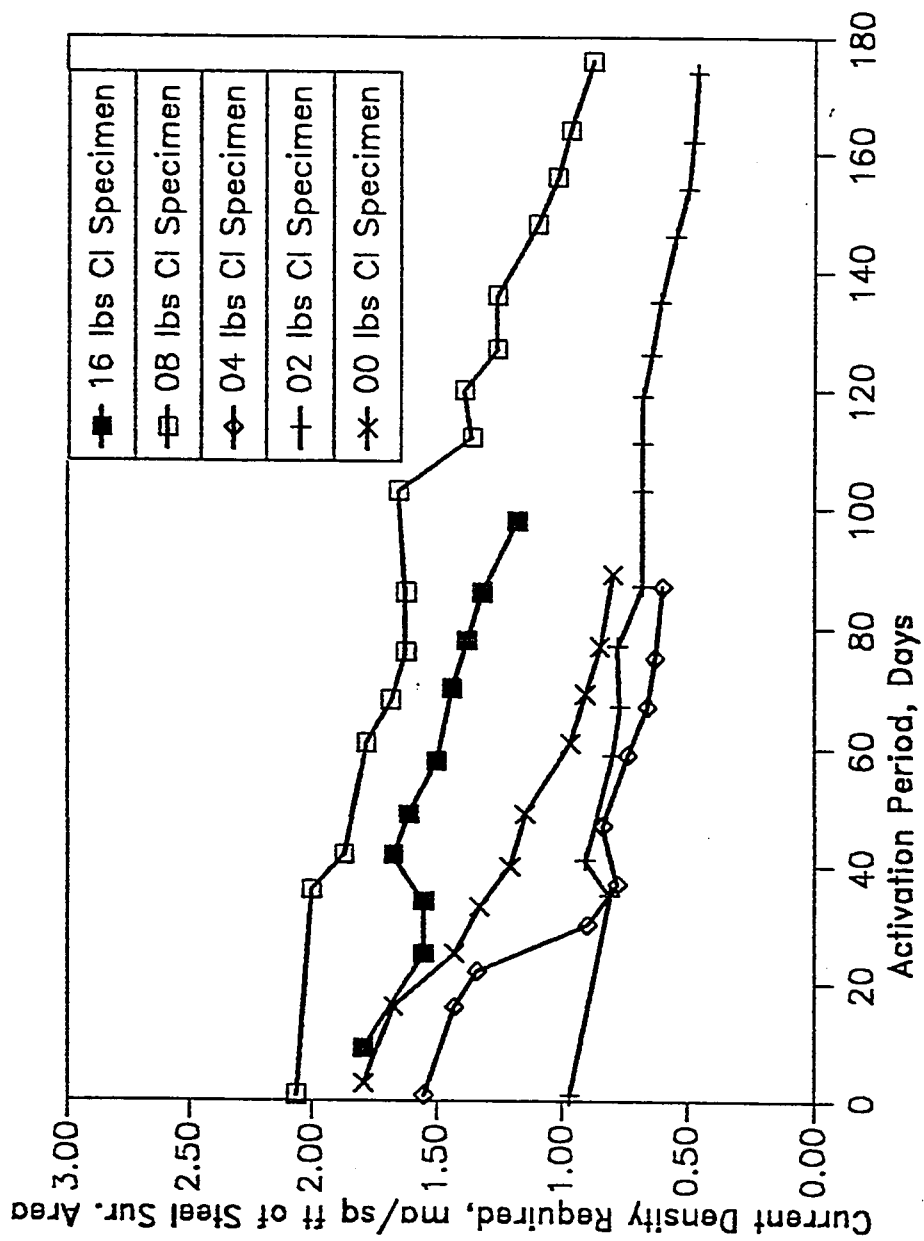


Fig. 5.2.15 Current Density Needed for Protection of Steel in Concrete Having 8 lbs Chloride Differential

only during the initial period of activation. For example, the current density requirement was reduced by 55 percent at the end of six months activation period for a 2 lbs-chloride bearing specimen coupled with 10 lbs chloride bearing macrocell. A decreased level of current density needed with prolonged period of activation may be attributable to the migration of chloride ions away from the vicinity of steel concrete interface. When CP current is applied, the negatively charged steel repulses the chloride ions whereas the positively charged anode attracts this chloride anions from the concrete pore solutions. The electromigration of chloride ions from steel concrete interface to a distance away from the steel thus reduces the chloride concentrations near the steel. This reduced chloride level near the vicinity of steel surface has a two fold effect; first, the reduction of corrosion activity at the steel surface and second, the reduction of potential difference between the specimen steel and the macrocell steel. A lower current density required with prolonged protection period is highly desirable due to several beneficial effects. Maintaining a reduced current density at the steel surface needs lesser power thereby implying economical benefits in terms of the energy costs as well a reduction in the secondary deleterious effects related to bond degradation and increased ASR effects caused by high CP current densities maintained for prolonged periods at the steel surface.

5.2.7 Effectiveness of CP in Arresting Corrosion of Steel

Table 5.2.2 shows the weight loss data for coupon steel and macrocell steel removed from the control specimen and cathodically protected specimen at the end of six months activation. The control specimens data show that the macrocell steel lost the weight by a relatively higher percentage in comparison to the

Table 5.2.2 Weight Loss of the Coupon Steel and Macrocell Steel for CP Specimen and Control Specimen in Chloride Effect Study. The Result of this Table Shows the Effectiveness of CP in Arresting the Corrosion

Specimen Chloride Content, lb/yd ³ of Concrete	Macrocell Chloride Content, lb/yd ³ of Concrete	Coupon Steel			Macrocell Steel		
		Weight loss, %		Weight Loss in CP Specimen in Comparison to Control Specimen, %	Weight Loss, %		Weight Loss in CP Specimen in Comparison to Control Specimen, %
		Control Specimen	CP Specimen		Control Specimen	CP Specimen	
02	10	1.15	0.09	7.8	2.18	0.10	4.50
08	16	3.25	0.10	3.0	4.93	0.19	3.80

coupon steel. For example, the weight losses by the coupon steel and the macrocell steel were 3.25 and 4.93 percents respectively in 8 lbs chloride bearing specimens coupled with 16 lbs chloride bearing macrocell. A relatively higher weight loss observed for the macrocell steel in comparison to the coupon steel is attributable to a relatively higher chloride presence in macrocell concrete. The data in this table show that the CP technique significantly control the chloride induced corrosion. For example, for 8 lbs chloride bearing concrete having 16 lbs chloride bearing macrocell, weight losses by the coupon and macrocell steels of a CP specimen were 3.0 percent and 3.8 percent of the corresponding weight losses observed in the control specimen. Similar results were observed for other chloride bearing specimens when CP current was applied.

5.2.8 Summarized Overview

Tables 5.2.3 and 5.2.4 show the protection level needed at the beginning of activation and the maximum protection level recorded during the observation period respectively. As pointed out before, the instant off potential, the decay potential, the shift potential and the current density needed for protection at the beginning of activation period are higher than the corresponding values after some period of activation with very few exceptions. The instant off potential and the current density needed for protection are directly related to the chloride gradient within the specimen as well as to the chloride content of the specimen. For example, for 16 lbs-chloride bearing specimen the current densities needed for protection are 2.5 and 1.79 ma/sq ft for chloride gradients of 2.0 and 1.5 respectively. The corresponding current density values are 2.98 and 2.78 ma/sq ft respectively for 32 lbs chloride bearing specimen. The data in these tables suggest

Table 5.2.3 Protection Level Needed at the Beginning of Activation

Specimen Chloride Content lb/cu. yd of Concrete	Macrocell Chloride Content lb/cu. yd of Concrete	Chloride Gradient Between Specimen and the Macrocell	Voltage Drop in Resistor Before CP mv	Static Potential of Steel mv CSE	Protection Level Needed			
					Current Density ma/sq. ft.	Instant off Potential mv CSE	4 Hour Decay, Potential mv	Shift Potential, mv
32	64	2.0	+8.36	556	2.98	634	60	78
	48	1.5	+3.80	556	2.78	613	61	57
16	32	2.0	+6.44	504	2.50	554	66	50
	24	1.5	+3.12	472	1.79	522	47	50
8	16	2.0	+5.84	432	2.06	502	61	70
	12	1.5	+2.71	410	1.31	466	48	56
4	12	3.0	+2.74	390	1.55	450	60	60
	8	2.0	+2.50	390	0.54	432	52	42
2	10	5.0	+3.86	350	0.97	390	65	40
	6	3.0	+2.52	350	0.48	346	32	
0	8	-	+4.65	200	1.79	376	64	176
	4	-	+3.65	200	1.55	346	46	146

Table 5.2.4 Maximum Protection Level Recorded During the Observation Period

Specimen Chloride Content lb/yd ³ of Concrete	Macrocell Chloride Content lb/yd ³ of Concrete	Chloride Gradient Between Specimen and the Macrocell	Voltage Drop Across Macro-cell, mV	Protection Level Needed			
				Current Density ma/ft ² of Steel	Instant off Pot-ential mV, CSE	Four Hour Decay Pot-ential mV	Shift Pot-ential, mV
32	64	2.0	+8.36	2.98	634	78	102
	48	1.5	+3.80	2.78	619	70	93
16	32	2.0	+6.44	2.50	554	72	104
	24	1.5	+3.12	1.79	526	48	99
8	16	2.0	+5.84	2.06	522	66	76
	12	1.5	+2.71	1.55	470	56	72
4	12	3.0	+2.74	1.55	478	66	112
	8	2.0	+2.50	0.60	442	60	78
2	10	5.0	+3.86	0.97	390	65	141
	6	3.0	+2.52	0.59	356	58	56
0	8	-	+4.65	1.79	378	62	192
	4	-	+3.65	1.55	362	58	170

that the normally used current density of 1 to 3 ma/sq.ft is sufficient to protect the steel embedded in high chloride contaminated concrete. The 0 lb chloride bearing concrete having 4 and 8 lbs chloride differentials within the same concrete may need current densities of 1.55 and 1.79 ma/sq ft respectively. However, for 2 lbs chloride bearing specimen having 4 and 8 lbs chloride differentials inside the specimen, the current density needed are below 0.50 and 1.0 ma/sq ft respectively. The lowest current density of 0.48 ma/sq ft is observed in the 2 lbs chloride bearing specimens having 4 lbs chloride differential within the specimen whereas the highest current density of 2.98 ma/sq ft is measured for the 32 lbs specimen having 32 lbs chloride differential. The current densities needed for other chloride bearing specimens lie in between the above two values. Like the current density requirement, the instant off potential needed is the lowest in the 2 lbs chloride-bearing specimen coupled with the 6 lbs chloride bearing macrocell and is the highest for 32 lbs chloride specimen coupled with 64 lbs chloride bearing macrocell. A relatively low 346 mV CSE instant off potential value is observed in 2 lbs specimen having 4 lbs chloride differential within the specimen whereas 634 mV CSE instant off potential value was noted for 32 lbs chloride bearing specimens with 32 lbs chloride differential. The instant off potential needed for protecting steel embedded in concrete having other chloride contents used in this study lie in between the above two values. These data indicate that the -850 mV CSE or -770 mV CSE instant off potential value proposed in the literature are overly conservative and need not to be invoked for protection when the chloride contents in the concrete are not excessive. The instant off potential value is dependent on the chloride content of the concrete as well as the chloride differential within the same concrete. The four hour decay potential and the shift potential needed for protection increase with an increase in the chloride gradient.

However, the data presented in Tables 5.2.3 and 5.2.4 (or Figs. 5.2.6 through 5.2.11) do not show a correlation between the decay potential or the shift potential and the chloride content of the specimen. The higher decay potential of 78 mV was observed in 32 lbs chloride bearing specimen having 32 lbs chloride differential and a highest shift potential is observed in the 0 lb specimen coupled with 8 lbs macrocell. These data suggest that the 100 mV decay potential in four hours is sufficient even for very high chloride content of 32 lbs/ yd³ in the concrete having a chloride gradient of upto 2.0 and the 300 mV shift potential is by and large an inadequate and overly conservative protection criterion.

5.2.9 Adequacy of Theoretical Model (Established in Art. 3.1) in Predicting the Effect of Chloride in Concrete on Cathodic Protection Potential

The theoretical study carried out for criteria establishment (Art. 3.1) recommended a potential value more negative than -0.650 V SHE (-0.960 V CSE) for adequate protection. The experimental results suggest that a potential value of -0.96 V CSE is significantly excessive even for the protection of steel in very high chloride content concrete (32 lbs/ yd³) having a chloride gradient of 2.0 within the same concrete. A -650 mV CSE instant off potential value may protect steel embedded in concrete containing chlorides upto 32 lbs/ yd³ and having a chloride gradient upto 2.0 within the same concrete. These findings suggest that a theoretically derived criterion may cause overprotection of steel. Also the theoretical model developed in Art. 3.1 does not demand a further lowering of the protection potential of steel for the presence of chlorides in concrete whereas the experimental findings indicated a relationship between the protection level and chloride contamination of concrete. A relatively higher protection level (higher

absolute value) was needed in the experimental study for higher chloride bearing concrete.

5.2.10 Effect of Primary Chloride in Concrete on Current-Potential Relationship

In the criteria evaluation study (Art. 5.1), it was found that a current density of 1.2 ma/sq ft was needed to achieve a potential corresponding to 100 mV decay in 4 hours on the steel in chloride free concrete. However, for chloride contaminated concrete having chloride differential within the same concrete, a current density value much higher than the above mentioned 1.2 ma/sq ft was needed to achieve even a 80 mV 4 hour decay potential. For example, for 32 lbs chloride bearing specimen coupled with 64 lbs chloride bearing macrocell, a four hour decay potential of 78 mV was recorded for adequate protection and the corresponding protection current density was 2.98 ma/sq ft. A shift potential value of 80 mV was found at 2.98 ma/sq ft current density in 32 lbs chloride bearing specimen having 64 lbs chloride bearing macrocell whereas at a current density of 3.2 ma/sq ft a shift potential of 300 mV was observed in chloride free concrete used in criteria reevaluation study. Thus, the presence of chloride and chloride differential in concrete complicates the current-potential relationship scanty available in the literature.

5.3 EFFECT OF TEMPERATURE ON CATHODIC PROTECTION CRITERIA AND CATHODIC PROTECTION APPLICATION

5.3.1 Temperature Effect on CP Criteria

The temperature attained by the specimens located in the temperature chamber had a peak value of 60°C for six hours and then it varied in the chamber in the 24 hours duration with time according to the regime which simulates the actual variation occurring on a typical summer day at Dhahran. The 24 hour temperature variation regime is shown in Fig. 4.5(Art. 4.1.3).

5.3.1.1 *Corrosion Activity*

Table 5.3.1 shows the comparative voltage drop in the resistor and the static potential of steel in concrete specimens which experience a constant room temperature of 25°C and a variable temperature regime having a peak value of 60°C .

The voltage drop in the resistor, prior to the application of CP, was found to be higher in the temperature treated specimens than that in the specimens exposed to the room temperature. For example, for 8 lbs-chloride-bearing concrete coupled with 16 lbs chloride bearing macrocell, the voltage drop values were 5.84 and 7.55 mV for room temperature exposed specimens and high temperature treated specimens, respectively. The percentage increase in the voltage drop value for high temperature treated specimens in comparison to the room temperature

Table 5.3.1 Comparison of the Voltage Drop in the Macrocell and the Static Potential of Steel at Room Temperature Exposure condition and High Temperature Exposure Condition

Chloride Content of the Specimen, lb/yd^3 of Concrete	Macro-cell Cl Content lb/yd^3 of Concrete	Voltage Drop Across the resistor (mV)		Static Potntial of Steel, mV CSE	
		At 25°C	At 60°C	At 25°C	At 60°C
08	16	+5.84	+7.55	429	460
32	48	+4.80	+5.95	543	568

exposed specimens was observed to be 29 percent for 8 lbs-chloride bearing specimen. Similar result was observed for 32 lbs-chloride-bearing specimen having 48 lbs-chloride bearing macrocell; the percentage increase in voltage drop due to high temperature treatment of the 32 lbs chloride bearing specimens was observed to be 24 percent. The resistor connects the steel embedded in high chloride bearing macrocell to the steel located in the relatively lower chloride bearing specimen. The voltage drop in the resistor is the result of corrosion current flow between the macrocell steel (anode) and the specimen steel (cathode); a higher voltage drop in the resistor is indicative of a higher corrosion current. A significantly increased voltage drop obtained in the temperature treated specimens, in comparison to the specimens exposed to room temperature, is attributable to an increased corrosion activity at the steel surface when concrete environment is characterized by a higher temperature regime.

The static potential of steel, prior to the application of CP, was found to be higher (more negative) in the high temperature treated specimens in comparison to the room temperature treated specimens. The static potential value obtained in high temperature treated specimen was 31 mV higher than the value obtained in room temperature exposed specimen for 8 lbs chloride bearing specimen coupled with 16 lbs chloride bearing macrocell. For 32 lbs chloride bearing specimen coupled with 48 lbs chloride bearing macrocell, the corresponding increase in static potential value (absolute value) was 25 mV. A higher static potential value is indicative of a higher corrosion activity (67,68).

Both of these voltage drop data and static potential data indicate an increased corrosion activity at the steel surface when concrete environment is characterized by a higher temperature regime.

5.3.1.2 *Protection Level Required*

Table 5.3.2 shows the comparative protection levels needed for the steel embedded in concrete specimens which experience a constant room temperature of 25°C and a variable temperature regime having a peak value of 60°C. The instant off potential values needed to protect the steel embedded in the temperature treated specimens were marginally higher compared to the values needed to protect steel embedded in the specimens exposed to room temperature. For example, instant off protection potential values observed in 8 lbs chloride bearing specimens having 16 lbs chloride bearing macrocells were 502 and 530 mv CSE for the 25°C and higher temperature exposure conditions respectively. For 32 lbs-chloride-bearing specimens having 48 lbs chloride bearing macrocell, the corresponding values were 608 mV and 628 mV respectively. The data obtained in both 8 and 32 lbs-chloride-bearing specimens indicate only marginal increase in instant off potential value due to high temperature exposure. Atleast, the effect of significantly different corrosion in high temperature treated specimens is not reflected that much on instant off potential value.

Likewise the instant off potential values, the 4 hour decay potential values needed to protect the steel in higher temperature treated specimens were marginally high compared to the values needed to protect steel in room temperature exposed specimens. For example, the four hour decay potential values observed in 8 lbs-chloride-bearing specimens coupled with 16 lbs chloride bearing macrocells were 70 and 80 mV for the 25°C and high temperature exposure conditions respectively. The corresponding values for 32 lbs-chloride-bearing specimen having 48 lbs-chloride-bearing macrocell were 60 and 66 mV respectively for room

Table 5.3.2 Comparison of the Protection Level Needed to Protect Steel in Concrete Exposed to Room Temperature of 25 C and Elevated Temperature of 60 C.

Chloride Content of Specimen, lb/cu. yd of Concrete	Macro-cell Chloride Content, lb/cu. yd of Concrete	Instant Off Potential mv, CSE		4 Hour Decay Potential, mv		Shift Potential mv		Current Density at Steel Surface ma/sq ft	
		At 25 C	At 60 C	At 25 C	At 60 C	At 25 C	At 60 C	At 25 C	At 60 C
08	16	502	530	70	80	73	70	2.06	2.54
32	48	608	628	60	66	65	60	2.68	3.18

temperature and high temperature treated specimens. The results indicate that the effect of significantly high corrosion activity in high temperature treated specimen is not reflected noticeably on four hour decay potential.

The influence of increased corrosion activity at high temperature is not reflected on the shift potential value. The shift potential values of 73 and 70 mV for the 25 C and high temperature exposure conditions respectively were noticed for 8 lbs-chloride-bearing specimen. For 32 lbs-chloride-bearing specimens, the corresponding values were 65 and 60 mV respectively.

The current density needed to protect the steel in temperature treated specimen is higher in comparison to the value required for the specimen exposed to room temperature. For example, the current densities in 8 lbs-chloride-bearing specimens were 2.06 and 2.54 ma/sq ft for the 25 C and high temperature exposure conditions respectively. The corresponding values for 32 lbs chloride bearing specimens were 2.68 and 3.18 ma/sq ft respectively for room temperature exposed specimens and high temperature treated specimens. As explained earlier, higher corrosion activity at higher ambient temperature would cause a higher current to flow through the resistor which connects the macrocell steel and the specimen steel. As the function of CP current is to reverse this local corrosion current flow, a higher CP current density would be needed in the temperature treated specimen to reverse the higher corrosion current generated here.

5.3.1.3 *Variation of the Protection Level Needed with Time*

Fig. 5.3.1 shows the static potential of steel at different activation ages. The static potential of steel varied up and down with activation age; however, the variation

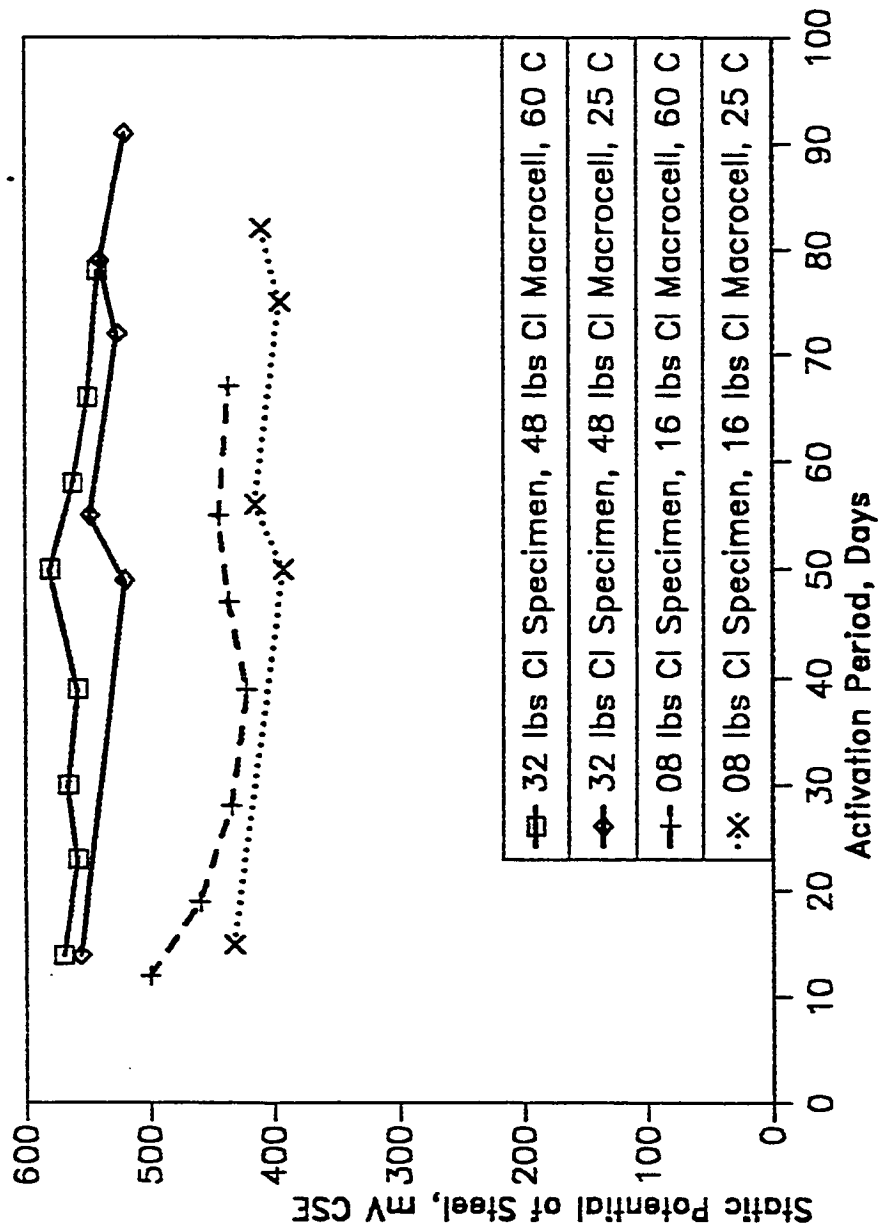


Fig. 5.3.1 Effect of High Ambient Temperature on Static Potential of Steel

was very marginal. A marginally higher static potential value was observed for temperature treated specimens in comparison to the room temperature exposed specimens. The higher static potential value in temperature treated specimens, in comparison to the specimens exposed to room temperature, is ascribable to an increased corrosion activity at the steel surface when concrete environment is characterized by a higher temperature regime.

Fig. 5.3.2 shows the instant off potential needed at different activation ages. Data of this Figure show that at the beginning of activation higher instant off potential values are needed for the temperature treated specimens in comparison to the specimens exposed to room temperature. Since the instant off potential value is dependent on the static base potential, the higher instant off potential obtained in the temperature treated specimens in comparison to the room temperature exposed specimens is attributable to the increased static potential of steel observed at elevated temperature. Data in Fig. 5.3.2 also show that at a later activation age, the instant off potential needed for the temperature treated specimen was lower(lower absolute value) in comparison to the room temperature exposed specimen.

Fig. 5.3.3 shows the 4 hour decay potential needed at different ages for the high temperature exposed specimens and the room temperature exposed specimens. A marginal up and down variation of the 4 hour decay potential values with activation period was observed.

Fig. 5.3.4 shows the shift potential values needed at different activation ages for high temperature treated specimens as well for room temperature exposed specimens. Likewise the decay potential, the shift potential values also varied up and down with activation period and the variation was marginal as in the case of

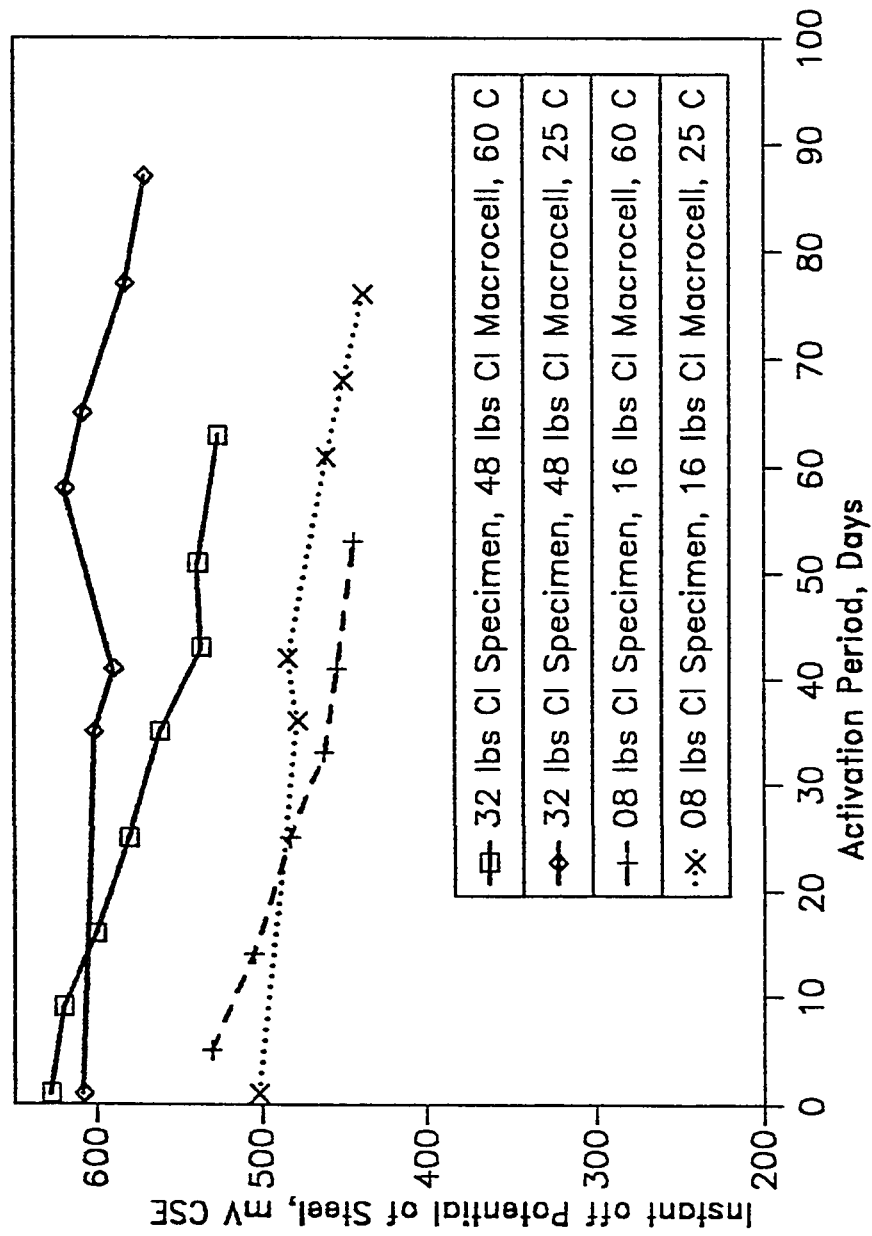


Fig. 5.3.2 Effect of Ambient Temperature on Instant off Potential Needed for Protection

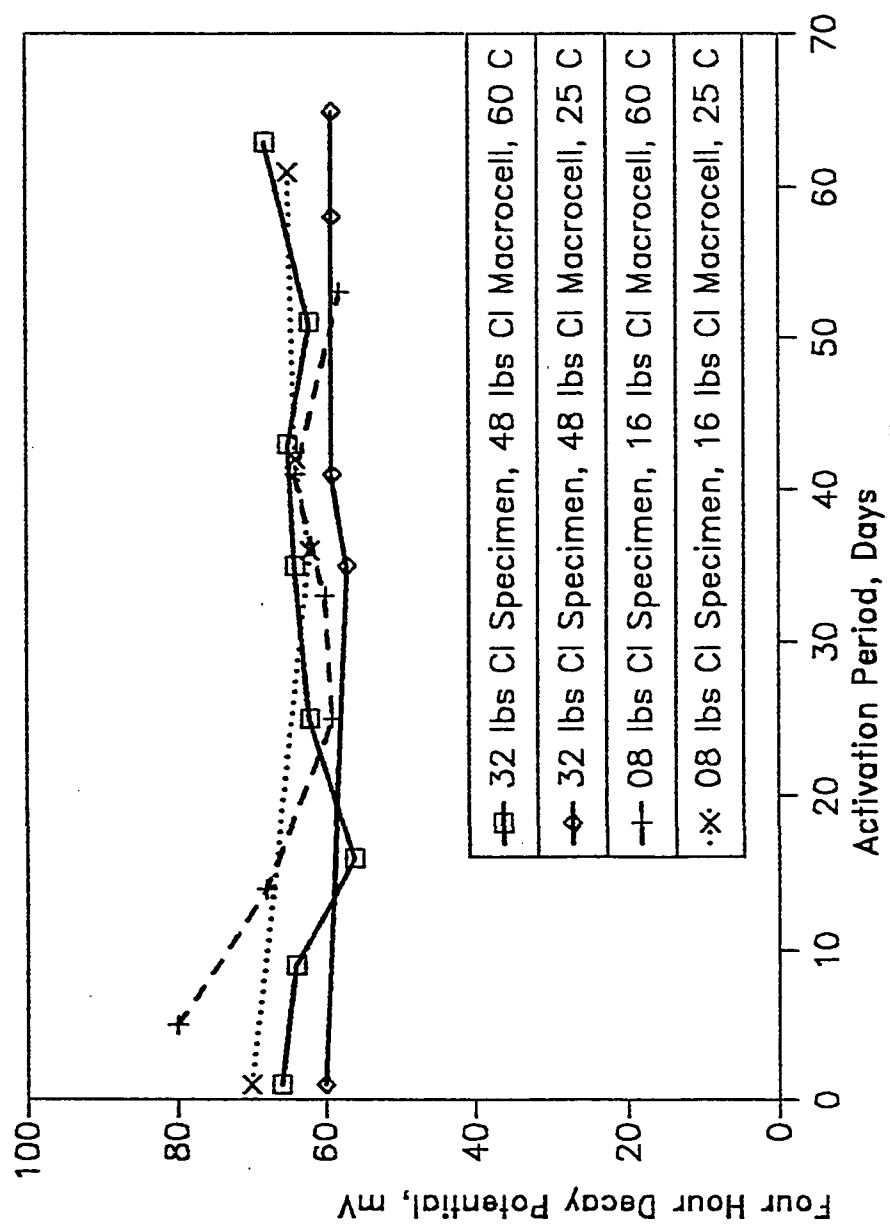


Fig. 5.3.3 Effect of Impressed Current on Four Hour Decay Potential Needed for Protection

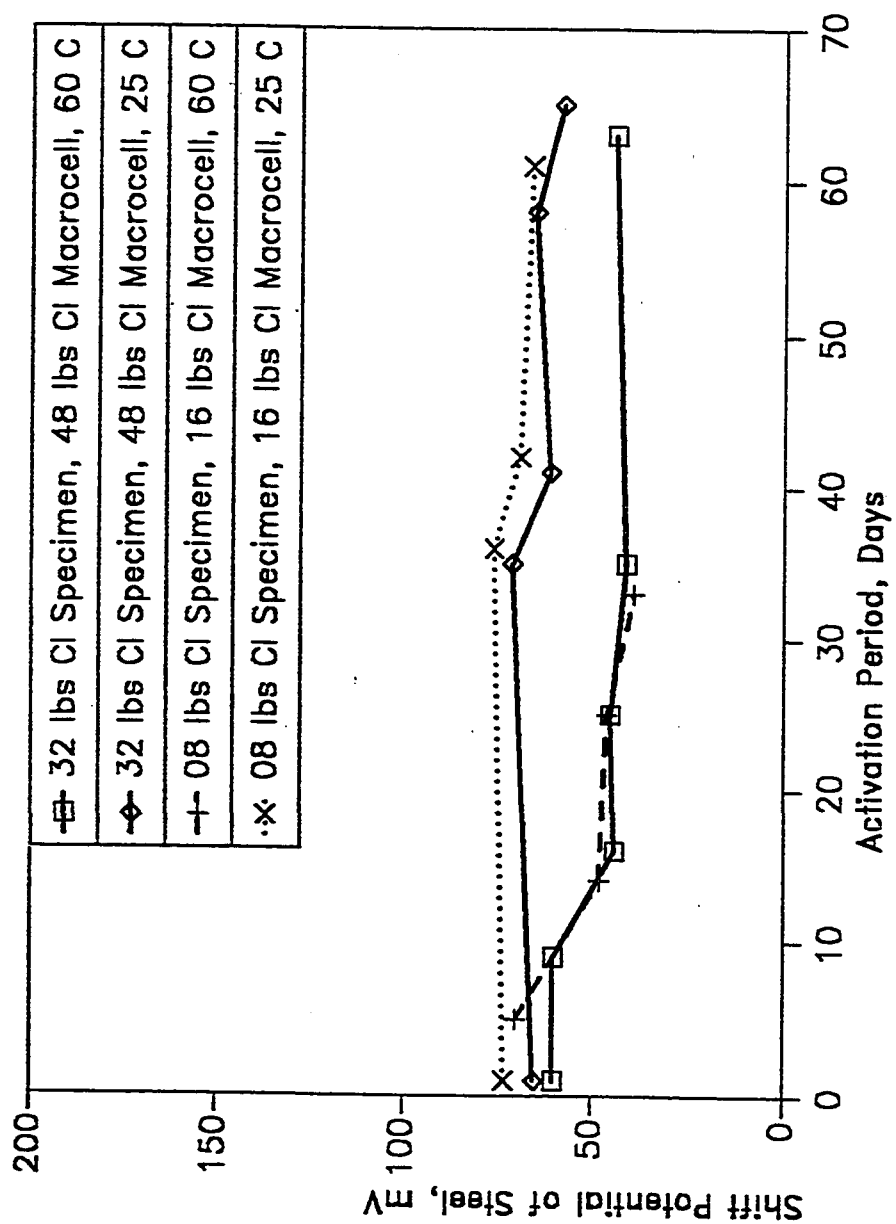


Fig. 5.3.4 Effect of Ambient Temperature on Shift Potential Needed for Protection

4 hour decay potential.

Fig. 5.3.5 shows the current density needed at different activation ages for the high temperature treated specimens and room temperature treated specimens. Likewise the room temperature exposed specimens, the current density needed for elevated temperature exposed specimens also decreases with activation period. The temperature treated specimens needed a higher current density for current reversal and cathodic protection. This higher current density would cause an increased electromigration of chloride ions from near the steel surface to regions away from steel in the temperature treated specimens. Enhanced electromigration of chlorides would result in the natural or base potential shift to a more positive value requiring lesser level of protection. As shown in Fig. 5.3.5, the current density needed for protection of the temperature treated specimens became equal to that needed for room temperature treated specimens after approximately two months activation period. A decreased level of current density needed at the later activation age in the temperature treated specimen in comparison to the room temperature exposed specimens is attributable to decrease in corrosion activity at the steel surface due to greater electromigration of chloride ions from the steel vicinity caused by a higher current density in the temperature treated specimens.

5.3.1.4 *Interactive Effect of Higher Corrosion Activity and Electromigration of Ions at High Temperature with Time*

The data presented above show two distinct effects of high temperature on corrosion activity and cathodic protection. First, a relatively higher corrosion activity at the steel surface when the concrete is exposed to a relatively higher temperature, second, an increased electromigration of ions in high temperature treated

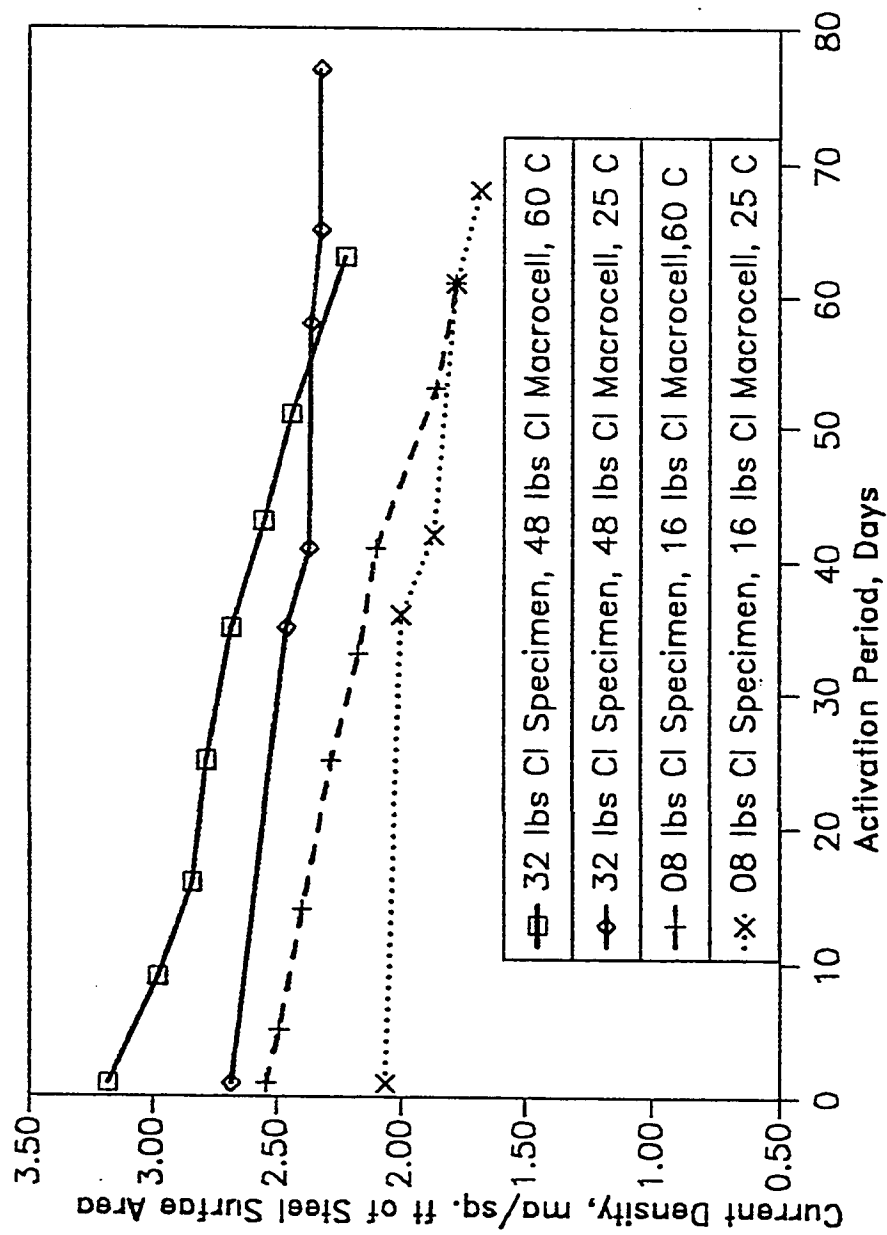


Fig. 5.3.5 Effect of Ambient Temperature on Current Density Needed for Protection

specimens in comparison to the room temperature treated specimens. Due to higher current in temperature treated specimens, there will be increased electromigration of both of chloride and alkali ions. This would result in two advantages: (i) electromigration of chloride ions away from the steel resulting in lowering the corrosion activity at the steel surface, (ii) increased migration of alkali ions to steel surface resulting in an enhanced build-up of alkalinity at the steel-concrete interface. Both will cause a shift of base potential to a more positive value. The interactive effects of higher corrosion activity and increased electromigration of ions at a relatively high temperature exposed specimens controls the protection level required; the increased corrosion activity warrants for a higher protection level whereas the increased electromigration of ions warrants for a lower protection level. A decreased level (more positive) of instant off potential value needed at the later activation age for the high temperature treated specimens in comparison to the room temperature exposed specimens indicates that the effect of the increased electromigration of ions really surpassed the effect of the increased corrosion activity. A decreased value of current density at a later activation period for both the high temperature treated specimen and room temperature exposed specimen is attributable to the reduction of corrosion activity near the steel caused by the electromigration of chloride ions from the vicinity of steel surface. As explained for instant off potential value, a decreased level of current density needed at the later activation age for the high temperature treated specimens in comparison to the room temperature exposed specimens indicates that the effect of the increased electromigration of ions exceeded the effect of the increased corrosion activity. However, the effect of the above stated interactive action of high corrosion activity and increased electromigration at high temperature exposure, on the 4 hour decay potential and shift potential could not be confirmed from the

data presented in this study.

5.3.1.5 *Adequacy of the Theoretical Model (Art. 3.1) to Predict the Temperature Effect on Cathodic Protection Potential*

The theoretical model established for prediction of cathodic protection potential (Art. 3.1) suggests a 20 mV increase (absolute value) of the protection potential for an increase of ambient temperature from 25°C to 60°C. The corresponding increase of the protection potential was found to be 25 mV in the experimental study. These findings suggest that the theoretical model is adequate for predicting the temperature effect on protection potential.

5.3.2 *Difficulties in Supplying Impressed Current to Steel in Concrete Specimens Kept at Hot-dry Environment at Outdoors*

The specimens were kept in hot-dry outdoor environment. The purpose of the study is to check the capacity of an easily available current source such as a 15 V DC battery in terms of supplying current to the steel on a long run basis. A current density range of 1-3 ma/ft² has been reported widely as the CP current used in practical CP installations. When the current supplied by this 15 V DC source gets reduced to below 1 ma/ft², the supply may be termed as completely inadequate. A supply source may be termed as inadequate or partially adequate when the current density at the steel surface drops below 3 ma/ft². The exposure period, the electrical resistivity of concrete and the moisture content of concrete corresponding to current density values of 1 and 3 ma/ft² are reported here.

The current passing to each of the specimens was divided by the steel area to obtain the current density. Fig. 5.3.6 shows the plot of current density that could be attained on the steel by a 15 V D.C. supply at different exposure periods. This Fig. shows that at the beginning of activation, a high current density close to 540 ma/ ft² was attained even by a low voltage supply source of 15 V D.C. However, the current passing to the steel, under the action of this constant voltage source, decreases rapidly with the exposure time. For a better picture of the current passing capacity at the later exposure periods, Fig. 5.3.7 is drawn which is a reproduction and enlargement of the later part of Fig. 5.3.6. At an exposure period of 94 days, the current density was at the level of 3 ma/ ft² and at the exposure period of 110 days, the current density dropped to a value close to 1 ma/ ft². At an exposure period of 120 days, the current density reduces to a value as small as 0.02 ma/ ft². The results demonstrate that in a period of less than 4 months, a constant D.C. supply of 15 V became unable to supply an adequate amount of current to the steel embedded in concrete specimens when the specimens are exposed in a hot and dry environment outdoors.

Fig. 5.3.8 shows the variation of concrete resistivity with exposure period. It is seen from the above paragraph that at 94 days exposure, the current density dropped below 3 ma/ ft². For this exposure period, the concrete resistivity value was 34,000 ohm-cm. It was also found in the above paragraph that at the age of 110 days, the current density dropped to a value less than 1 ma/ ft², and for this exposure period, the resistivity measured from the cylindrical specimen was reported to be 40,000 ohm-cm. This data shows that when the concrete resistivity measured in the concrete cylinder increased to a value of above 34,000 ohm-cm, the 15 V DC source was partially able to supply adequate current to the steel. At

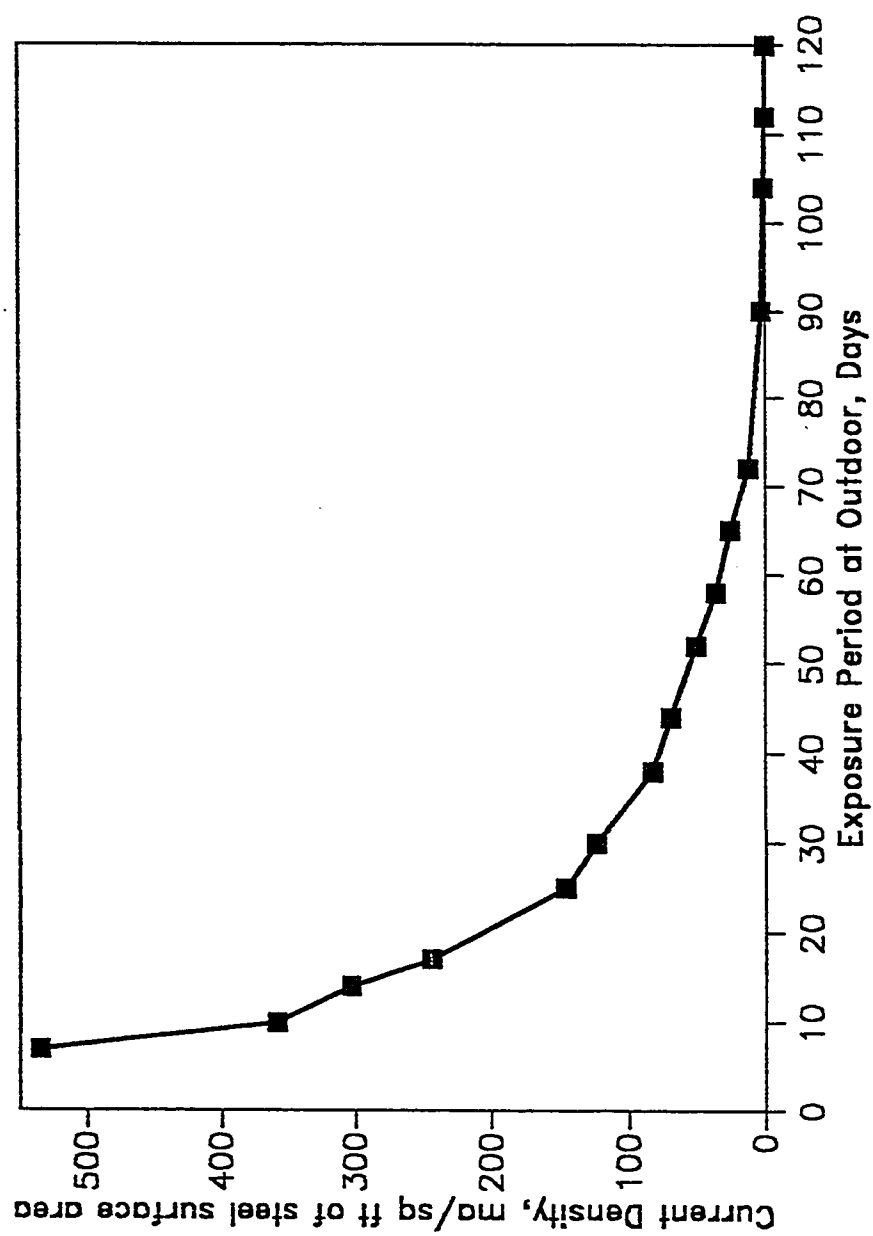


Fig. 5.3.6 Variation of Current Density With Exposure Period Outdoors

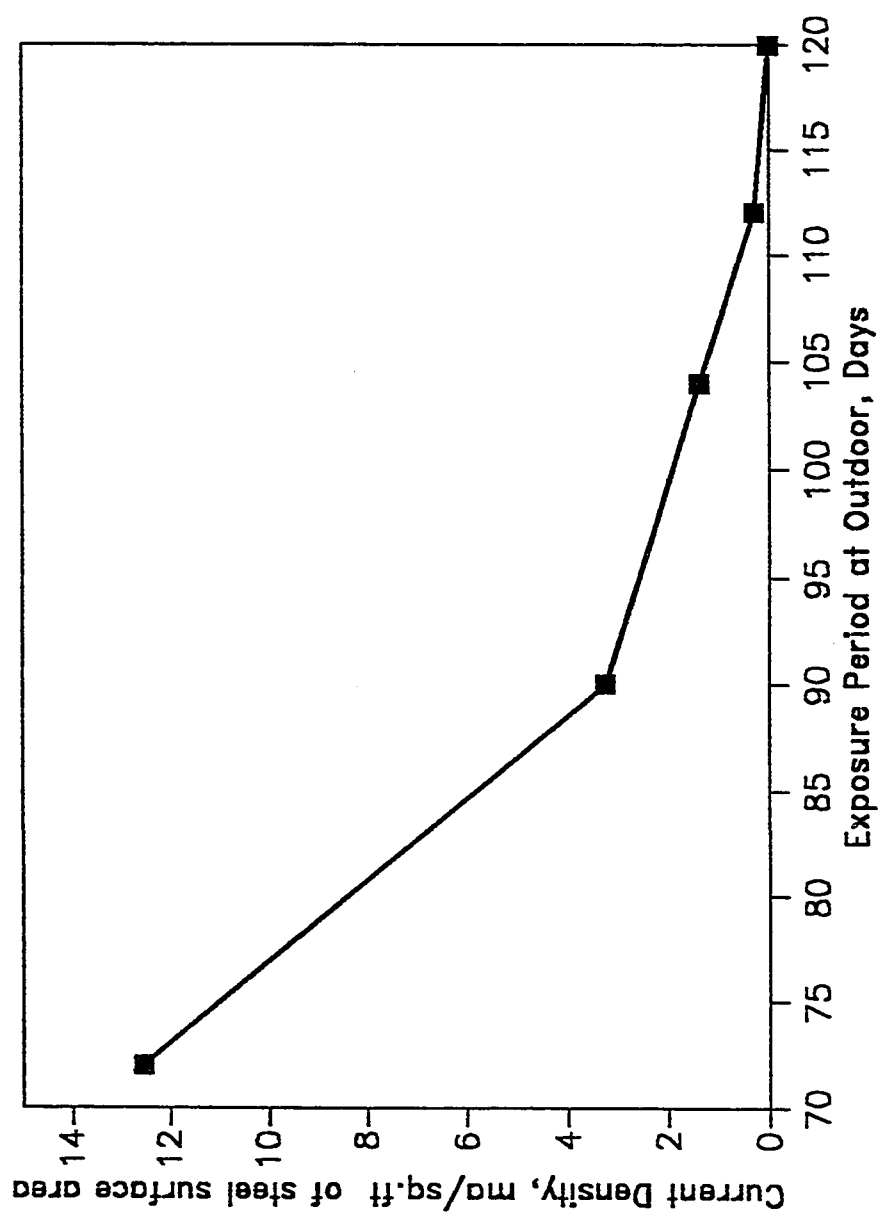


Fig. 5.3.7 Current Density During Final Stage of Exposure

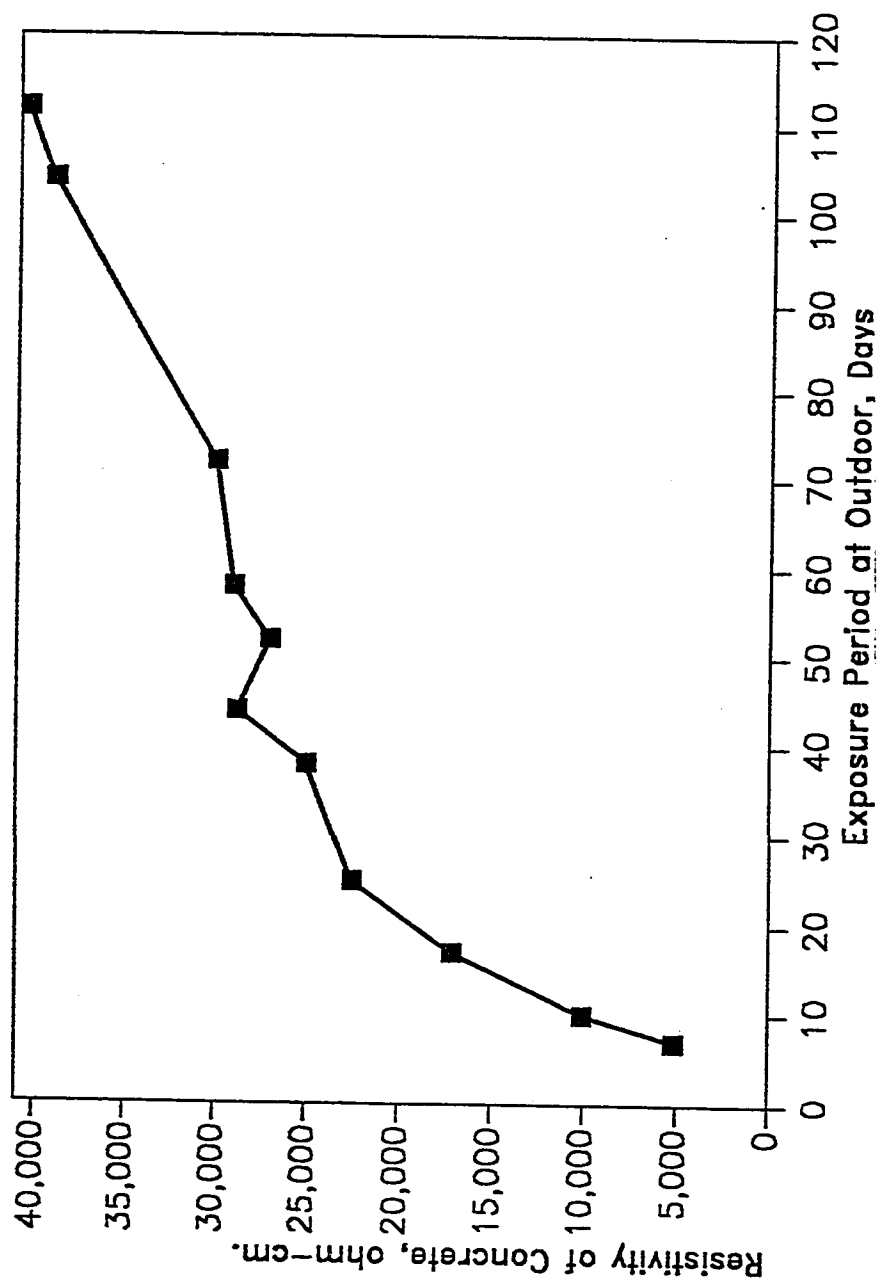


Fig. 5.3.8 Variation of Concrete Resistivity with Exposure Period at Outdoor

a resistivity of 40,000 ohm-cm, the current passing to the steel dropped below 1 ma/ ft² and hence the 15 V DC supply source at this resistivity may be termed as completely inadequate in sufficiently polarizing the steel.

Fig. 5.3.9 shows the variation in the moisture content of concrete with the exposure period in the outdoor environment. As the powdered concrete samples were heated up to only 110°C for the moisture content measurement, it is only the uncombined water which has left the concrete at this temperature. A value of 5.4 percent uncombined water by weight of concrete was found in concrete samples exposed to the outdoor environment for 7 days. The moisture content, however, reduced from this peak value of 5.4 percent to a low value of 1.30 percent at an exposure period of 70 days. It is seen earlier that at 94 days and 110 days, the current density dropped below 3 ma/ ft² and 1 ma/ ft² respectively. The moisture content at these two ages were found to be 1.24 and 1.20 percent respectively. The moisture contents reported here were measured from representative samples which consist of powder from all depths of the concrete slab. The overlay concrete and the concrete immediately below the anode dried out almost completely and corresponding moisture contents were found to be 0.54 and 0.75 percent respectively. Although the moisture content of the representative sample was found to be in the range of 1.2 percent at the final day of exposure, because of the low moisture content of the concrete immediately below the anode layer, an adequate quantity of current could not flow from the anode to the cathode. Thus, it is not the moisture content of the representative concrete, but the moisture content of the concrete immediately below the anode layer that really controls the flow of current from anode to steel. To maintain sufficient current flow from anode to steel, the moisture from the concrete immediately below the anode

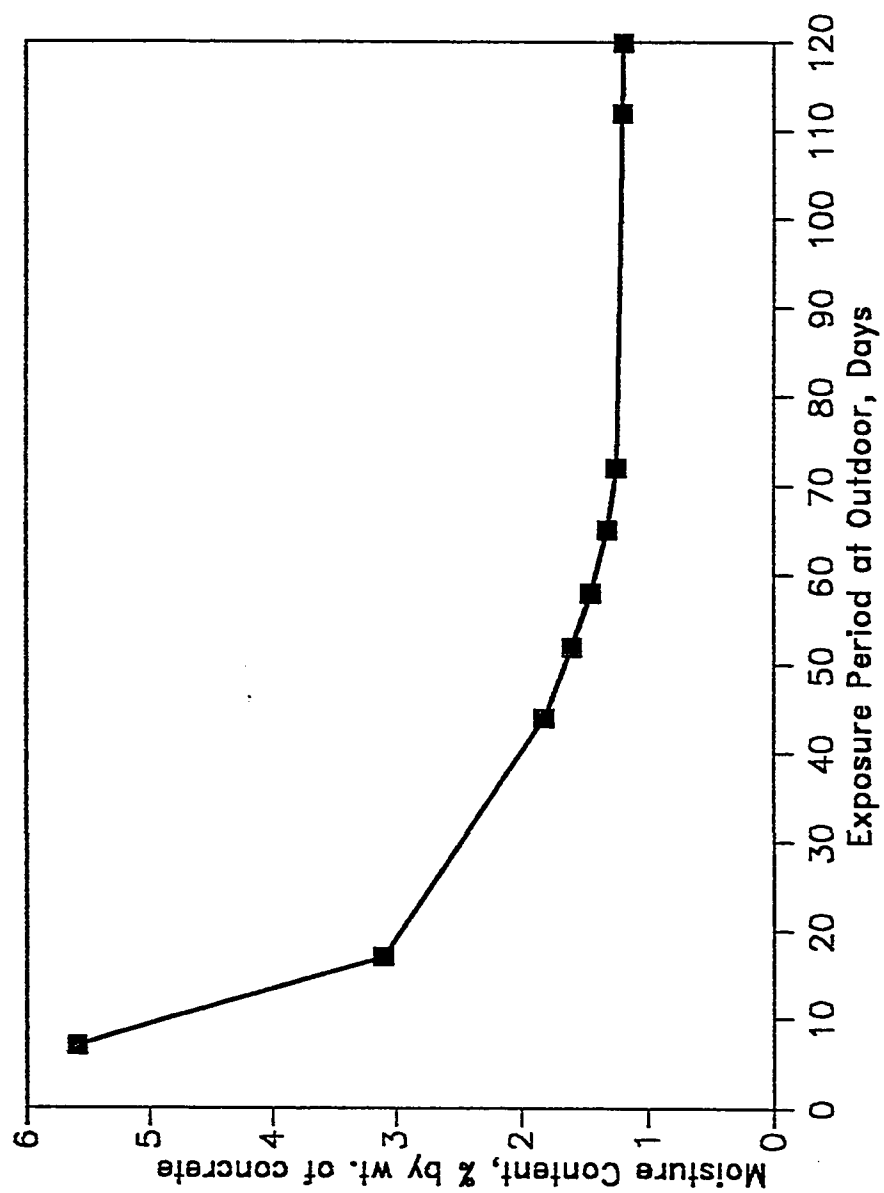


Fig. 5.3.9 Variation of Moisture Content with Exposure Period Outdoors

layer should not be allowed to evaporate. This is possible by properly designing the overlay concrete. A low slump, highly dense water retaining overlay will help in stopping the evaporation of water from the concrete immediately below the anode layer. A conductive polymeric paint as an anode may supply current to steel relatively easily in concrete exposed to a hot-dry environment because of the high anode to cathode area ratio in this situation.

Fig. 5.3.10 shows the plot of current density against the resistivity of concrete. As expected, the current density decreases with the increase of the concrete resistivity. The current density falls to an inadequate level with respect to the protection of steel against corrosion at a concrete resistivity of 35,000 to 40,000 ohm-cm.

5.4 DEPTH EFFECT ON CATHODIC PROTECTION CRITERIA

In the test program, both the top and bottom mat reinforcements of a two mat reinforced concrete slab were protected by placing anode near the top surface of the slab. Current reversal technique was used to select the level for adequate protection. Artificial corrosion macrocells were positioned at the levels of the reinforcements. Two sets of specimens were used; in the first set the difference in chloride content of the specimen and the macrocell was 64 lbs Cl/cu yds of concrete and in the other set the difference was 16 lbs/cu yds of concrete. The specimen chloride content was 32 lbs /cu. yds of concrete. The top mat protection was achieved first and the corresponding current density and the steel

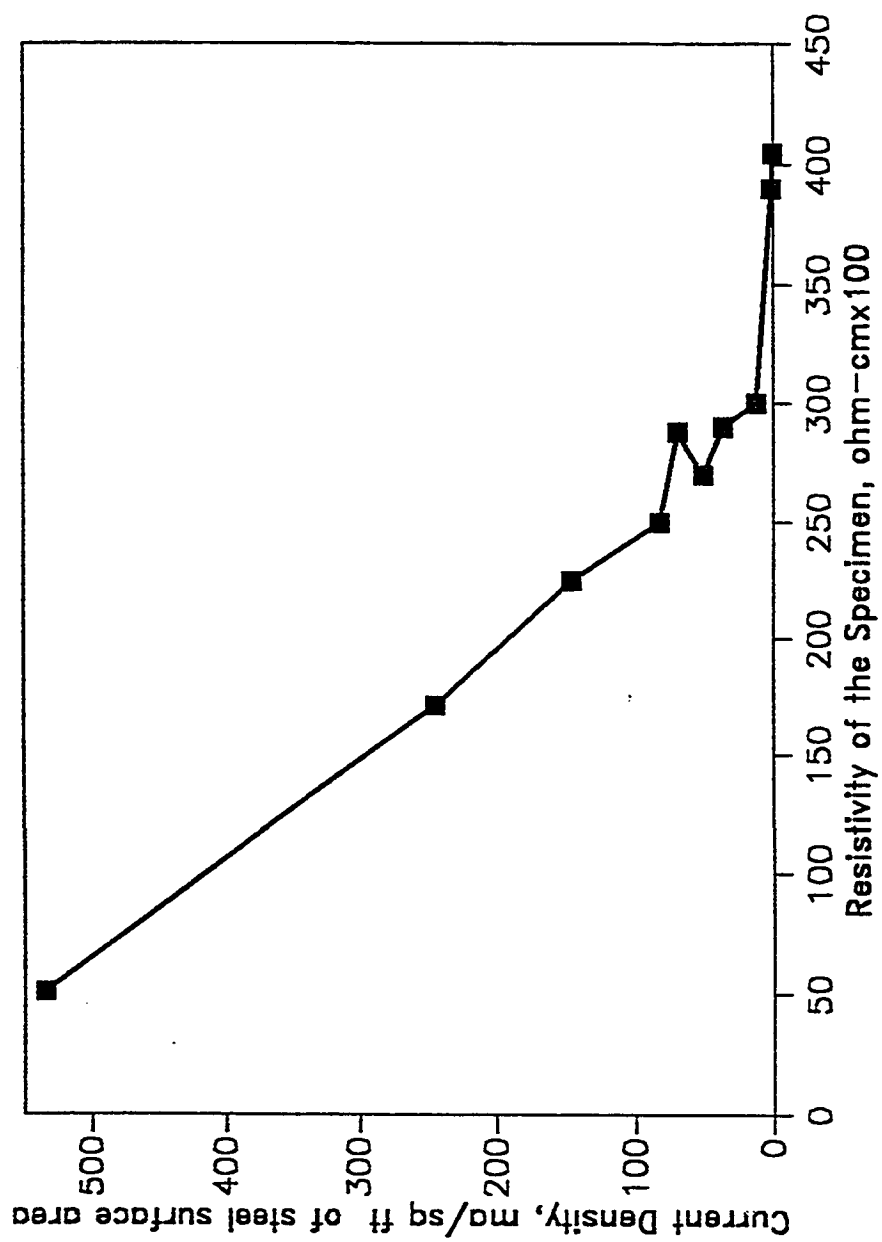


Fig. 5.3.10 Variation of Current Density With Resistivity of Concrete

potentials were noted. Subsequently, the bottom mat protection was achieved and the protection levels for the bottom mat as well as the overprotection levels of the top mat reinforcements were recorded. The protection of the steel was continued for an activation period of six months.

The data obtained from the control specimens (never received current) are shown in Tables 5.4.1 and 5.4.2. Table 5.4.1 shows the static potential of the main steel and the current flow through the resistor which connects the main steel embedded in 32 lbs-chloride-bearing concrete and the macrocell steel embedded in 96 lbs-chloride-bearing macrocells concrete. Table 5.4.2 shows the results obtained from 32 lbs chloride bearing specimens having 48 lbs chloride bearing macrocells. Data from both these Tables suggest a marginal variation of the static potential with time. Most of the static potential values are around 550 mV CSE. The voltage drop across the resistor also varies slightly with time. The differential in potentials of the macrocell steel and the specimen steel causes the corrosion current to flow in the circuit; the voltage drop across the resistor is caused by this current flow. The variation of voltage drop across the resistor, with time, is attributable to the variation of steel potential with time. The voltage drop in the resistor observed in the specimens having 96 lbs-chloride-bearing macrocells was higher than the corresponding value observed in the specimens having 48 lbs-chloride-bearing macrocells. Static potential of steel is directly related to the chloride content of concrete around the steel. A higher differential in chloride content between the specimen concrete and the macrocell concrete causes a higher differential in static potential of specimen steel and the macrocell steel. At this higher static potential differential, an increased corrosion current will flow through the resistor connecting the main steel and the macrocell steel.

Table 5.4.1 Static Potential of the Main Steels and the Voltage Drop Across the Macrocell in Control Specimen Which Never Received CP Current (32 lbs Chloride Bearing Specimen, 96 lbs Chloride Bearing Macrocell

Age of the Specimen (days)	TOP MAT			BOTTOM MAT		
	Voltage Drop in the Resistor, (mv)	Current Flow Through the Resistor, (μ A)	Static Potential of steel, mv CSE	Voltage Drop in the Resistor, (mv)	Current Flow Through the Resistor, (μ A)	Static Potential of Steel, mv CSE
7	14.80	292	570	14.80	292	562
8	14.60	286	570	11.80	231	586
17	12.52	246	562	10.20	198	594
25	12.30	241	570	10.70	227	562
37	11.57	226	578	10.80	210	545
45	11.84	232	562	10.00	196	551
62	12.55	246	570	11.50	225	586
70	14.41	282	554	12.50	245	566
105	14.30	281	562	15.30	300	522
130	16.63	326	522	14.80	292	490
150	15.50	304	562	15.40	302	516
190	12.80	251	552	13.20	259	546
200	13.10	256	534	12.40	243	530

Table 5.4.2 Static Potential of the Main Steels and the Voltage Drop Across the Macrocell in Control Specimen Which Never Received CP Current (32 lbs Chloride Bearing Specimen, 48 lbs Chloride Bearing Macrocell

Age of the Specimen (days)	TOP MAT			BOTTOM MAT		
	Voltage Drop in the Resistor, (mv)	Current Flow Through the Resistor, (A)	Static potential of steel, mv CSE	Voltage Drop in the Resistor, (mv)	Current Flow Through the Resistor, (A)	Static potential of steel, mv CSE
7	4.84	95	592	5.60	110	592
14	5.11	100	570	5.33	105	578
52	4.80	94	586	6.30	123	538
58	4.86	95	586	5.30	104	546
84	5.12	100	578	4.70	92	546
104	4.97	97	578	4.90	96	530
120	4.47	87	588	5.89	115	570
137	3.99	78	562	4.95	97	556
154	4.89	96	560	5.00	98	538
165	4.78	94	568	5.50	108	542

Table 5.4.3 shows the cathodic protection level needed for the reinforcements in the two mat reinforced concrete slabs.

To protect the top mat steel in 32 lbs chloride bearing specimen having pockets or zones of 96 lbs chloride concentration within the specimen, the instant off potential, the decay potential and the current density recorded were 620 mV CSE, 78 mV and 4.40 ma/sq ft respectively. When attempt was made to protect the bottom mat reinforcement, adequate protection was achieved at 632 mV CSE instant off potential, 82 mV decay potential and at a current density of 3.87 ma/sq ft in the bottom steel. At the time when bottom mat is protected, the situation in the top mat is characterized by 726 mV CSE instant off potential, 126 mV decay potential and a current density of 9.6 ma/sq ft. The overprotection of the top mat is to the extent of: 116 mV CSE instant off potential, 48 mV decay potential and 5.2 ma/sq ft current density. It may be observed that when bottom mat has adequate protection (current densities in top and bottom mats were 9.6 and 3.87 ma/sq ft respectively), the four hour decay potential value for the top mat (126 mV) was higher than the 100 mV 4 hour decay criterion used in certain CP installations.

A 590 mV CSE instant off potential, 60 mV 4 hour decay potential and 2.84 ma/sq ft current density were needed to protect the top mat steel embedded in 32 lbs-chloride-bearing concrete having 48 lbs chloride rich pockets within the specimen. The bottom mat protection level was achieved at 592 mV CSE instant off potential, 58 mV 4 hour decay potential and 2.89 ma/sq ft current density. When the bottom mat had just adequate level of protection, the top mat was overprotected and had achieved 654 mV CSE instant off potential, 90 mV 4 hour decay potential and 5.44 ma/sq ft current density. Thus, whereas the bottom mat

Table 5.4.3 Protection Level Needed to Reverse the Current Flow. Depth Effect and Chloride Gradient Effect Are Incorporated Here

Chloride Content in the Specimen	Top mat OR Bottom mat	Macro-cell Reading Before CP (mV)	TOP MAT PROTECTION ONLY				BOTTOM MAT PROTECTION			
			Macro-cell reading after CP (mV)	Instant off potential, mV CSE	4 Hour Decay Potential, mV	Current Density ma/sq. ft	Macro-cell Reading After CP, mV	Instant off potential, mV CSE	4 Hour Decay Potential, mV	Current Density, ma/sq. ft.
32 lbs in Specimen, 96 lbs in Macrocell	top	+12.90	-0.10	620	78	4.40	-4.64	726	126	9.60
	Bot	+12.80	+1.58	584	32	2.14	-0.05	632	82	3.87
32 lbs in Specimen, 48 lbs in Macrocell	top	+ 4.84	-0.15	590	60	2.84	-2.51	654	90	5.44
	Bot	+5.06	+2.74	546	48	1.81	-0.13	592	58	2.89

achieves protection at a value of current density which is less than 3 ma/sq ft, this being the upper limit in CP practice of protecting reinforcing steel in concrete structures (72,73), the top mat current density of 5.5 ma/sq ft is indicative of overprotection.

Results of Table 5.4.3 show that the top mat steel experiences overprotection when both the top and bottom mat reinforcements are treated from the same anode source located close to the top mat steel (Fig. 4.19). The effect of chloride gradients which are obtainable due to commonly occurring unavoidable significant differentials in the chloride concentrations within the chloride-bearing concrete on the protection level is also observable in the results presented in this Table. For a chloride gradient of 3 which is obtainable when the steel is embedded in 32 lbs chloride bearing specimen having 96 lbs chloride rich concrete pockets within the specimen, protection of the bottom mat was achieved at a current density of 3.87 ma/sq ft and the corresponding overprotection of the top mat was found to be at a level of 9.6 ma/sq ft current density. On the otherhand, for a chloride gradient of 1.5 which is obtainable when the steel is embedded in 32 lbs chloride bearing concrete specimens having 48 lbs chloride rich concrete pockets within the same specimen, protection is achieved for the bottom mat at a current density of 2.89 ma/sq ft, whereas the corresponding top mat steel current density was observed to be 5.44 ma/sq ft. A higher chloride gradient within the concrete also adversely affects the instant off potential values and the 4 hour decay potential values as shown in Table 5.4.3.

Table 5.4.4 shows the current density and the potentials of steel for the just adequate protection of the bottom mat reinforcement and the corresponding overprotection values for the top mat steel at different activation ages for the 32

**Table 5.4.4 The Operation Current/Potential Needed for Protection of Bottom Mat
at Different Activation Periods (for 32 lbs Chloride Bearing
Specimen Having 96 lbs Chloride Bearing Macrocell**

Acti- vation Period (days)	Current Density ma/sq ft.		Instant off Po- tential, mv CSE		Four Hour Decay Potential	
	Top Mat	Bottom Mat	Top Mat	Bottom Mat	Top Mat	Bottom Mat
9	9.60	3.89	726	632	126	82
17	9.32	3.62	716	622	126	86
30	9.23	4.92	692	618	122	86
38	9.06	4.66	682	624	118	81
55	7.77	4.92	682	618	122	84
92	8.63	4.14	690	590	106	84
98	8.29	4.92	684	602	108	84
125	8.52	5.06	686	590	126	88
146			678	610	118	85
176	8.63	4.08	672	618	110	80
185	7.78	3.63	680	615	118	80
195	7.99	3.85	670	610	122	76

lbs-chloride-bearing specimens having 96 lbs chloride rich pockets within the specimen. A maximum bottom mat current density of 5 ma/sq ft and a top mat current density of 9.60 ma/sq ft were observed over a 195 days activation period. Both the bottom and top mat steel current densities varied with activation period; no well defined effect of activation period on the protection current density was noticed. The 96 lbs chloride bearing concrete differential pocket probably induces a progressively higher level of corrosion activity in the steel with time so that a current density higher than the initial current density of 3.89 ma/sq ft was required at a later phase of the activation period. The instant off potential values recorded for the top and bottom mat steels were highest at the beginning of the activation period and then vary with the activation period without showing any apparent relationship between the instant off potential value and the activation period. Although the instant off potential value varied up and down with the activation period, the values measured at the end of a 195 days activation period were relatively higher (lower absolute value) than those obtained at the beginning of activation period. For example, at a nine days activation period, the instant off potential values for top and bottom mats were measured to 726 and 632 mV CSE respectively whereas the corresponding values were measured to 670 and 610 mV CSE for top and bottom mats respectively after 195 days of activation. A low instant off potential value at a later activation age is ascribable to the impressed current which progressively reduces the chloride level at the steel surface. The electromigration of chloride ions from near the steel towards the anode causes a reduction in chloride level near the steel; a relatively lower (in absolute value) instant off potential is needed for a relatively lower chloride content concrete (Figs. 5.2.2 through 5.2.5, the results of chloride effects study). The decay potential values also varied up and down with activation period and the maximum 4

hour decay potential values of 122 and 86 mV were reported at the top and bottom mat steels respectively.

Table 5.4.5 shows the current density and the potentials of steel for protection of bottom mat and the corresponding overprotection level of the top mat steel at different activation ages for the 32 lbs-chloride-bearing specimen having 48 lbs chloride rich pockets. Both the top and bottom mat current densities were highest at the beginning of the activation and varied up and down during the activation period. The instant off potential measured at top and bottom mat reinforcements also varied in an irregular fashion during the activation period. Likewise is the situation for the decay potentials recorded for the top and bottom mat steels.

As discussed before, the top mat steel is overprotected in the process of protecting the bottom mat steel if the anode source is the same one placed at the top of the slab close to the top reinforcement. Both the top and bottom mat steels were connected to the negative terminal of the same supply source; the voltage difference, generated by the DC supply, between the anode and the top or the bottom mat reinforcement was the same. Top mat reinforcement being nearer to the anode, the resistance between the anode and the top mat is significantly lower than between the anode and the bottom mat steel. Since the current always flows along the path of relatively lower resistance, the top mat would receive more current than the bottom mat. The current densities of 9.60 and 5.44 ma/sq ft for the top steel surface as reported in Tables 5.4.4 and 5.4.5 respectively would clearly have adverse effects. These higher current densities may cause possible secondary deleterious effects such as steel-concrete bond degradation and increased cracking due to an enhancement of alkali-silica reaction if reactive

Table 5.4.5 The Operation Current/Potential Needed for Protection of Bottom Mat at Different Activation Periods (for 32 lbs Chloride Bearing Specimen Having 48 lbs Chloride Bearing Macrocell)

Acti- vation Period (days)	Current Density ma/sq ft.		Instant Off Potential, mv CSE		Four Hour Decay Potential	
	Top Mat	Bottom Mat	Top Mat	Bottom Mat	Top Mat	Bottom Mat
1	5.44	2.89	654	592	90	56
38	5.18	2.89	644	580	88	52
44	5.31	2.71	636	568	84	56
54	4.92	2.62	622	566	88	56
70	5.44	2.35	632	580	84	52
81			628	572	108	60
92	5.05	2.53	616	586	96	60
107	5.44	2.62	624	560	88	56
140	4.66	2.53	634	558	92	56

aggregates are used in the construction.

Results of Tables 5.4.4 and 5.4.5 show that when steel is embedded in concrete having chloride differentials within the concrete resulting a chloride gradient, a high protection level is required and the extra level of protection will have to commensurate with the value of the chloride gradient determined by the extent of chloride differential. This is attributable to the fact that higher chloride differentials and therefore higher chloride gradients within the concrete surrounding the steel would create a higher potential differences on the steel. When points having the above mentioned high potential differential are connected through an external resistor, a high corrosion current will flow through the resistor. Therefore a higher CP current would be needed in the circuit to reverse the flow of this high corrosion current.

From the results obtained in this section of the study, it may reasonably be concluded that the -770 mV CSE or -850 mV CSE instant off potentials values are higher than required to attain for adequate protection. Even the instant off potential value corresponding to significant overprotection of the top mat reinforcement lies below (i.e. more positive) the -770 mV CSE. An instant off potential of 632 mV CSE was found sufficient to protect steel embedded in chloride rich concrete ($32\text{lbs} / \text{yd}^3$) even in the presence of extremely high chloride rich pockets corresponding to chloride gradient of 3. The 100 mV 4 hour decay potential was found to be just enough to protect steel embedded in 32 lbs-chloride-bearing concrete having 96 lbs chloride bearing concrete pockets (chloride gradient: 3) within the same concrete member. A maximum 4 hour decay potential of 126 mV was recorded as the overprotection potential for the top mat steel. When the steel was embedded in 32 lbs chloride bearing concrete having 48 lbs

chloride bearing concrete pocket (corresponding to a chloride gradient of 1.5), a maximum value of 60 mV 4 hour decay potential was measured to achieve protection of the bottom mat. The overprotection potential of the top mat reinforcement in this case was below 100 mV value as a maximum overprotection potential of 96 mV decay in 4 hour was recorded at the level of top mat steel.

To examine the effects of CP current on deeply buried reinforcing steel shaded by steel lying closer to the anode network, two current pickup probes were placed one behind the other at distances of 2.5 in and 3.5 in from the anode. Each of the current pickup probes was attached to a lead wire which was connected to the anode. Table 5.4.6 shows the current drawn by the pick up probes at different circuit currents. The results show that higher amount of current was received by the probes located near the steel in comparison to the probes located away from the steel. The current received by the probe located at 3.5 in away from the anode was 40 % of the current received by the probe at 2.5 in away from the anode. A relatively lower current received by the probe located at a relatively higher distance from the anode in comparison to the one located at a relatively lower distance from the anode is ascribable to the higher resistance between the anode and steel in the former case. Since both of the pickup probes are able to draw current from the supply system, the anode system employed here can be considered an efficient system in terms of supplying currents at different depths. It can also be inferred that the current pickup probes proved useful in examining current distribution relative to anode positions.

The effectiveness of CP in arresting the corrosion may be checked from the results provided by the corrosometer probes. These corrosometer probes were placed at the level of steel during casting of the specimen. The corrosion rates of

Table 5.4.6 Current Drawn up by the Pickup Probes. The Results Show the Efficiency of the Anode System in Supplying Current to the Steel Located at Different Distances From the Anode

Total Current in the Circuit, ma	Current Drawn up by the Pickup Probes	
	Probe 2.5 in Away From the Anode	Probe 3.5 in Away From the Anode
8.2	4.96	1.95
6.5	3.80	1.50
7.8	4.50	1.65

the steel embedded in control specimen as well as in cathodically protected specimens were measured. The CK-3 corrosometer dial readings obtained from the embedded corrosion probes were converted to mills per year (MPY) using the standard formula. The corrosion rate in the control specimen was found to be 0.198 MPY compare to an insignificant average corrosion rate of 0.013 MPY recorded in the cathodically protected specimens.

The effectiveness of CP may also be checked from the weight loss data of the coupon steel and macrocell steel. Table 5.4.7 shows the weight loss data for coupon and macrocell steels removed from the control and CP specimens at the end of six months activation. The data in this table show that the CP technique significantly control the chloride induced corrosion. For example, for 32 lbs chloride bearing specimen having 96 lbs chloride bearing macrocell, the weight losses for the top and bottom macrocell steels of a CP specimen were 0.90 percent and 5.9 percent of the corresponding weight losses observed in top and bottom macrocell steels of the control specimen.

5.5 ENHANCEMENT OF ALKALI-SILICA REACTION DUE TO CATHODIC PROTECTION

The effect of current density on the enhancement of alkali-silica reaction is studied in this section. Steel embedded in mortar specimens made of high alkali cement and reactive crushed pyrex glass were subjected to 20 and 100 ma/ft² cathodic protection (CP) current densities for a period of 80 days. The observations made in alkali-silica reaction study are: time for appearance of the first sign

Table 5.4.7 Weight Loss of the Coupon Steel and Macrocell Steel for CP Specimen and Control Specimen in Depth Effect Study. The Result of this Table Shows the Effectiveness of CP in Arresting the Corrosion

Specimen Chloride Content, lb/yd of Concrete	Macrocell Chloride Content, lb/yd of Concrete	Top Mat or Bottom Mat	Coupon Steel		Macrocell Steel		
			Weight loss, %		Weight Loss, %		Weight Loss in CP Specimen in Comparison to Control Specimen, %
			Control Specimen	CP Specimen	Control Specimen	CP Specimen	
32	96	top	7.93	0.23	25.5	0.23	0.90
		bott	5.30	0.43	19.2	1.15	5.90

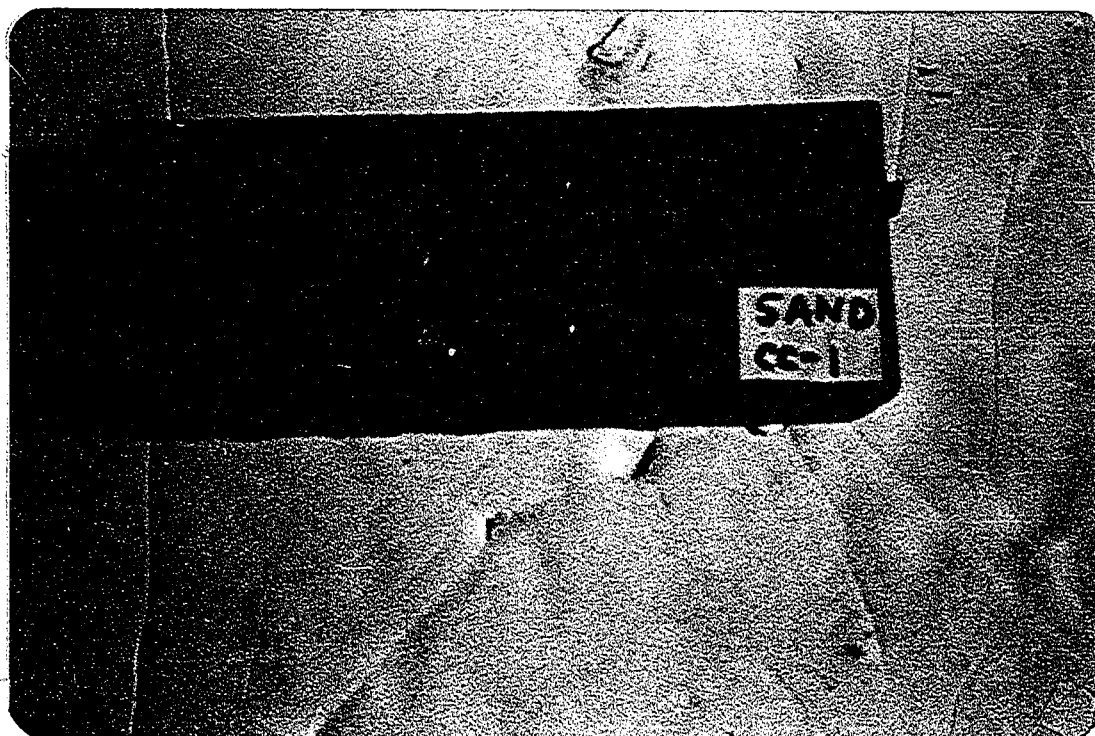
of crack, total expansion at the end of the observation period, compressive strength and hardness number of mortar removed from different locations with respect to the cathode position, possible change in steel properties due to CP current and the volume of the alkali-silica gel formed at the steel concrete interface.

5.5.1 Initiation of Cracks and Total Expansion at the End

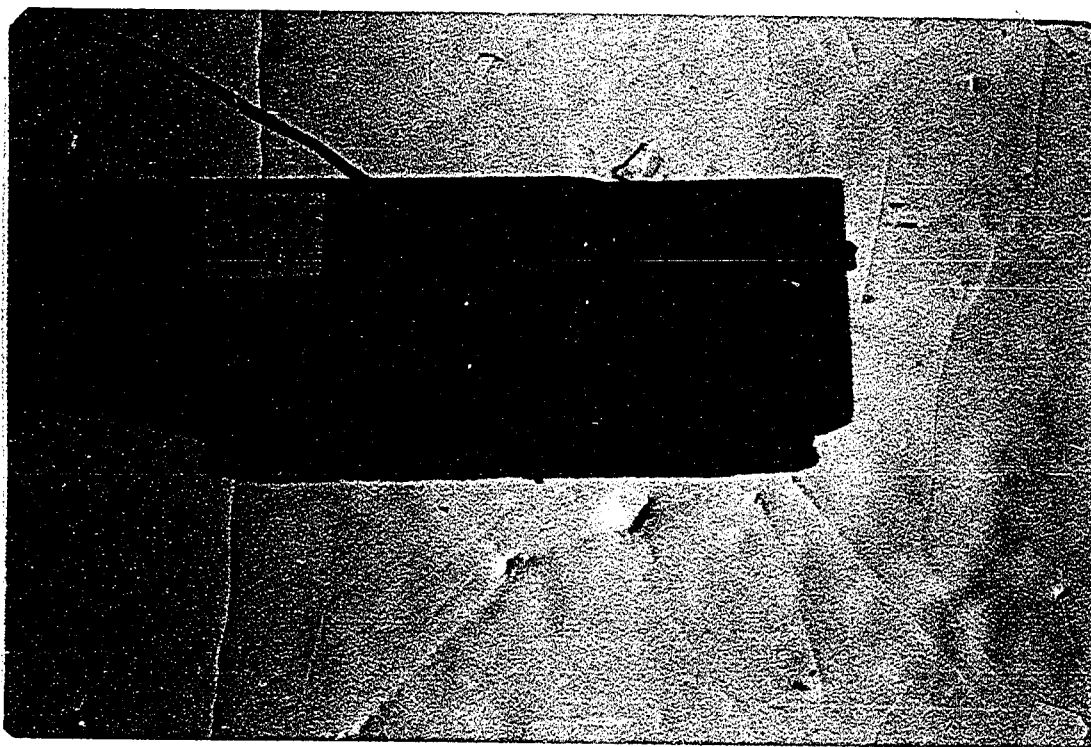
Table 5.5.1 shows the effect of the CP current on expansion and the initiation of cracks due to alkali-silica reaction at the end of the observation period. In specimens with nonreactive aggregate and no CP current, as expected no crack appeared. In control specimens (no current) made with reactive aggregates, the first sign of crack appeared after 75 days from the time of casting. In control specimens, total expansion at failure based on 2 in (50.8 mm) gauge length, was measured equal to 0.151 mm. A CP current of 20 ma/sq. ft (215 ma/ sq m) advanced the cracking initiation period to 45 days. At a current density of 100 ma/ sq. ft (1076 ma/sq m) the first sign of cracks appeared at a very early age of 30 days. Even without CP, disruptive alkali-silica reaction would commence in due course of time if reactive aggregates are used; but the application of CP in concrete made with reactive aggregates would cause disruption at a significantly earlier age. Fig. 5.5.1 shows the cracking patterns in different specimens. It is notable that the first sign of crack appeared just above the steel in specimens where CP currents were applied. The cracks at other locations in these specimens appeared at a later age. The cracks above the steel could not widen due to the possible restraining effect of the steel presence. For widening of these cracks the mortar has to move over the circumference of the steel bar when it is presumed that for the movement the mortar has to overcome the friction of the steel sur-

Table 5.5.1 Effect of Current Density on Initiation of Crack and Expansion at the End of Observation Period

Specimen and CP Current	Water Cement Ratio	First Sign of Crack at, (days)	Total Expansion at the End of Observation Period, mm
Cement + Sand, no CP	0.40	Did not appear	0.0
Cement + Pyrex, no CP	0.40	75	0.151
Cement + Pyrex, 20 ma/sq ft	0.40	45	0.184
Cement + Pyrex, 100 ma/sq ft	0.40	30	0.183

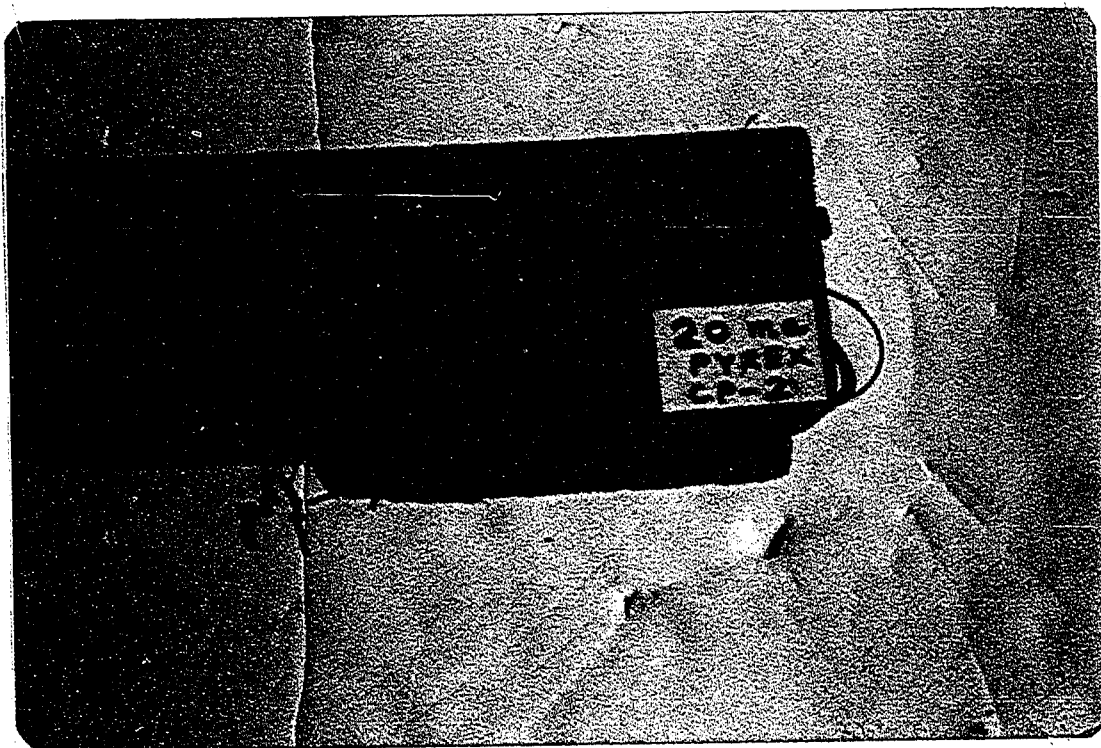


(a) No Reactive Aggregate, No CP

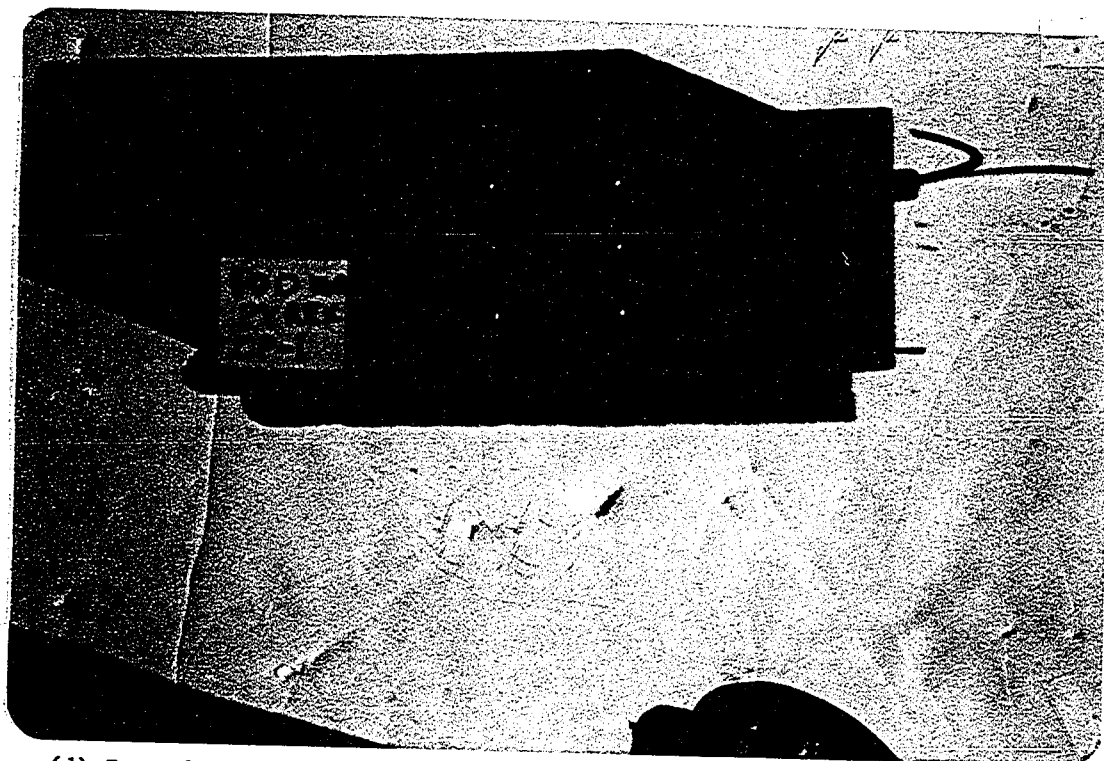


(b) Reactive Aggregate , No CP

Fig. 5.5.1 Cracking Pattern for Different Specimens
Used in Alkali-Silica Study



(c) Reactive Aggregate, 20 ma/sq ft CP



(d) Reactive Aggregate, 100 ma/sq ft CP Current

Fig. 5.5.1 Contd. Cracking Pattern for Different Specimen Used
in Alkali-Silica Reactivity Study

face. The first crack in the control specimen having crushed pyrex glass as aggregate appeared at a location away from the steel. As expected, no crack appeared on the control specimen where nonreactive sand was used as aggregate. The much earlier appearance of the first sign of crack near the steel in specimens subjected to CP current is attributable to the negative polarities of steel which attract Na and K ions near the steel. This high concentration of cations in the steel vicinity together with OH formation due to electrolysis of water creates an environment most conducive to an increased alkali-silica reaction. These results provide warning to the CP users when CP corrosion prevention technique is employed in reinforced concrete structures where reactive aggregates have been used in construction.

5.5.2 Compressive Strength

Due to the formation of alkali-silica gel, the mortar may get softened. This softening effect should be reflected in a reduction in the compressive strength of the mortar. Fig. 5.5.2 shows the effect of CP current densities on compressive strength of 1/2 in (12.7 mm) mortar cubes removed from different locations of the alkali-silica reactive specimens with respect to the position of the cathode(steel). It seems significant amount of alkali-silica gel formed near the steel due to CP current causes appreciable softening of concrete. This is reflected in the considerable reduction in the compressive strength of mortar near the steel of the specimens in which CP currents were applied. In specimens subjected to 100 ma/sq. ft (1076 ma/sq m) of CP current, the compressive strength of cubes taken from near the steel is 34 percent lower than that of the cubes taken from a distance away from the steel near the anode. The corresponding compression

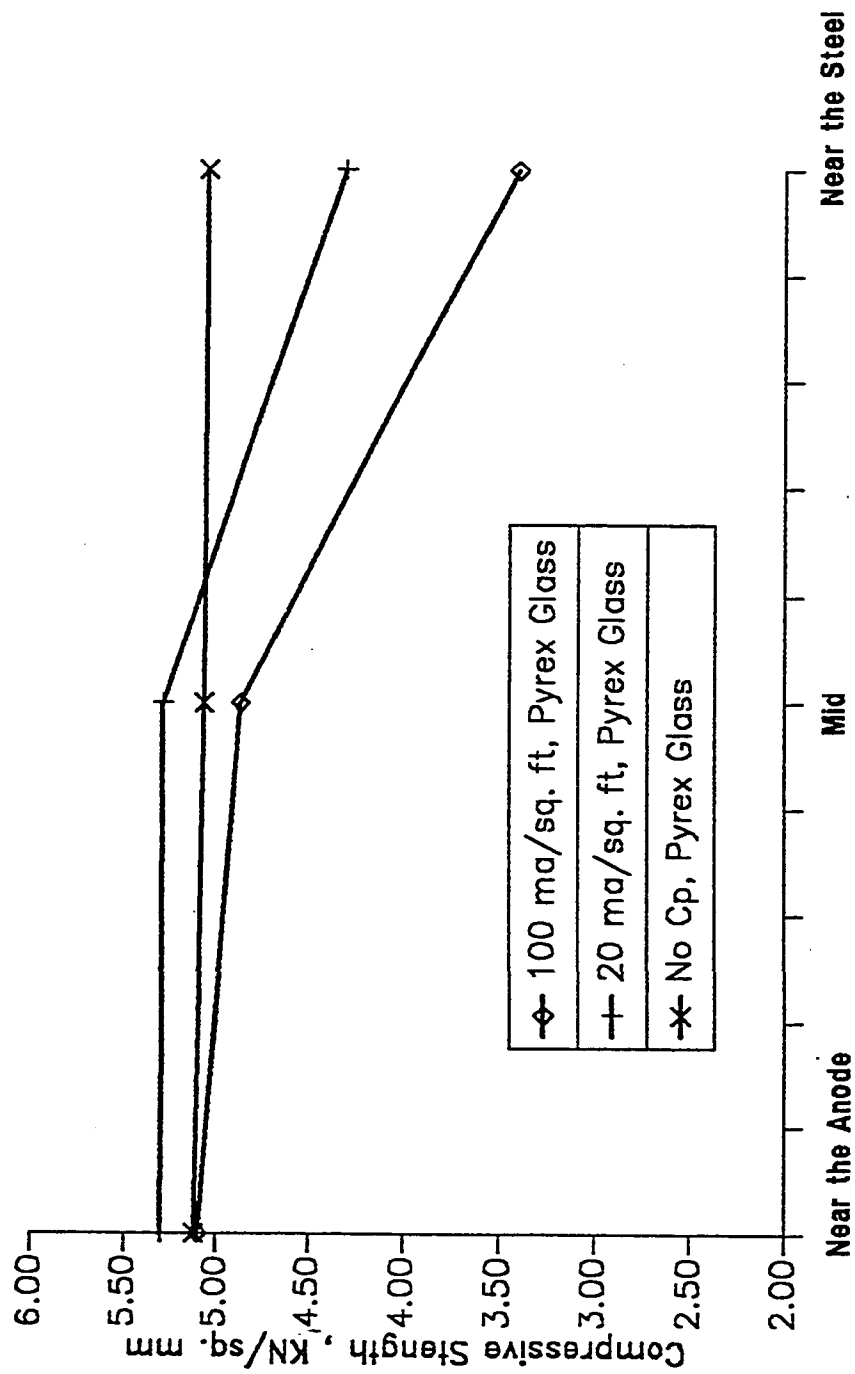


Fig. 5.5.2 Effect of Cathodic Protection Current on Compressive Strength of Mortar

strength reduction value is 15 percent in specimens subjected to 20 ma/ sq ft (215 ma/ sq m) of CP current. Fig. 5.5.2 also shows that compressive strength of cubes removed from similar locations of control specimens (never received current) is not dependent on the locations from which the cubes were taken. This reduction in the compressive strength is most likely to reduce the bond between steel and concrete when CP is applied for a long period of time in a reinforced concrete structure where reactive aggregate is used. It is to be noted that the results presented here show a highly accelerated effect due to the fact that a very high current density of 100 ma/sq. ft was applied. Such a current density is very high in comparison to the normal protection current of 1 to 3 ma/sq. ft required to satisfy different CP criteria(72). Also the use of reactive crushed pyrex glass with a cement to aggregate ratio of unity also gives an accelerated disruptive effect. These two measures were adopted to study the phenomena of possible softening within a reasonable period of time. The results do show that CP current will strongly promote the alkali-silica reaction in the vicinity of steel and that a softening phenomena would take place due to the alkali-silica reaction in the concrete surrounding the steel.

5.5.3 Hardness of the Mortar

Rockwell hardness numbers were measured on mortar plate specimens removed from different locations with respect to the position of the cathode (steel); these positions were near the steel, near the anode and at midpoint between steel and anode. Fig. 5.5.3 shows the effect of current density on the hardness of cement mortar removed from the aforesaid locations. Hardness numbers for control specimens (nonreactive sand used as aggregate and no CP

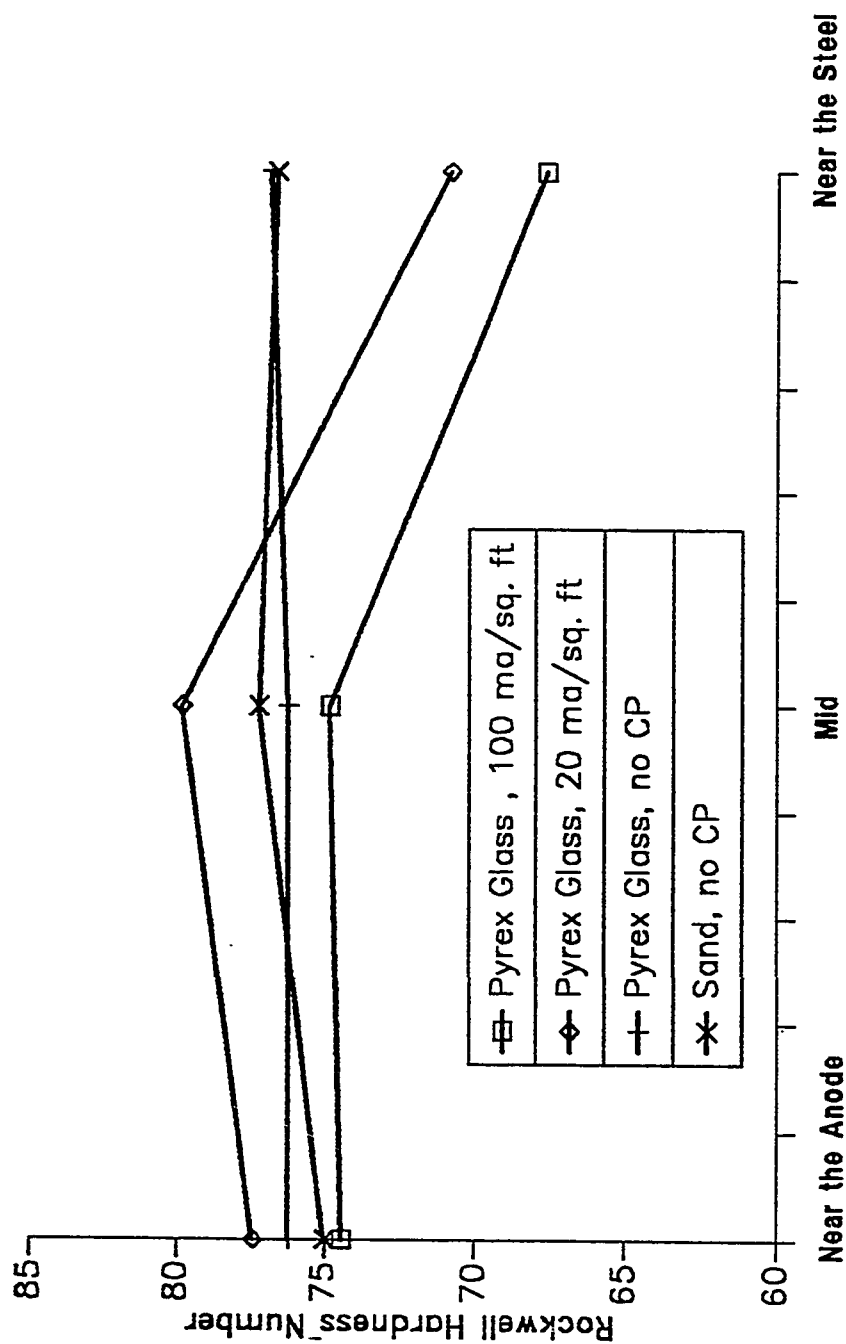


Fig. 5.5.3 Effect of Cathodic Protection Current on Hardness of Mortar

current, reactive crushed pyrex glass and no CP current) are almost same at all the three locations for which the tests were performed. However, considerable reduction in the hardness number at locations near the cathode (the steel) is observed in specimens where CP current was applied. In specimens subjected to 100 ma CP current per square ft of steel surface area, an average hardness number of 67 is measured near the cathode whereas the corresponding value is around 75 near the anode (farthest point from the cathode).

5.5.4 Effect on Steel Properties

The effect of CP current on steel properties is shown in Table 5.5.2. It is reported elsewhere(27) that a CP current reduces the ductility of steel thereby imparting brittleness. From the total elongation data reported in Table 5.5.2, it is clear that the CP current has no definite adverse effect on the ductility of steel. Thus the effect of CP current on the induction of brittleness in the steel embedded in concrete structures is not supported by these data for the short term tests conducted in this study. A small reduction in ultimate load is noticed at high current density; however, this reduction is rather insignificant. It is also clear that there is no effect of CP current on the rupture strength of steel embedded in concrete.

5.5.5 Volume of Gel Formed

Simple staining technique was employed on powdered sample taken from near the steel. In this technique, the measured absorbance is the indicator of the volume of the gel forms. Table 5.5.3 shows the effect of current densities on the

Table 5.5.2 Effect of Current Density on Ductility, Ultimate Strength and Rupture Load of Steel

Specimen and CP Current	Total Elongation (mm)	Ultimate load, KN	Rupture Load, KN
Cement + Pyrex, no CP	30.8	75.5	58.0
Cement + Pyrex, 20 ma/sq ft	32.0	74.0	54.0
Cement + Pyrex, 100 ma/sq ft	30.0	72.0	55.0

Table 5.5.3 Results Obtained From Simple Staining Technique

Type of Aggregate	CP or Without CP	Absorbance
Cement + Pyrex Glass	no CP	0.391
Cement + Pyrex Glass	20 ma/sq ft Current	0.855
Cement + Pyrex Glass	100 ma/sq ft Current	1.029

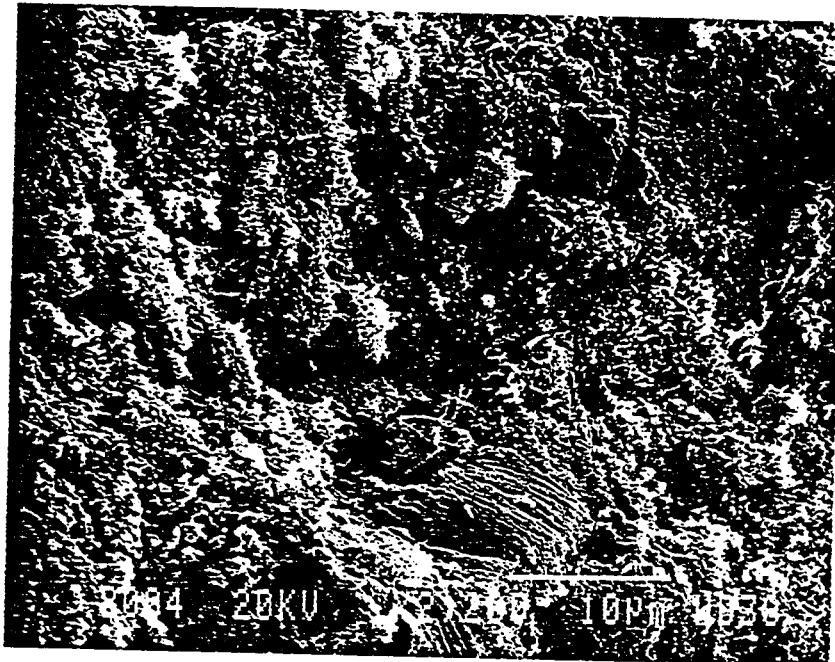
measured absorbance. A high absorbance has been observed in powdered samples removed from specimens in which 100 ma/ sq. ft current density was applied. Higher absorbance implying the higher volume of the gel formed in the specimens subjected to CP current indicates an acceleration of the disruptive activity due to the alkali-silica gel when CP is applied.

5.5.6 Scanning Electron Microscopy

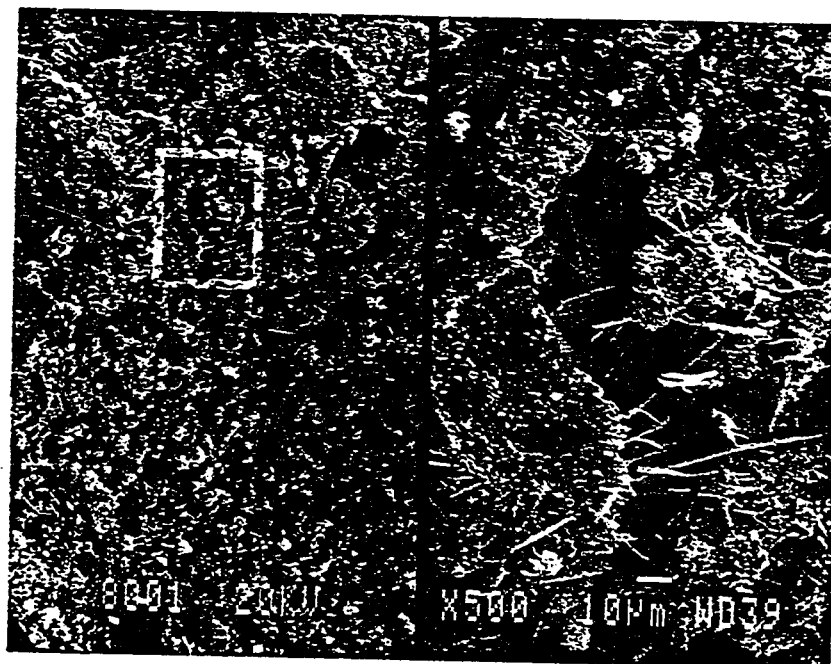
Scanning electron microscopy analysis have been performed on control specimens as well as specimens where CP current was applied. Presence of massive gel were noticed as shown in Fig. 5.5.4.

5.5.7 Summarized Overview

Results of the alkali-silica reaction study indicate an increased disruption of concrete due to an enhanced alkali-silica reaction when CP current was applied. In the laboratory sample, a normal reactive environment was created by using high alkali cement and a reactive aggregate simulated by crushed pyrex glass. The test was accelerated by using a cement to aggregate ratio of unity and a high current density of 100 ma/sq ft. The results of the criteria establishment study (Art. 5.2) show that a maximum current density of the order of 3.0 ma/sq ft is required for protecting steel in concrete located in Gulf environment. It was also found in the criteria establishment study that the current density requirement decreases with activation period. Under the action of a low CP current of the order of 3 ma/sq ft, the alkali-silica reaction will be relatively much slower and will take much more time to manifest disruptive deterioration than observed in the present accelerated test.



(a)



(b)

Fig. 5.5.4 Photographs of Scanning Electron Microscopy Analysis. The Mortar Samples were removed from Steel-Concrete Interface (a) Control Specimen (No CP Current), (b) CP Specimen

5.6 DEGRADATION OF STEEL-CONCRETE BOND DUE TO CATHODIC PROTECTION

Four constant current densities of 3, 10, 20 and 50 ma/ ft² (32.3, 108, 215 and 538 ma/ m²) at the steel surface were used in the test program which also include chloride content of concrete as the second variable. Chloride contents of 2 and 8 lbs/ yd³ (0.364 and 1.455 percent by weight of cement) were added to concrete as sodium chloride (NaCl) through mix water. After 14 months of impressed current, the cathodically protected specimens along with control specimens were tested for bond strength. After the completion of the bond test on each specimen, the steel bar was removed and inspected for the corrosion condition. Concrete powdered samples were obtained for testing from three locations; near the steel, near the anode and midpoint of the steel and the anode. The powdered samples were chemically analyzed for determination of K⁺, Na⁺ and Cl⁻. Bond strength and chemical analysis results obtained from current-treated specimens were compared with the corresponding values measured in the control specimens.

5.6.1 Degradation of Steel-Concrete Bond

Fig. 5.6.1 shows the typical load versus free-end slip and loaded-end slip relationship. This presentation shows a nearly linear relationship between load and slip upto 70 percent of the ultimate bond strength. Thereafter at 35 KN the load-slip curve changes trend sharply, signifying a breakdown of bond between reinforcing steel and concrete. The descending portion o the load-slip curve after a slip of 3 mm indicates progressive deterioration of bond at the steel-concrete

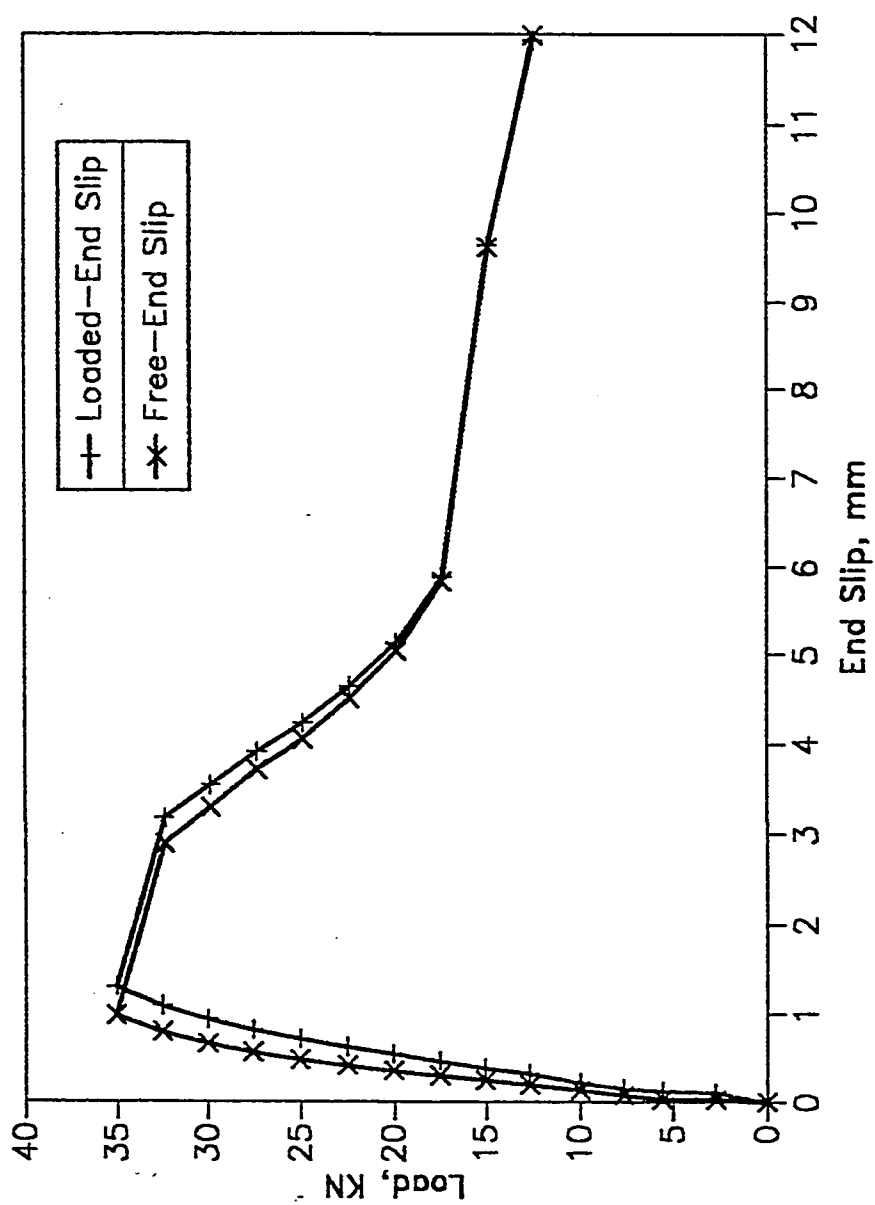


Fig. 5.6.1 Typical Load vs. Free-End and Loaded-End Slips from Bond Strength Test on a Current-Treated Specimen (Impressed Current: 50 ma/sq. ft, Chloride Content: 2 lbs/cu yd)

interface, till the curve becomes horizontal, indicating continued slip at about 50 percent of the ultimate load. The load eventually decreased to near-zero at a very high slip value not shown in Fig. 5.6.1, as it is of little significance. The behavior also shows that during the increasing bond resistance phase, as well as the early stage of the bond breakdown phase, the loaded-end slip is somewhat higher than the free-end slip. This is attributable to the elastic deformation of steel bar which is reflected only in the loaded-end slip values.

Figs. 5.6.2 and 5.6.3 show the load and free-end slip relationships for 2 lbs/ yd³ (1.19 kg/ m³) chloride-bearing concrete specimens treated with 3 ma/ ft² (32.3 ma/ m²) and 50 ma/ ft² (538 ma/ m²) impressed current densities along with the behavior of control specimens. It is seen that after the 14 months of treatment with 3 ma/ ft² impressed current, the reduction in the ultimate bond strength is only an insignificant 2 percent. However, for the 50 ma/ ft² current density, there is a 20 percent reduction in the bond strength. Also, whereas the control specimens show virtually no slip upto a pullout load of 30 KN, the 50 ma/ ft² current-treated specimens show appreciable slips even in the early stage of loading; the slip at 30 KN being 0.75 mm in CP specimens compared to near-zero in control specimens.

Fig. 5.6.4 shows the percentage reduction in the ultimate bond strength between reinforcing steel and the two chloride bearing concretes for the four current densities impressed for a period of fourteen months. Bond strength reduction evaluation is based on the differential in the values of the CP specimens and the corresponding control specimens. These data show a good correlation between the impressed current density and reduction in the bond strength, and shows that the loss of bond is roughly proportional to the applied current for both levels of chloride content in concrete. The data also show that

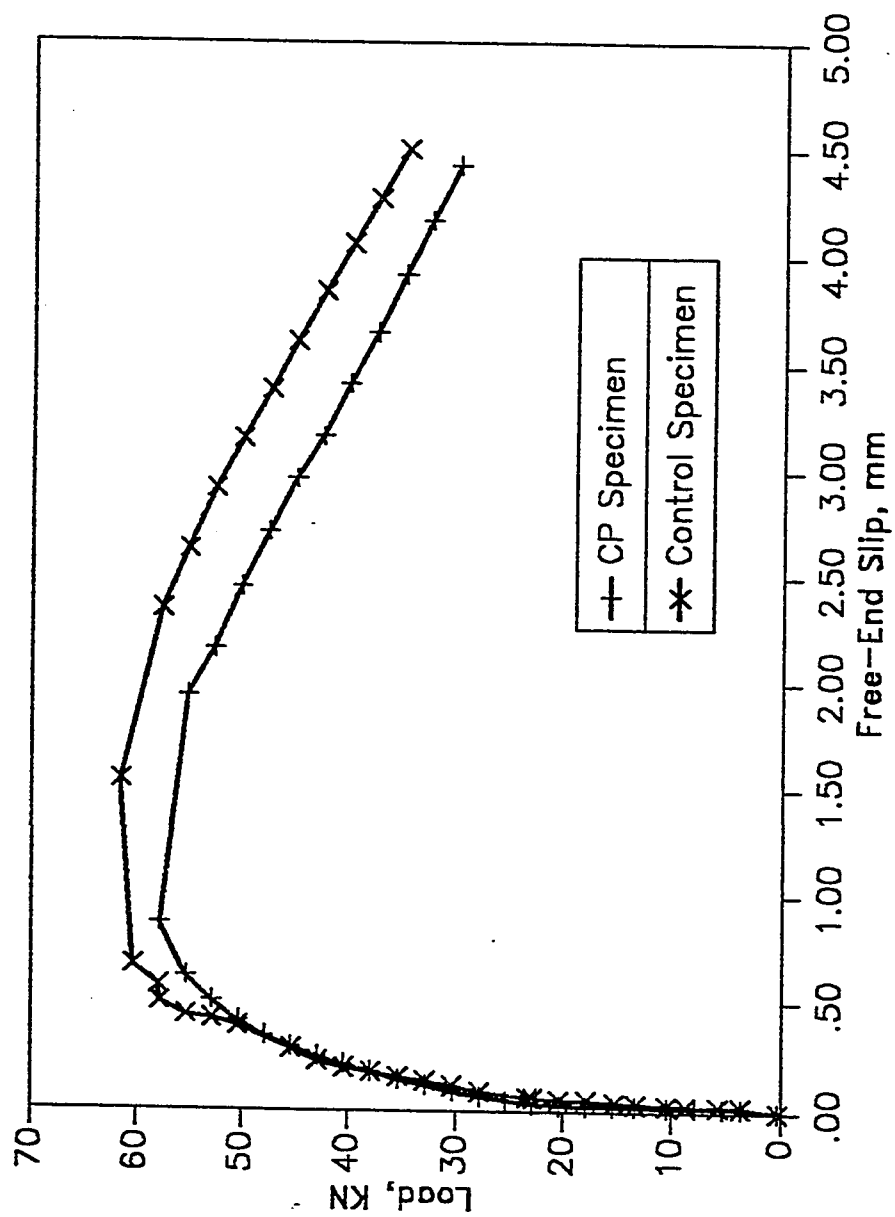


Fig. 5.6.2 Free-End Slips Under Bond Test for Cathodic Protection Current-Treated and Control Specimens (Impressed Current: 3 ma/sq.ft, Chloride Content: 2 lbs/cu yd)

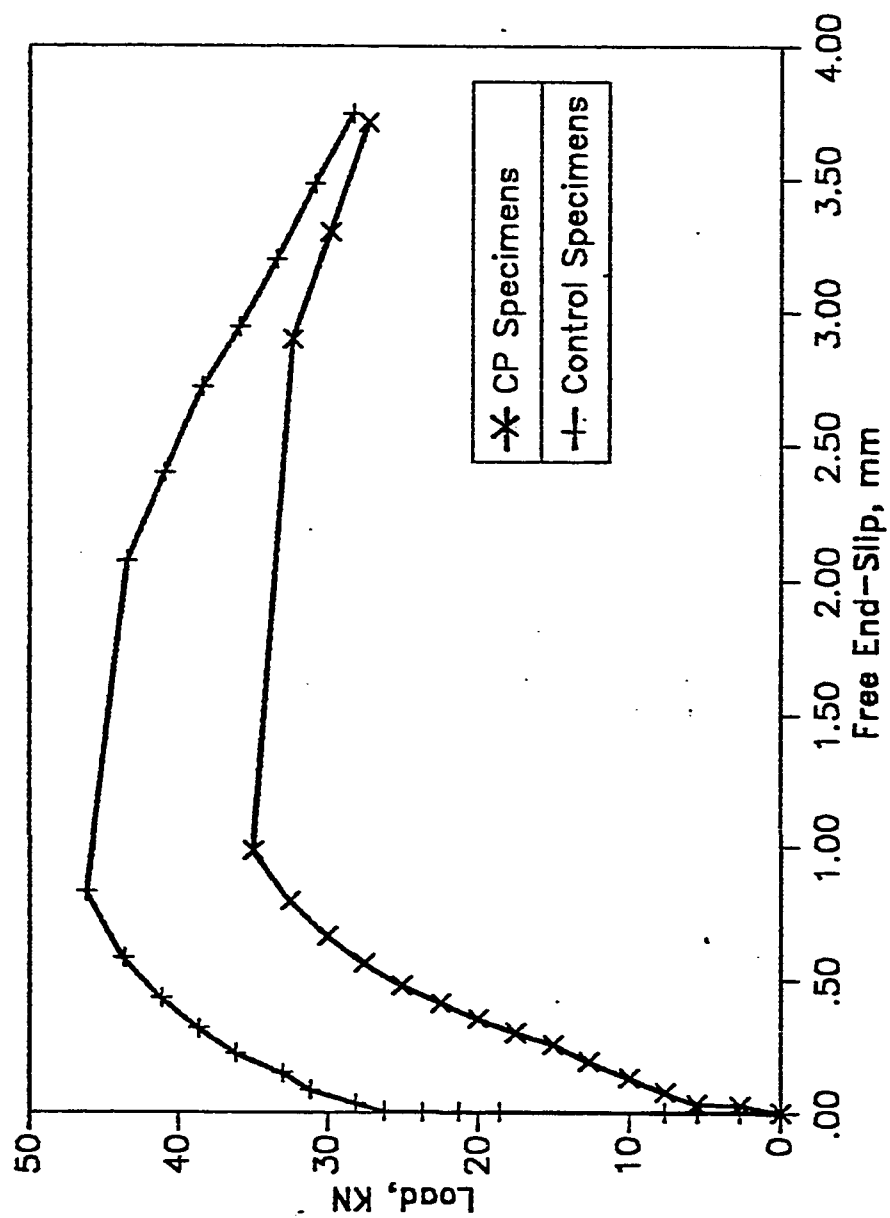


Fig. 5.6.3 Free End Slips Under Bond Test for Cathodic Protection
Current-treated Specimens and Control Specimens (Impressed
Current: 50 ma/sq.ft, Chloride Content: 2 lbs/cu yd)

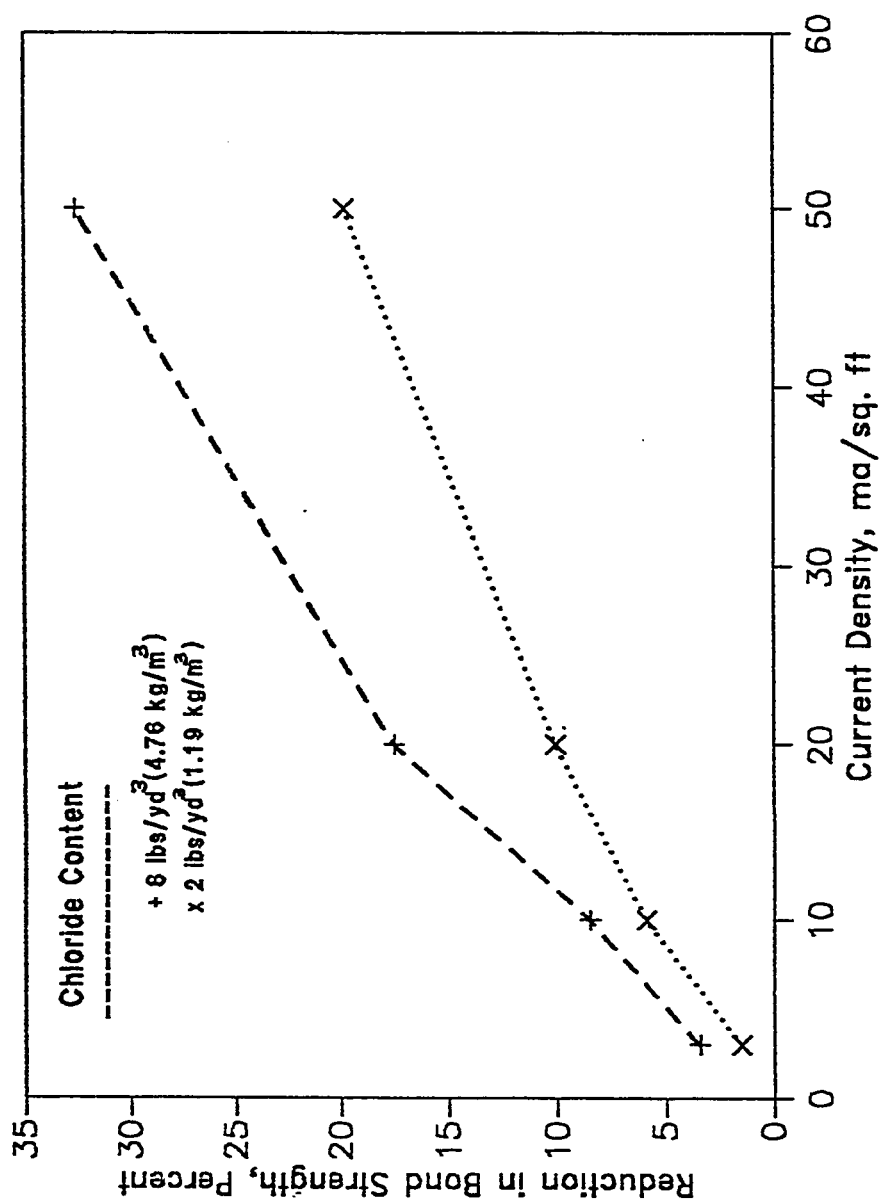


Fig. 5.6.4 Reduction in Bond Strength for Different Cathodic Protection Current Densities Impressed on Reinforcing Steel in Chloride Contaminated Concrete

for the same current density, significantly higher bond reductions occur when the chloride content is increased from 2 to 8 lbs/ yd³ (1.19 to 4.76 kg/ m³). For example, for a 50 ma/ ft² current density the ultimate bond reduction is increased from 19 to 33 percent when the chloride concentration in concrete increases from 2 to 8 lbs/ yd³.

5.6.2 Movement of Alkali-Cations Due to CP Current

Figs. 5.6.5 and 5.6.6 show the effect of current density and chloride (supplied as NaCl) content of concrete on the concentration of Na⁺ and K⁺ near the steel surface, with control specimens providing results corresponding to zero current density. Fig. 5.6.5 shows that the concentration of Na⁺ near the steel surface is a function of current density as well as chloride content of concrete. The positively charged sodium ions get attracted and accumulated near the negatively charged steel. Since current is carried from anode to cathode (steel reinforcement) through ionic movement, a higher CP current density impressed on steel causes a greater concentration of sodium ions close to the steel-concrete interface. A significantly higher concentration of sodium ions was measured in the 8 lbs-chloride specimens in comparison with those containing 2 lbs/ yd³ of chloride. For CP current densities of 0, 3, 10, 20 and 50 ma/ ft², Na⁺ concentrations, expressed as the percentage weight of cement, for 2 lbs- and 8 lbs-chloride specimens were 0.359, 0.395, 0.581, 0.746, 0.983 and 1.29, 1.65, 1.77, 1.89, 2.41 respectively. These data show that for the 8 lbs-chloride concrete, the Na⁺ concentration was, on an average, 200 percent higher than for the 2 lbs-chloride concrete. The significantly increased presence of Na⁺ at the steel level for the 8 lbs-chloride concrete is ascribable to higher concentration of Na⁺ in the pore solution from

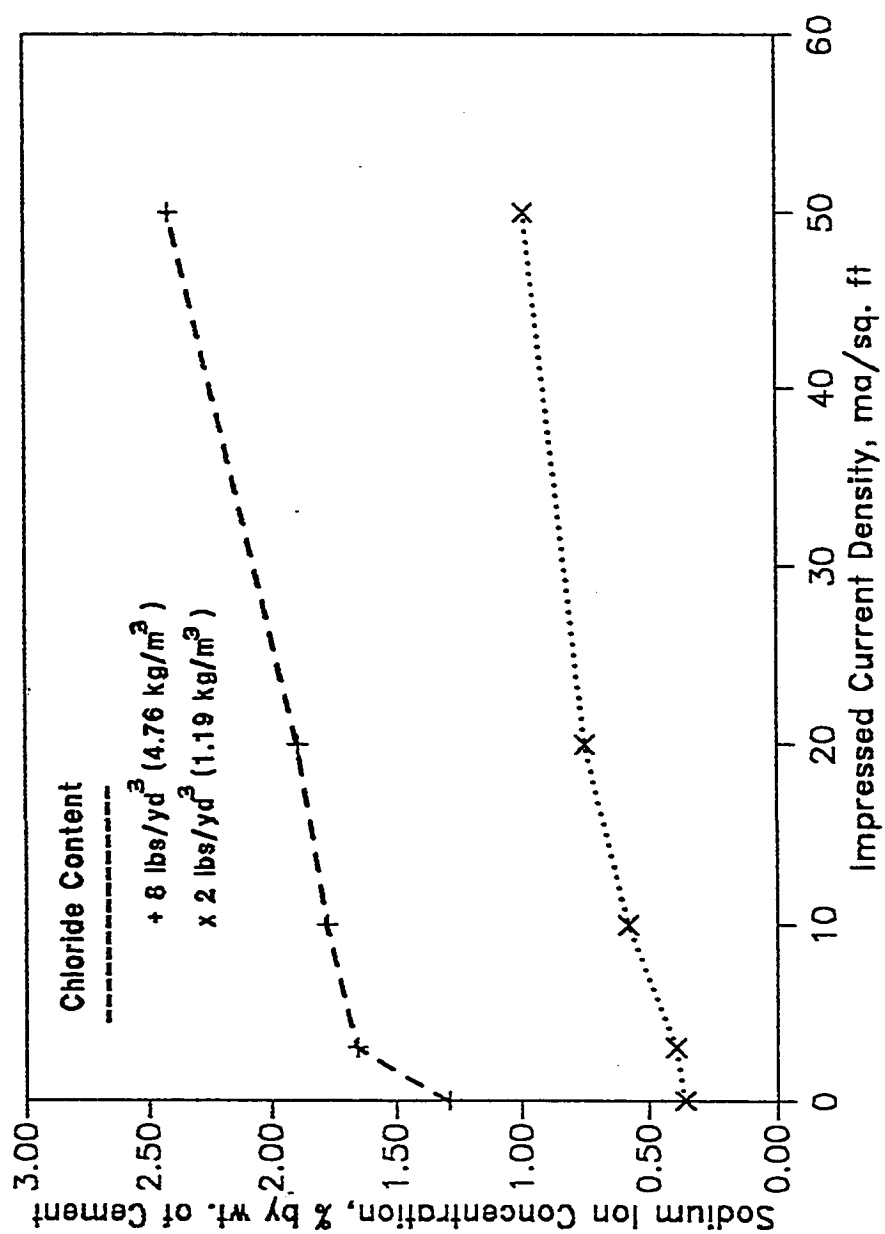


Fig. 5.6.5 Effect of Impressed Current Density on the Concentration of Sodium Ions Near the Reinforcing Steel Surface

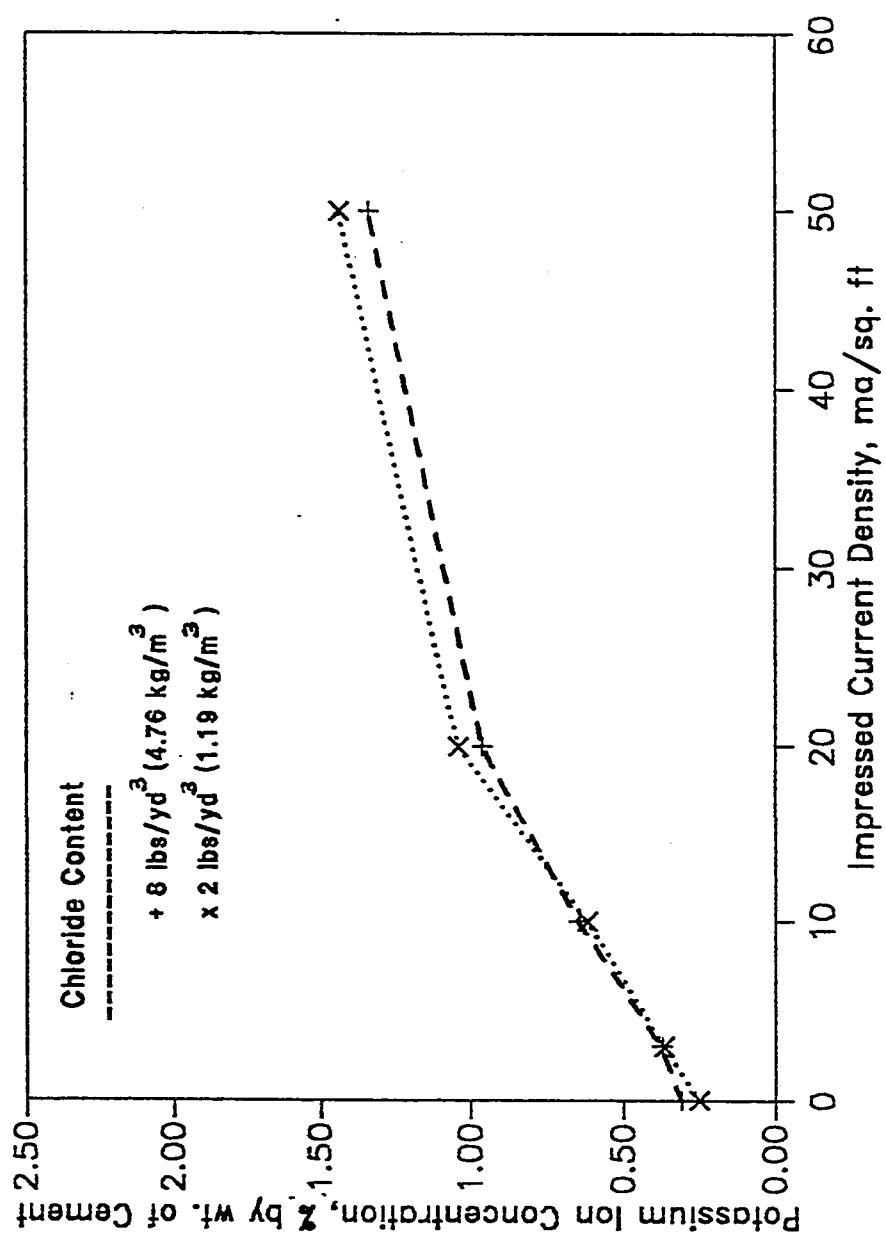


Fig. 5.6.6 Effect of Impressed Current Density on the Concentration of Potassium Ions Near the Reinforcing Steel Surface

the increased NaCl addition. Understandably, a similar situation is not obtainable for K^+ (Fig. 5.6.6) which shows similar order of concentration for both 2 lbs- and 8 lbs-chloride concretes with increase in CP current density. K^+ concentration in the pore solution being a function of the potassium associated alkali content in the portland cement composition, is unaffected by chloride addition as NaCl.

It is interesting to note that for a given current density and chloride contamination in concrete, the accumulation of K^+ near the steel surface is much higher than that of the Na^+ . For example, the percentage increases (in comparison to the control specimens, zero ma/ft^2 of CP current) in sodium ions accumulated near the steel at current densities of 3, 10, 20 and 50 ma/ft^2 were respectively 10, 62, 108 and 174 for specimens having 2.0 $lb\ Cl^- / yd^3$ of concrete. The percentage increases (in comparison to the control specimen, zero ma/ft^2 CP current) in K^+ ion concentration near the steel for current densities of 3, 10, 20 and 50 ma/ft^2 were respectively 46, 146, 342 and 488 for specimens having 2 $lb\ Cl^- / yd^3$ of concrete. These data show that K^+ migrates by an average of 173 percent faster than the Na^+ . The experimental results found here are in line with the theoretical findings reported in Art. 3.2 wherein the K^+ migration was found to be 153 percent faster than the Na^+ . A possible explanation of this relatively higher accumulation of K^+ in comparison to Na^+ lies on the fact that the conductance of concrete depends upon the velocities as well as the concentrations of the ions present in the pore solutions. These ions move through the concrete electrolytic medium at different velocities. The absolute velocities of K^+ and Na^+ ions are reported to be 0.000665 and 0.000456 cm/sec respectively at a particular condition(78). It is this higher velocity of the

K^+ ion which causes the rapid migration of this cation toward the cathode.

Typical concentration profiles for Na^+ ions as a function of distance from the rebar are shown in Figs. 5.6.7 and 5.6.8. The results show that the concentration of Na^+ ions accumulated at the regions near the rebar is higher than that at the mid section (25.4 mm from the rebar) and at regions near the anode (50.8 mm from the rebar). However, for the control specimen the general trend is opposite and the Na^+ ion concentration in the anode vicinity is slightly higher than at the mid section and the regions near the rebar.

Figs. 5.6.9 and 5.6.10 show the concentration profiles for K^+ ions as a function of distance from the rebar. The results show that in the cathodically protected specimen the K^+ ions, like the Na^+ ions, migrate toward the rebar section (cathode). However, like Na^+ ions, the general trend is opposite in the control specimen and the concentration of K^+ ions increases with the distance from the the cathode. Like Cl^- ions, the migration of Na^+ and K^+ ions from the regions near the rebar toward the concrete surface in the control specimen is probably due to the evaporation of water from the concrete which will carry the ions toward the concrete surface.

5.6.3 Relationship Between the Bond Reduction and Alkali Cations Concentration at Steel Surface

Fig 5.6.11 shows the relationship between bond reduction and the two alkali ion concentrations ($K^+ + Na^+$) in the vicinity of the reinforcing steel for the 2 lbs-and 8 lbs-chloride concretes. The bond reduction is found to be roughly proportional to the concentrations of sodium and potassium ions near the steel-concrete interface. A bond loss of upto 33 percent is measured when the

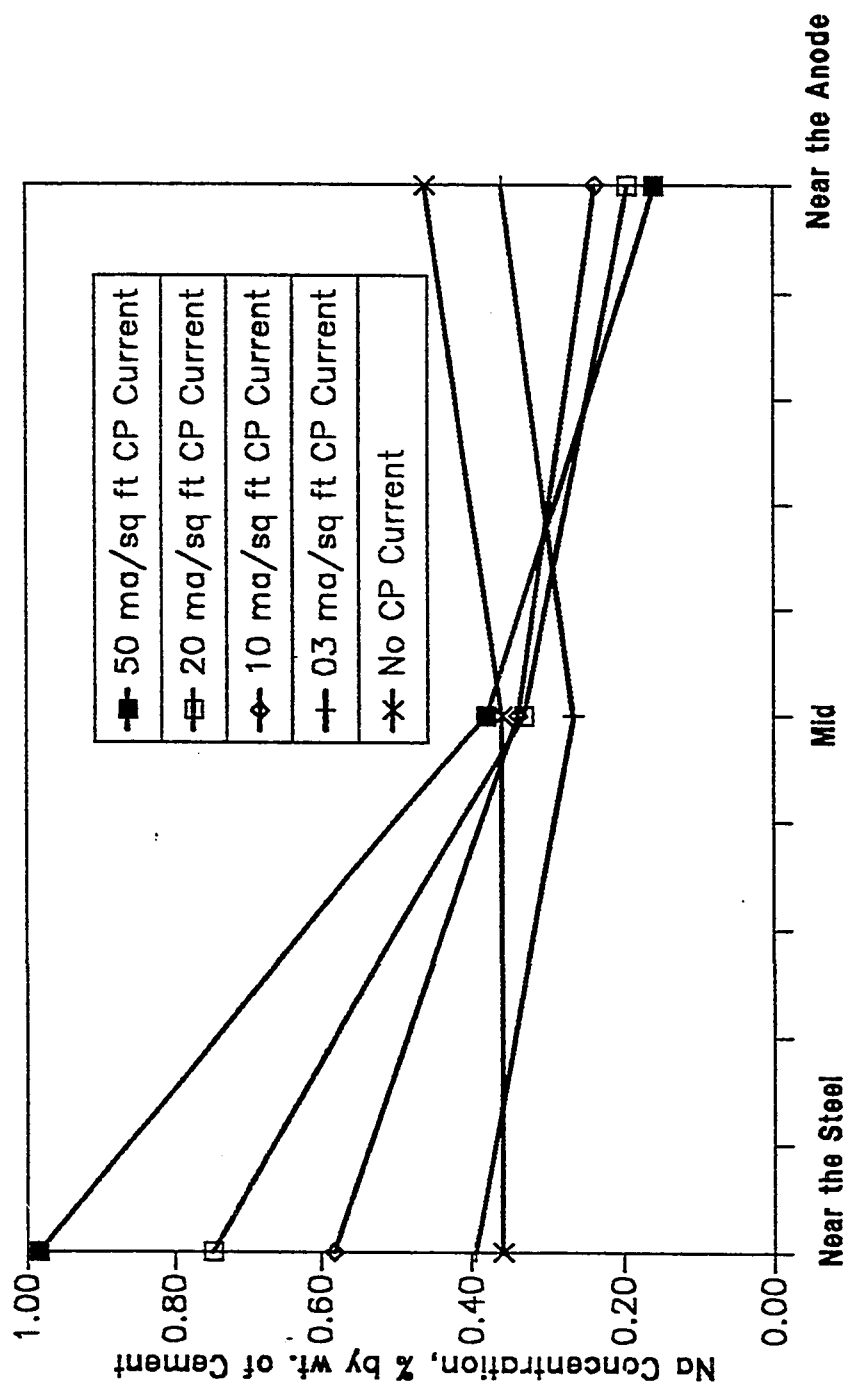


Fig. 5.6.7 Na Ion Concentration at Different Locations for Specimens Containing 2 lbs $\text{Cl}^-/\text{cu. yd}$ of Concrete

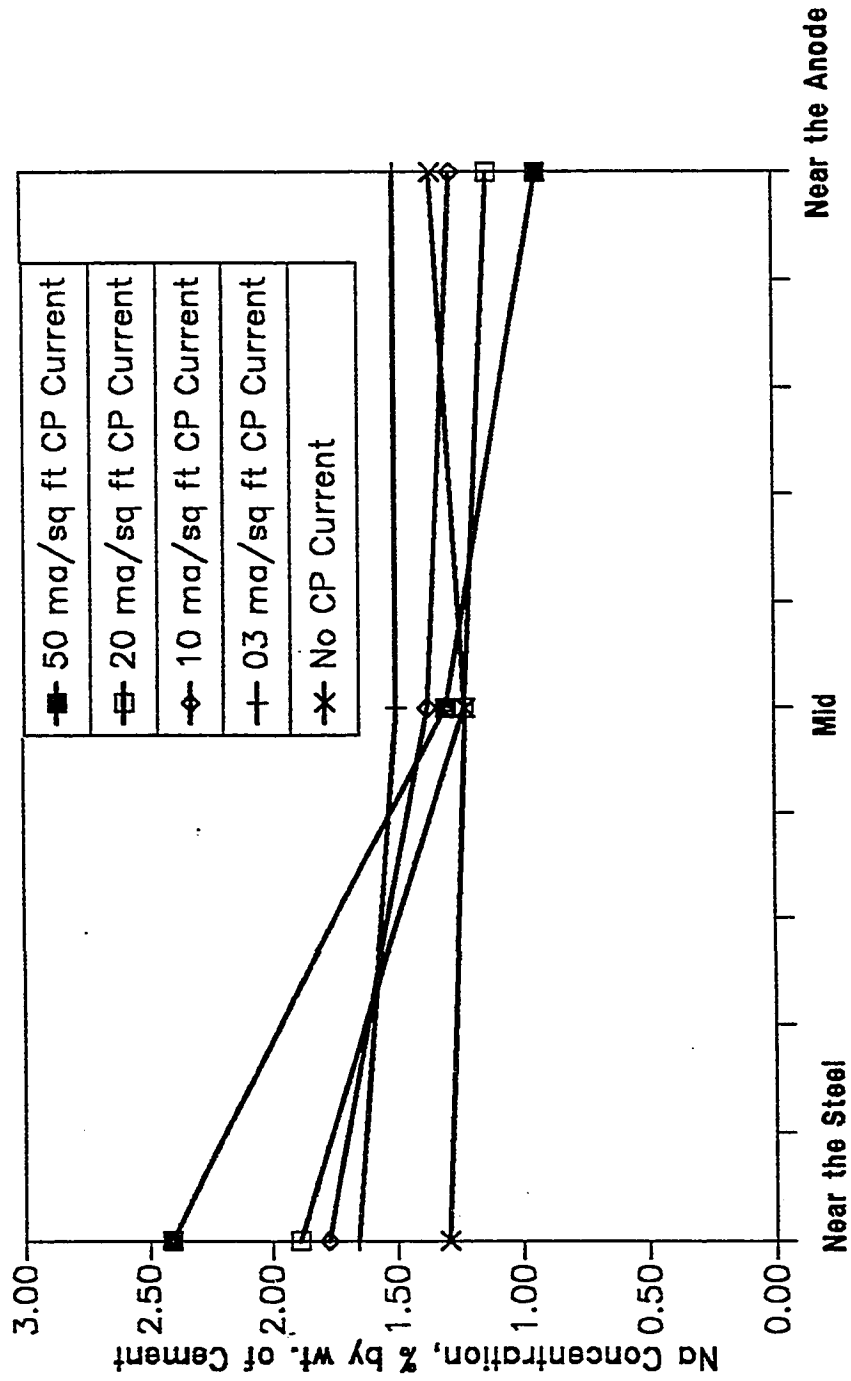


Fig. 5.6.8 Na Ion Concentration at Different Locations for Specimens Containing 8 lbs $\text{Cl}^-/\text{cu yd}$ of Concrete

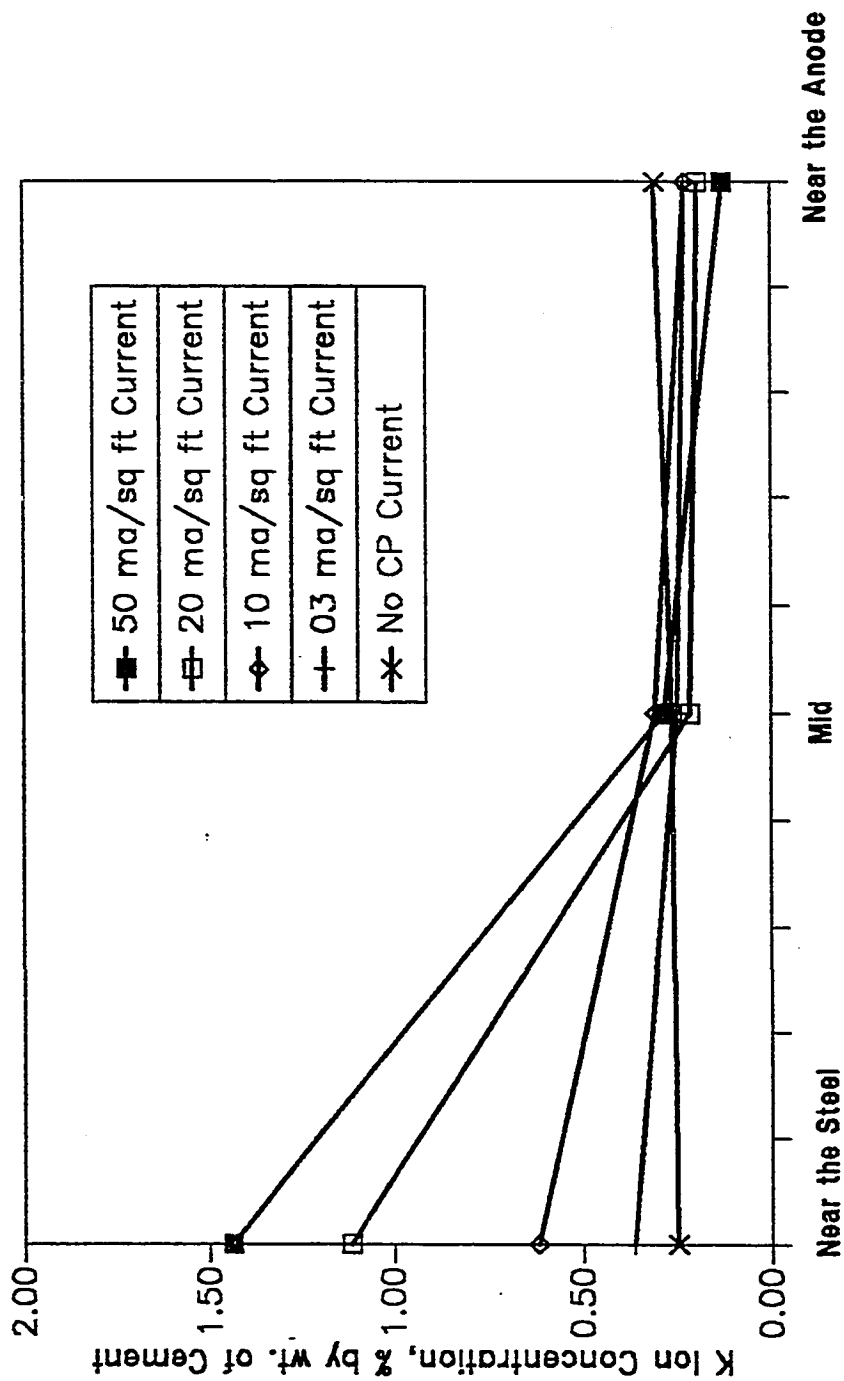


Fig. 5.6.9 K Ion Concentration at Different Locations for Specimens Containing 2 lbs $\text{Cl}^-/\text{cu. yd}$ of Concrete

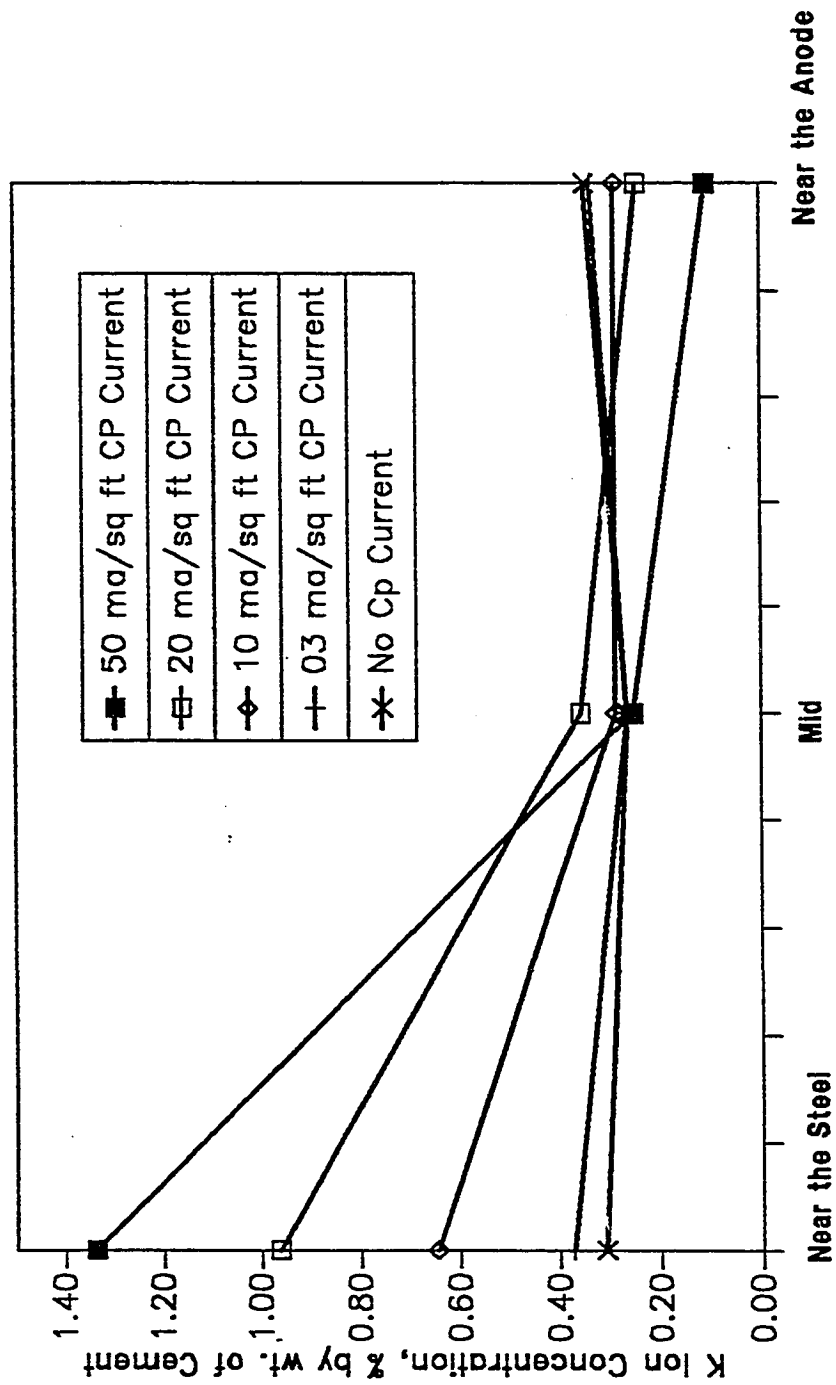


Fig. 5.6.10 K Ion Concentration at Different Locations for Specimens Having 8 lbs $\text{Cl}^-/\text{cu yd}$ of Concrete

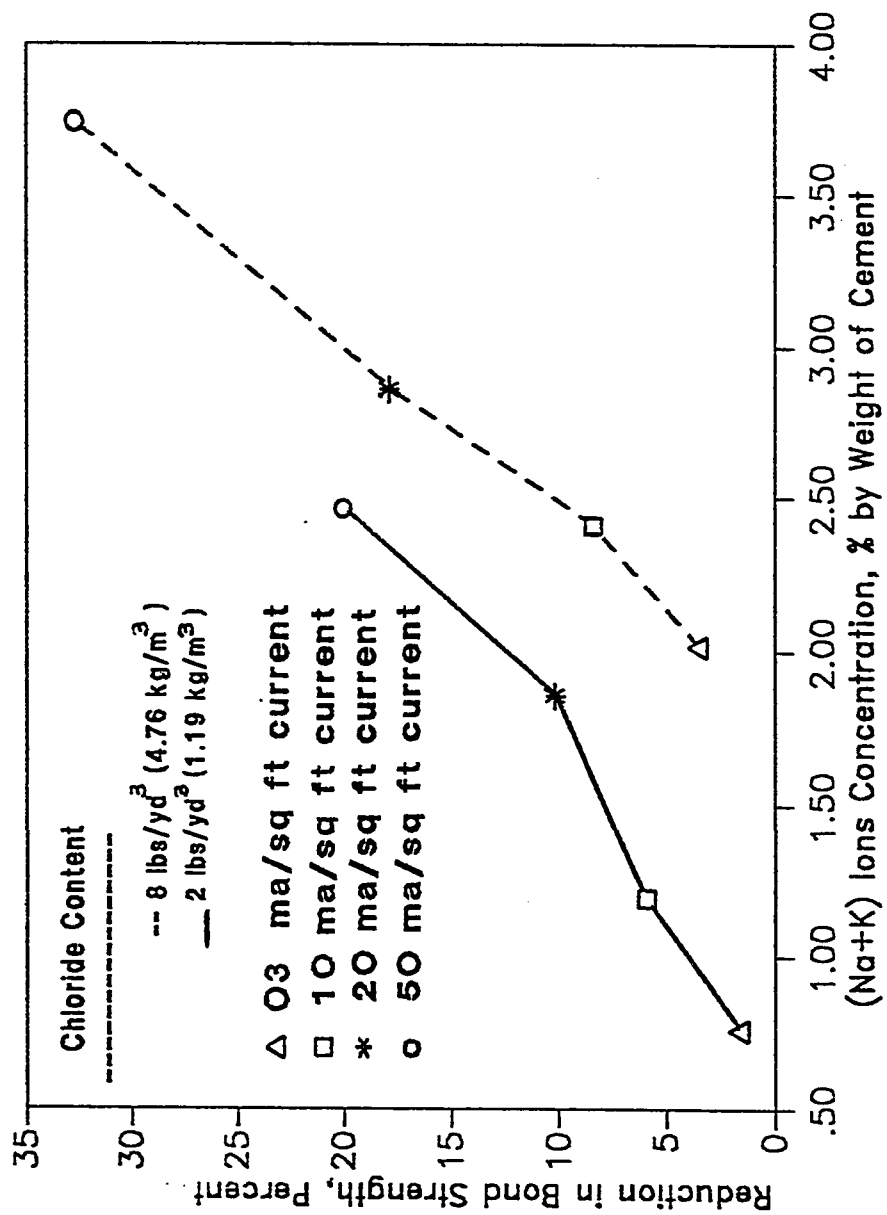


Fig. 5.6.11 Reduction in Bond Strength Due to ($\text{Na}^+ + \text{K}^+$) Concentrations Near the Reinforcing Steel Surface

potassium and sodium accumulation level reaches 3.74 percent by weight of cement for a current density of 50 ma/ ft² impressed on steel embedded in the 8 lbs/ yd³ chloride-bearing concrete.

5.6.4 Movement of Chloride Ions Due to CP Current

Plot in Fig. 5.6.12 is the result of chloride analysis on concrete powder taken from the region near the reinforcing steel for the 2 lbs-and 8 lbs-chloride concretes. Chloride data corresponding to zero ma/ ft² current density show the results for control specimens (never received current). This presentation shows that impressed current causes an electromigration of chlorides away from the reinforcing steel toward the concrete surface. The removal of chlorides from the vicinity of reinforcement increases with the current density. The percentage reductions of Cl⁻ from near the steel at current densities of 3, 10, 20 and 50 ma/ ft² are 26, 38, 58, and 69 respectively for the 2 lbs/ yd³ (1.19 kg/ m³) chloride-bearing specimens, whereas the corresponding reductions for specimens with 8 lbs-chloride (4.76 kg/ m³) are 9, 16, 36 and 51 respectively. The level of chloride migration is found to decrease with an increase in the chloride content of concrete. This is possibly because in high chloride contaminated concrete, in addition to chloride anions, a higher concentration of sodium ions are available for carrying the current from anode to cathode. In order to maintain a constant current flow between anode and cathode (the steel), a significantly higher percentage of available chloride anions have to take part in transferring the currents from anode to cathode in the low chloride contaminated concrete.

Figs. 5.6.13 and 5.6.14 show the chloride concentration profiles for specimens having 2.0 and 8.0 lb Chloride/ yd³ of concrete respectively. It is clear

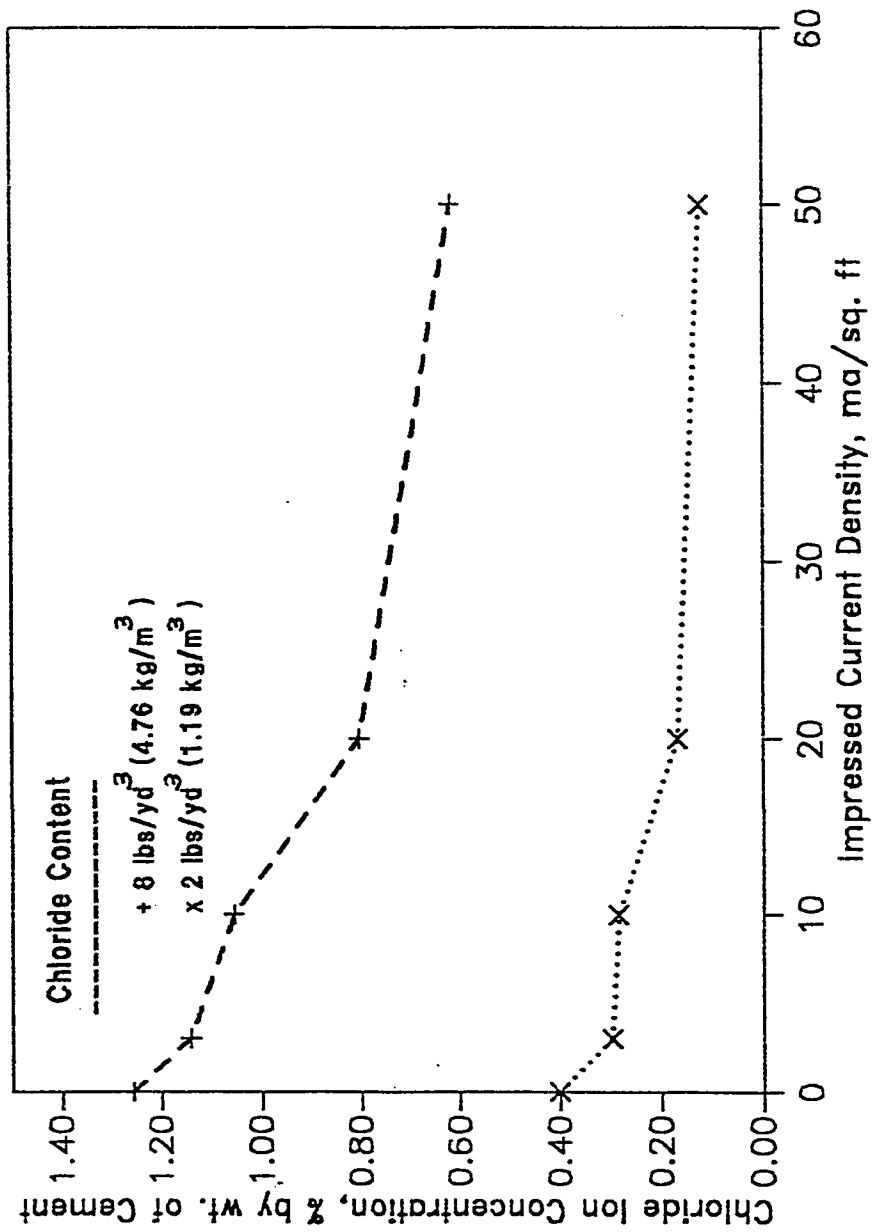


Fig. 5.6.12 Effect of Impressed Current Density on the Chloride Ion Concentration Near the Reinforcing Steel Surface

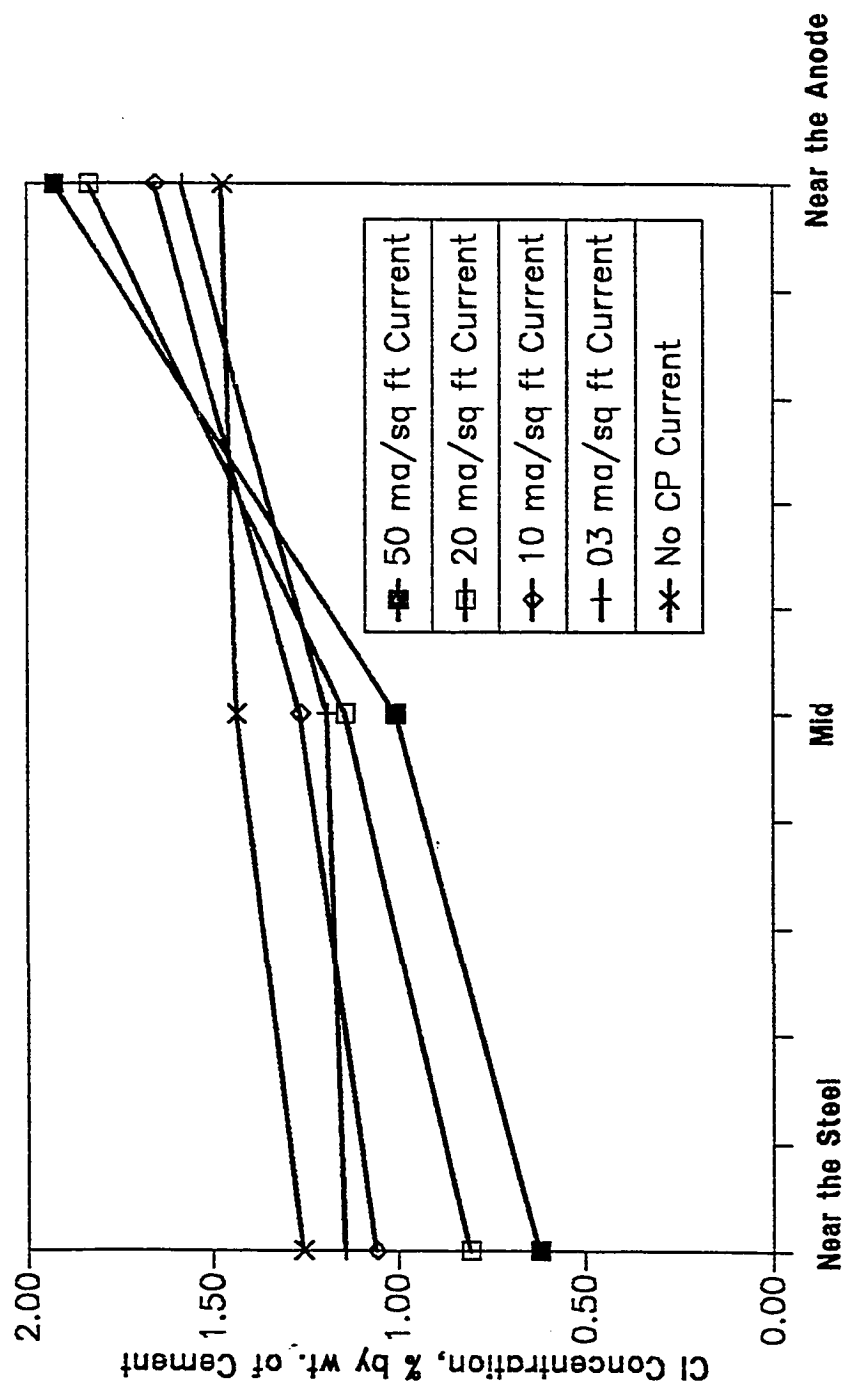


Fig. 5.6.13 Chloride Concentrations at Different Locations for Specimens Containing 2 lbs Cl^- / yd^3 of Concrete

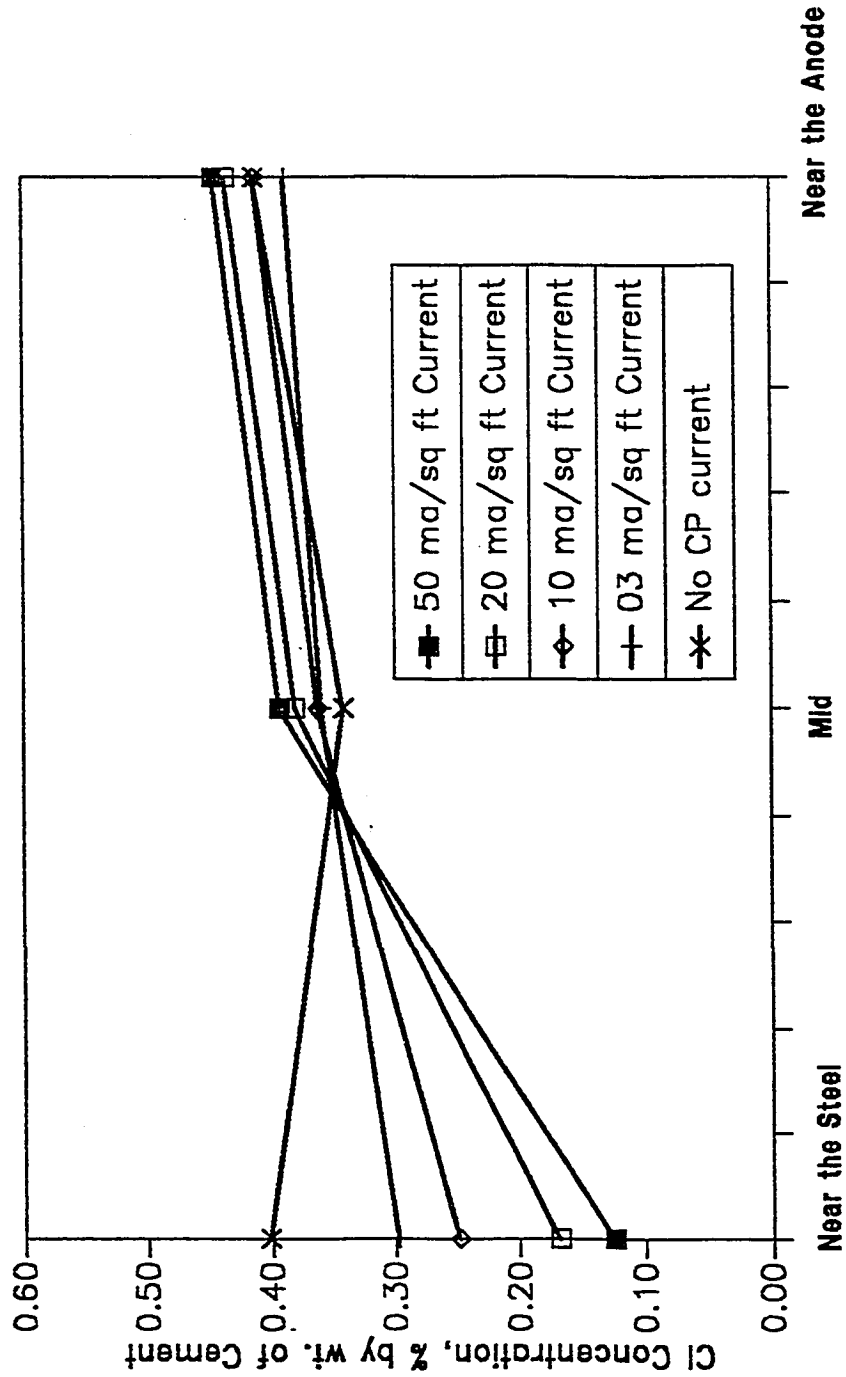


Fig. 5.6.14 Chloride Ion Concentrations at Different Locations for Specimens Containing 8 lbs Cl⁻/cu yd of Concrete

from these Figures that the Chloride ions in the CP specimens moved away from the regions near the rebar toward the anode area. This is expected because the anions in the concrete pore solutions have an affinity towards the positively charged electrode (anode); as a result the Cl^- ions will migrate toward the anode area. In some cases, in bridge decks, this technique is used to remove the Cl^- ions from the vicinity of the steel surface in the reinforced concrete bridge deck. The Cl^- ions determined in the control specimens showed that a little amount of this anion moved away from the regions near the rebar toward the anode area. This is probably due to evaporation of water from the concrete which will carry the ions toward the concrete surface.

Fig. 5.6.15 shows the condition of the reinforcing bars removed from the specimens after 14 months of activation period. Of the five bars shown in this Figure, four are retrieved from specimens subjected to CP current whereas one is from the control specimen. The bars retrieved from CP current treated specimens were totally rust-free and shiny, whereas significant rust is found on the bars removed from the control specimens. This significant corrosion differential in the conditions of the bars shows the effectiveness of CP as a corrosion control measure in reinforced concrete structures.

5.6.5 Discussion

The data show that a sustained impressed current on reinforcing steel in concrete will cause a deterioration in the bond between steel and concrete. The magnitude of bond deterioration is shown to be a function of the current density and chloride(NaCl) content of concrete, these being the two variables included in this study. Other studies show that it also depends on the polarization time. The

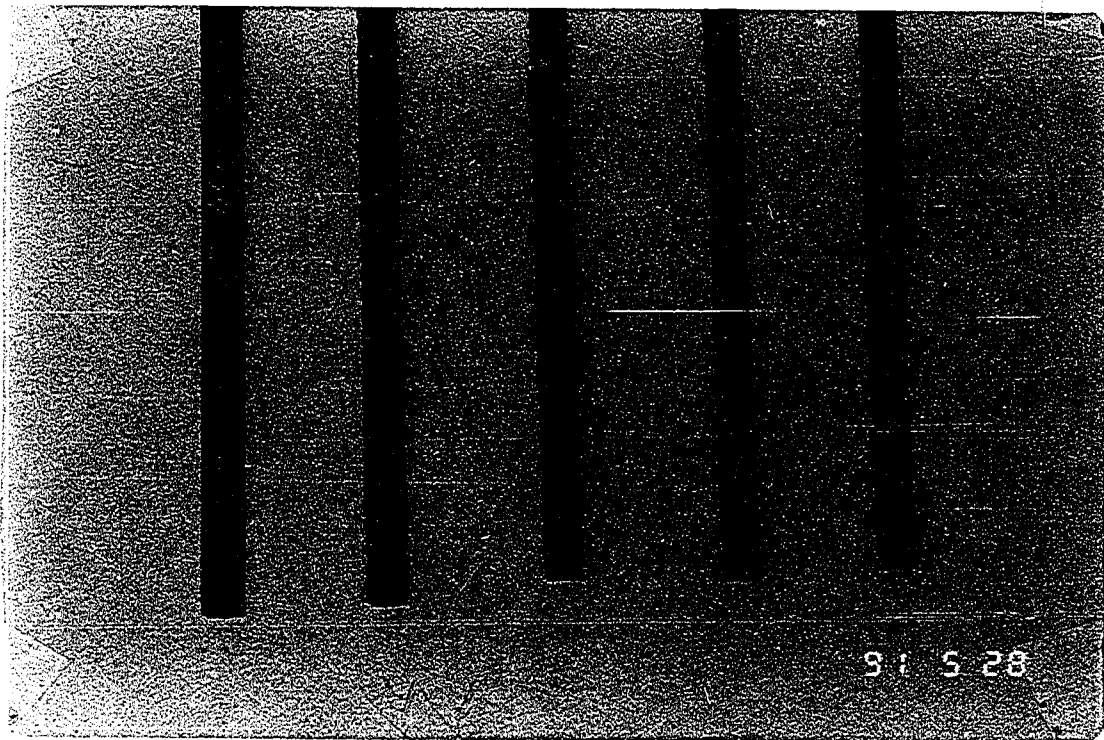


Fig. 5.6.15 Corrosion Conditions of Steel Bars Removed From Cathodic Protection Current-treated and Control Specimens (First Bar From Left is From Control Specimen, Other Four Bars Are From Current-treated Specimens)

14 month treatment data show only an insignificant 1.5 and 3 percents reduction in bond in 2 lbs-and 8 lbs-chloride concrete specimens respectively for a 03 ma/ft² practical cathodic protection current density used to protect reinforcing steel from chloride based corrosion. A relatively much higher current density of 50 ma/ft² results in a bond reduction of the order of 19 and 33 percents in 2 lbs-and 8 lbs-chloride specimens respectively with reductions lying in between these values for other current densities (10 and 20 ma/ft²) used in this study. The data related to bond reduction with current density show, that for both levels of chloride content in concrete, bond loss is roughly proportional to the current density. Assuming no appreciable change in the intrinsic mechanism of bond degradation at the steel-concrete interface, 50 ma/ft² for 14 months (504 amp-hour/ft²) is equivalent to some 30 years at a cathodic protection current density of 2 ma/ft² (average of 1 - 3 ma/ft², which is the usual range of practical CP current densities). However, in certain structural situations, characterized by high chloride gradients and significant depth effect due to an increased distance between bottom steel and the anode, cathodic current densities as high as 10 ma/ft² may be employed. In such a situation, 504 amp-hour/ft² is equivalent to about 6 years at a current density of 10 ma/ft². These data, however, indicate that practical values of CP current densities (1-3 ma/ft²) do not cause loss of bond to an extent which would cause concern.

Data developed in this study also show that when CP current is impressed on reinforcing steel in concrete, it causes electromigration of cations and anions present in the pore solution of concrete due to the hydration kinetics and additives. Na⁺ and K⁺ undergo ionic migration between anode and cathode (steel reinforcement) with an accumulation at regions near the reinforcing steel which increases with current density. The concomitant reduction in bond and a

build up of Na^+ and K^+ in the vicinity of the steel-concrete interface is indicative of a weakening of concrete in this region, most probably due to a softening effect of these cations. Na^+ and K^+ form alkali hydroxides with the hydroxyl ions which are abundantly present in the alkaline pore fluid. These hydroxides are known to react with the calcium silicate hydrate binder in the cement system producing soluble silicates which render the concrete relatively soft(26,42,43,44).

Softening of the concrete at the steel-concrete interface is indicated by the form of the load-slip curve(Figs.5.6.2-5.6.3) for the current treated specimens. It is observed that contrary to the position for the control specimens, slip starts in the treated specimens at quite low loads and is about 4 fold the value for control specimens by the time pull out load reaches ultimate bond strength for the treated specimens. Hardness tests carried out on small concrete specimens removed from the steel-concrete interface also confirm the softening of concrete.

The data also show that for the same current density, increase in chlorides inducted into concrete as NaCl, increase bond reduction significantly. For the range of current densities applied in this program, loss of bond increased about 1.75 fold when chlorides were increased from 2 lbs/ yd³ (1.19 kg/ m³) to 8 lbs/ yd³ (4.76 kg/ m³). The effect is attributable to a very significant increase in the Na^+ build up near steel-concrete interface with higher levels of chlorides with associated sodium cation. This is clearly demonstrated by a near-linear relationship between increase in the ($\text{K}^+ + \text{Na}^+$) concentration and reduction in bond as shown in Fig. 5.6.11

Another phenomenon of some significance is the electromigration of chlorides away from the region of the reinforcing steel. Chloride migration is

activated by the mechanism of attraction of negatively charged chloride ions by a positively charged electrode(anode). Since the chloride concentration at the steel-concrete interface is the controlling factor in the initiation and subsequent kinetics of corrosion of reinforcing steel, the removal of chlorides from the vicinity of steel signifies an appreciable reduction in the corrosion risk. For 2 lbs- and 8 lbs-chloride concretes, reductions of 69 and 51 percents were obtained with a CP current density of 50 ma/ ft^2 . The initial concentrations of 0.40 and 1.30 percent by weight of cement were thus reduced to 0.124 and 0.61 percent by weight of cement for the 2 lbs- and 8 lbs-chloride bearing concretes respectively. The after-treatment chloride level(0.124 percent by weight of cement) for 2 lbs-chloride bearing concrete is reduced below the threshold chloride content(0.15 percent, ACI specification), whereas for the 8 lbs-chloride bearing concrete it is reduced to half its original value which may fall below the threshold value after a longer activation period. Also the condition of the retrieved bars from current-treated and control specimens showed that active corrosion had ceased. This is possibly due to the interactive beneficial effect of the cathodic polarization of the reinforcing steel and the removal of chlorides from the vicinity of reinforcing steel.

In the criteria formulation study (Art. 5.2) which incorporated the effect of chloride and temperature, a maximum protection current density of 3.18 ma/sq ft was found for the temperature treated specimens. The bond degradation study showed that a current density of 3 ma/sq ft causes a very insignificant bond reduction ($< 2 \%$) in 14 months activation period. A positive point which merits importance is that the protection current densities for temperature treated specimens and also for the room temperature exposed specimens decrease with the activation period. Under the action of the above mentioned lower current

density at a later activation age, the bond deterioration will be insignificant and negligible. However, in a high chloride contamination (32 lbs/ yd^3) and high chloride gradient (a gradient equal to 3.0) situation, when the bottom mat had to be protected through an anode near the top surface in a two mat reinforced concrete slab, a current density as high as 9 ma/ ft^2 was observed in the top mat reinforcement (Art. 5.4). Bond deterioration is a severe problem in this situation. It seems that in a two mat structural situation in slab, attempts should be made to develop mechanisms specially in new construction to provide well distributed paths of lesser electrical resistivity to facilitate the flow of current to the bottom mat.

CHAPTER 6

CONCLUSIONS AND RECOMMENDATIONS

1. Theoretical study shows:

- (i) Temperature effect on CP criteria is relatively small. At a higher concrete temperature of 80°C , the absolute value of CP potential of steel needed to be increased by around 33 mV from the normal potential value at a room temperature of 25°C . A CP potential value more negative than -960 mV CSE can be used for adequate protection.
- (ii) Ambient relative humidity has an indirect effect on cathodic protection potential as at higher humidities more iron ions go into pore solution thereby requiring higher protection potentials.
- (iii) The concentrations of alkali cations near the steel increase with the increase in current density and activation period.

2. Tests on chloride-free concrete establish the following potential-current relationship at the very beginning of the polarization period:

Potential	Current
100 mV potential decay	1.2 ma/sq.ft
-850 mV CSE instant off potential	14.0 ma/sq.ft
300 mV potential shift	3.2 ma/sq.ft

3. However, cathodic protection is facilitated with time as instant off potential and decay potential values increase with continued polarization at a given current density. For example whereas 1 ma/ft^2 CP current density achieved a decay potential of only 40 mV at the beginning of the activation period, the same 1 ma/ft^2 satisfied 100 mV decay potential after 6 weeks of polarization. Similarly, whereas a 3 ma/ft^2 practical CP current density completely fails to provide the -850 mV CSE instant off potential at the beginning of activation period, the trend of data show that this same 3 ma/ft^2 CP protection current density is likely to provide the -850 mV instant off potential after several months.
4. The static potential of reinforcing steel is directly dependent on the chloride content of the concrete; a higher static potential of steel is observed for a higher chloride content. This is attributable to an enhanced aggressivity of the corrosion environment in concrete contaminated with a higher level of chlorides.
5. The corrosion current flow between the anode and the cathode is more strongly dependent on the chloride gradients and less on absolute chloride content of concrete. The corrosion current flow increases significantly with the chloride gradient in the concrete. Also for a given chloride gradient, the corrosion current flow increases with an increase in the chloride content of the concrete.

6. The instant off potential, shift potential, decay potential and current density needed for adequate protection of steel are all dependent on the chloride gradient as well as the chloride content in concrete. The prevalent -850 mV CSE instant off potential, 100 mV decay potential and the 300 mV shift potential were all found to be conservative for chloride contents of upto 32 lb/yd³ and a chloride gradient of 2.
7. An instant off potential of -500 mV CSE can be safely adopted as a criterion to protect steel embedded in chloride-bearing concrete containing upto an average of 8 lbs chloride and having upto 12 lbs chloride rich zones within the same concrete. This indicates that steel experiencing high chloride gradients can be protected with 500 mV CSE provided the maximum chloride content does not exceed 12 lb/yd³.

A -650 mV CSE instant off potential value would protect steel embedded in concrete containing chlorides upto 32 lbs/ yd³ and having a chloride gradient of upto 2.0 within the same concrete.

8. The decay potential was found to be least sensitive to chloride content and chloride gradients. For a change of chloride from a small value to 32 lbs/ yd³, the decay potential variation was only 20 mV.

A 60 mV decay in 4 hours was found to be adequate for upto 8 lbs chloride contaminated concrete having upto 12 lbs chloride rich zones within the same concrete.

A 70 mV four hour decay potential was found to be adequate for upto 16 lbs

chloride contaminated concrete having upto 24 lbs chloride rich zones within the same concrete.

A 80 mV decay potential was found to be sufficient for 16 and 32 lbs-chloride bearing concretes having a chloride gradient of upto 2.0.

9. Shift potential is mainly controlled by the chloride gradient and not by the average absolute values of chloride content. In a low chloride contaminated concrete with high gradients a larger shift will be necessary to protect steel compared to the situation when chloride contents may be very high but the gradients relatively low. For a chloride gradients of 2, 4 and 8, potential shifts of the order of 100 mV, 140 mV and 200 mV respectively were required for adequate protection. In terms of absolute chloride contents a shift of 100 mV was found sufficient for as high as 32 lbs/ yd³ chloride bearing concrete with low chloride gradient whereas a shift of 200 mV was required for almost chloride free concrete but having a high gradient of about 8.
10. Protection current density was found to be dependent more on chloride gradient than on absolute average chloride content of concrete. For example, a protection current density of 2.1 ma/ ft² was required for 8 lbs chloride bearing concrete having a chloride gradient of 2.0 whereas a current density of 1.7 ma/ ft² was required for 16 lbs chloride bearing concrete having a chloride gradient of 1.5.
11. A CP current density level of 1 to 3 ma/sq ft was found to be adequate for

protection of steel embedded in concrete having a chloride content of upto 32 lbs and a chloride gradient of upto 2.0. A current density of 2 ma/sq ft may be safely adopted to protect steel in chloride bearing concrete containing upto 16 lbs chloride and having a maximum 8 lbs chloride differential within the same concrete. A current density of 3 ma/sq ft may be safely adopted to protect steel embedded in concrete containing upto 32 lbs chlorides having a chloride gradient of 2.0.

12. A higher static potential as well as a higher intensity of corrosion current observed for concrete exposed to a higher temperature of 60°C (as compared to 20°C) indicate an increased corrosion activity with an increase in the ambient temperature to which concrete is exposed.

Increased corrosion activity at 60°C required an increased level of cathodic protection as indicated by higher protection current density, higher instant off protection potential and marginally higher decay potential at the beginning of polarization period.

As polarization continues a higher protection current density required for 60°C exposure results in an increased electromigration of ions. This electromigration of ions provides a two fold benefits in reducing corrosion activity. **Firstly**, chloride ions move away from steel-concrete interface reducing chloride attack on steel and **secondly**, alkali cations move toward the steel-concrete interface resulting in an enhanced build-up of alkalinity at the steel-concrete interface. Both these effects cause a shift of base potential to a more positive value. The reduction in corrosion activity is confirmed by a reduction in the

required level of protection with the progress of polarization. The level of protection at 60°C after 2 months was observed to be lesser than required for 25°C concrete exposure as well as the protection required at the beginning of the activation period.

The reduction in required cathodic protection at higher temperature exposure is indicative of a dominant influence of the electromigration factor in the interactive relationship between increased corrosion activity and the beneficial electromigration of ions caused by the higher temperature.

The temperature effect therefore requires only about 20 percent higher level of protection in terms of current density/instant off potential/decay potential for an initial polarization period of two months. Thereafter no additional protection is required for temperature. These data also indicate that significant benefits in reducing long term cathodic protection requirement could be derived by adopting a higher level of protection in terms of higher protection current/instant off/decay potentials in the initial period of activation. The longer is the period of this enhanced activation the greater would be the reduction in the corrosion activity due to beneficial electromigration eventually requiring reduced protection in a long term basis. It is also possible that in low or moderate conditions of chloride corrosion with initial high level of protection for a finite period the corrosion activity may stop completely. This needs further research.

13. In case of usual primary chloride-bearing concrete in the Gulf region, both the top and bottom reinforcement mats have to be protected against corrosion. In

such cases the cathodic protection data show that the top mat is significantly overprotected when the bottom mat is just adequately protected for the anode source located above the top mat.

In a 32 lbs chloride bearing concrete with chloride gradients of 3.0 and 1.5, the top mat received 9.6 ma/ ft² and 5.44 ma/ ft² CP current compared to 3.87 ma/ ft² and 2.89 ma/ ft² respectively required to protect the bottom mat. Likewise, the instant off potential and decay potential values of 730 mV CSE and 128 mV respectively for the top mat also indicate significant overprotection of the top mat.

The bond deterioration data presented subsequently indicates that in high chloride bearing concretes with high chloride gradients the protection of bottom mat would result in the overprotection of top mat to such an extent that an appreciable 30 percent reduction in steel-concrete bond may occur in a period of approximately 8 years. However, in concrete subjected to high currents of 100 ma/ ft² for upto 80 days no reduction in steel ductility and ultimate/rupture strength were observed.

It seems that in two mat structural situation in slabs attempts should be made to develop mechanism specially in new construction to facilitate the flow of current to the bottom mat.

14. When reinforcing steel is subjected to an impressed current of 50 ma/ ft² for 14 month period, softening of the concrete at the steel-concrete interface is indicated by the form of the load-slip curve for the current-treated specimens. Slip starts in the treated specimens at quite low load and is about 4 fold the

value of control specimens by the time pull out load reaches ultimate bond strength for the treated specimens.

15. Bond deterioration is a function of current density and chloride content of concrete from NaCl source. This degradation of steel concrete bond increases with an increase in the impressed current density and chloride content of concrete.
16. Bond reduction in a 14 month polarization period for a practical CP current density of 3 ma/ ft^2 is negligible. However, a 19 percent reduction in bond strength is observed in specimens having $2 \text{ lbs Cl}^- / \text{yd}^3$ (0.364 percent by weight of cement) of concrete subjected to a CP current of 50 ma/ ft^2 (538 ma/ m^2) applied over a period of 14 months. The corresponding value for specimens having $8 \text{ lbs Cl}^- / \text{yd}^3$ (1.45 percent by weight of cement) of concrete was found to be 33 percent.
17. A 50 ma/ ft^2 current applied for 14 months required 504 amp-hr/ ft^2 to cause 19 to 33 percent bond loss. 504 amp-hr/ ft^2 is equivalent to some 30 years at a practical cathodic protection current density of 2 ma/ ft^2 (21.5 ma/ m^2).
18. Accumulation of sodium ions in the vicinity of reinforcing steel is a function of sustained impressed current density at the steel surface and the NaCl supplied chloride content of the concrete, whereas the potassium build up near

the steel surface is a function of current density only and is independent of the chloride content of concrete specimen. Potassium ions migrate towards the cathode at a higher rate when compared with the migrations of sodium ions present in the concrete pore solutions.

19. The degradation of bond between steel and concrete is most probably caused by the build up of sodium and potassium ions at the steel-concrete interface which results in the softening of the concrete. Bond loss is shown to be almost proportional to the accumulation of sodium and potassium ions in the vicinity of reinforcing steel.
20. Electromigration of negatively charged chloride ions away from the reinforcing steel is caused by the attraction of the positively charged anode. The migration of chloride ions increases with current density but is found to be relatively more effective in low chloride contaminated concrete in comparison to the high chloride contaminated concrete. The migration of chlorides away from the steel significantly brings down the chloride ion concentration at the steel concrete interface thereby reducing the corrosion risk.
21. In control specimens where CP current was not applied, the concentrations of Cl^- , Na^+ , and K^+ increase with the distance from the steel. Evaporation of water from the concrete carries the ions toward the concrete surface.
22. In high alkali-cement concrete containing reactive aggregates CP current

significantly advances the cracking time and softens the mortar at the steel-concrete interface reducing compressive strength and hardness. This is attributable to the formation of alkali-silica gel as evidenced in absorbance tests and scanning electron microscopy. The absorbance measured in 20 ma/ ft² and 100 ma/ ft² current treated specimens were 0.855 and 1.029 respectively whereas an absorbance of only 0.391 was observed in control specimen which was not treated with CP current.

Current densities of 20 and 100 ma/ ft² advanced the cracking time by 40 and 60 percents respectively compared to cracking time in specimens which were not current-treated. 34 and 15 percents reduction in strength were observed when treated with 100 ma/ ft² and 20 ma/ ft² respectively for 80 days. For the same specimens the hardness number was reduced to 66 and 72 from 77.

In a normal cathodic protection situation for a high alkali-cement concrete made with reactive aggregate and a CP current of the order of 3 ma/ ft², the alkali-silica reaction will be relatively much slower and will take significantly more time to manifest disruptive deterioration than was observed in the present accelerated test. The data indicate that CP applied to structures with alkali-silica reaction problem will result in cracking and deterioration of concrete.

23. At an outdoor exposure period of 4 months, a 15 V D.C. supply was found to be inadequate to supply the normally required amount of current of 1-3 ma/ ft² to the steel embedded in a reinforced concrete slab. In the typical hot-dry exposure the current supply dropped below 3 ma/ ft² in 95 days and below 1

ma/ ft² in 110 days.

24. An electrical resistivity value of 35,000 ohm-cm resulted in currents below 3 ma/ ft² whereas a value of 40,000 ohm-cm reduced the current flow below 1 ma/ ft². These data indicate that to achieve normal CP current of 1-3 ma/ ft² the concrete resistivity should be below 35,000 ohm-cm for a normally available 15 V DC supply.

The moisture content data show that the in overlay region and in the vicinity of the anode the concrete was very dry (0.6 percent moisture content) compared to concrete sufficiently remote from the anode area. The difficulty in the flow of current may be attributable to this loss of moisture from the overlay region. This indicates that overlays designed with moisture retaining material would significantly reduce the problem of current flow from the anode to the reinforcing steel. Further research is needed for the designing of such moisture retaining overlays.

25. The effectiveness of cathodic protection was confirmed through measurements by:
 - (i) Weight loss data for coupon steel and macrocell steel. For chloride bearing concrete, the weight loss was reduced to negligible values in coupon steel and macrocell steel compared to corresponding control specimens (0.9 to 4.3 percent of the loss in corroding control specimens).
 - (ii) Corrosion rate data from corrosometer probes. When effective CP was

applied the corrosion rate decreased from 0.197 MPY (for corroding control specimen) to 0.013 MPY for protected specimen.

26. The decay potential data were found to be least sensitive to chloride content, chloride gradient and temperature effect although it does not explicitly indicate the level of protection current flow which is automatically adjusted to accommodate the various factors influencing the level of corrosion activity. Based on its capacity to accommodate large fluctuation in corrosion conditions without showing significant variations in the numerical decay value and its independence of IR drop and measuring reference cell, a decay potential concept is recommended as a preferred cathodic protection approach.
27. The current-potential relationship obtainable in chloride-free concrete is different from the one applicable to concrete having primary chlorides and chloride differential. For example, a current density of 1.2 ma/ft^2 was needed to achieve a potential of 100 mV decay in 4 hour for a chloride free concrete as compared to current density of 2.98 ma/ft^2 required to attain 80 mV decay in 32 lbs chloride bearing concrete with a chloride gradient of 2. Similarly, current-instant off and the current-shift potentials relationships obtained in chloride free concrete were different from those obtained in primary chloride-bearing concrete. An elucidation of current-potential relationship in chloride bearing concrete needs further research.

CHAPTER 7

REFERENCES

1. Rasheeduzzafar, Dakhil,F.H., and Gahtani,A.S., " The Deterioration of Concrete Structures in the Environment of the Middle East", ACI Journal, Proceedings Vol.81, No. 1, January-February 1984, pp 13-20.
2. Rasheeduzzafar, Dakhil,F.H., and Gahtani,A.S., " The Deterioration of Concrete Structures in the Environment of Eastern Saudi Arabia", The Arabian Journal of Science and Engineering, Vol. 7, No. 3, 1982, pp 191-209.
3. Rasheeduzzafar, and Dakhil,F.H., " Field Studies on the Durability of Concrete Construction in a High Chloride-Sulphate Environment", International Journal of Housing Science, Vol. 4, No. 3, 1980, pp 203-232.
4. Tarigoe, R.M., " Corrosion Control for Reinforced Concrete", Report for M.S. Degree, University of Florida, 1983.
5. " Economic Effects of Metallic Corrosion in the United States Part I", A report to the Congress by the National Bureau of Standard, US Dept. of Commerce, NBS Special Publication No. 511-1, May 1978.
6. " Deteriorating Highways and Lagging Revenues: A Need to Reassess the Federal Highway Program", Publication No. CED-81-42, U.S. General Accounting Office, Washington D.C., March 1981, 90 pp.
7. Al-Sulaimani, G.J., Kaleemullah,M., Basunbul,I.A., and Rasheeduzzafar, " Influence of Corrosion and Cracking on Bond Behavior and Strength of Reinforced concrete", To be Published in ACI Journal.
8. Rasheeduzzafar, Dakhil,F.H., and Gahtani,A.S., " Corrosion of Reinforcement in Concrete Structures in the Middle East", Concrete International: Design and Construction, Vol. 7, No. 9, September 1985, pp 48-55.
9. Pourbaix, M., " Applications of Electrochemistry in Corrosion Science and in Practice", Vol. 14, 1974, pp 25-82.
10. Powers, T.C., " A Discussion of Cement Hydration in Relation to the Curing of Concrete", Proceedings Highway Research Board, Vol. 27, 1947, pp 178-188.

11. Glass, G.K., " The Effect of a Change in Surface Conditions Produced by Anodic and Cathodic Reactions on the Passivation of Mild Steel", Corrosion Science, Vol. 26, No. 6, 1986, pp 441-454.
12. Henriksen, J.F., " The Corrosion and Protection of Steel in Saturated $\text{Ca}(\text{OH})_2$ Contaminated with NaCl", Corrosion Science, Vol. 20, 1980, pp 1241-1249.
13. Gjørsv, O.E., " Steel Corrosion in Reinforced and Prestressed Concrete Structures:" nordisk betong, Vol.2, No.4, 1982, p 147.
14. Verbeck, G.J., " Mechanisms of Corrosion of Steel in Concrete". ACI Special Publication SP-49, 1975, pp 21-38.
15. Roberts, M.H., " Carbonation of Concrete Made with Dense Natural Aggregates", Building Research Establishment Information , Paper IP 6/81, April 1981.
16. Reports on " Study of Concrete Cracks in High Voltage Transmission Tower Footings in Sabhka Environments", Research Institute, KFUPM, 1985.
17. Hausmann, D.A., " Steel Corrosion in Concrete: How Does It Occur", Material Protection, Vol. 6, No. 11, 1967, pp 19-23.
18. Weiher, H., and Segmuller, E., " Action of Chlorides on Concrete", Betonwerk und Fertigteil- Technik, 1973, Vol. 8, pp 577- 584.
19. " Guide to Durable Concrete", Journal, American Concrete Institute, December 1977, pp 573-609.
20. Viramani, Y.P., " Cost Effective Rigid Concrete Construction and Rehabilitation in Adverse Environments". Project No. 4k, FCP Annual Progress Report, Sept. 1982, 35 pp.
21. Viramani, Y.P., Jones, W.R., and Jones, D.H., " Steel Corrosion in Concrete: PH at Corrosion Sites", Public Roads, December 1984, p 96.
22. Rasheeduzzafar, Dakhil, F.H., Al-Gahtani, A.S., Al-Saadoun, S.S., Bader.

- M.A., and Medallah, K.Y., "Proposal for a Code of Practice to Ensure Durability of Concrete-Construction in the Arabian Gulf Environment", Proceedings, Second International Conference on the Deterioration and Repair of Reinforced Concrete in the Arabian Gulf, Bahrain, 11-13 October, 1987, pp 595-631.
23. Pocock, D.C., and Gibbs, B., "Diagnosis, Prevention and Repair of Deterioration in Concrete Bridges- An Overview", Taywood Engineering Ltd., London.
 24. Stratfull, R.F., "Experimental Cathodic Protection of a Bridge Deck", Trans. Res. Record No. 451 (1973), pp 44-52.
 25. FHWA Memorandum of 23/4/82.
 26. Locke, C.E., Dehghanian, C., Gibbs, L., "Effect of Impressed Current on Bond Strength Between Steel Rebar and Concrete", Paper presented at Corrosion'83, NACE, Anaheim, 1983.
 27. Arpaia, M., Orsini, P.G., and Pernice, P., "Hydrogen Embrittlement of High Strength Steel Wires under Cathodic Polarization", Materials Chemistry and Physics, Vol 15, 1987, pp501-509.
 28. Uhlig, Corrosion and Corrosion Control, 2nd Edition, Wiley, pp 409.
 29. Hover, K.C., "Cathodic Protection for Reinforced Concrete Structures", ACI SP-85-8, American Concrete Institute, PP 175-209, 1985.
 30. Stratfull, R.F., "Experimental Cathodic Protection of Bridge Deck", TRB Record 500, 1974.
 31. Nicholson, J.P., "New Approach to Cathodic Protection of Bridge Decks and Concrete Structures", NACE East Canadian Region Meeting, 1978.
 32. Ratliff, J.L., "A Study of Cathodic Protection for Corrosion Control in Reinforced Concrete Bridge Piles", Report to Fla. Dept. of Transp., 1975.
 33. Fromm, H.J., and Wilson, G.P., "Cathodic Protection of Bridge Decks, A Study of Three Ontario Bridges", Transportation Research Record No. 604, 1976.

34. Chou, G.K., " Cathodic Protection : An Emerging Solution to the Rebar Corrosion Problem", Concrete Construction, June 1984, pp 562- 565.
35. Lea, F.M., The Chemistry of Cement and Concrete", London, Arnold, 1970.
36. Monfore, G.E., " The Electrical Resistivity of Concrete", Journal, PCA Research and Development Laboratories, Vol. 10, No. 2, May, 1968, pp 35-48.
37. Waddel, J.J., Concrete Construction Handbook, 2nd Edition, McGraw-Hill, 1974.
38. Maguire, D., and Olen, M., " Report on an Investigation into the Electrical Properties of Concrete", Transaction, S. African Institute of Electrical Engineers, Vol.31, No. 11, Nov. 1940, pp 301-303.
39. Lewis, D.A., and Copenhagen, W.J., " Corrosion of Reinforcing Steel in Concrete in Marine Atmosphere", Corrosion, NACE, Vol. 15, July 1959, P. 382.
40. Hymers, W., " Electrical Conductive Concrete", Concrete Construction, May 1980, pp 44-45.
41. Moore, A.E., " Effect of Electrical Current on Alkali-Silica Reactions", a Recent Conference Paper Sponsored by Cement and Concrete Research.
42. Rosa, E.B., McCollum,B., and Peters, O.S., " Electrolysis in Concrete", Tech. Paper B.S. T18, National Bureau of Standards, 1913.
43. Locke, C.E. and Dehghanian, C., " Related Studies to Cathodic Protection of Reinforced Concrete", Report No. FIIWA/OK 83(06), University of Oklahoma, Oklahoma, USA, 1983.
44. Casad, B.M., " The Effect of Cathodic Protection Current on Bond Between Concrete and Reinforcing Steel", M.S. Thesis, Oklahoma State University, Oklahoma, USA, August, 1981.
45. Diamond, S., " A review of Alkali-Silica Reaction and Expansion Mechanism -2, Reactive Aggregates", Cement and Concrete Research, Vol. 6, No.

- 4, pp 549-560, July 1976.
46. Glasser, L.S., and Kataoka, N., "The Chemistry of Alkali-Silica Reaction", *Cement and Concrete Research*, Vol. 11, No. 1, Jan. 1981.
 47. Vrabie, J.B., "Cathodic Protection for Reinforcing Steel in Concrete; Chloride Corrosion of Steel in Concrete", *ASTM STP-629*, 1977, pp 124-149.
 48. Chang, G.C., Apostololos, J.H., and Myhres, F.A., "Cathodic Protection Studies of Reinforced Concrete", *California Dept. of Transp., Report No. FHWA/CA/TL*, March 1981.
 49. French, W.J., and Poole, A.B., "Alkali-Aggregate Reactions and the Middle East", *Concrete*, January 1976, p 18.
 50. Sims, I., and Poole, A.B., "Potentially Alkali-Reactive Aggregates from the Middle East", *Concrete*, May 1980, p 27.
 51. Stern, M., and Geary, A.L., "Electrochemical Polarization", *Journal Electrochemical Society*, Vol. 104, No. 1, p 56, 1957.
 52. Schutt, W.R., "Practical Experiences with Bridge Deck Cathodic Protection", *Paper No. 74, NACE CORROSION/78*, Houston, Texas, 1978.
 53. Schell, H.C., and Manning, D.G., "Evaluating the Performance of Cathodic Protection Systems on Reinforced Concrete Bridge Substructures", *Material Performance*, July 1985, p 18.
 54. Stratfull, R.F., "Criteria for the Cathodic Protection of Bridge Decks", *Corrosion of Reinforcement in Concrete Construction*, Alan P. Crane, Ed., *Society of Chemical Industry*, London, England, p 287, 1983.
 55. Gummon, R.A., *Paper No. 343, NACE Corrosion*, Houston, March 1986.
 56. Hausmann, D.A., "Criteria for Cathodic Protection of Steel in Reinforced Concrete Structures", *Materials Protection*, Vol. 8, No. 10, 1969, pp 23-25.
 57. Vrabie, J.B., "Cathodic Protection for Reinforced Concrete Bridge Decks: Laboratory Phase", *NCHRP Report No. 180, Transportation Research Board*, Washington, D.C., 1977, 135 pp.

58. Kuhn, R.J., "Cathodic Protection of Underground Pipelines From Soil Corrosion", Proc. Amer. Pet. Institute, 1933.
59. Munger, C.G., and Robinson, R.C., "Coatings and Cathodic Protection", Materials Performance, July 1981, p 46.
60. Ward, P.M., "Cathodic Protection : A User's Perspective", ASTM Special Technical Publication STP 629, Chloride Corrosion of Steel in Concrete, 1976, pp 150-163.
61. Slater, J.E., "Criteria for Adequate Cathodic Protection of Steel in Concrete", Paper 132, Corrosion'79, NACE, 1979.
62. Brown, R.H., and Mears, R.B., "A Theory of Cathodic Protection", Transaction, Electrochemical Society, Vol. 74, 1938.
63. LaQue, F.L., Marine Corrosion Causes and Prevention, J. Wiley and Sons, New York, 1975.
64. Locke, C.E., "Specialized Studies of Cathodic Protection of Rebars in Bridge Decks", Final Report, Oklahoma Department of Highways, 1975.
65. Logan, K.H., "Comparison of Cathodic Protection Test Methods", Corrosion, Vol. 8, No. 9, 1974, pp 300-304.
66. Husock, B., "Evaluation of Cathodic Protection Criteria", U.S. Department of Commerce, National Technical Information Service, Report No. AD-A084-783, April 1979.
67. Page, C.L., Havdah, J., "Electrochemical Monitoring of Corrosion of Steel in Microsilica Cement Pastes", Materiaux et Construction, Vol. 18, No. 103, Jan. 1985, pp 41-49.
68. Lambert, P., Page, C.L., and Vassie, P.R.W., "Investigation Of Reinforcement Corrosion 2, Electrochemical Monitoring of Steel in Chloride Contaminated Concrete", Materials and Structures(in Press).
69. Kendell, K., "The Cathodic Protection of Reinforced Concrete", U.K. Corrosion' 84, Hacrrigate, November 1985.

70. Cathodic Protection of Steel in Concrete, Report of Committee E-4-9, NACE, 1988.
71. Kendell, K., and Pithouse, K.B., "Field Observations on the Depolarization Assessment of Cathodic Protection System for Reinforced Concrete, with an Initial Study of Concrete in the Anode Vicinity", Draft Paper.
72. Rog, J.W., and Swait, W.J., "Selecting a Cathodic Protection System for Reinforced Concrete", Construction Specifier, Vol. 14, No. 12, Dec. 1987, pp 51-55.
73. Weyers, R.E., and Cady, P.D., "Cathodic Protection of Concrete Bridge Decks", ACI Journal, Proceeding Vol. 81, No. 6, Nov-Dec. 1984, pp 618-622.
74. Perenchio, W.F., Landgren, J.R., and West, R.F., "Cathodic Protection of Concrete Bridge Substructures", TRB, Oct. 1985, NCHRP 278, 59p.
75. Al-Kurdi, S.M.A., "Durability Assessment Criterion for Concrete and Reinforcement Exposed to Simulated Environmental Conditions of Saudi Arabia", M.Sc. Thesis, Dept. of Civil Engineering, KFUPM, 1984.
76. Pourbaix, M., Lectures on Electrochemical Corrosion, Plenum Press, New York, London, 1973 p 336.
77. Thangavel, K., Rengaswamy, N.S., and Balakrishnan, K., "Potential Criteria for Cathodic Protection of Steel in Concrete: Simulated Environment", Arabian Journal of Science and Engineering, Vol. 14, No.2, April, 1989, pp 357-364.
78. Creighton, H.J., Principles and Applications of Electrochemistry, Vol.1., Fourth Edition, John Wiley and Sons, May 1947.
79. Bailar, J.C. and Coauthors, Comprehensive Inorganic Chemistry, Pergamon Press, Vol. 1, First Edition, 1973.
80. Oldermann, I., and Wonnermann, R., "Effect of Alkalies on Portland Cement Hydration II, Alkalies Present in Form of Sulphate", Cement and Concrete Research, Vol. 13, 1983, pp 771-777.

81. Standard Test Methods for Potentially Alkali-Reactivity of Cement Aggregate Combinations (Mortar Bar Method), ASTM C-227, pp 121-125.
82. Brotschi, J., and Mehta, P.K., " Test Methods for Determining Potential Alkali-Silica Reactivity in Cement", Cement and Concrete Research, Vol. 8, pp 191-200, 1978.
83. Diamond, S., " A review of Alkali-Silica Reaction and Expansion Mechanism 2- Reactive Aggregates", Cement and Concrete Research, Vol. 6, NO. 4, pp 549-560, 1976.
84. Rockwell Hardness Test, ASTM.
85. Poole, A.B., McLachlan, A., and Ellis, D.J., " A Simple Staining Technique for the Identification of Alkali-Silica Gel in Concrete and Aggregate", Cement and Concrete Research, Vol. 18, pp 116-120, 1988.
86. Shayan, A., and Quick, G., " Microstructure and Composition of AAR Products in Conventional Standard and New Accelerated Testing", 8th International Conference on Alkali-Aggregate Reaction, 1989, KYOTO, pp 475-482.
87. Moranville, M.R., " Products of Reaction and Petrographic Examination", 8th International Conference on Alkali-Aggregate Reaction, 1989, KYOTO, pp 445-456.
88. Parkin Elmer, Atomic Absorption Analysis Methods.
89. Clear, K.C., and Harrigan, E.T., " Sampling and Testing for Chloride Ion in Concrete", Report No. FHWA-RD-77-85, Federal Highway Administration, Washington, DC, 1977.